NEW STRATEGIES FOR RUTHENIUM CATALYZED C-C BOND FORMATION

A Dissertation
Submitted to the Graduate Faculty
of the
North Dakota State University
of Agricultural and Applied Science

By

Jing Zhang

In Partial Fulfillment of the Requirements
for the Degree of
DOCTOR OF PHILOSOPHY

Major Department:
Chemistry and Biochemistry

November 2014

Fargo, North Dakota

North Dakota State University
Graduate School

Title

New Strategies for Ruthenium catalyzed C-C bond Formation

By

Jing Zhang

The Supervisory Committee certifies that this ***disquisition*** complies with North Dakota State University's regulations and meets the accepted standards for the degree of

DOCTOR OF PHILOSOPHY

SUPERVISORY COMMITTEE:

Prof. Pinjing Zhao
Chair

Prof. Gregory Cook

Prof. Mukund Sibi

Prof. Chengwen Sun

Approved:

12-03-2014
Date

Prof. Gregory Cook
Department Chair

ABSTRACT

Transition metal-catalyzed C-H bond activation allows direct functionalization of the ubiquitous C-H bonds in organic molecules to increase the molecular complexity. Since Murai's pioneering work in ruthenium catalyzed regioselective arene-alkene coupling reaction, a number of transition metal catalysts have been developed for C-C bond formation via C-H bond activation. However, metal-catalyzed C-H functionalization faces a number of long-standing challenges such as the control over regio- and stereoselectivity and harsh reaction conditions. Presented herein is our research on the development of ruthenium(II)-based catalysts for new and improved methods in C-C bond formations by formal activation of sp^2 C-H bonds and subsequent coupling with alkyne substrates.

Chapter 1 introduces the background of alkyne hydroarylation initiated by transition metal-catalyzed C-H bond activation and the significance to develop new strategies to overcome the limitations of current methods.

In Chapter 2 and Chapter 3, ruthenium(II)-N-heterocyclic carbene (NHC) catalyst systems were developed for efficient [3+2] carbocyclization between N-H aromatic ketimines or aromatic ketones and internal alkynes under very mild conditions. This process incorporates the *ortho*-directing imine and ketone groups for C-H bond activation into the overall transformation in a tandem manner and enables efficient access to indenyl amines and alcohols in high yields.

Chapter 4 describes the development of bis-cyclometalated ruthenium(II) complexes with readily available N-H aromatic ketimine and ketone ligands as a new class of catalyst precursors for C-C coupling reactions. The catalytic activity of the bis(imine) complex is evaluated in several catalytic coupling reactions of alkene and alkyne substrates. The coupling reactions are proposed to proceed by Ru(II)/Ru(IV) catalytic cycles involving C-C bond formation by oxidative cyclization.

Chapter 5 details the development of a decarboxylative alkyne hydroarylation process to synthesize arylalkenes with controlled and versatile regiochemistry of aromatic substituents. Following a tandem sequence of C-H bond activation and alkyne coupling, the subsequent decarboxylation is facilitated by the newly installed *ortho*-alkenyl moiety and is compatible with various aromatic substituents at *para*-, *meta*- and *ortho*-positions. This new decarboxylation strategy eliminates the prerequisite of

substrate activation by *ortho*-substitution and allows a broad scope of substituted benzoic acids to serve as aromatic building blocks for alkyne hydroarylation.

ACKNOWLEDGMENTS

I express my deepest gratitude to all the people who made my time at NDSU an important and memorable experience in my life.

Firstly, I would like to thank the most influential person, my advisor, Dr. Pinjing Zhao, for his excellent guidance through my PhD study. Dr. Zhao, I consider myself very lucky to have an advisor like you. You led me into the field of organometallic chemistry, which I deeply love. You taught me how to read and write chemistry. You showed me how to approach a problem in different ways and guided me when I made mistakes. You gave me a lot of freedom in my research and encouraged me to pursue my interests. You taught me how to present chemistry and supported me to go to many conferences. You have devoted endless time to me, even though you were extremely busy. You are the perfect mentor because you are always there for your students and ready to help. I will forever appreciate everything you have done for me. I hope that you will continue to be a significant person in my life and be my role model in personality, intelligence, and career.

I would like to thank my committee members for their support and advice. Dr. Cook, thank you very much for giving me some of the most important advice at the very beginning of my graduate study. You said, “do not compete with your colleagues; compete with the students in the top institutes”. Your advice encouraged me greatly through my graduate study. No matter if I succeeded or failed, it kept me calm and focused. I also appreciate all of your help and support during my time at NDSU. Dr. Sibi, I have learned a lot in your classes, in WOrMs discussions, and in my committee meetings. I also saw an important and valuable character trait in you: *dedication*—I tried to develop this trait in myself, and I think it would benefit me forever. Thank you very much for all your help and insightful comments at different stages of my research. Dr, Sun, although we were not in the same department and did not meet frequently, every time I met you, I learned something from you. You taught me how to communicate effectively, and gave me valuable suggestions on how to organize data and write research summaries. I am very grateful to your help. I also thank you for bringing a different perspective to my committee.

I could not complete the research described in this dissertation without the help from my colleagues in our department and my collaborators in other institutes. I want to thank Dr. Zhong-Ming Sun for training me to be an organometallic chemist at the beginning of my graduate study and letting me

participate in his projects and share the credit. I also want to thank Dr. Angel Ugrinov for being a patient teacher on mass spectrometry, also thank you for your extensive feedback and for solving crystal structures for me. I want to thank Mr. Daniel Wanner and Dr. John Bagu for training me and helping me to use NMR. I am very grateful to Dr. Vesela Ugrinova, Dr. Yonghua Yang, Dr. Jun Deng, Dr. Shinya Adachi, Dr. Xuguang Liu, Dr. Selvakumar Sermadurai, Dr. Chengkui Pei, and Dr. Nicolas Zimmerman for being thought-provoking consultants for helping me to address all of my questions about organic chemistry. I also want to thanks Professor John. F. Hartwig and Dr. Ruja Shrestha from UC Berkeley for collaborating on the project of decarboxylative hydroarylation. Finally I would like to thank Professor Yong Zhang from the Stevens Institute of Technology for his calculations on the project of alkene-alkyne coupling.

I also have been lucky to have very supportive friends in our department. Jing Yi, I am very lucky to have met you as the first friend in Fargo. You are so optimistic about life and nice to me. When I first came to Fargo and knew nobody, you let me stay in your apartment and made me breakfast for weeks. You taught me many things and answered my endless questions about living in the US and working in the lab—all of these turned out to be very helpful to me. Thank you very much for always being approachable when I needed your help. Gaoyuan, I am so happy that you joined our department after Jing's departure. I knew you would be a good friend after our first conversation because I could see intelligence sparkling in your eyes and you felt like an old friend. Indeed, you have been a great friend and helped me out many times. You also encouraged me because you worked so hard in your lab that left me no excuse to be lazy. Thank you so much for always being around. I also want to thank Xuguang, Zhongjing and Chengzhe for all of your help, and for being good friends.

I am very grateful to Wendy, Linda, Amy, and Tina for addressing my endless administrative questions and problems. I also want to thank David for helping me to get my chemicals and reagents, washing my lab-coats, and taking care of lots of things, even those I had not noticed. Without your help, I could not have completed my graduate study at NDSU so smoothly.

Last, but not least, I want to thank my family—my parents, my grandparents, my sister, and my brother—for your unconditional support and encouragement to pursue my dreams.

DEDICATION

This thesis is dedicated to the memory of my grandfather.

TABLE OF CONTENTS

LIST OF TABLES

Table Page

LIST OF FIGURES

Figure Page

LIST OF SCHEMES

Scheme Page

LIST OF ABBREVIATIONS

AcOH……acetic acid

Ag……silver

Au……gold

BINAP……..2,2'-bis(diphenylphosphino)-1,1'-binaphthyl

Bn……....benzyl

*n*Bu……..*normal*-butyl

*t*Bu……...*tertiary*-butyl

Bz……....benzoyl

$CDCl_3$……..deuterated chloroform

cod……..1,5-cyclooctadiene

coe……..cyclooctene

cot……..1,3,5,7-cyclooctatetraene

Co……...cobalt

CO……..carbon monooxide

Cp……...cyclopentadienyl

Cp*……..pentamethylcyclopentadienyl

Cs……...cesium

Cu……...copper

dba……..dibenzylideneacetone

DCE……1,2-dichloroethane

DCM……....dichloromethane

DG……...directing group

DIOP……2,3-O-isopropylidene-2,3-dihydroxy-1,4-bis(diphenylphosphino)butane

DMA……N,N-dimethylacrylamide

DME……1,2-dimethoxyethane

DMF……N,N-dimethylformamide

DMSO……..dimethylsulfoxide

DPPP……1,3-bis(diphenylphosphino)propane

EDG……..electron donating group

Et……ethyl

EtOAc……ethyl acetate

Et_2O……...diethyl ether

EWG……..electron withdrawing group

$FcPCy_2$…….. (dicyclohexylphosphinyl)ferrocene

FG……..functional group

GC…….gas chromatography

GC/MS……..gas chromatography/mass spectrometry

HRMS……...high resolution mass spectrometry

IMes……..1,3-bis(2,4,6-trimethylphenyl)imidazole-2-ylidene

IPr…….1,3-bis(2,6-diisopropylphenyl)imidazole-2-ylidene

Ir ……...iridium

K……potassium

L…….ligand

M……..metal

Me…….methyl

MeO…….methoxy

Mn…….manganese

Na……sodium

NHC……N-heterocyclic carbene

Ni…….nickel

NMP……N-methyl-2-pyrrolidone

^{1}H-NMR……..nuclear magnetic resonance (detecting protons)

^{13}C-NMR……..nuclear magnetic resonance (detecting carbon isotope ^{13}C)

OAc……acetate

OBz……benzoate

OPiv……pivalate

PCy_3……tricyclohexylphosphine

Pd……palladium

phen……1,10-phenanthroline

Ph……phenyl

PivOH……..pivalic acid

*i*Pr……isopropyl

*i*PrOAc……isopropyl acetate

PPh_3……triphenylphosphine

Pt……platinum

P*t*Bu……tri-*tertiary*-butylphosphine

rac……racemic

Re……rhenium

Rh……rhodium

Ru……ruthenium

Sb……antimony

SIMes……1,3-bis(2,6-diisopropylphenyl) -4,5-dihydroimidazole-2-ylidene

SIPr……1,3-bis(2,6-diisopropylphenyl)-4,5-dihydroimidazole-2-ylidene

TEA……triethylamine

TLC……thin-layer chromatography

TMS……trimethylsilyl

Zn……zinc

CHAPTER 1. INTRODUCTION

Carbon skeletons are the basis of organic structures. Thus, the investigation of new and versatile methods for the construction of C–C bonds is fundamental for the development of organic synthesis and materials chemistry. Classic organic reactions for C-C bond formation usually require prefunctionalized starting materials, which might be challenging to access. In contrast, unactivated carbon-hydrogen (C-H) bonds are ubiquitous in organic molecules. Therefore, direct transformation of these C-H bonds would provide atom-and step-economic routes to C-C bonds.

Transition metal complexes have been used to cleave unactivated C-H bonds to furnish more reactive carbon-metal bonds, which is termed C-H bond activation (Scheme 1.1). In 1963, the first example of this concept is reported by Kleiman and Dubeck (Scheme 1.2).[1] An *ortho*-C-H bond of azobenzene (**1.01**) was cleaved with stoichiometric Cp_2Ni (**1.02**), forming a 5-membered nickellacycle (**1.03**) after heating at 135 ^{o}C for 4h. The azo functional group works as a coordinating directing group to bring the metal in close proximity to the *ortho* C–H bond to be cleaved, resulting in high levels of regioselectivity. Later, the first ruthenium mediated C-H bond cleavage was published in 1965 by Chatt and Davidson (Scheme 1.3).[2] They observed that a ruthenium(0) complex (**1.04**) with a π-coordinated naphthalene was in equilibrium with a naphthyl-ruthenium(II) hydride complex (**1.05**) via C-H oxidative addition. After these pioneering results, a large amount of studies were reported on unactivated C-H bond cleavage using a stoichiometric amount of various transition metal complexes.[3-6]

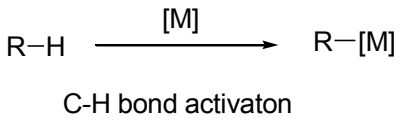

Scheme 1.1. Transition metal-assisted C-H bond activation

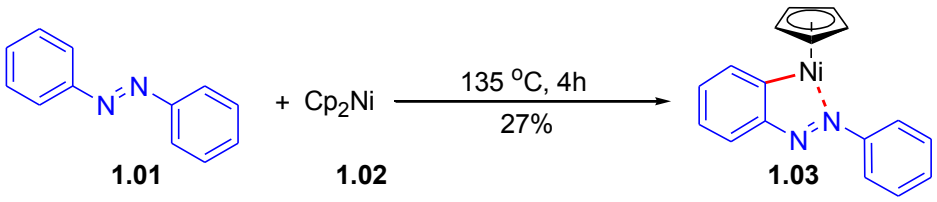

Scheme 1.2. First example of transition metal-mediated C-H bond cleavage

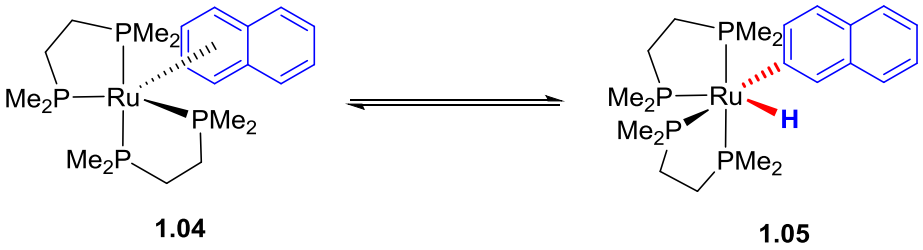

Scheme 1.3. First example of ruthenium mediated C-H bond cleavage

Since the manipulation of unreactive C-H bond was demonstrated in stoichiometric reactions, many efforts have been devoted into developing catalytic versions of C-H bond activation.[7-12] The first synthetically useful catalytic C-H activation for carbon-carbon (C-C) bond formation was reported in 1993 by Murai and co-workers (Scheme 1.4).[13] This work described a ruthenium catalyzed highly efficient and regioselective hydroarylation of terminal olefins (**1.07**) with aromatic ketones (**1.06**). The coordination of the carbonyl group with ruthenium complex resulted in highly site-selective *ortho* C-H bond cleavage and led to the ruthenacycle intermediate (**1.08**), which then reacted with the olefin substrates to produce alkylated ketones (**1.09**). This report highlighted the importance of a chelating group in order to achieve highly reactive and selective system for C-H activation processes.

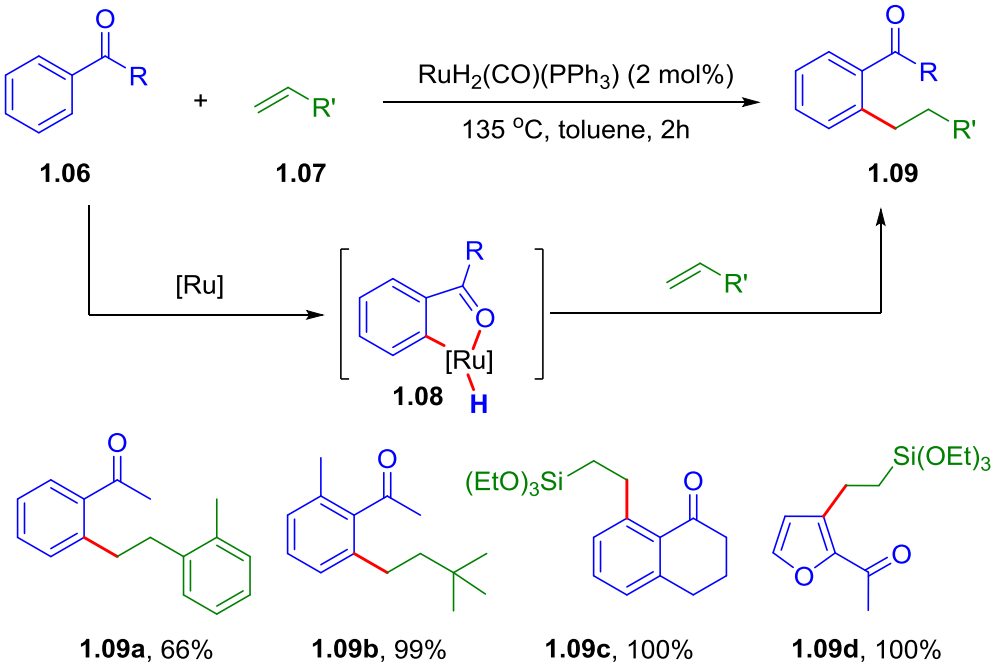

Scheme 1.4. Murai's ruthenium catalyzed aromatic ketone alkylation with terminal alkenes initiated by carbonyl directed C-H bond activation

Following this breakthrough discovery, a variety of functional groups containing oxygen and nitrogen atom were identified as suitable directing groups for ruthenium catalyzed C-H bond cleavage/olefin insertion process, such as ester,[14] aldehyde,[15] aldimine,[16,17] pyridine,[18] oxazoline,[19] and nitrile.[20] *This reaction featured high efficiency and regioselectivity without any byproducts, which represented one important direction of organic synthesis to develop atom-, step- and redox-economic reactions*.[21]

Attempts have been made to develop more reactive catalysts and to understand the reaction mechanism.[22-28] In 1998, Chaudret and coworkers synthesized a ruthenium complex with dihydrogen ligand (**1.10**) and prepared a ruthenacycle (**1.11**) with η^2-coordinated acetophenone via C-H bond cleavage (Scheme 1.5, Equation 1).[29] The stoichiometric reaction of **1.11** with triethoxyvinylsilane at room temperature gave the mono-insertion product, which was consistent with Murai's hypothesis. Catalytic insertion of ethylene was also achieved at room temperature with acetophenone in the presence of catalytic amount of **1.10** or **1.11** (Equation 2). Similar results were reported by Leitner and coworkers.[30-32] These results provided very useful information on C-H bond activation reaction mechanism and

demonstrated cyclometalated ruthenium complexes as highly promising catalyst precursor for mild C-H bond activation.

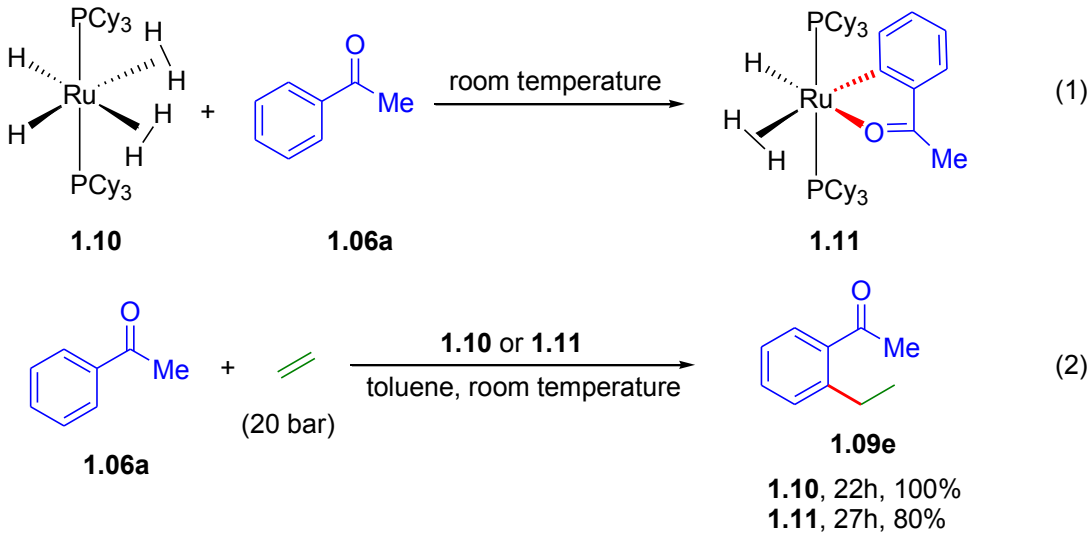

Scheme 1.5. Room temperature aromatic ketone alkylation using Chaudret's catalyst

The generally accepted mechanism for *ortho*-alkylation via C-H bond activation is depicted in Scheme 1.6. First, coordination of transition metal to the chelating oxygen facilitates cleavage of the C-H bond in the *ortho* position and generates a matallacycle intermediate (**1.08**). Next, olefin coordination and subsequent migratory insertion give a metal alkyl intermediate (**1.13**). Lastly, reductive elimination produces the *ortho* alkylated product (**1.09**) and regenerates the initial catalyst, completing the catalytic cycle. The reductive elimination for C-C bond formation was generally proposed as the rate-determining step.

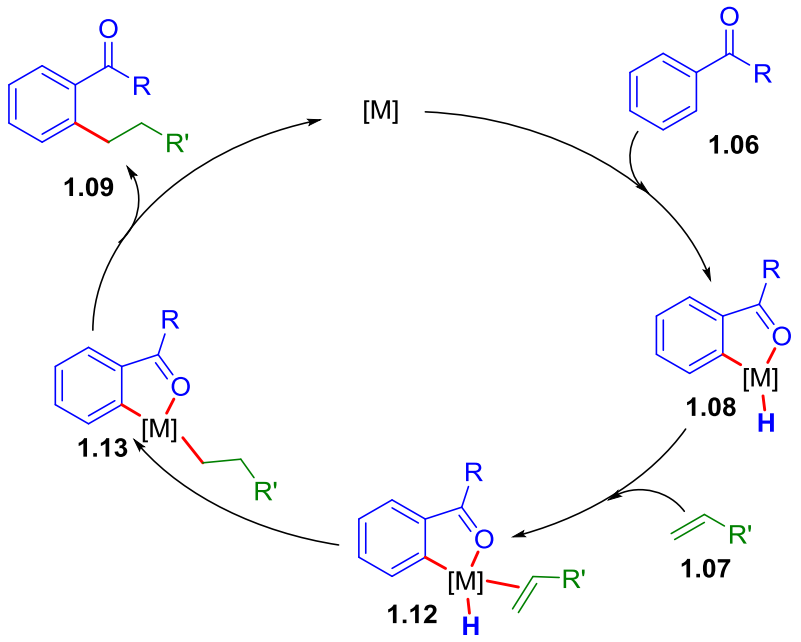

Scheme 1.6. Generally accepted reaction mechanism for Murai reaction

In 1995, internal alkynes were used for the first time as the acceptor of the C-H bond to generate substituted alkene products.[33] Highly site-selective hydroarylation of alkynes was achieved *ortho* to the directing carbonyl group by a ruthenium catalyst (Scheme 1.7). In the presence of catalytic amount of $RuH_2(CO)(PPh_3)_3$, α-tetralone (**1.06b**) reacted with internal alkynes generating the alkenylated arenes (**1.15**). Two possible stereoisomers were obtained in the case of symmetrically substituted internal alkynes, such as 4-octyne, in favor of the *syn*-hydroarylation products. This result indicated a *syn*-migratory insertion of alkynes. In comparison, for the unsymmetrically substituted internal alkynes such as 1-phenyl-1-butyne, all of the four regio- and stereoisomers of the products were observed.

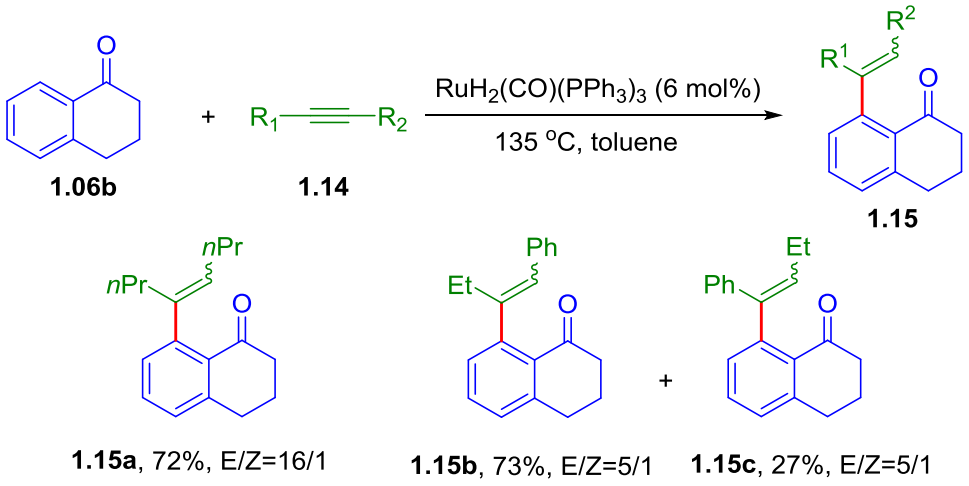

Scheme 1.7. Ruthenium catalyzed alkyne hydroarylation with cyclic α-tetralone

The regio- and stereochemistry results in catalytic alkyne hydroarylation with aromatic ketones were rationalized with a proposed mechanism that is analogous to the hydroarylation of olefins via directed C-H bond oxidative addition (Scheme 1.8). Following the formation of metallacycle (**1.08**), alkyne coordination and migratory insertion into the M-H linkage would form alkenyl-metal intermediates **1.17** and **1.17'** in favor of generating a more electronically stable vinyl-metal intermediate, while the steric effects might favor the other regioisomer. Thus, the combined electronic and steric effects of alkyne substrates make it relatively difficult to reach high regioselectivity. Besides, there is no strong geometry restriction, allowing both *E* and *Z* isomers to be formed after reductive elimination.

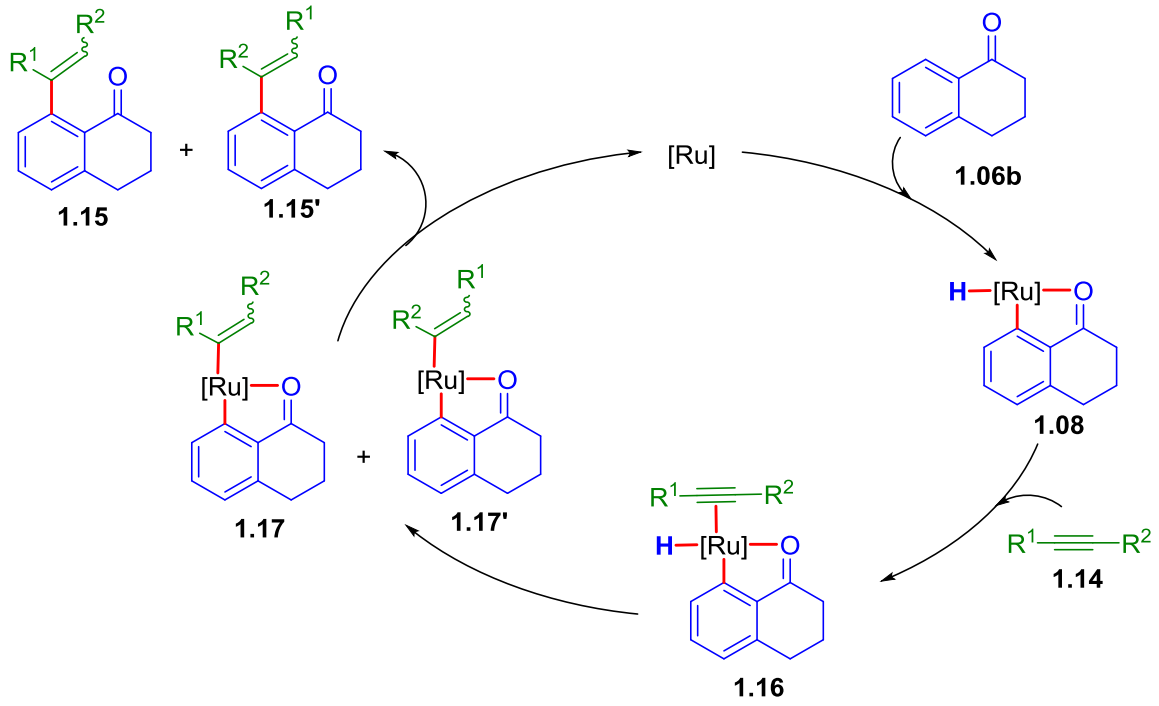

Scheme 1.8. Proposed reaction mechanism for alkyne hydroarylation with aromatic ketones initiated by C-H bond oxidative addition

This transformation completes the net insertion of C-C triple bonds into aromatic C-H bonds and represents the most straightforward and economic methods to access trisubstituted styrene derivatives, which are prevalent structures in biologically active compounds and used extensively as synthetic intermediates for fine chemicals and materials. However, unlike alkene hydroarylation, the development of transition metal-catalyzed alkyne hydroarylation based on directed C-H bond activation was not as well established and there were only a few catalytic systems reported 15 years after the first report.[34-38] In 1999, Miura and coworkers disclosed a catalyst system of iridium(I) catalyst precursor and P*t*Bu$_3$ ligand for regioselective hydroarylation of dialkyl alkynes with 1-naphthol (**1.18**) in the presence of a catalytic amount of $NaCO_3$ in refluxing toluene (Scheme 1.9).[34] Alkenylation occurred at the *ortho* position of the hydroxyl group producing only *E*-isomers, probably due to the presence of bulky phosphine ligand on the catalyst. In 2001, a rhodium(I) catalyst was successfully applied in internal alkyne hydroarylation with 2-phenylpyridines (**1.20**) in the presence of a catalytic amount of PPh_3 in refluxing toluene (Scheme 1.10).[35]

However, double alkenylated products (**1.22**) would be formed when the other *ortho* C-H bond is not blocked.

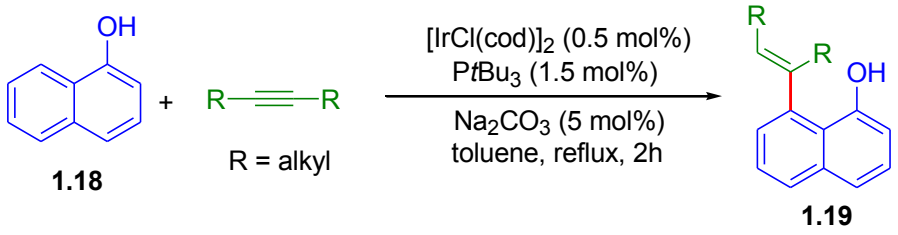

1.18 **1.19**

Scheme 1.9. Iridium catalyzed alkyne hydroarylation with 1-naphthol

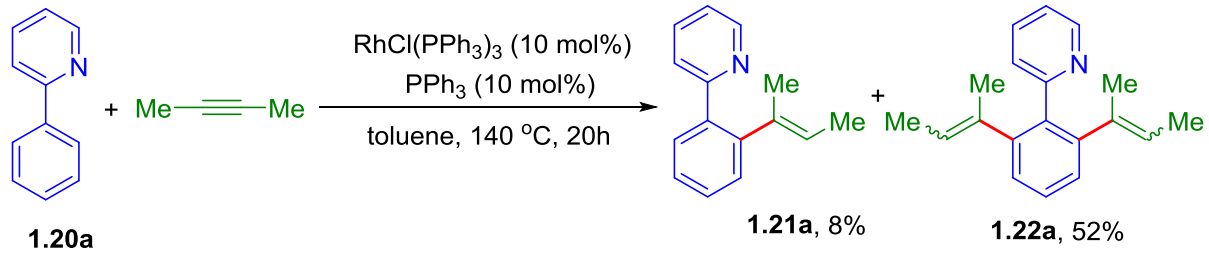

1.20a **1.21a**, 8% **1.22a**, 52%

Scheme 1.10. Rhodium catalyzed alkyne hydroarylation with 2-phenylpyridine

In 2008, Shibata and coworkers reported a cationic iridium catalyzed alkyne hydroarylation of ketones in refluxing DCE (Scheme 1.11).[36] In the case of aryl ketones with both *ortho* C-H bonds available, over-alkenylation occurred. In the same year, Kuninobu and Takai revealed a rhenium catalyzed alkyne hydroarylation with heteroaryl aldimines in DCE at 115 °C (Scheme 1.12).[37] High regioselectivity and stereoselectivity for alkyne addition were achieved. Similar reaction mechanisms via transition metal-mediated C-H bond oxidative addition were proposed in these reports.

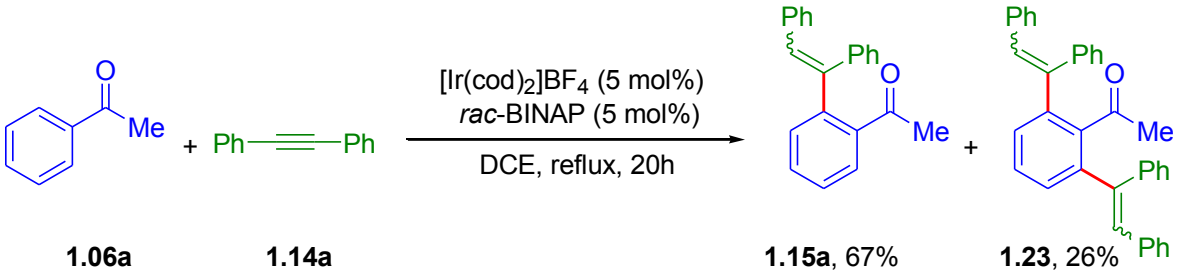

Scheme 1.11. Cationic iridium catalyzed alkyne hydroarylation with acetophenone

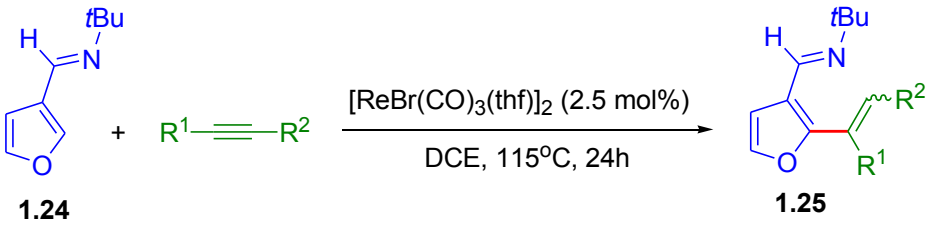

Scheme 1.12. Rhenium catalyzed alkyne hydroarylation with heteroaryl aldimines

In 2008, Zhang and coworkers first introduced another C-H bond cleavage mechanism for alkyne hydroarylation.[38] In the presence of catalytic amount of $RuCl_3$, alkenylation of 2-arylpyridines (**1.20**) at the *ortho* C−H bond proceeded in high regio- and stereoselectivity with the assistance of stoichiometric benzoyl peroxide or benzoic acid (Scheme 1.13). Besides arylpyridines, phenylpyrimidine and phenylpyridazine also underwent alkenylation under the same reaction conditions.

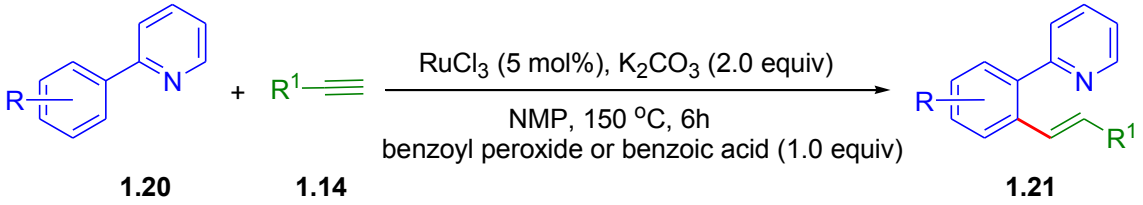

Scheme 1.13. Ruthenium catalyzed terminal alkyne hydroarylation with 2-phenylpyridines

The authors proposed a reaction mechanism involving C-H bond cleavage via concerted metalation-deprotonation pathway instead of an oxidative addition pathway (Scheme 1.14). The catalytic reaction proceeds via coordination-assisted benzoate-accelerated deprotonation at the *ortho* C-H position of the pyridyl group by ruthenium through the formation of intermediate **1.26**, generating a ruthenacycle intermediate (**1.27**). Alkyne coordination and migratory insertion into the Ru-C linkage provide a cyclic vinyl-Ru intermediate (**1.29**). Subsequent protonation gives the alkenylated product (**1.21**) and regenerates the initial active catalyst. Notably, the internal alkynes were inactive under these reaction conditions.

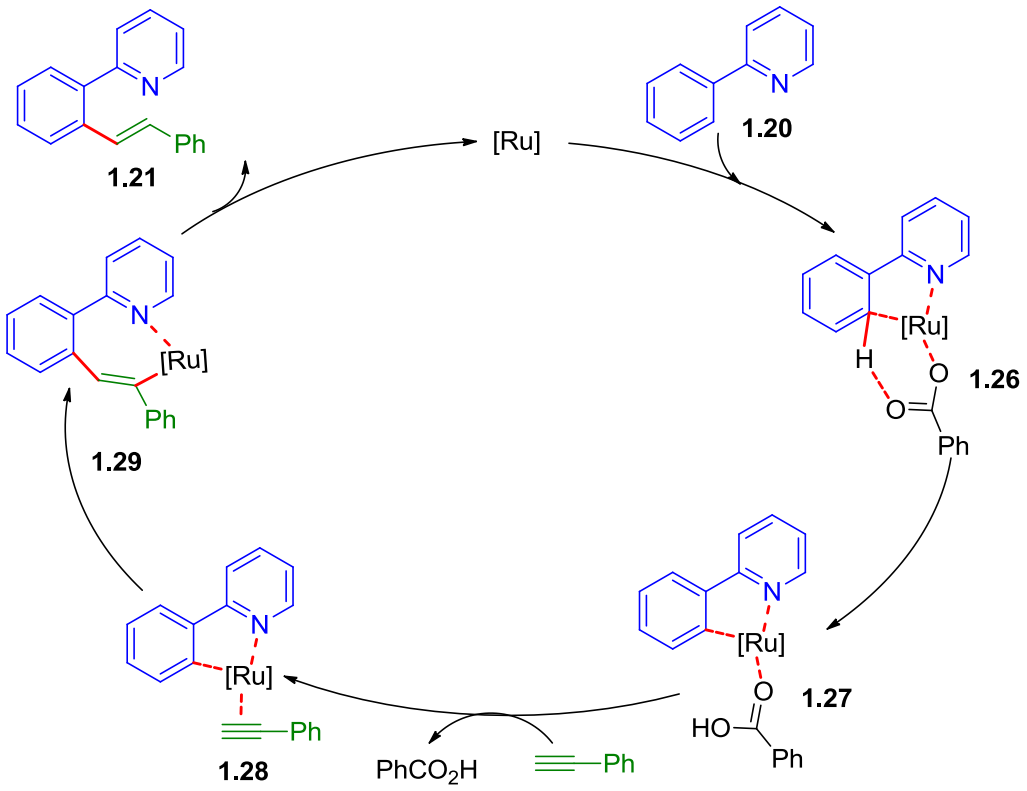

Scheme 1.14. Proposed reaction mechanism for ruthenium catalyzed alkyne hydroarylation with 2-phenylpyridine initiated by C-H bond concerted metalation-deprotonation

In 2010, Fagnou and coworkers reported a cationic rhodium complex catalyzed alkyne hydroarylation with indole derivatives (**1.30**) initiated by C-H bond activation via a proposed concerted

metalation-deprotonation mechanism for C-H bond activation (Scheme 1.15).[39] With the aid of PivOH additive, 2-alkenylindoles (**1.31**) were obtained in good yields with high regio- and stereoselectivity in *i*PrOAc under relatively lower reaction temperature. This catalytic system for *ortho*-C-H alkenylation could also be applied to other heterocycles, such as pyrroles, furans, and benzamides.

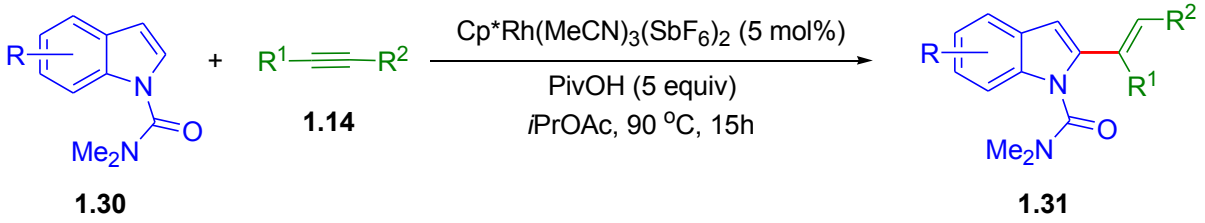

Scheme 1.15. Rhodium catalyzed alkyne hydroarylation with indoles initiated by C-H bond concerted metalation-deprotonation

These reactions showed good reactivity towards internal alkynes with high regio- and stereoselectivity favoring the *E*-stereoisomers. Compared with C-H oxidative addition, the metallacycle intermediate (**1.32**) generated via concerted metalation-deprotonation pathway does not possess a hydride ligand. Thus, the alkyne insertion is into M-C bond instead of M-H bond. The cationic nature of the metal complex promotes metal-carbon σ bonding to the carbon with a substituent that is capable of sharing its positive charge through inductive or resonance effect (Scheme 1.16). In addition, the geometry requirement for the formation of metallacycle intermediate **1.33** highly prefers the *syn*-insertion.

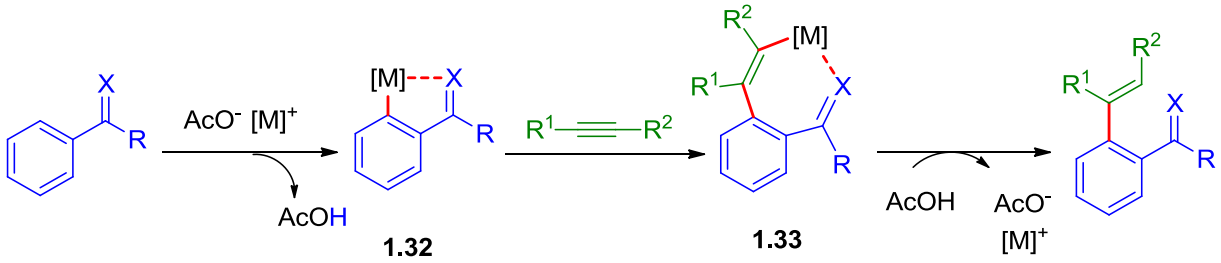

Scheme 1.16. Selectivity in alkyne hydroarylation initiated by C-H bond concerted metalation-deprotonation

During the development of this thesis, a variety of catalysts have been reported for effective alkyne hydroarylation with arenes bearing different directing groups, such as ruthenium, rhodium, iridium and cobalt catalysts.[40-45] Although the directing group allows precise regiocontrol of alkenylation at the *ortho* position, it typically remains intact on the product structure after the reaction and leads to several limitations. First, the directing group on the product could cause over-reaction, which leads to a mixture of mono-and dialkenylated products. Second, additional synthetic steps would be required to remove these directing groups or transform them into more synthetically useful functionalities. Third, the general inability of common directing groups to access *meta*- and *para*-alkenylated products limits its application. Besides, all of the current catalyst systems of functional group-directed alkyne hydroarylation require harsh reaction conditions, such as high reaction temperatures and requirement of heavy salt additives, which restricts the utility and functional group compatibility. Lastly, the precise control over regio- and stereoselectivity is still an unsolved problem.

All these longstanding challenges have incited us to develop new catalytic methods for C-H functionalization that involve rational catalyst design and novel strategy for directing group transformation. The following chapters describes our research on the development of ruthenium(II)-based catalysts for new and improved methods in C-C bond formations by formal activation of sp^2 C-H bonds and subsequent coupling with alkyne substrates. Results from the following three major projects are summarized: (1) mild [3+2] annulations by involving the *ortho*-directing group for aromatic C-H activation into the overall transformation in a tandem manner; (2) development of new, bis-cyclometalated Ru(II) catalysts with internal templates for mild C-C coupling; (3) decarboxylative alkyne hydroarylation by utilizing the carboxyl functionality as a traceless-removable directing group.

1.1. References

1. Kleiman, J. P.; Dubeck, M. The Preparation of Cyclopentadienyl [*o*-(Phenylazo)phenyl]nickel. *J. Am. Chem. Soc.* **1963**, *85*, 1544-1545.

2. Chatt, J.; Davidson, J. M. The Tautomerism of Arene and Ditertiary Phosphine Complexes of Ruthenium(0), and the Preparation of New Types of Hydrido-Complexes of Ruthenium(II). *J. Chem. Soc.* **1965**, 843-855.

3. Shilov, A. E.; Shul'pin, G. B. Activation of C−H Bonds by Metal Complexes. *Chem. Rev.* **1997**, *97*, 2879-2932.

4. Ryabov, A. D. Mechanisms of Intramolecular Activation of Carbon-Hydrogen Bonds in Transition-Metal Complexes. *Chem. Rev.* **1990**, *90*, 403-424.

5. Newkome, G. R.; Puckett, W. E.; Gupta, V. K.; Kiefer, G. E. Cyclometalation of the Platinum Metals with Nitrogen and Alkyl, Alkenyl, and Benzyl Carbon Donors. *Chem. Rev.* **1986**, *86*, 451-489.

6. Ryabov, A. D. Cyclopalladated Complexes in Organic Synthesis. *Synthesis* **1985**, *1985*, 233-252.

7. Kashiwagi, K.; Sugise, R.; Shimakawa, T.; Matuura, T.; Shirai, M.; Kakiuchi, F.; Murai, S. Catalytic Dimerization of Acrylonitrile. *Organometallics* **1997**, *16*, 2233-2235.

8. Moore, E. J.; Pretzer, W. R.; O'Connell, T. J.; Harris, J.; LaBounty, L.; Chou, L.; Grimmer, S. S. Catalytic and Regioselective Acylation of Aromatic Heterocycles Using Carbon Monoxide and Olefins. *J. Am. Chem. Soc.* **1992**, *114*, 5888-5890.

9. Jordan, R. F.; Taylor, D. F. Zirconium-Catalyzed Coupling of Propene and α-Picoline. *J. Am. Chem. Soc.* **1989**, *111*, 778-779.

10. Tsou, D. T.; Burrington, J. D.; Maher, E. A.; Grasselli, R. K. Mechanism of Ruthenium-Catalyzed Linear Dimerization of Acrylonitrile: a Kinetic Study. *J. Mol. Catal.* **1985**, *30*, 219-239.

11. Hong, P.; Yamazaki, H.; Sonogashira, K.; Hagihara, N. Rhodium Carbony Cluster Catalyzed Addition of Arenes to Diphenylketene and Aryl Isocyanates. *Chem. Lett.* **1978**, *7*, 535-538.

12. Fujiwara, Y.; Moritani, I.; Matsuda, M.; Teranishi, S. Aromatic Substitution of Olefin. IV Reaction with Palladium Metal and Silver Acetate. *Tetrahedron Lett.* **1968**, *9*, 3863-3865.

13. Murai, S.; Kakiuchi, F.; Sekine, S.; Tanaka, Y.; Kamatani, A.; Sonoda, M.; Chatani, N. Efficient Catalytic Addition of Aromatic Carbon-Hydrogen Bonds to Olefins. *Nature* **1993**, *366*, 529-531.

14. Sonoda, M.; Kakiuchi, F.; Kamatani, A.; Chatani, N.; Murai, S. Ruthenium-Catalyzed Addition of Aromatic Esters at the *ortho* C-H Bonds to Olefins. *Chem. Lett.* **1996**, *25*, 109-110.

15. Kakiuchi, F.; Sato, T.; Igi, K.; Chatani, N.; Murai, S. The Ruthenium-Catalyzed Addition of β-C-H Bonds in Aldehydes to Olefins. *Chem. Lett.* **2001**, *30*, 386-387.

16. Kakiuchi, F.; Yamauchi, M.; Chatani, N.; Murai, S. Ruthenium-Catalyzed Addition of Aromatic Imines at the *ortho*-C-H Bonds to Olefins. *Chem. Lett.* **1996**, *25*, 111-112.

17. Kakiuchi, F.; Sato, T.; Tsujimoto, T.; Yamauchi, M.; Chatani, N.; Murai, S. New Protocol for the Siteselective Alkylation and Vinylation of Aromatic Compounds. Catalyst-Specific Reactions. *Chem. Lett.* **1998**, *27*, 1053-1054.

18. Schinkel, M.; Marek, I.; Ackermann, L. Carboxylate-Assisted Ruthenium(II)-Catalyzed Hydroarylations of Unactivated Alkenes through C-H Cleavage. *Angew. Chem. Int. Ed.* **2013**, *52*, 3977-3980.

19. Kakiuchi, F.; Sato, T.; Yamauchi, M.; Chatani, N.; Murai, S. Ruthenium-Catalyzed Coupling of Aromatic Carbon-Hydrogen Bonds in Aromatic Imidates with Olefins. *Chem. Lett.* **1999**, *28*, 19-20.

20. Kakiuchi, F.; Sonoda, M.; Tsujimoto, T.; Chatani, N.; Murai, S. The Ruthenium-Catalyzed Addition of C-H Bonds in Aromatic Nitriles to Olefins. *Chem. Lett.* **1999**, *28*, 1083-1084.

21. Burns, N. Z.; Baran, P. S.; Hoffmann, R. W. Redox Economy in Organic Synthesis. *Angew. Chem. Int. Ed.* **2009**, *48*, 2854-2867.

22. Jazzar, R. F. R.; Mahon, M. F.; Whittlesey, M. K. Synthesis and X-ray Structural Characterization of $Ru(PPh_3)_3(CO)(C_2H_4)$ and $RuH(o\text{-}C_6H_4C(O)CH_3)(PPh_3)_2L$ (L = PPh_3, CO, DMSO): Ruthenium Complexes with Relevance to the Murai Reaction. *Organometallics* **2001**, *20*, 3745-3751.

23. Drouin, S. D.; Amoroso, D.; Yap, G. P. A.; Fogg, D. E. Multifunctional Ruthenium Catalysts: A Novel Borohydride-Stabilized Polyhydride Complex Containing the Basic, Chelating Diphosphine 1,4-Bis(dicyclohexylphosphino)butane and Its Application to Hydrogenation and Murai Catalysis. *Organometallics* **2002**, *21*, 1042-1049.

24. Trost, B. M.; Imi, K.; Davies, I. W. Elaboration of Conjugated Alkenes Initiated by Insertion into a Vinylic C-H Bond. *J. Am. Chem. Soc.* **1995**, *117*, 5371-5372.

25. Hiraki, K.; Ishimoto, T.; Kawano, H. An NMR Study on the Ruthenium Complex-Catalyzed C-H/Olefin Coupling Reaction. *Bull. Chem. Soc. Jpn.* **2000**, *73*, 2099-2108.

26. Kakiuchi, F.; Ohtaki, H.; Sonoda, M.; Chatani, N.; Murai, S. Mechanistic Study of the $Ru(H)_2(CO)(PPh_3)_3$-Catalyzed Addition of C-H Bonds in Aromatic Esters to Olefins. *Chem. Lett.* **2001**, *30*, 918-919.

27. Matsubara, T.; Koga, N.; Musaev, D. G.; Morokuma, K. Density Functional Study on Activation of *ortho*-C-H Bond in Aromatic Ketone by Ru Complex. Role of Unusual Five-Coordinated d^6 Metallacycle Intermediate with Agostic Interaction. *J. Am. Chem. Soc.* **1998**, *120*, 12692-12693.

28. Matsubara, T.; Koga, N.; Musaev, D. G.; Morokuma, K. Density Functional Study on Highly *Ortho*-Selective Addition of an Aromatic CH Bond to Olefins Catalyzed by a $Ru(H)_2(CO)(PR_3)_3$ Complex. *Organometallics* **2000**, *19*, 2318-2329.

29. Guari, Y.; Sabo-Etienne, S.; Chaudret, B. Exchange Couplings Between a Hydride and a Stretched Dihydrogen Ligand in Ruthenium Complexes. *J. Am. Chem. Soc.* **1998**, *120*, 4228-4229.

30. Busch, S.; Leitner, W. Convenient Preparation of Mononuclear and Dinuclear Ruthenium Hydride Complexes for Catalytic Application. *Chem. Commun.* **1999**, 2305-2306.

31. Busch, S.; Leitner, W. Ruthenium-Catalysed Murai-Type Couplings at Room Temperature. *Adv. Synth. Catal.* **2001**, *343*, 192-195.

32. Giunta, D.; Hölscher, M.; Lehmann, C. W.; Mynott, R.; Wirtz, C.; Leitner, W. Room Temperature Activation of Aromatic C-H Bonds by Non-Classical Ruthenium Hydride Complexes Containing Carbene Ligands. *Adv. Synth. Catal.* **2003**, *345*, 1139-1145.

33. Kakiuchi, F.; Yamamoto, Y.; Chatani, N.; Murai, S. Catalytic Addition of Aromatic C-H Bonds to Acetylenes. *Chem. Lett.* **1995**, *24*, 681-682.

34. Satoh, T.; Nishinaka, Y.; Miura, M.; Nomura, M. Iridium-Catalyzed Regioselective Reaction of 1-Naphthols with Alkynes at the *peri*-Position. *Chem. Lett.* **1999**, *28*, 615-616.

35. Lim, Y.-G.; Lee, K.-H.; Koo, B. T.; Kang, J.-B. Rhodium(I)-Catalyzed *ortho*-Alkenylation of 2-Phenylpyridines with Alkynes. *Tetrahedron Lett.* **2001**, *42*, 7609-7612.

36. Kuninobu, Y.; Kikuchi, K.; Tokunaga, Y.; Nishina, Y.; Takai, K. Hydroarylation of Acetylenes, Acrylates, and Isocyanates with Heteroaromatic Compounds under Rhenium Catalysis. *Tetrahedron* **2008**, *64*, 5974-5981.

37. Tsuchikama, K.; Kasagawa, M.; Hashimoto, Y.-K.; Endo, K.; Shibata, T. Cationic Iridium–BINAP Complex-Catalyzed Addition of Aryl ketones to Alkynes and Alkenes via Directed C–H Bond Cleavage. *J. Organomet. Chem.* **2008**, *693*, 3939-3942.

38. Cheng, K.; Yao, B.; Zhao, J.; Zhang, Y. $RuCl_3$-Catalyzed Alkenylation of Aromatic C−H Bonds with Terminal Alkynes. *Org. Lett.* **2008**, *10*, 5309-5312.

39. Schipper, D. J.; Hutchinson, M.; Fagnou, K. Rhodium(III)-Catalyzed Intermolecular Hydroarylation of Alkynes. *J. Am. Chem. Soc.* **2010**, *132*, 6910-6911.

40. Hashimoto, Y.; Hirano, K.; Satoh, T.; Kakiuchi, F.; Miura, M. Ruthenium(II)-Catalyzed Regio- and Stereoselective Hydroarylation of Alkynes via Directed C-H Functionalization. *Org. Lett.* **2012**, *14*, 2058-2061.

41. Lee, P.-S.; Fujita, T.; Yoshikai, N. Cobalt-Catalyzed, Room-Temperature Addition of Aromatic Imines to Alkynes via Directed C-H Bond Activation. *J. Am. Chem. Soc.* **2011**, *133*, 17283-95.

42. Yamakawa, T.; Yoshikai, N. Cobalt-Catalyzed *ortho*-Alkenylation of Aromatic Aldimines via Chelation-Assisted C–H Bond Activation. *Tetrahedron* **2013**, *69*, 4459-4465.

43. Zhao, P.; Niu, R.; Wang, F.; Han, K.; Li, X. Rhodium(III)- and Ruthenium(II)-Catalyzed Olefination of Isoquinolones. *Org. Lett.* **2012**, *14*, 4166-4169.

44. Reddy, M. C.; Jeganmohan, M. Ruthenium-Catalyzed Highly Regio- and Stereoselective Hydroarylation of Aryl Carbamates with Alkynes via C-H Bond Activation. *Chem. Commun.* **2013**, *49*, 481-483.

45. Liang, L.; Fu, S.; Lin, D.; Zhang, X.-Q.; Deng, Y.; Jiang, H.; Zeng, W. Ruthenium(II)-Catalyzed Direct Addition of Indole/Pyrrole C2–H Bonds to Alkynes. *J. Org. Chem.* **2014**, *79*, 9472-9480.

CHAPTER 2. RUTHENIUM(II)/N-HETEROCYCLIC CARBENE CATALYZED [3+2] CARBOCYCLIZATION WITH AROMATIC N-H KETIMENES AND INTERNAL ALKYNES

2.1. Background and Significance

Direct incorporation of the directing groups into transition metal-catalyzed C-H bond functionalization in a tandem manner provides an additional utility to the directing group. Thus, it is highly desirable to apply this strategy in alkyne hydroarylation to increase the diversity and molecular complexity.

In 1995, Kisch reported the first example of transformation of the directing group initiated by C-H bond activation (Scheme 2.1).[1] Indoles (**2.03**) were obtained from the reaction between 1,2-diarylazenes (**2.01**) and internal alkynes (**2.02**) in the presence of catalytic amount of Wilkinson's catalyst. Strong electronic effect was observed in the substituents in the alkynes. Electron-withdrawing substituents induced a decrease of the turnover numbers.

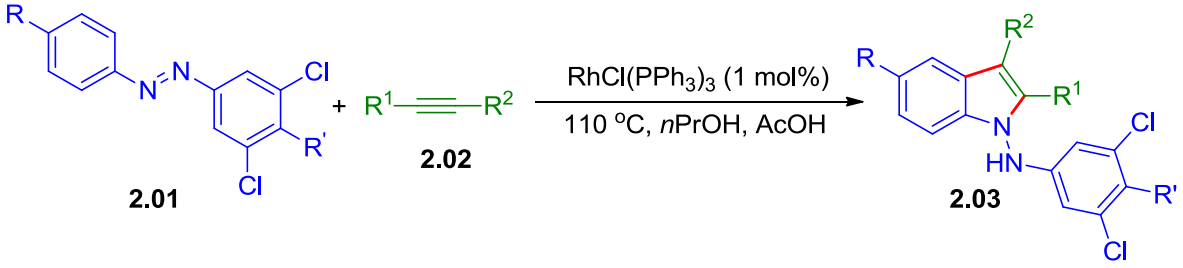

Scheme 2.1. The first example of transformation of the directing group initiated by C-H bond activation

The mechanism was proposed to be a hydroarylation of an alkyne followed by an acid catalyzed rearrangement (Scheme 2.2). Wilkinson's catalyst promoted C-H cleavage at the *ortho*-position of the diazo group via oxidative addition, generating a rhodacycle (**2.05**). Alkyne migratory insertion into Rh-H bond gave a Rh alkenyl intermediate (**2.06**). Subsequent C-C reductive elimination afforded alkenylated

intermediate (**2.07**) and regenerated the active rhodium catalyst (**2.08**) to complete the catalytic cycle. In the presence of a Brønsted acid, intermediate (**2.07**) rearranged to give the final indole product.

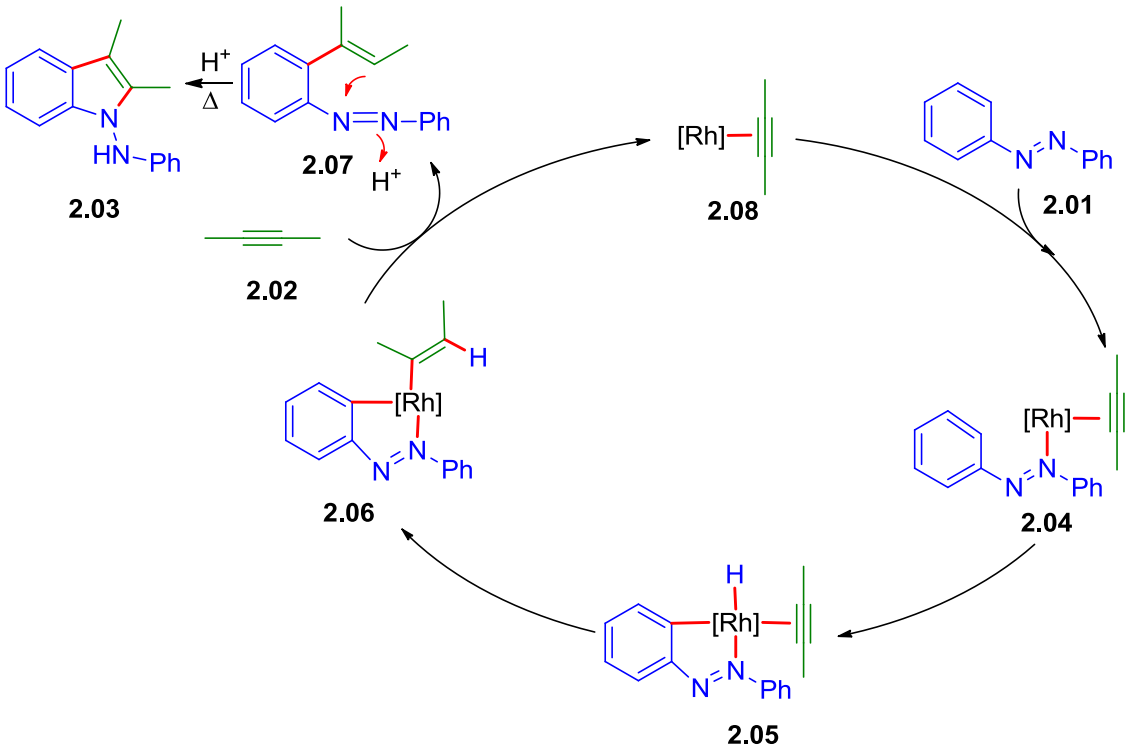

Scheme 2.2. Proposed reaction mechanism for indole formation initiated by rhodium catalyzed C-H bond oxidative addition

However, the concept of involving directing group into transition metal-catalyzed C-H bond functionalization did not receive much attention in the next ten years. In 2005, Kuninobu, Takai and coworkers disclosed one of the first examples of transition metal-catalyzed carbocyclization in a tandem fashion initiated by C-H bond cleavage (Scheme 2.3).[2] The initial imine directed C-H bond activation via oxidative addition catalyzed by rhenium complex generates rhenacycle (**2.11**). Alkyne coordination and subsequent migratory insertion produce alkenyl rhenium complex (**2.12**). This rhenium species undergoes intramolecular addition to the ketimine moiety, forming amido rhenium complex (**2.13**). Successive reductive elimination and double bond isomerization afford indenyl amine products. The reaction yields were strongly influenced by the electronic properties of the aromatic ring of aldimine substrate. Electron-

rich and -neutral aldimines gave higher yields. On the other hand, electron-poor or hindered aldimines exhibited no reactivity or very poor reactivities. This [3+2] carbocyclization is highly attractive as the directing group participated in a redox-neutral transformation, producing valuable indene derivatives. However, the reaction is limited to protected aldimines and aromatic internal alkynes. When ketimine was utilized, deamination took place due to the harsh reaction conditions.[3]

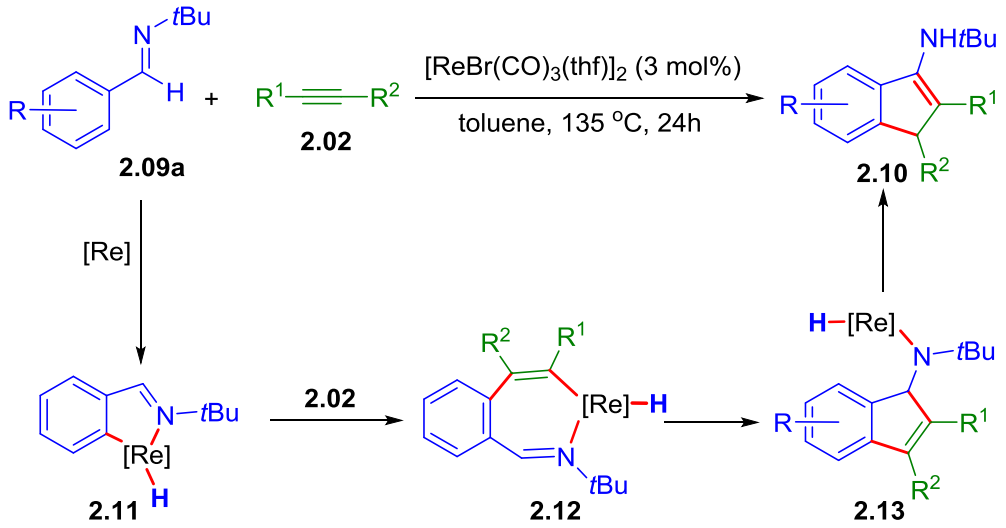

Scheme 2.3. Rhenium catalyzed carbocyclization with aromatic aldimines and internal alkynes

In 2009, Satoh, Miura and coworkers reported an oxidative [3+2] carbocyclization of aldimines and internal alkynes using a rhodium catalyst (Scheme 2.4).[4] Unlike the rhenium mediated C-H bond oxidative addition generating M-H complex, this reaction is initiated by C-H bond deprotonation with the assistance of acetate giving a rhodacycle (**2.15a**) without hydride ligand. Alkyne insertion and subsequent intramolecular imine addition afford a rhodium amido intermediate (**2.17a**). Subsequent β-hydride elimination yields indenone imines (**2.14**). Oxidation of the released rhodium(I) by copper(II) salt regenerates the initial active rhodium (III) catalyst. The scope of alkynes was limited to diaryl-alkynes. When benzophenone phenylimine (**2.09c**) was used in order to avoid β-hydride elimination, the reaction stopped before intramolecular imine addition and produced the *ortho*-alkenylated product (**2.18a**) in low

yield (Scheme 2.5). When unprotected benzophenone imine (**2.09d**) was subjected in similar reaction conditions, oxidative heterocyclization took place yielding 1,3,4-triphenylisoquinoline (**2.19a**) in quantitative yield via C-H and N-H activation (Scheme 2.6).

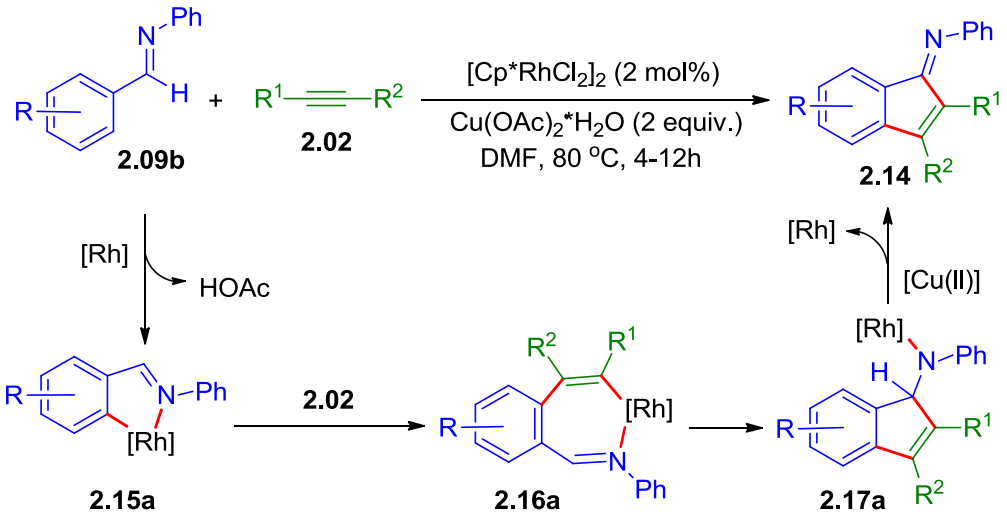

Scheme 2.4. Rhodium(III) catalyzed carbocyclization with aromatic aldimines and internal alkynes

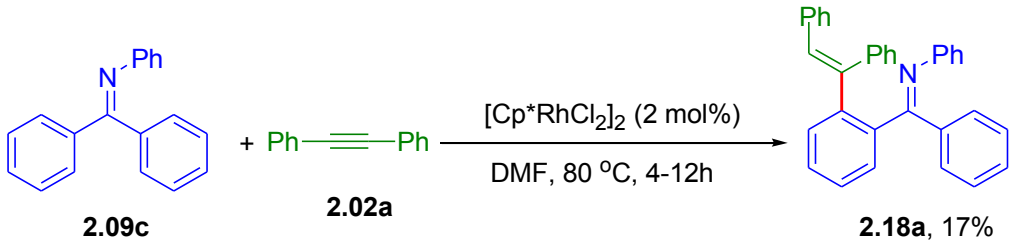

Scheme 2.5. Rhodium(III) catalyzed benzophenone phenylimine alkenylation with diphenylacetylene

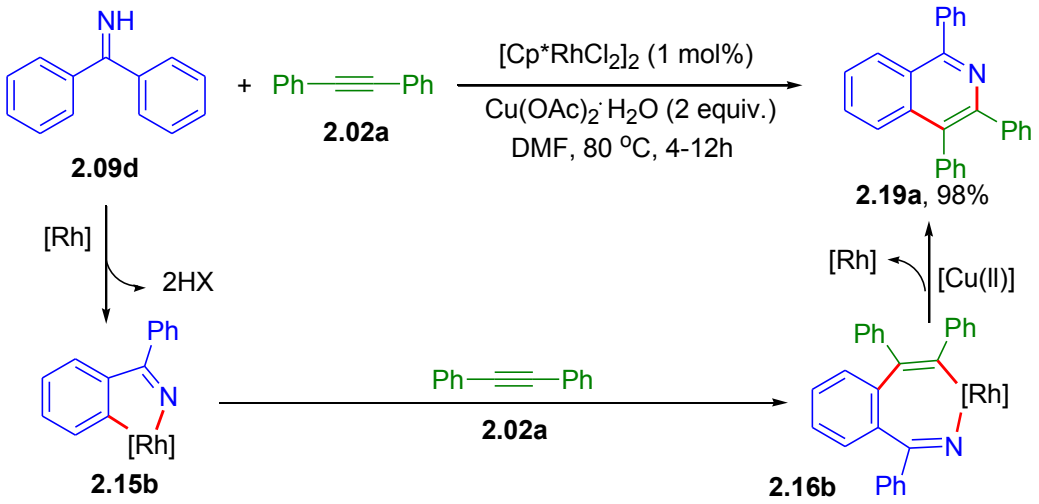

Scheme 2.6. Rhodium(III) catalyzed oxidative heterocyclization with benzophenone imine and diphenylacetylene

Based on these early works, our group envisioned that it would be of high synthetic value to be able to intercept the amido-metal intermediate (**2.22**) prior to β-H elimination, which would give a useful amine functional group upon protonation (Scheme 2.7).[5] Furthermore, to avoid the isomerization and elimination as previously observed in rhenium and rhodium catalytic systems, a new catalyst would be required. With a proper catalyst precursor the overall reaction would be a redox-neutral process, which would provide a convenient and waste-free complement to current synthetic routes towards tertiary carbinamines.[6-12]

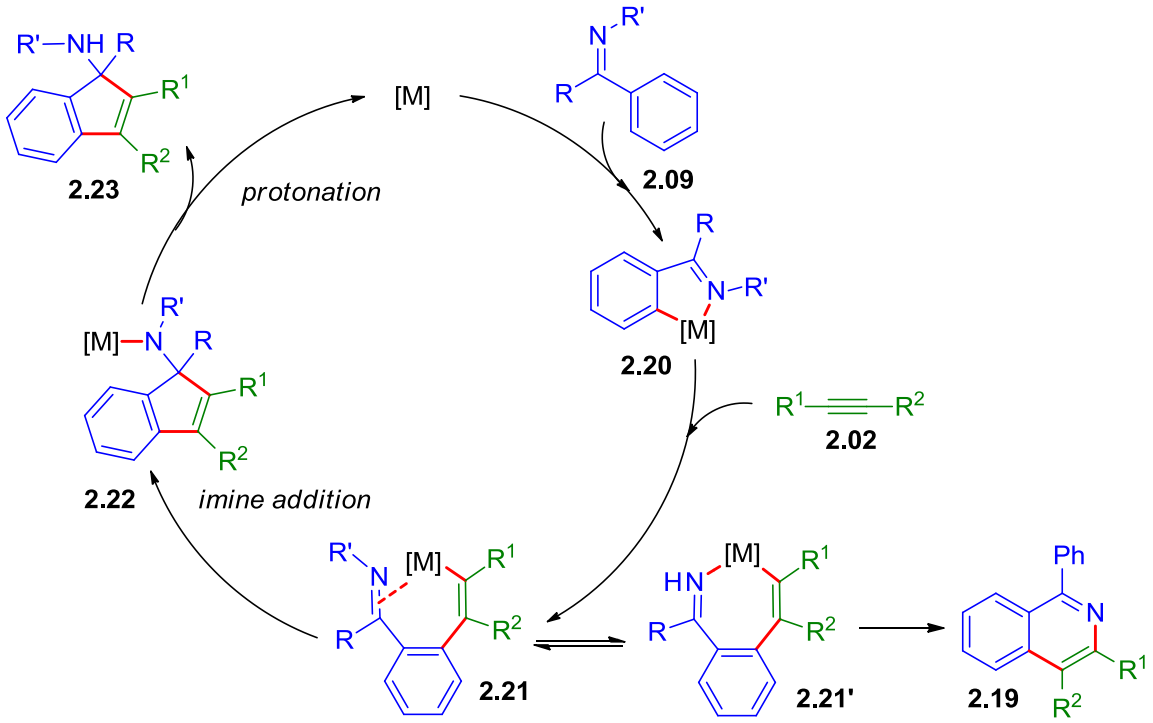

Scheme 2.7. Envisioned catalytic cycle for transition metal-catalyzed redox-neutral carbocyclization initiated by C-H bond activation

In the envisioned catalytic cycle, a key step is the generation of a nucleophilic transition metal–alkenyl intermediate (**2.21**) with a π-coordinated imine moiety, which is reactive towards intramolecular ketimine addition. The corresponding σ-complexation by the nitrogen atom would limit the rotation of the electrophile (C=N moiety). This would disturb the orbital interaction that is necessary for the proposed intramolecular imine insertion and, as a result, inhibit the formation of the carbocycle. The intermediate **2.21'** with σ-coordinated nitrogen would prefer reductive elimination for C-N bond formation, giving the isoquinoline derivative (**2.19**).

With the envisioned catalytic cycle, N-unsubstituted diaryl ketimine substrates were initially selected with the following considerations. First, N-unsubstituted diaryl ketimines were less studied compare with protected aldimines and ketimines. Second, diaryl ketimines can be prepared conveniently by Grignard reactions by using readily available aryl halides and aryl cyanides.[13,14] This modular synthetic approach is convenient for exploration of reactivity dependence on various aromatic substituents. Third, [3+2] annulations with N-unsubstituted diaryl ketimines would be operationally simple and without the

need for additional deprotection procedures. Lastly, reactions with diaryl ketimines will avoid potential interference by imine/enamine tautomerization.

With these considerations, our group successfully developed a formal [3+2] carbocyclization to produce indenyl amines based on the envisioned catalytic cycle described in Scheme 2.7.[5] In the presence of catalytic amounts of $[Rh(cod)Cl]_2$ and DPPP, N-unprotected aromatic ketimines reacted with internal alkynes in toluene at 120 °C generating carbinamines in high yields with very good regioselectivity for alkyne addition (Scheme 2.8). As for the diaryl ketimines, intramolecular competition reactions revealed the C-H bond cleavage highly preferred the electron deficient aromatic ring (Scheme 2.9). Valerophenone imine (**2.09f**) was not a reactive substrate, which might be due to the ketimine-enamine isomerization. An electron withdrawing substituent, CF_3 group, was required to activate aryl-alkyl ketimine (Scheme 2.10). Compared with previously reported rhenium and rhodium catalytic systems, this catalytic system incorporated a steering phosphine ligand, which provided a potential synthetic route to chiral indenyl amines. Indeed, by using a chiral bisphosphine ligand, (R,R)-DIOP, moderate enantioselectivity was achieved.

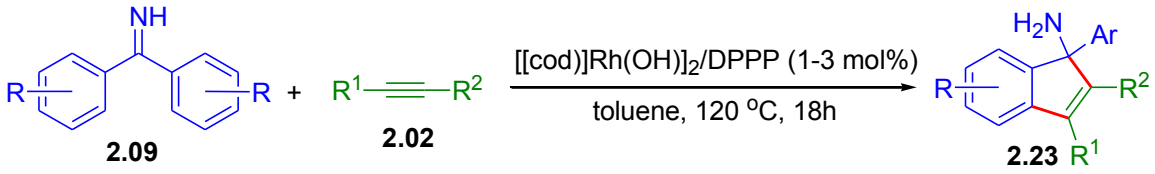

Scheme 2.8. Rhodium(I) catalyzed [3+2] carbocyclization with aromatic ketimines and internal alkynes

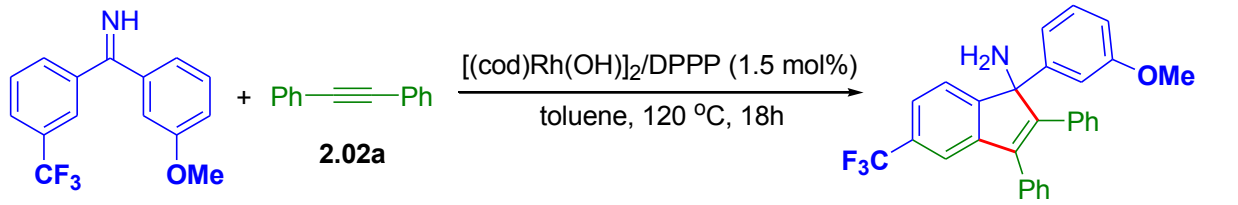

detected as the only product, 84%

Scheme 2.9. Intramolecular competition in rhodium(I) catalyzed [3+2] carbocyclization with diaryl ketimines and internal alkynes

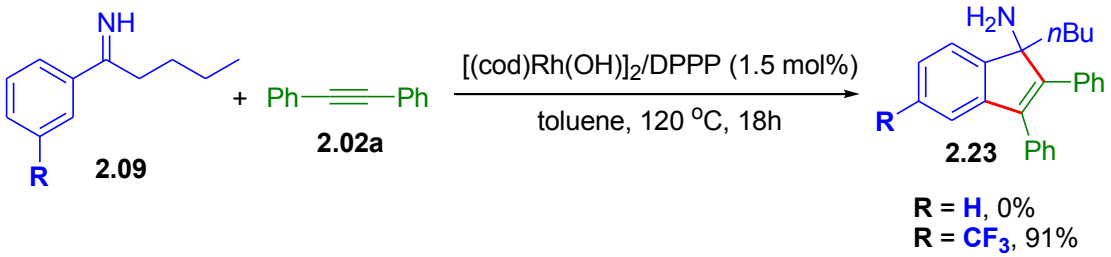

Scheme 2.10. Rhodium(I) catalyzed [3+2] carbocyclization with aryl-alkyl ketimines and diphenylacetylene

During the development of this thesis, Cramer and coworkers developed a chiral version of this reaction with diaryl ketimines and internal alkynes.[15] Good enantioselectivity was achieved for internal alkynes with coordinating substituent at α position, such as 1,4-dimethoxyl-2-butyne. Cramer and Takai independently applied their catalytic systems to terminal allenes as the C-H bond acceptor.[16,17] However, most of these reactions were performed at 120 °C. By carrying out stoichiometric reactions between Rh(I) catalyst precursors and benzophenone imine, we have found that cyclometalation was very slow even at elevated temperature, which indicated that C-H bond activation was likely involved in the turnover-limiting step. Thus, it is highly desirable to introduce new transition metal complexes, which could efficiently mediate C-H bond cleavage under milder conditions, allowing broader functional-group compatibility and wider synthetic applications.

Ruthenium complexes have been demonstrated to be powerful catalyst for directed C-H bond alkylation in the last two decades. In Murai's breakthrough discovery, alkylation of aromatic ketones was conducted in refluxing toluene with $Ru(H)_2(CO)_2(PPh_3)_3$ as catalyst precursor (Scheme 1.4).[18] Later, Chaudret and Leitner found that $Ru(H)_2(H_2)_2(PCy_3)_2$ could cleave the *ortho*-C-H bond of aromatic ketones at room temperature to give a ruthenacycle intermediate (**1.11**), which was catalytically active for aryl C-H bond ethylation with ethylene under ambient temperature (Scheme 1.5).[19-21] Recently, Murai and coworkers discovered cyclometalated Ru(II) hydride complexes for C-H bond alkylation of aromatic ketones at room temperature (Scheme 2.11).[22] A group of ruthenacycles, generated from the reaction of $Ru(H)_2(CO)_2(PPh_3)_3$ and trimethylvinylsilane, exhibited high catalytic efficiency to catalyze Murai reaction under room temperature. In reaction mechanism study, ruthenacycle (**2.24**) was detected by NMR during

the reaction and assigned as the key intermediate. In a related study, Davies and coworkers reported a room temperature alkyne insertion of a cyclometalated ruthenium complex (**2.25**), leading to the formation of an alkenylruthenium(II) complex (**2.26**).[23] In addition, several studies revealed Ru(II)-mediated stoichiometric cyclometalation of aromatic imine derivatives and subsequent alkyne insertions under mild conditions.[24,25] These work inspired us to develop a ruthenium catalytic system for formal carbocyclization of imines and alkynes under mild reaction conditions.

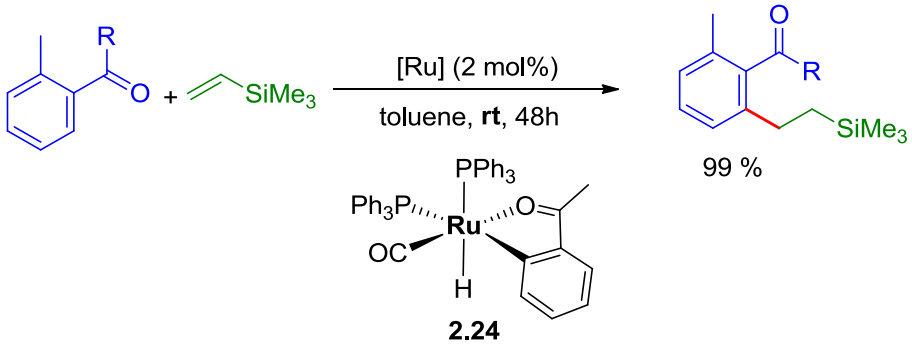

Scheme 2.11. Ruthenium-hydride complex catalyzed Murai reaction at room temperature

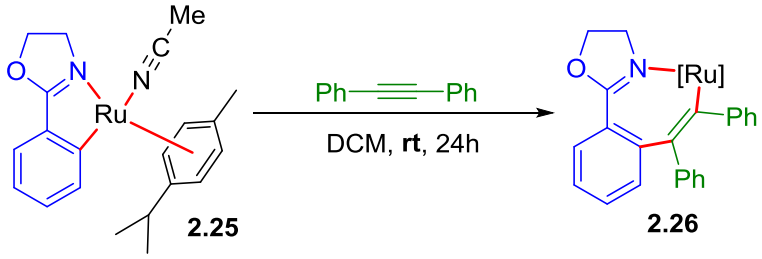

Scheme 2.12. Ruthenacycle mediated alkyne insertion at room temperature

2.2. Initial Results

To exploit such mild ruthenium catalysis for [3+2] carbocyclizations, we envisioned an important distinction between different pathways for ruthenium-mediated C-H activations (Scheme 2.13). In the well-established Murai reaction mechanism (Path A), both Ru(0) and Ru(II)-hydride catalyst precursors are expected to activate aromatic C-H bonds and form a cyclometalated Ru(II)-hydride intermediate **2.20a** via C-H oxidative addition or hydride metathesis. Alkyne insertion into the Ru-H linkage is generally much more favored over insertion into Ru-C linkage, resulting in the formation of a Ru(II) phenyl alkenyl intermediate **2.21a** and subsequent C-C reductive elimination to form an acyclic alkenylation product. To promote the desired [3+2] carbocyclization product instead, we aimed to eliminate potential involvement of ruthenium-hydride species by using alkylruthenium(II) catalyst precursors that would promote deprotonation pathway for C-H activation (Path B). Alkyne insertion into Ru-C linkage of non-hydride intermediate **2.20b** would occur to form **2.21b**, which leads to the desired cyclization sequence as described in Scheme 2.13.

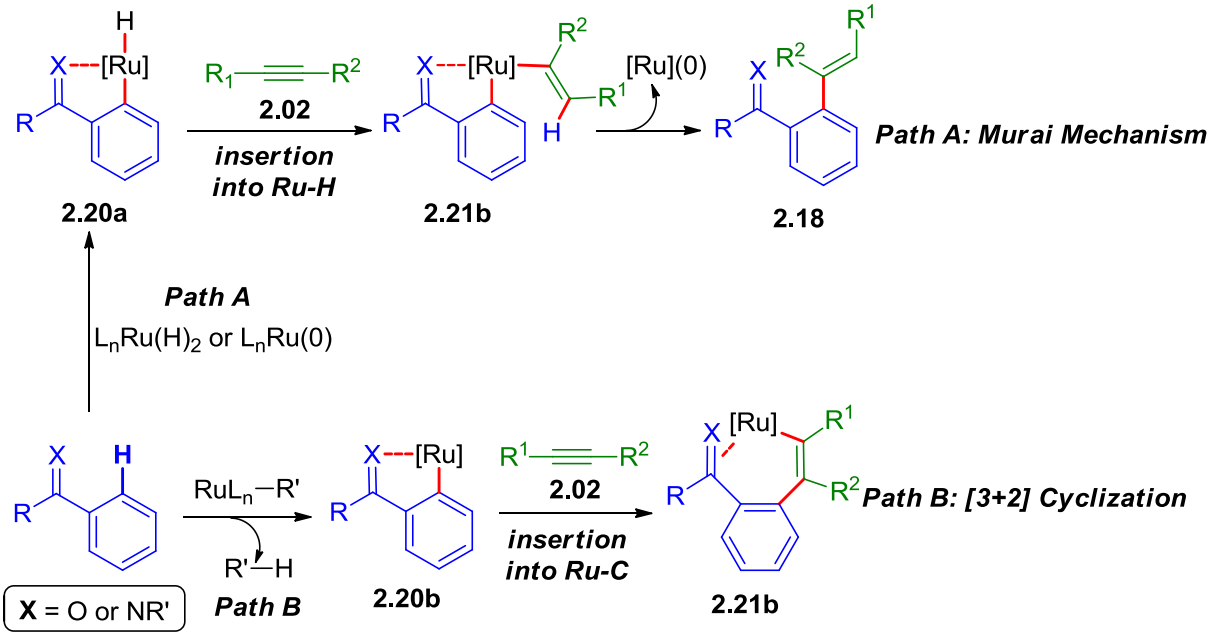

Scheme 2.13. Possible pathways for ruthenium-catalyzed tandem C-H activation/alkyne coupling

To explore the key process of C-H activation with N-H ketimines, we first studied stoichiometric reactions between benzophenone imine and selected Rh(I) and Ru(II) catalyst precursors (Scheme 2.14). $[(cod)Rh(OH)]_2$ and 1,3-bis(diphenylphosphino) propane (dppp) ligand did not react with benzophenone imine at 80 ^{o}C, which is comparable to the high reaction temperatures required for similar Rh(I) catalyzed reactions.[5,15,16] In contrast, the Ru(II)/π-allyl complex $[(cod)Ru(\eta^3\text{-methallyl})_2]$ reacted with benzophenone imine at room temperature quantitatively to form the doubly cyclometalated Ru(II) bis(imine) complex, $\{Ru(cod)[\eta^2\text{-}HNC(C_6H_5)C_6H_4]_2\}$ (**2.27**) (Figure 2.1). The solid-state structure of complex **2.27** was determined by single crystal X-ray diffraction, which shows a near-octahedral Ru(II) center with the two N atoms of the imine ligands *trans* to each other, and two Ru-C bonds *cis* to each other (Figure 2.1).

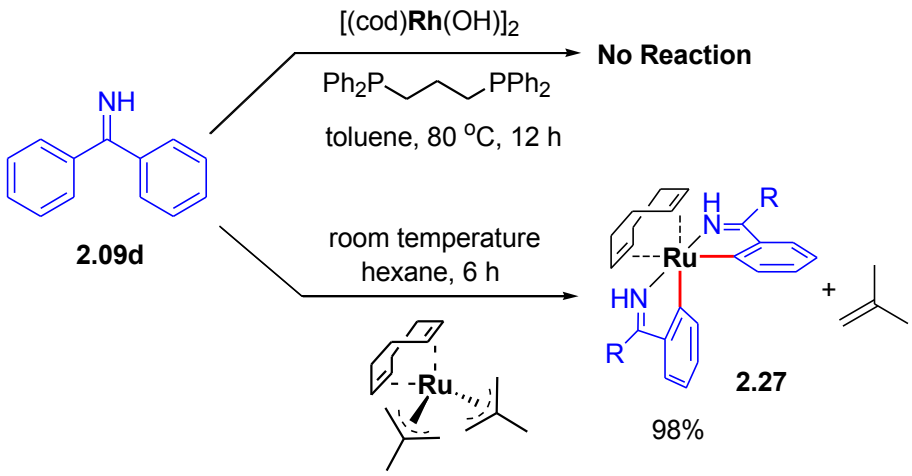

Scheme 2.14. Attempted cyclometalation with benzophenone imine and rhodium(I) and ruthenium(II) complexes

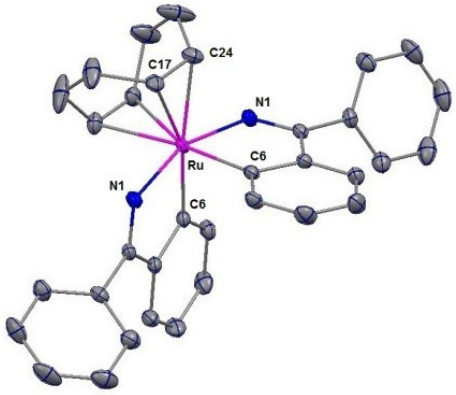

Figure 2.1 ORTEP diagram of {Ru(cod)[η^2-HNC(C_6H_5)C_6H_4]$_2$} (**2.27**) at 50% thermal ellipsoid

2.3. Optimization of Reaction Conditions

The Ru(II)-mediated room-temperature imine C-H bond activation encouraged us to evaluate Ru(II) catalyst precursors for ligand-assisted [3+2] ketimine/alkyne carbocyclization at room temperature. In toluene, ruthenacycle **2.27** failed to catalyze coupling between benzophenone imine and diphenylacetylene at room temperature (Table 2.1, entry 1). In contrast, we found in the presence of catalytic amount of N-heterocyclic carbene (NHC) ligand, 1,3-bis(2,6-diisopropylphenyl)imidazole-2-ylidene (IPr) and **2.27**, [3+2] carbocyclization occurred at room temperature with moderate yield after 24 hours (entry 2). When **2.27** was replaced with the Ru(II) π–allyl complex, [(cod)Ru(η^3-methallyl)$_2$], as catalyst precursor, similar yield was obtained (entry 3), suggesting that ruthenacycle **2.27** is a catalytically active intermediate and can be readily generated *in situ* from commercially available [(cod)Ru(η^3-methallyl)$_2$] and benzophenone imine (entry 3). Thus, [(cod)Ru(η^3-methallyl)$_2$] was explored as the general catalyst precursor with various phosphine and NHC ligands (entries 4-10). None of the tested mono- or bis-phosphine ligands could promote the [3+2] annulation effectively (entries 7-10), whereas 1,3-bis(2,4,6-trimethylphenyl)imidazole-2-ylidene (IMes) showed comparable activity to IPr, yielding 57% of the product (**2.23a**) (entry 4). Saturated NHC ligands, such as 1,3-bis(2,6-diisopropylphenyl)-4,5-dihydroimidazole-2-ylidene (SIMes) and 1,3-bis(2,6-diisopropylphenyl)-4,5-dihydroimidazole-2-ylidene (SIPr), led to significantly reduced yields (entries 5-6). Several other Ru(II) complexes were tested as

catalyst precursors with IPr ligand, but none of them exhibited catalytic reactivity to promote the formation of the indenyl amine (**2.23a**) (entries 11-15).

Table 2.1. Effects of ligand and catalyst precursor in ruthenium catalyzed [3+2] carbocyclization with benzophenone imine and diphenylacetylene at room temperature[a]

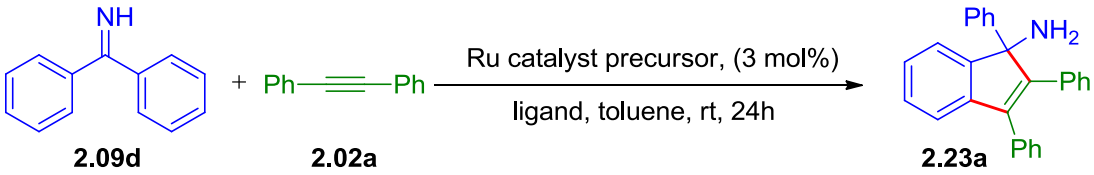

2.09d **2.02a** **2.23a**

entry	catalyst precursor	ligand (mol%)	yield (%) [b]
1	[Ru(cod)[η^2-HNC(C_6H_5)C_6H_4]$_2$] (**2.27**)	none	< 2
2	[Ru(cod)[η^2-HNC(C_6H_5)C_6H_4]$_2$] (**2.27**)	IPr (6)	45
3	Ru(methylallyl)$_2$(cod)	IPr (6)	44
4	Ru(methylallyl)$_2$(cod)	IMes (3.3)	57
5	Ru(methylallyl)$_2$(cod)	SIPr (3.3)	< 2
6	Ru(methylallyl)$_2$(cod)	SIMes (3.3)	5
7	Ru(methylallyl)$_2$(cod)	PPh_3 (6)	< 2
8	Ru(methylallyl)$_2$(cod)	PCy_3 (6)	< 2
9	Ru(methylallyl)$_2$(cod)	DPPP (3)	<2
10	Ru(methylallyl)$_2$(cod)	DPPBenzene (3)	0
11	Ru(cod)Cl_2[c]	IPr (3.3)	13
12	Ru(CO)$(H)_2(PPh_3)_3$	IPr (3.3)	< 2
13	CpRu$(PPh_3)_2$Cl	IPr (3.3)	0
14	Cp^*RuCl_2	IPr (3.3)	< 2
15	Grubb's catalyst (1st generation)	none	0

[a] Reaction conditions: diphenylacetylene (0.1 mmol, 1.0 equiv), benzophenone imine (1.1 equiv), toluene (0.5 mL), rt, 24h. [b] Yields were based on GC analysis. [c] In the presence of 10 mol% of LiHMDS.

In terms of solvent effect, significantly higher reactivity was observed in non-polar solvents than in polar solvents (Table 2.2). Room-temperature coupling between benzophenone imine (1.1 equiv.) and diphenylacetylene (1.0 equiv.) was effectively carried out in hexane solvent with 3.0 mol% [(cod)Ru(η^3-

methallyl)$_2$] and 3.3 mol% IPr, giving the desired product as the single product in 95% yield (entry 3). In comparison, the combination of hexane as solvent and IMes as ligand only slightly improved the yield from 57% to 68% (entry 4). Only a trace amount of product was detected from reactions without ligand IPr (entry 5). Among ethereal solvents, diethyl ether gave the best yield 64% (entries 8-11). The protic solvent, methanol, totally shut off the reaction. Other polar solvents, like DMF, DCE, led to only trace amount of the desired product.

Table 2.2. Effects of solvent and ligand in ruthenium catalyzed [3+2] carbocyclization with benzophenone imine and diphenylacetylene at room temperature[a]

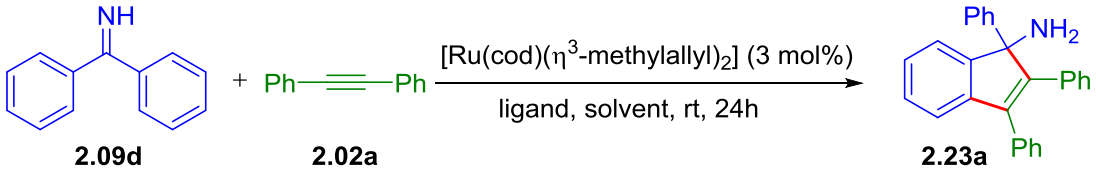

2.09d **2.02a** **2.23a**

entry	solvent	ligand (3.3 mol%)	yield (%) [b]
1	toluene	IPr	44
2	toluene	Mes	57
3	hexane	IPr	95
4	hexane	Mes	68
5	hexane	Mes	0
6	hexane	SiPr	<2
7	hexane	SMes	9
8	THF	IPr	9
9	DME	IPr	16
10	Et_2O	IPr	64
11	Dioxane	IPr	8
12	DMF	IPr	<2
13	DCE	IPr	<2
14	methonal	IPr	0

[a] Reaction conditions: diphenylacetylene (0.1 mmol, 1.0 equiv), benzophenone imine (1.1 equiv), solvent (0.5 mL), rt, 24h. [b] Yields were based on GC analysis.

The ruthenium catalyst precursor, [(cod)Ru(η^3-methallyl)$_2$], was proved pivotal to the reaction (Table 2.3). Decrease in [(cod)Ru(η^3-methallyl)$_2$] loading to 1 mol% dramatically reduced the yield of product (entry 2). In the absence of Ru catalyst precursor there was no reaction (entry 3). The catalytic system was very sensitive to air, when the reaction was conducted under an atmosphere of air, the starting materials were left unreacted (entry 4). Inorganic salts have been utilized to assist C-H bond deprotonation in transition metal-catalyzed C-H bond functionalization. Thus, various bases were tested in this ruthenium catalytic system in the presence and absence of NHC ligand. The results showed that these salts hindered the reaction (entries 5-17).

Table 2.3. Effects of catalyst loading and basic additive in ruthenium catalyzed [3+2] carbocyclization with benzophenone imine and diphenylacetylene at room temperature[a]

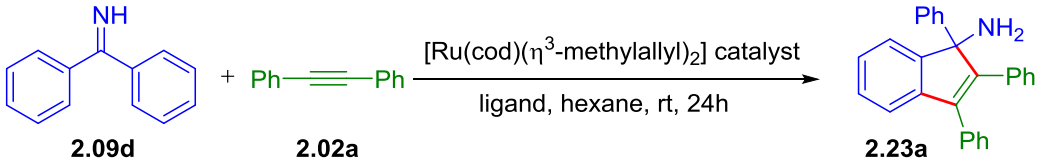

2.09d **2.02a** **2.23a**

entry	[Ru(cod)(methyallyl)$_2$] (mol%)	ligand (mol%)	base	yield (%) [b]
1	3	IPr (3.3)	none	95
2	1	IPr (1.1)	none	23
3	0	IPr (3.3)	none	0
4	3	IPr (3.3)	none	0 [c]
5	3	none	Cs_2CO_3	6
6	3	none	K_3PO_4	12
7	3	none	NaO*t*Bu	12
8	3	none	KO^{t}Bu	<2
9	3	none	LiOAc	<2
10	3	none	NH_4OAc	<2
11	3	IPr (3.3)	Cs_2CO_3	65
12	3	IPr (3.3)	K_3PO_4	52
13	3	IPr (3.3)	NaO*t*Bu	22
14	3	IPr (3.3)	KO*t*Bu	14
15	3	IPr (3.3)	LiHMDS	<2
16	3	IPr (3.3)	LiOAc	<2
17	3	IPr (3.3)	NH_4OAc	<2

[a] Reaction conditions: diphenylacetylene (0.1 mmol, 1.0 equiv.), benzophenone imine (1.1 equiv.), hexane (0.5 mL), rt, 24h. [b] Yields were base on GC analysis. [c] Under an atmosphere of air.

2.4. Substrate Scope

With the standard reaction conditions established, various internal alkynes and diaryl N-H ketimines were studied for Ru(II)-catalyzed room temperature [3+2] annulation. High yields and regioselectivity were achieved for reactions between benzophenone imine and nonsymmetrical phenylacetylene derivatives having an alkyl, alkenyl, or 2-thiophenyl substituent (Figure 2.2). For aryl-alkyl acetylenes, the alkyl groups were connected to the carbon attached to position of C-H bond cleavage and aryl group connected to the iminyl carbon (**2.23b**-**d**). Notably, a cyclopropyl group, which is known to undergo ring opening in the presence of transition metal catalysts, was compatible with the catalyst system (**2.23d**). For conjugated enyne substrate, the C-C triple bond participated in carbocyclization while leaving the C-C double bond untouched (**2.23e**). Phenyl-2-thiophyl-acetylene showed very good reactivity and regioselectivity (**2.23f**). The alkyne regioselectivity of these two substrate indicated the functional groups (alkene and thiophenyl) might be able stabilize the intermediate **2.21b** via coordination to the ruthenium center. Reactions between benzophenone imine and aliphatic internal alkynes required the use of IMes as ligand and toluene as solvent (**2.23g**, **2.23h**). Heating at 60 ^{o}C was necessary to form the diethyl-substituted product **2.23g** in high yield.

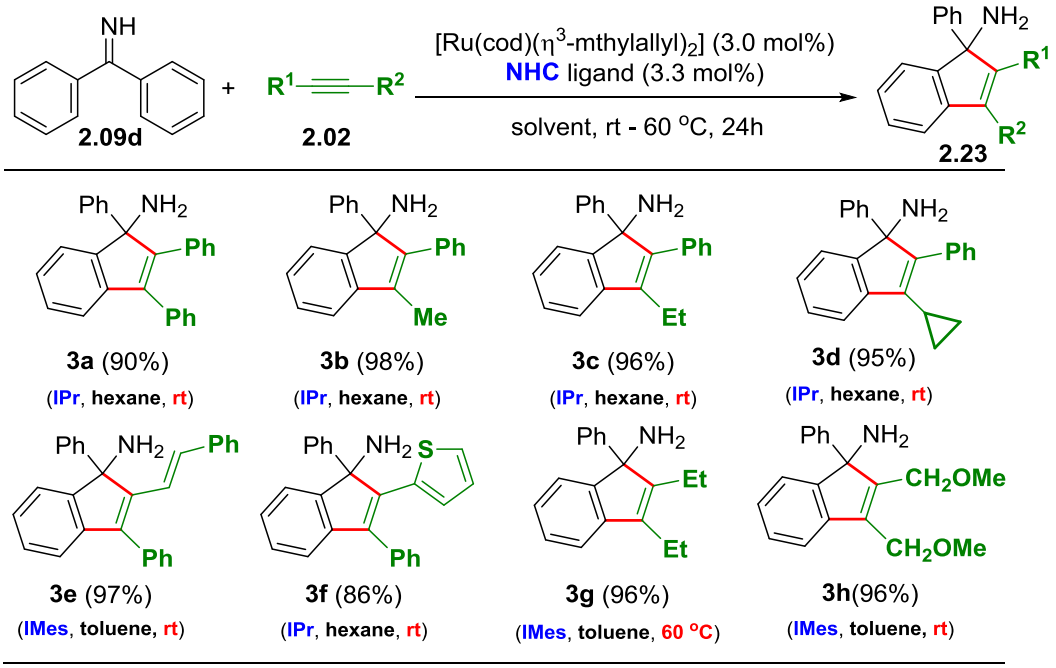

[a] Reaction conditons: benzophenone imine (0.11 mmol, 1.1 equiv.), alkyne (0.1 mol, 1.0 equiv.), [Ru(cod)(η^3-mthylallyl)$_2$] 3.0 mol%, NHC 3.3mol%, hexane 0.5 mL, room temperature, 24h. [b] Yields were average yields based on at least two runs.

Figure 2.2. Alkyne substrate scope in ruthenium(II)/NHC catalyzed [3+2] carbocyclization with aromatic ketimines and internal alkynes[a,b]

Among ketimine substrates, diaryl ketimines with electron-withdrawing F, Cl, and CF_3 groups at *para*- and *meta*-positions readily reacted with diphenylacetylene to give [3+2] adducts in high yields (Figure 2.3, **2.23i**-**n**). In comparison, lower reactivity was observed for imines with a *para*- or *meta*-methoxy group, the reactions of which were carried out at 60 °C to achieve high yields (**2.23o**, **2.23p**). A temperature of 60 °C was also necessary for 3,3'-bis-CF_3-substituted benzophenone imine (**2.23k**). Ketimine substrates with *ortho*-CH_3 or -OCH_3 groups showed no reactivity under current catalytic conditions, presumably owing to steric inhibition of the cyclometalation process. Nonsymmetrical diaryl ketimines coupled to diphenylacetylene with moderate regioselectivity (ca. 2:1 to 4:1); C-H activation at the more electron-deficient aryl was favored. This electronic influence on regioselective C-H bond activation was most pronounced with product **2.23p**, which was formed by exclusive reaction at the *meta*-CF_3 substituted phenyl ring over the *meta*-methoxy substituted one.[5]

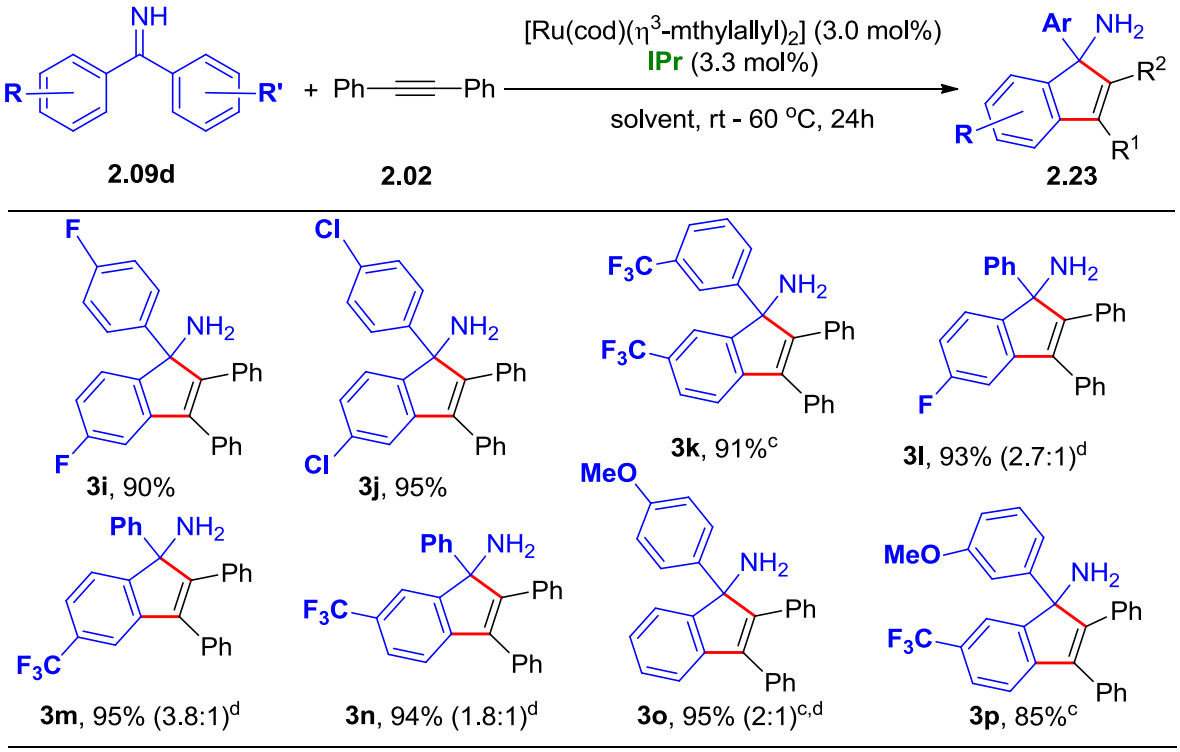

[a] Reaction conditons: benzophenone imine (0.11 mmol, 1.1 equiv.), alkyne (0.1 mol, 1.0 equiv.), [Ru(cod)(η^3-mthylallyl)$_2$] 3.0 mol%, IPr 3.3mol%, hexane 0.5 mL, 24h. [b] Yields were average yields based on at least two runs. [c] At 60 °C. [d] Combided yield of two isomers; the ratio was determined by NMR analysis; structure of the major isomer is shown.

Figure 2.3. Aromatic ketimine substrate scope in ruthenium(II)/NHC catalyzed [3+2] carbocyclization with aromatic ketimines and internal alkynes[a,b]

With high catalytic efficiency and tunable ancillary ligands, the Ru(II)-NHC catalyst system is expected to facilitate mild [3+2] annulations for more challenging substrates. Valerophenone imine, which is an inactive substrate in rhodium catalytic system (Scheme 2.10),[5] reacted with [Ru(cod)(methylallyl)$_2$] under room temperature forming the doubly cyclometalated Ru(II) bis(imine) complex [Ru(cod)[η^2-HNC(*n*-C_4H_9)C_6H_4)$_2$] (**2.28**) in 85% yield (Scheme 2.15). The solid-state structure of complex **2.28** was determined by single crystal X-ray diffraction, which showed a similar structure as its analogue complex **2.27** (Figure 2.2). This result indicated a feasible C-H bond activation of aryl-alkyl ketimines in stoichiometric cyclometalation with [Ru(cod)(methylallyl)$_2$]. Under catalytic conditions, effective coupling of diphenylacetylene with valerophenone imine was promoted by 3 mol% of [Ru(cod)(methylallyl)$_s$] and IMes at 60 °C (Scheme 2.16). The requirement for elevated reaction temperature also suggested that the C-H

bond activation was likely not involved in the rate-determining step, which may occur during subsequent alkyne insertion or cyclization steps. This reaction represented a very rare example of mild C-H functionalization with unactivated and unprotected aryl-alkyl N-H ketimines.[5]

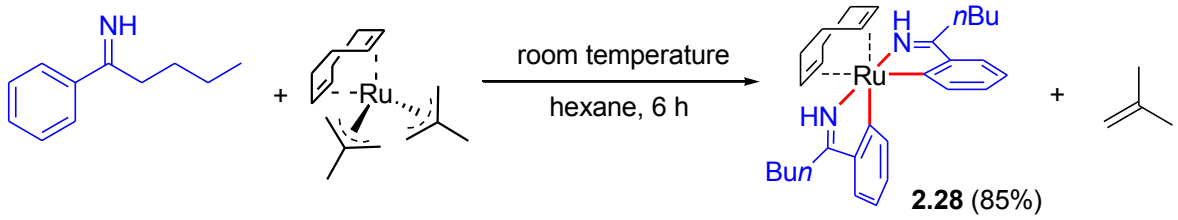

Scheme 2.15. Stoichiometric cyclometalation with valerophenone imine and [Ru(cod)(η^3-methylallyl)$_2$]

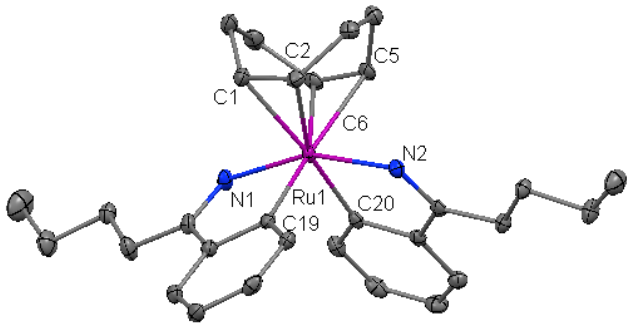

Figure 2.4. ORTEP diagram of {Ru(cod)[η^2-HNC(*n*Bu)C$_6$H$_4$]$_2$} (**2.28**) at 50% thermal ellipsoid

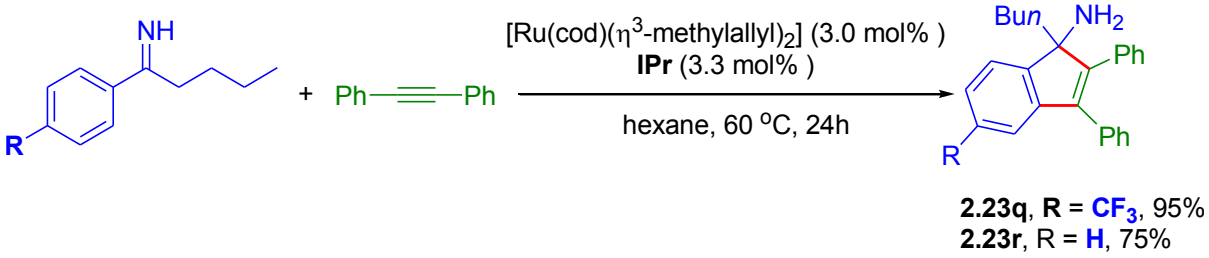

Scheme 2.16. Ruthenium(II)/NHC catalyzed [3+2] carbocyclization with valerophenone imines and diphenylacetylene

2.5. Proposed Reaction Mechanism

Current results on the substrate scope and substituent effects provide significant insights into the reaction mechanism. Firstly, high regioselectivity with non-symmetric alkyne substrates supported the proposed alkyne insertion into a Ru-aryl rather than Ru-H linkage (Scheme 2.13, Path B). As observed with unsymmetrically substituted aryl-alkyl alkynes, alkyne insertion into Ru-aryl linkage placed the Ru center preferentially at the more stabilized benzylic position in the alkenylruthenium(II) intermediate (**2.21b**) (Scheme 2.13, R^2=alkyl, R^1=aryl). Secondly, the relatively low reactivity with 3-hexyne compared to aromatic alkynes was consistent with a rate-limiting alkyne insertion step. Thus, the remarkable reactivity enhancement by NHC ligands was likely due to their electron richness and ability to promote insertions of organic π systems into metal-carbon linkages. Thirdly, the stoichiometric reaction of valerophenone imine with [Ru(cod)(methylallyl)$_2$] under room temperature and catalytic reaction with diphenylacetylene under 60 ^{o}C also indicated that C-H bond activation was not the turnover-limiting step. Lastly, regioselective functionalization at the more electron-deficient arenes suggested a C-H activation pathway via σ-bond metathesis or nucleophilic deprotonation rather than electrophilic aromatic substitution.[26-28] Therefore, the catalytic cycle proposed for rhodium catalytic system is also applicable to this ruthenium catalyzed [3+2] carbocyclization (Scheme 2.7).

2.6. Conclusion

In summary, we have developed a Ru(II)-catalyzed [3+2] annulation between N-H ketimines and internal alkynes to form indenamines under mild reaction conditions. Room-temperature C-H activation and subsequent carbocyclization was achieved by using a Ru(II)/η^3-methylallyl catalyst precursor, NHC ligands, and without strong oxidant or acid/base additives. Future efforts will be focused on gaining a better understanding of the reaction mechanism and exploration of NHC ligands for selective functionalization of C-H bonds for broader synthetic applications.

2.7. Experimental Procedures

2.7.1. General Information

Unless otherwise noted, all manipulations were carried out under a nitrogen atmosphere using standard Schlenk-line or glovebox techniques. All glassware was oven-dried for at least 1 h prior to use. THF, toluene, ether, and hexane were degassed by purging with nitrogen for 45 min and dried with a solvent purification system (MBraun MB-SPS). DMF, dioxane, dimethoxyethane, dichloroethane, methanol, and ethanol were dried over activated 3 Å molecular sieves and degassed by purging with nitrogen. Other reagents and substrates were commercially available used as received, including unprotected forms of NHC ligands IPr, IMes, SIPr, and SIMes. TLC plates were visualized by exposure to ultraviolet light. Organic solutions were concentrated by rotary evaporation at ~10 torr. Flash column chromatography was performed with 32–63 microns silica gel. GC analyses were performed on a Shimadzu GC-2010 with n-dodecane as the internal standard. ^{1}H NMR spectra were obtained on a 400 MHz spectrometer, and chemical shifts were recorded relative to residual protiated solvent. ^{13}C NMR spectra were obtained at 100 MHz, and chemical shifts were recorded to the solvent resonance. Both ^{1}H and ^{13}C NMR chemical shifts were reported in parts per million downfield from tetramethylsilane (δ = 0 ppm). ^{19}F NMR spectra were obtained at 282.4 MHz, and all chemical shifts were reported in parts per million upfield of CF_3COOH (δ = -78.5 ppm). High-resolution mass spectra were obtained from a Bruker Daltronics BioTOF HRMS spectrometer.

2.7.2. General Procedure for the Preparation of N-H Diaryl Ketimines[5]

Into a 20 mL vial equipped with a magnetic stir bar was added the aryl Grignard reagent (6.0 mmol) and 2 mL THF inside a N_2-filled glovebox. The corresponding arylnitrile (5.4 mmol) in 2 mL THF was added dropwise to allow good mixing and controlled heat release. The mixture was stirred at room temperature for 30 minutes before being capped with a screw-cap, sealed with electric tape, and transferred out of glovebox and put into an 85 °C oil bath. After stirring for 12h, the reaction mixture was cooled to room temperature and quenched by slow addition of anhydrous MeOH while stirring at 0 ^{o}C. The resulting mixture was stirred at room temperature for 30 minutes, and the volatile materials were

evaporated under vacuum. The residue was further purified by flash-column chromatography, with 1.5 mL of triethylamine (TEA) added into every 100 mL of eluent (ethyl acetate/Hexane). The imine products were generally acquired with over 95% purity and less than 5% ketone impurities based on GC analysis.

2.7.3. Preparation of Alkyne Substrates[28,29]

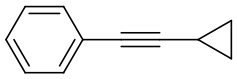

2,02d

(Cyclopropylethynyl)benzene: Into a flame-dried 100 mL flask equipped with a magnetic stir bar was added iodobenzene (5.25 mmol), bis(triphenylphosphine)-palladium(II) chloride [$Pd(PPh_3)_2Cl_2$] (2 mol%), copper(I) iodide (CuI) (4 mol%) and triethylamine (30 mL). The corresponding ethynylcyclopropane (5 mmol) was dissolved into 3mL TEA and added dropwise. The reaction was performed at room temperature under nitrogen overnight. The reaction mixture was then poured into water, and the aqueous layer was extracted three times with dichloromethane. After drying the combined organic layers over magnesium sulfate, the solution was filtered and the solvent was removed in vacuum. The solid residue was further purified by column chromatography using hexane solvent to afford the product as a yellow oil (0.54 g, 76%).

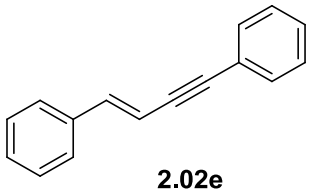

2.02e

(*E*)-But-1-en-3-yne-1,4-diyldibenzene: into a flame-dried 100 mL flask equipped with a magnetic stir bar was added β-bromostyrene (5.25 mmol), bis(triphenylphosphine)-palladium(II) chloride [$Pd(PPh_3)_2Cl_2$] (2 mol%), copper(I) iodide (CuI) (2 mol%), tetrabutylammonium fluoride hydrate (2.0 equiv.) and THF (15 mL). The corresponding alkyne phenylacetylene (5 mmol) was dissolved in 3mL THF and added dropwise. The reaction was performed at room temperature under nitrogen overnight.

The workup procedure was the same as for the synthesis of (cyclopropylethynyl)benzene. The product was acquired as a white solid (0.76 g, 73%).

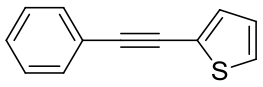

2.02f

2-(Phenylethynyl)thiophene: a mixture of the 2-iodothiophene (5mmol), phenylacetylene (6 mmol), $[Pd(PPh_3)_2Cl_2]$ (2 mol %), PPh3 (1%) and TEA (5 mL) in 20 mL of THF was stirred for 20 min at room temperature, and CuI (1 mol %) was then added. The mixture was stirred under room temperature for 1.5 hour. The workup procedure is same as synthesis of (cyclopropylethynyl)benzene. The product is a white solid (0.88 g, 95%).

2.7.4. Preparation and X-Ray Diffraction Analysis of Ruthenium(II) Catalyst Precursors

Ru(cod)[η^2-HNC(C_6H_5)C_6H_4]$_2$ (**2.27**) and Ru(cod)[η^2-HNC(*n*Bu)C_6H_4]$_2$ (**2.28**): Into a 20 mL scintillation vial equipped with a magnetic stir bar was added Ru(cod)(methylallyl)$_2$ (320 mg, 1.0 mmol), imine (2.0 mmol) and 10 mL toluene. The mixture was stirred overnight at room temperature. Then, the solvent was removed under reduced pressure. The residue was washed with hexane (3X), dried under vacuum, and afforded an orange powder (**2.27**, 513 mg, 90 %; **2.28**, 451 mg, 85%).

Single crystal X-ray diffraction data of Ru(cod)[η^2-HNC(C_6H_5)C_6H_4]$_2$ (**2.27**) and Ru(cod)[η^2-HNC(*n*Bu)C_6H_4]$_2$ (**2.28**) were collected on a Bruker Apex Duo diffractometer with a Apex 2 CCD area detector at T = 100K. Cu radiation was used for both of these 2 samples. Structures were process with Apex 2 v2013.4-1 software package with the most recent SAINT and SHELX software. Multi-scan absorption correction (SADABS 2012/1) was applied to **2.27** and **2.28**. Direct method was used to solve these two structures. Details of data collection and refinement are given in Table 2.4-2.7.

Table 2.4. Summary of cell parameters, data collection and structural refinements for {Ru(cod)[η^2-HNC(C_6H_5)C_6H_4]$_2$} (**2.27**).

Empirical formula	$C_{34}H_{30}N_2Ru \cdot C_6H_6$
Formula weight	647.79
Temperature, K	100
Wavelength, (Å)	0.71073
space group	C2/c
a/Å	11.6901(2)
b/Å	16.1927(3)
c/Å	16.7863(3)
α, deg	90
β,deg	96.6000(10)
γ, deg	90
V, Å	3156.49(10)
Z	4
d_{calcd}, g/cm^3	1.363
μ, mm^{-1}	.528
F(000)	1344
Theta range, deg	2.80 ÷ 27.49
h, k, l ranges	-15 ÷ 15, -21 ÷ 20, -21 ÷ 21
Reflections collected/unique	13384
Unique Reflections/gt	3606/3429
COOF on F^2	1.179
R_1, wR_2 $(I>2\sigma(I))^a$	2.5%, 7.02%
R_1, wR_2 *(all data)*	2.76%, 8.06%
Largest diff. peak and hole (e. Å $^{-3)}$	0.101

[a] $R1 = \Sigma||F_o| - |F_c|| / \Sigma|F_o|$, $wR2 = [\Sigma w[(F_o)^2 - (F_c)^2]^2 / \Sigma w(F_o^2)^2]^{1/2}$ for $F_o^2 > 2\sigma(F_o^2)$, $w = [\sigma^2(F_o)^2 + (AP)^2 + BP]^{-1}$ where $P = [[(F_o)^2 + 2(F_c)^2] / 3$ and A (B) = 0.0455 (3.9724);

Table 2.5. Selected bond lengths [Å] and bond angles [degree] for {Ru(cod)[η^2-HNC(C_6H_5)C_6H_4]$_2$} (**2.27**).

bond length [Å]		bond angles [degree]	
Ru(1)-N(1)	2.072(2)	N(1)#1-Ru(1)-C(6)#1	77.31(7)
Ru(1)-C(17)	2.256(2)	N(1)#2-Ru(1)-C(6)#2	87.35(7)
Ru(1)-C(6)	2.053(2)	N(1)#1-Ru(1)-C(17)	81.47(6)
Ru(1)-C(24)	2.262(2)	N(1)#1-Ru(1)-C(24)	117.72(7)
N(1)-C(3)	1.295(2)	N(1)-Ru(1)-N(1)	158.28(6)
C(3)-C(11)	1.452(2)	C(6)-Ru(1)-C(6)	90.27(7)
C(6)-C(11)	1.421(3)	C(6)-Ru(1)-C(17)	158.15(7
C(1)-C(5)	1.391(3)	C(17)-Ru(1)-C(24)	79.26(7)
C(3)-C(5)	1.484(3)	N(1)-C(3)-C(5)	122.0(2)
C(17)-C(24)	1.375(3)	N(1)-C(3)-C(11)	114.7(2)
		Ru(1)-N(1)-C(3)	118.9(1)
		Ru(1)-C(6)-C(11)	114.8(1)
		C(5)-C(3)-C(11)	123.4(2)
		C(17)-Ru(1)-C(24)	123.4(2)
		N(1)-C(3)-C(5)-C(1)	65.3(3)
		N(1)-Ru(1)-N(1)-C(3)	42.1(2)

Table 2.6. Summary of cell parameters, data collection and structural refinements for {Ru(cod)[η^2-HNC(*n*Bu)C_6H_4]$_2$} (**2.28**).

Empirical formula	$C_{30}H_{40}N_2Ru$
Formula weight	529.71
Temperature, K	100
Wavelength, (Å)	0.71073
space group	*P-1*
a/Å	9.2597(13)
b/Å	10.5632(15)
c/Å	14.336(2)
α, deg	103.701(2)
β,deg	94.033(2)
γ, deg	109.012(2)
V, Å	1271.3(3)
Z	2
d_{calcd}, g/cm^3	1.384
μ, mm^{-1}	0.637
F(000)	556.0
Theta range, deg	2.23 ÷ 27.17
h, k, l ranges	-11÷ 11, -13 ÷ 13, -18 ÷ 18
Reflections collected/unique	28500
Unique Reflections/gt	5629/5009
COOF on F^2	1.028
R_1, wR_2 $(I>2\sigma(I))^a$	2.52%, 5.64%
R_1, wR_2 *(all data)*	3.18%, 5.93%
Largest diff. peak and hole (e. Å $^{-3)}$	0.068

[a] $R1 = \Sigma||F_o| - |F_c|| / \Sigma|F_o|$, $wR2 = [\Sigma w[(F_o)^2 - (F_c)^2]^2 / \Sigma w(F_o^2)^2]^{1/2}$ for $F_o^2 > 2\sigma(F_o^2)$, $w = [\sigma^2(F_o)^2 + (AP)^2 + BP]^{-1}$ where $P = [[(F_o)^2 + 2(F_c)^2] / 3$ and A (B) = 0.0241(0.9582);

Table 2.7. Selected bond lengths [Å] and bond angles [degree] for {Ru(cod)[η^2-HNC(*n*Bu)C_6H_4]$_2$} (**2.28**).

bond length [Å]		bond angles [degree]	
Ru(1)-N(1)	2.074(2)	N(1)-Ru(1)-N(2)	156.68(7)
Ru(1)-N(2)	2.094(2)	N(1)-Ru(1)-C(1)	80.37(7)
Ru(1)-C(1)	2.256(2)	N(1)-Ru(1)-C(2)	114.80(6)
Ru(1)-C(2)	2.244(2)	N(1)-Ru(1)-C(5)	117.19(7)
Ru(1)-C(5)	2.272(2)	N(1)-Ru(1)-C(6)	81.57(6)
Ru(1)-C(6)	2.250(2)	N(1)-Ru(1)-C(19)	76.53(7)
Ru(1)-C(19)	2.052(2)	N(1)-Ru(1)-C(20)	86.87(7)
Ru(1)-C(20)	2.060(2)	N(2)-Ru(1)-C(1)	118.33(7)
C(1)-C(2)	1.383(3)	N(2)-Ru(1)-C(2)	82.54(7)
C(5)-C(6)	1.383(3)	N(2)-Ru(1)-C(5)	80.06(7)
		N(2)-Ru(1)-C(6)	114.14(2)
		N(2)-Ru(1)-C(19)	88.76(7)
		N(2)-Ru(1)-C(20)	76.55(7)
		C(1)-Ru(1)-C(2)	35.80(7)
		C(5)-Ru(1)-C(6)	35.62(7)
		C(1)-Ru(1)-C(6)	79.02(7)
		C(1)-Ru(1)-C(5)	85.79(7)
		C(2)-Ru(1)-C(6)	93.76(7)
		C(2)-Ru(1)-C(5)	79.13(7)

2.7.5. General Procedure for Ruthenium(II)/NHC-Catalyzed [3+2] Annulation

Into a 4.0 mL scintillation vial equipped with a magnetic stir bar was placed the alkyne substrate **2.02** (0.1 mmol, 1.0 equiv.), the ketimine substrate **2.09** (1.1 equiv.) and a stock solution of Ru(II) catalyst precursor and carbene ligand in hexane solvent (0.5 mL). The stock solution contains [Ru(cod)(methylallyl)$_2$] (0.030 equiv.) and IPr ligand (0.033 equiv.). The vial was sealed with a silicone-lined screw-cap and stirred at room temperature in glovebox for 24 h. In case heating is needed for complete conversion, the vial was transferred out of the glovebox and stirred in a 60 °C or 80 °C oil bath

for 24 h. The reaction mixture was then cooled to room temperature, and all volatile materials were removed under reduced pressure. Further purification was achieved by flash column chromatography. Yields of the isolated products are based on the average of two runs under identical conditions.

2.7.6. Spectral Data for Isolated [3+2] Annulation Products

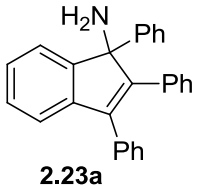

2.23a

1, 2, 3-Triphenyl-1H-inden-1-ylamine (**2.23a**): Chromatography (1:4 ethyl acetate/hexane, R_f = 0.35) gave **2.23a** as a white solid (32.4 mg, 90 %). ^{1}H NMR (400 MHz, $CDCl_3$): δ = 7.58–7.55 (m, 2H), 7.45–7.00 (m, 15H), 6.90–6.85 (m, 2 H), 1.86 ppm (s, -NH_2); ^{13}C NMR (100 MHz, $CDCl_3$): δ = 154.2, 151.2, 143.0, 139.6, 135.2, 134.6, 129.9, 129.8, 129.7, 128.8, 128.8, 128.2, 127.9, 127.8, 127.4, 127.1, 126.9, 125.8, 123.3, 121.2, 71.8 ppm; HRMS: m/z calcd for $C_{27}H_{19}^+$ (loss of -NH_2 group): 343.1481; found: 343.1476.

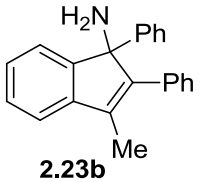

2.23b

3-Methyl-1,2-diphenyl-1H-inden-1-ylamine (**2.23b**): Chromatography (1:3 ethyl acetate/hexane, R_f = 0.40) gave **2.23b** as a white solid (29.2 mg, 98 %). ^{1}H NMR (400 MHz, $CDCl_3$): δ = 7.40–7.13 (m, 12 H), 6.98-6.96 (m, 2H), 2.20 (s, 3 H), 1.75 ppm (s, 2H; -NH_2); ^{13}C NMR (100 MHz, $CDCl_3$): δ = 153.1, 150.5, 144.3, 142.9, 135.2, 134.7, 129.4, 128.6, 128.3, 127.9, 127.4, 126.9, 126.7, 125.9, 122.7, 119.7, 71.9, 12.0; HRMS: m/z calcd for $C_{22}H_{17}^+$ (loss of -NH_2 group): 281.1325; found: 281.1322.

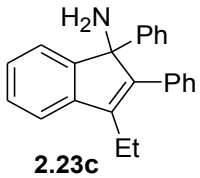

2.23c

3-Ethyl-1,2-diphenyl-1H-inden-1-ylamine (**2.23c**): Chromatography (1:3 ethyl acetate/hexane, R_f=0.40) gave **2.23c** as a white solid (29.9 mg, 96%). ^{1}H NMR (400 MHz, $CDCl_3$): δ = 7.36–7.12 (m, 12 H), 6.94–6.90 (m, 2H), 2.59 (m, 2 H), 1.76 (s, 2H; -NH_2), 1.26 ppm (td, *J* = 7.6, 1.7, 3H); ^{13}C NMR (100 MHz, $CDCl_3$): δ = 153.4, 150.4, 143.3, 142.6, 140.5, 135.3, 129.4, 128.5, 128.3, 127.8, 127.5, 126.9, 126.5, 126.0, 123.1, 120.1, 71.9, 19.6, 13.9 ppm; HRMS: m/z calcd for $C_{23}H_{19}^+$ (loss of -NH_2 group): 295.1481; found: 295.1476.

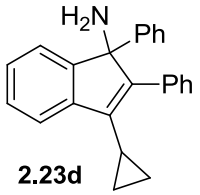

2.23d

3-Cyclopropyl-1,2-diphenyl-1H-inden-1-ylamine (**2.23d**): Chromatography (1:4 ethyl acetate/hexane, R_f=0.30) gave **2.23d** as a white solid (30.7 mg, 95%). ^{1}H NMR (400 MHz, $CDCl_3$): δ = 7.50–7.07 (m, 14 H), 1.86 (tt, *J* = 8.5, 5.5 Hz, 1H), 1.77 (br s, 2H), 0.96 (m, 1H), 0.77 (m, 1 H), 0.64 (m, 1H), 0.52 ppm (m, 1H); ^{13}C NMR (100 MHz, $CDCl_3$): δ = 153.1, 151.0, 143.7, 143.0, 139.5, 135.0, 129.7, 128.6, 128.5, 128.5, 128.0, 127.8, 127.5, 126.9, 126.6, 125.7, 122.9, 120.6, 71.5,9.0, 7.5, 6.4 ppm; HRMS: m/z calcd for $C_{24}H_{19}^+$ (loss of -NH_2 group): 307.1481; found: 307.1492.

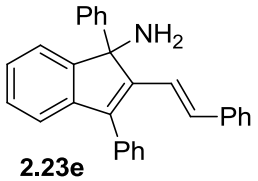

2.23e

(E)-1,2-Diphenyl-3-styryl-1H-inden-1-ylamine (**2.23e**): Chromatography (1:4 ethyl acetate/hexane, R_f=0.30) gave **2.23e** as a white solid (37.4 mg, 97%). ^{1}H NMR (400 MHz, $CDCl_3$): δ = 7.60 (m, 7H), 7.49 (tt, *J* = 7.2, 1.6 Hz, 1H), 7.33 (td, *J* = 7.4, 1.3 Hz, 4H), 7.21 (m, 7H), 7.10 (d, *J* = 16.6, 1H), 6.43 (d, *J* = 16.6, 1H), 2.09 ppm (s, 1H; -NH_2); ^{13}C NMR (100 MHz, $CDCl_3$): δ = 154.3, 148.3, 143.7, 142.2, 142.1, 137.8, 134.6, 132.4, 129.9, 129.0, 128.9, 128.7, 128.3, 128.0, 127.8, 127.3, 127.1, 126.7, 125.5, 123.2, 121.3, 120.6, 69.6 ppm; HRMS: m/z calcd for $C_{29}H_{21}^+$ (loss of -NH_2 group): 369.1638; found: 369.1634.

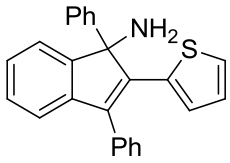

2.23f

1,3-Diphenyl-2-(thiophen-2-yl)-1H-inden-1-ylamine (**2.23f**): Chromatography (1:3 ethyl acetate/hexane, R_f=0.30) gave **2.23f** as a colorless solid (31.5 mg, 86 %). ^{1}H NMR (400 MHz, $CDCl_3$): δ = 7.63 (dt, *J* = 8.5, 2.4 Hz, 2H), 7.51-7.45 (m, 5H), 7.30 (m, 2H), 7.23 (m, 2H), 7.18 (dd, *J* = 7.4, 1.3 Hz, 1H), 7.13 (dd, *J* = 7.4, 1.2 Hz, 1H), 7.07 (d, *J* = 7.4 Hz, 1H), 7.04 (dd, *J* = 5.1, 1.1 Hz, 1H), 6.75 (d*d, J* = 5.1, 3.7 Hz, 1H), 6.58 (dd, *J* = 3.7, 1.1 Hz, 1H), 1.99 ppm (s, 2H; -NH_2); ^{13}C NMR (100 MHz, $CDCl_3$): δ = 152.6, 144.5, 143.1, 142.9, 139.1, 136.6, 135.1, 129.8, 129.3, 128.9, 128.4, 128.1, 127.6, 127.3, 126.9, 126.8, 126.2, 125.8, 123.2, 121.1, 71.6 ppm; HRMS: m/z calcd for $C_{25}H_{17}S^+$ (loss of -NH_2 group): 349.1045; found: 349.1041.

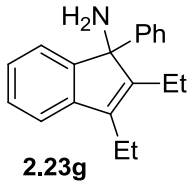

2.23g

2, 3-Diethyl-1-phenyl-1H-inden-1-ylamine (**2.23g**): Chromatography (1:2 ethyl acetate/hexane, R_f = 0.30) gave **2.23g** as a colorless oil (25.3 mg, 96 %). ^{1}H NMR (400 MHz, $CDCl_3$): δ = 7.31 (dt, *J* = 6.8, 0.8 Hz, 2H), 7.25–7.16 (m, 5H), 7.10–7.05 (m, 2H), 2.61-2.48 (m, 2 H), 2.29–2.09 (m, 2H), 1.70 (br s, 2H; -NH_2), 1.23 (t, *J* = 7.2 Hz, 3H), 0.84 ppm (t, *J* = 7.6 Hz, 3H); ^{13}C NMR (100 MHz, $CDCl_3$): δ = 153.9, 151.7, 144.0, 143.0, 138.3, 128.3, 127.5, 126.8, 126.0, 125.6, 122.3, 119.0, 71.3, 18.9, 18.5, 14.8, 13.7 ppm; HRMS: m/z calcd for $C_{19}H_{19}^+$ (loss of -NH_2 group): 247.1481; found: 247.1475.

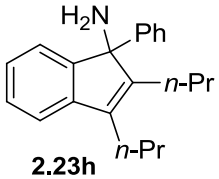

2.23h

1-Phenyl-2,3-dipropyl-1H-inden-1-ylamine (**2.23h**): Chromatography (1:2 ethyl acetate/hexane, R_f = 0.35) gave **2.23h** as a colorless oil (27.4 mg, 94 %). ^{1}H NMR (400 MHz, $CDCl_3$): δ = 7.32 (d, *J* = 6.8 Hz, 2H), 7.24–7.15 (m, 5H), 7.05 (m, 2H), 2.50 (t, *J* = 7.6 Hz, 2H), 2.21 (m, 1H), 2.06 (m, 1H), 1.71 (br s, 2H; -

NH_2), 1.66 (m, 2H), 1.32 (m, 1H), 1.14 (m, 1H), 1.03 (td, *J* = 7.2, 2.2 Hz, 3H), 0.82 ppm (td, *J* = 7.2, 2.2 Hz, 3H); ^{13}C NMR (100 MHz, $CDCl_3$): δ = 154.0, 151.0, 144.2, 143.1, 137.2, 128.3, 127.5, 126.8, 126.0, 125.6, 122.3, 119.1, 71.3, 28.1, 27.9, 23.2, 22.2, 15.0, 14.7 ppm; HRMS: m/z calcd for $C_{21}H_{23}^+$ (loss of -NH_2 group): 275.1794; found: 275.1787.

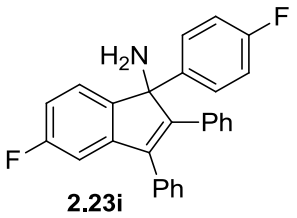

2.23i

5-Fluoro-1-(4-fluorophenyl)-2,3-diphenyl-1H-inden-1-amine (**2.23i**): Chromatography (1:3 ethyl acetate/hexane, R_f = 0.30) gave **2.23i** as a white solid (35.6 mg, 90%). ^1H NMR (400 MHz, $CDCl_3$): δ = 7.49 (dd, *J* = 8.2, 5.5 Hz, 2H), 7.37-7.31 (m, 5H), 7.14-7.05 (m, 4H), 6.98 (t, *J* = 8.2 Hz, 3H), 6.83 (m, 3H), 1.81 ppm (s, 2H; -NH_2); ^{13}C NMR (100 MHz, $CDCl_3$): δ = 164.0 (d, *J* = 242.7 Hz), 161.5 (d, *J* = 244.1 Hz), 152.9, 148.3, 145.0 (d, *J* = 8.1 Hz), 138.7, 138.4, 134.5, 134.1, 132.6 (d, *J* = 8.1 Hz), 129.7, 129.5, 129.0, 128.3, 128.1, 127.8, 127.4 (d, *J* = 8.1 Hz), 124.3 (d, *J* = 9.5 Hz), 115.8, 115.6, 113.5, 113.1, 108.8, 108.6, 71.0 ppm; ^{19}F NMR (282.4 MHz, $CDCl_3$): δ = -114.8 (td, *J* = 9.0, 5.0 Hz, 1F), -116.3 ppm (m, 1F); HRMS: m/z calcd for $C_{27}H_{19}NF_2Na^+$: 418.1378; found: 418.1387.

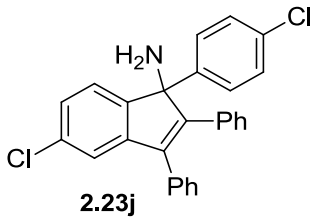

2.23j

5-Chloro-1-(4-chlorophenyl)-2,3-diphenyl-1H-inden-1-ylamine (**2.23j**): Chromatography (1:3 ethyl acetate/hexane, R_f = 0.30) gave **2.23j** as a white solid (40.7 mg, 95%). ^1H NMR (400 MHz, $CDCl_3$): δ = 7.48 (dt, *J* = 8.7, 2.3 Hz, 2H), 7.41-7.31 (m, 4H), 7.26 (m, 3H), 7.11-7.05 (m, 6H), 6.86 (m, 2H), 1.86 ppm (s, 2H; -NH_2); ^{13}C NMR (100 MHz, $CDCl_3$): δ = 152.2, 150.9, 144.7, 141.1, 138.9, 134.3, 134.1, 133.9, 133.1, 129.7, 129.4, 129.1, 129.0, 128.3, 128.2, 127.9, 127.2, 126.8, 124.3, 121.5, 71.1 ppm; HRMS: m/z calcd for $C_{27}H_{17}Cl_2^+$ (loss of -NH_2 group): 411.0702; found: 411. 0715.

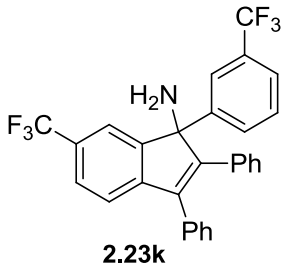

2.23k

2,3-Diphenyl-6-(trifluoromethyl)-1-(3-(trifluoromethyl)phenyl)-1H-inden-1-ylamine (**2.23k**): Chromatography (1:3 ethyl acetate/hexane, R_f = 0.30) gave **2.23k** as a light yellow solid (45.1 mg, 91%). ^{1}H NMR (400 MHz, $CDCl_3$): δ = 7.98 (s, 1H), 7.66 (d, J = 7.9 Hz, 1H), 7.55 (d, *J* = 8.0 Hz, 2H), 7.46–7.36 (m, 8H), 7.15–7.07 (m, 3H), 6.84 (dd, *J* = 7.2, 1.2 Hz, 2H), 1.91 ppm (s, 2H; -NH_2); ^{13}C NMR (100 MHz, $CDCl_3$): δ = 153.3, 152.9, 146.4, 143.3, 139.3, 134.2, 133.6, 131.4 (q, *J* = 32.4 Hz), 129.6, 129.51, 129.46, 129.3, 129.1, 128.5, 128.3, 128.1, 125.8 (q, *J* = 4.1 Hz), 124.5 (q, *J* = 272.0 Hz), 123.1 (q, *J* = 272.7 Hz), 122.6 (q, *J* = 4.0 Hz), 121.5, 120.2 (q, *J* = 4.1 Hz), 71.7 ppm; 8, 124.3, 121.5, 71.1 ppm; ^{19}F NMR (282.4 MHz, $CDCl_3$): d = -62.7, -63.4 ppm; HRMS: m/z calcd for $C_{29}H_{17}F_6^+$: 479.1229; found: 479.1228.

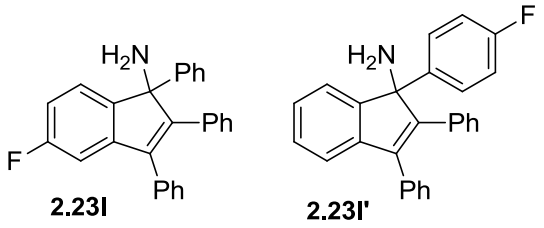

2.23l **2.23l'**

5-Fluoro-1,2,3-triphenyl-1H-inden-1-ylamine (**2.23l**) and 1-(4-fluorophenyl)-2,3-di-phenyl-1H-inden-1-ylamine (**2.23l'**): Chromatography (1:4 ethyl acetate/hexane, R_f = 0.30) gave a mixture of **2.23l** and **2.23l'** as a white solid (35.1 mg, 93%). Compounds **2.23l** and **2.23l'** could not be separated by chromatography. Based on ^{19}F NMR spectroscopy, **2.23l** and **2.23l'** have a ratio of 73 to 27%. ^{1}H NMR (400 MHz, $CDCl_3$): δ = 7.55–6.80 (m, 18H), 1.83 ppm (s, 2H; -NH_2); ^{13}C NMR (100 MHz, CDCl3): δ = 163.9 (d, *J* = 242.8 Hz), 161.5 (d, *J* = 244.2 Hz), 153.1, 153.0, 150.9, 148.52, 148.50, 145.1 (d, *J* = 8.1 Hz), 142.8, 142.6, 139.6, 138.68, 138.65, 135.1, 134.7, 134.5, 134.3, 129.8, 129.6, 129.5, 128.94, 128.91, 128.82, 128.2, 128.0, 127.9, 127.6, 127.55, 127.52, 127.5, 127.2, 127.0, 125.6, 124.4 (d, *J* = 9.5 Hz), 123.2, 121.3, 115.7, 115.5, 113.3, 113.1, 108.6, 108.4, 71.5, 71.3 ppm; ^{19}F NMR (282.4 MHz,

$CDCl_3$): δ = -115.7 (t, *J* = 9.0 Hz), -117.1 ppm (t, *J* = 9.0 Hz); HRMS: m/z calcd for $C_{27}H_{18}F^+$ (loss of -NH_2 group): 361.1387; found: 361.1392.

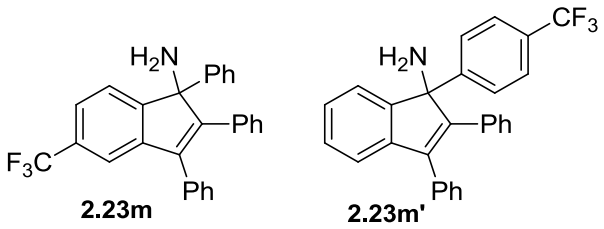

2.23m **2.23m'**

1, 2, 3-Triphenyl-5-trifluoromethyl-1H-inden-1-ylamine (**2.23m**) and 2,3-diphenyl- 1-(4-trifluoromethylphenyl)-1H-inden-1-ylamine (**2.23m'**): Chromatography (1:4 ethyl acetate/hexane, R_f = 0.40) gave a mixture of **2.23m** and **2.23m'** as a white solid (40.6 mg, 95%). Compounds **2.23m** and **2.23m'** could not be separated by chromatography. Based on the analysis by ^{19}F NMR spectroscopy, **2.23m** and **2.23m'** have a ratio of 79 to 21%. ^1H NMR (400 MHz, $CDCl_3$): δ = 7.69 (d, *J* = 8.0 Hz, 1H), 7.56–7.51 (m, 3H), 7.43–7.04 (m, 12H), 6.88–6.83 (m, 2H), 1.86 ppm (s, 2H; -NH_2); ^{13}C NMR (100 MHz, $CDCl_3$): δ = 156.6, 152.8, 152.5, 150.6, 147.7, 143.7, 142.9, 141.8, 138.7, 134.9, 134.4, 134.2, 134.0, 130.40 (q, J = 31.8 Hz), 129.8, 129.7, 129.6, 129.5, 129.10, 129.05, 128.4, 128.29, 128.25, 128.20, 128.0, 127.8, 127.6, 127.1, 126.2, 125.8 (q, *J* = 3.7 Hz), 125.7, 124.0 (q, *J* = 3.8 Hz), 123.6, 123.3, 121.5, 117.9 (q, *J* = 4.6 Hz), 71.8, 71.7 ppm; ^{19}F NMR (282.4 MHz, $CDCl_3$): δ = - 62.7 (s), - 63.0 ppm (s); HRMS: m/z calcd for $C_{28}H_{18}F_3^+$ (loss of -NH_2 group): 411.1355; found: 411.1355.

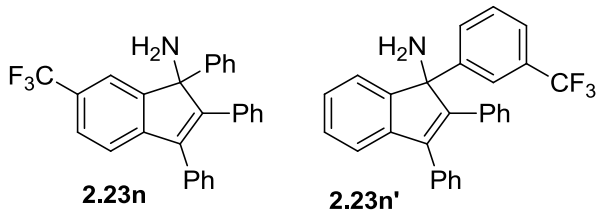

2.23n **2.23n'**

1,2,3-Triphenyl-6-trifluoromethyl-1H-inden-1-ylamine (**2.23n**) and 2,3-diphenyl-1-(3-trifluoromethylphenyl)-1H-inden-1-ylamine (**2.23n'**): Chromatography (1:4 ethyl acetate/hexane, R_f=0.40 for **3n**, R_f=0.30 for **3n'**) gave **2.23n** (25.7 mg), **2.23n'** (14.2 mg), and **2.23n**+**2.2 3n'** (40.2 mg) as white solids (total yield: 94%, **3n**/**3n'** = 1.8:1). **2.23n**: ^1H NMR (400 MHz, $CDCl_3$): δ = 7.54–7.22 (m, 13H), 7.12–7.02 (m, 3H), 6.86 (m, 2H), 1.86 ppm (s, 2H; -NH_2); ^{13}C NMR (100 MHz, $CDCl_3$): δ = 153.9, 153.6, 146.5, 141.7, 138.6, 134.5, 134.0, 129.8, 129.5, 129.1, 129.0, 128.3, 128.1, 127.9, 127.6, 125.7, 125.4 (q, *J* =

3.8,), 121.2, 120.2 (q, *J* = 3.6 Hz), 71.9 ppm; ^{19}F NMR (282.4 MHz, $CDCl_3$): δ = -62.6 ppm (s). **2.23n'**: ^{1}H NMR (400 MHz, $CDCl_3$): δ = 8.00 (s, 1H), 7.63–7.06 (m, 15H), 6.84 (m, 2H), 1.89 ppm (s, 2H; -NH_2); ^{13}C NMR (100 MHz, $CDCl_3$): δ = 152.5, 150.5, 144.6, 142.8, 140.2, 134.9, 134.2, 129.7, 129.6, 129.4, 129.2, 128.9, 128.3, 128.2, 128.0, 127.6, 127.1, 124.1 (dd, *J* = 3.5, 7.2 Hz), 123.3, 122.7 (dd, *J* = 3.1, 6.9 Hz), 121.5, 71.6 ppm; ^{19}F NMR (282.4 MHz, $CDCl_3$): δ = -63.4 ppm (s); HRMS: m/z calcd for $C_{28}H_{18}F_3^+$ (loss of -NH_2 group): 411.1355; found:411.1376.

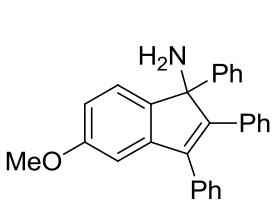

2.23o

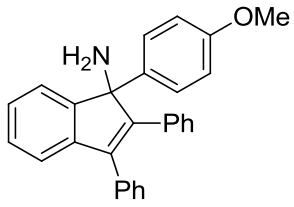

2.23o'

5-Methoxy-1,2,3-triphenyl-1H-inden-1-ylamine (**2.23o**) and 1-(4-methoxyphenyl)-2,3-diphenyl-1H-inden-1-ylamine (**2.23o'**): Chromatography (1:1 ethyl acetate /hexane, R_f = 0.35) gave a mixture of **2.23o** and **2.23o'** as a white solid (36.9 mg, 95 %). Compounds **2.23o** and **2.23o'** could not be separated by chromatography. Based on the analyses by ^{1}H NMR spectroscopy, **2.23o** and **2.23o'** have a ratio of 67 to 33%. ^{1}H NMR (400 MHz, $CDCl_3$): δ = 7.54 (m, 2H), 7.47–7.02 (m, 12H), 6.89–6.82 (m, 3H), 6.69 (dd, *J* = 8.2, 2.4 Hz, 1H), 3.78, 3.76 (s, 3H), 1.83 ppm (s, 2H; -NH_2); ^{13}C NMR (100 MHz, $CDCl_3$): δ = 160.0, 158.8, 153.4, 152.6, 151.3, 145.5, 144.5, 143.4, 142.8, 139.3, 135.3, 135.2, 134.8, 134.6, 129.9, 129.8, 129.6, 128.84, 128.81, 128.2, 127.8, 127.7, 127.4, 127.0, 126.95, 126.90, 125.7, 124.0, 123.2, 121.1, 114.2, 111.8, 107.6, 71.5, 71.3, 55.7, 55.4 ppm; HRMS: m/z calcd for $C_{28}H_{21}O^+$ (loss of -NH_2 group): 373.1587; found: 373.1580.

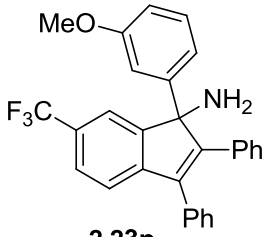

2.23p

1-(3-Methoxy-phenyl)-2,3-diphenyl-6-trifluoromethyl-1H-inden-1-ylamine (**2.23p**): Chromatography (1:4 ethyl acetate: hexane, R_f=0.30) gave **2.23p** as a white solid (38.9mg, 85%). ^{1}H

NMR (400 MHz, $CDCl_3$): δ = 7.50 (d, *J* = 8.0 Hz, 1H), 7.48 (s, 1H), 7.23 (m, 2H), 7.13-7.05 (m, 4H), 6.89 (m, 2H), 6.82 (dd, *J* =8.1, 2.6 Hz, 1H), 3.78 (s, 3H), 1.85 ppm (s, 2H; $-NH_2$); ^{13}C NMR (100 MHz, $CDCl_3$): δ = 160.3, 153.7, 153.4, 146.4, 143.6, 138.7, 134.6, 133.9, 130.1, 129.8, 129.5, 129.0, 128.7 (q, J = 38 Hz), 128.3, 128.2, 127.9 , 124.7 (q, *J* = 280 Hz), 125.4 (q, *J* = 3.8 Hz), 121.2, 120.1 (q, *J* = 3.8 Hz), 118.0, 112.6, 111.8, 71.8, 55.4 ppm; ^{19}F NMR (282.4 MHz, $CDCl_3$): δ = 62.2 ppm (s); HRMS: m/z calcd for $C_{29}H_{20}OF_3^+$ (loss of $-NH_2$ group): 441.1461; found: 441.1474.

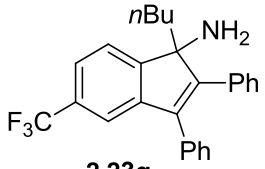

2.23q

1-Butyl-2,3-diphenyl-6-trifluoromethyl-1H-inden-1-ylamine (**2.23q**): Chromatography (1:4 ethyl acetate/hexane, R_f=0.40) gave **2.23q** as a light yellow solid (38.7 mg, 95 %). ^1H NMR (400 MHz, $CDCl_3$): δ =7.53 (d, *J* = 1.1 Hz, 2H), 7.48 (s, 1H), 7.33–7.20 (m, 10H), 1.97 (dt, *J* = 12.0, 4.6 Hz, 1H), 1.85 (dt, *J* = 13.1, 3.9Hz, 1H), 1.62 (s, 2H; $-NH_2$), 1.15 (m, 3H), 0.76 ppm (m, 4H); ^{13}C NMR (100 MHz, $CDCl_3$): δ = 154.4, 151.2, 144.1, 138.9, 135.2, 134.3, 130.2 (q, *J* = 32 Hz), 129.7, 129.5, 128.7, 128.5, 127.8, 127.7 (q, J = 310 Hz), 127.4, 123.4 (q, *J* = 3.5 Hz), 122.2, 117.5 (q, *J* = 3.5 Hz), 69.8, 38.2, 26.0, 23.0, 14.0 ppm; ^{19}F NMR (282.4 MHz, $CDCl_3$): δ = -62.8 ppm (s); HRMS: m/z calcd for $C_{26}H_{22}F_3^+$ (loss of $-NH_2$ group): 391.1668; found: 391.1674.

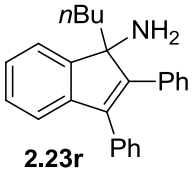

2.23r

1-Butyl-2,3-diphenyl-1H-inden-1-ylamine (**2.23r**): Chromatography (1:4 ethyl acetate/hexane, R_f=0.30) gave **2.23r** as a light yellow oil (25.5 mg, 75 %). ^1H NMR (400 MHz, $CDCl_3$): δ = 7.48-7.45(m, 1H), 7.31-7.23 (m, 13H), 2.01-1.83(m, 2H), 1.68 (s, 2H, $-NH_2$), 1.22-1.13 (m, 3H), 0.87-0.79(m, 1H), 0.76 ppm (t, *J* = 7.2 Hz, 3H); ^{13}C NMR (100 MHz, $CDCl_3$): δ = 150.7, 149.5, 143.4, 139.7, 135.9, 135.1, 129.8, 129.6, 128.5, 128.4, 127.7, 127.41, 127.39. 126.3, 122.0, 120.8, 69.8, 38.5, 26.1, 23.0, 14.1 ppm; HRMS: m/z calcd for $C_{25}H_{23}^+$ (loss of $-NH_2$ group): 323.1794; found: 323.1789.

2.8. References

1. Aulwurm, U. R.; Melchinger, J. U.; Kisch, H. Transition Metal Complexes of Diazenes. 35. Synthesis of 1-(Arylamino)indoles by Rhodium-Catalyzed Addition of Alkynes to 1,2-Diaryldiazenes. *Organometallics* **1995**, *14*, 3385-3395.

2. Kuninobu, Y.; Tokunaga, Y.; Kawata, A.; Takai, K. Insertion of Polar and Nonpolar Unsaturated Molecules into Carbon−Rhenium Bonds Generated by C−H Bond Activation: Synthesis of Phthalimidine and Indene Derivatives. *J. Am. Chem. Soc.* **2005**, *128*, 202-209.

3. Kuninobu, Y.; Nishina, Y.; Shouho, M.; Takai, K. Rhenium- and Aniline-Catalyzed One-Pot Annulation of Aromatic Ketones and α, β-Unsaturated Esters Initiated by C-H Bond Activation. *Angew. Chem. Int. Ed.* **2006**, *45*, 2766-2768.

4. Fukutani, T.; Umeda, N.; Hirano, K.; Satoh, T.; Miura, M. Rhodium-Catalyzed Oxidative Coupling of Aromatic Imines with Internal Alkynes via Regioselective C-H Bond Cleavage. *Chem. Commun.* **2009**, 5141-5143.

5. Sun, Z.-M.; Chen, S.-P.; Zhao, P. Tertiary Carbinamine Synthesis by Rhodium-Catalyzed [3+2] Annulation of N-Unsubstituted Aromatic Ketimines and Alkynes. *Chem. – Eur. J.* **2010**, *16*, 2619-2627.

6. Friestad, G. K.; Mathies, A. K. Recent Developments in Asymmetric Catalytic Addition to C=N bonds. *Tetrahedron* **2007**, *63*, 2541-2569.

7. Shibasaki, M.; Kanai, M. Asymmetric Synthesis of Tertiary Alcohols and α-Tertiary Amines via Cu-Catalyzed C−C Bond Formation to Ketones and Ketimines. *Chem. Rev.* **2008**, *108*, 2853-2873.

8. Kobayashi, S.; Konishi, H.; Schneider, U. Indium(I) Iodide-Catalyzed Regio- and Diastereoselective Formal α-Addition of an α-Methylallylboronate to N-Acylhydrazones. *Chem. Commun.* **2008**, 2313-2315.

9. Fu, P.; Snapper, M. L.; Hoveyda, A. H. Catalytic Asymmetric Alkylations of Ketoimines. Enantioselective Synthesis of N-Substituted Quaternary Carbon Stereogenic Centers by Zr-Catalyzed Additions of Dialkylzinc Reagents to Aryl-, Alkyl-, and Trifluoroalkyl-Substituted Ketoimines. *J. Am. Chem. Soc.* **2008**, *130*, 5530-5541.

10. Dilman, A. D.; Arkhipov, D. E.; Levin, V. V.; Belyakov, P. A.; Korlyukov, A. A.; Struchkova, M. I.; Tartakovsky, V. A. Trifluoromethylation of N-Benzoylhydrazones. *J. Org. Chem.* **2008**, *73*, 5643-5646.

11. Notte, G. T.; Leighton, J. L. A New Silicon Lewis Acid for Highly Enantioselective Mannich Reactions of Aliphatic Ketone-Derived Hydrazones. *J. Am. Chem. Soc.* **2008**, *130*, 6676-6677.

12. Johns, A. M.; Liu, Z.; Hartwig, J. F. Primary *tert*- and *sec*-Allylamines via Palladium-Catalyzed Hydroamination and Allylic Substitution with Hydrazine and Hydroxylamine Derivatives. *Angew. Chem. Int. Ed.* **2007**, *46*, 7259-7261.

13. Dejaegher, Y.; Mangelinckx, S.; Kimpe, N. D. Synthesis of Substituted Benzhydrylamines. *Synlett* **2002**, *2002*, 0113-0115.

14. Hou, G.; Gosselin, F.; Li, W.; McWilliams, J. C.; Sun, Y.; Weisel, M.; O'Shea, P. D.; Chen, C.-y.; Davies, I. W.; Zhang, X. Enantioselective Hydrogenation of N−H Imines. *J. Am. Chem. Soc.* **2009**, *131*, 9882-9883.

15. Tran, D. N.; Cramer, N. Enantioselective Rhodium(I)-Catalyzed [3+2] Annulations of Aromatic Ketimines Induced by Directed C-H Activations. *Angew. Chem. Int. Ed.* **2011**, *50*, 11098-11102.

16. Tran, D. N.; Cramer, N. *syn*-Selective Rhodium(I)-Catalyzed Allylations of Ketimines Proceeding Through a Directed C-H Activation/Allene Addition Sequence. *Angew. Chem. Int. Ed.* **2010**, *49*, 8181-8184.

17. Kuninobu, Y.; Yu, P.; Takai, K. Rhenium-Catalyzed Diastereoselective Synthesis of Aminoindanes via the Insertion of Allenes into a C−H Bond. *Org. Lett.* **2010**, *12*, 4274-4276.

18. Murai, S.; Kakiuchi, F.; Sekine, S.; Tanaka, Y.; Kamatani, A.; Sonoda, M.; Chatani, N. Efficient Catalytic Addition of Aromatic Carbon-Hydrogen Bonds to Olefins. *Nature* **1993**, *366*, 529-531.

19. Guari, Y.; Sabo-Etienne, S.; Chaudret, B. Exchange Couplings Between a Hydride and a Stretched Dihydrogen Ligand in Ruthenium Complexes. *J. Am. Chem. Soc.* **1998**, *120*, 4228-4229.

20. Busch, S.; Leitner, W. Convenient Preparation of Mononuclear and Dinuclear Ruthenium Hydride Complexes for Catalytic Application. *Chem. Commun.* **1999**, 2305-2306.

21. Busch, S.; Leitner, W. Ruthenium-Catalysed Murai-Type Couplings at Room Temperature. *Adv. Synth. Catal.* **2001**, *343*, 192-195.

22. Kakiuchi, F.; Kochi, T.; Mizushima, E.; Murai, S. Room-Temperature Regioselective C-H/Olefin Coupling of Aromatic Ketones Using an Activated Ruthenium Catalyst with a Carbonyl Ligand and Structural Elucidation of Key Intermediates. *J. Am. Chem. Soc.* **2010**, *132*, 17741-50.

23. Davies, D. L.; Al-Duaij, O.; Fawcett, J.; Singh, K. Reactions of Cyclometalated Oxazoline Half-Sandwich Complexes of Iridium and Ruthenium with Alkynes and CO. *Organometallics* **2010**, *29*, 1413-1420.

24. Aguilar, D.; Bielsa, R.; Soler, T.; Urriolabeitia, E. P. Cycloruthenated Complexes from Iminophosphoranes: Synthesis, Structure, and Reactivity with Internal Alkynes. *Organometallics* **2011**, *30*, 642-648.

25. Li, B.; Roisnel, T.; Darcel, C.; Dixneuf, P. H. Cyclometallation of Arylimines and Nitrogen-Containing Heterocycles via Room-Temperature C-H Bond Activation with Arene Ruthenium(ii) Acetate Complexes. *Dalton Trans.* **2012**, *41*, 10934-10937.

26. Li, L.; Brennessel, W. W.; Jones, W. D. An Efficient Low-Temperature Route to Polycyclic Isoquinoline Salt Synthesis via C-H Activation with $[Cp^*MCl_2]_2$ (M = Rh, Ir). *J. Am. Chem. Soc.* **2008**, *130*, 12414-12419.

27. Li, L.; Brennessel, W. W.; Jones, W. D. C−H Activation of Phenyl Imines and 2-Phenylpyridines with $[Cp^*MCl_2]_2$(M = Ir, Rh): Regioselectivity, Kinetics, and Mechanism. *Organometallics* **2009**, *28*, 3492-3500.

28. Yang, C.-Y.; Lin, M.-S.; Liao, H.-H.; Liu, R.-S. Diversity of Products in the Gold-Catalyzed Cyclization of 1-Epoxy-1-alkynylcyclopropanes by Using 1-Oxyallyl Cations. *Chem. – Eur. J.* **2010**, *16*, 2696-2699.

29. Mori, A.; Shimada, T.; Kondo, T.; Sekiguchi, A. A Highly Effective Pd/Cu-Catalyzed Coupling Reaction of Terminal Alkynes with Organic Halides Promoted by Tetrabutylammonium Fluoride or Hydroxide. *Synlett* **2001**, *2001*, 649-651.

CHAPTER 3. RUTHENIUM(II)/N-HETEROCYCLIC CARBENE CATALYZED [3+2] CARBOCYCLIZATION WITH ARYL KETONES AND INTERNAL ALKYNES

3.1. Background and Significance

The indenol moiety is an important structural unit present in various biologically active compounds that showed insecticidal, analgesic, and myorelaxation properties.[1-4] Despite their high utility, only a few synthetic routes are available in the literature.[1-18]

Transition metal-catalyzed carbocyclization is a powerful method for the construction of indenol derivatives in organic synthesis.[19-23] Liebeskind et al. reported a stoichiometric reaction of alkynes with *ortho*-manganated acetophenones (**3.02**) to give indenols (**3.03**) (Scheme 3.1).[1] The reaction exhibited a surprisingly high degree of regiochemical control over the range of alkynes studied. Vicente and coworkers reported stoichiometric and catalytic synthesis of indenols from *mono*- and disubstituted alkynes and organomercuric compounds using palladium complexes.[5,6]

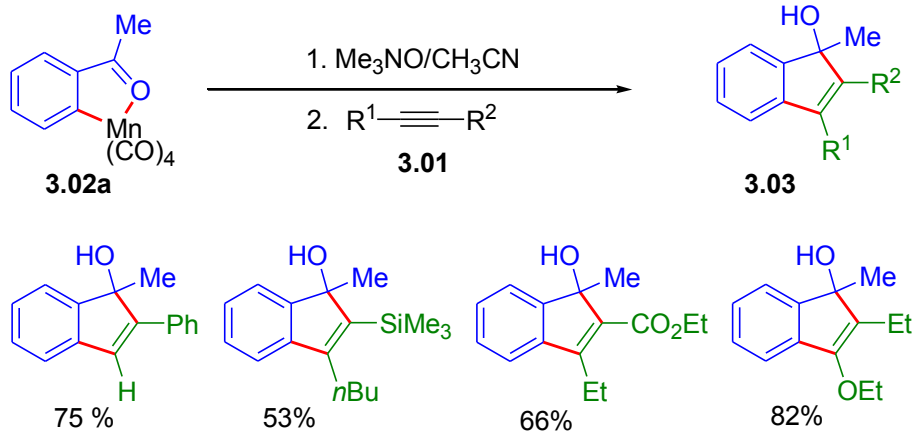

Scheme 3.1. Carbocyclization with *ortho*-manganated acetophenones and alkynes

Carbocyclization of *ortho*-haloaromatic ketones or aldehydes (**3.04**) with alkynes to give substituted indenols utilizing palladium catalyst was reported by Yamamoto and co-workers (Scheme 3.2, **A**).[7,8] Similar catalytic reactions with nickel catalyst in the presence of stoichiometric amount of zinc as

reductant were reported by the Cheng group (Scheme 3.2, **B**).[9,11] Notably, cobalt catalytic system developed by Cheng and coworkers extended the arene substrate scope to aromatic aldehydes (Scheme 3.2, **C**).[10,12] These reactions proceeded via oxidative addition of the C-X bonds in *ortho*-haloaromatic ketones/aldehydes (**3.04**), generating the metallacycle intermediate **3.05**, followed by alkyne insertion that gave the vinyl-metal intermediate **3.06**. Subsequent intramolecular addition of M-C linkage to the C=O bond affording the alkoxy-metal intermediate **3.07**. Successive transmetalation and protonation afforded the indenol products. Although stoichiometric amount of organometallic substrates were not required in these reactions, regeneration of the catalysts in nickel and cobalt catalytic systems demanded stoichiometric amount of zinc as reductant to generate low-valent and active catalysts.

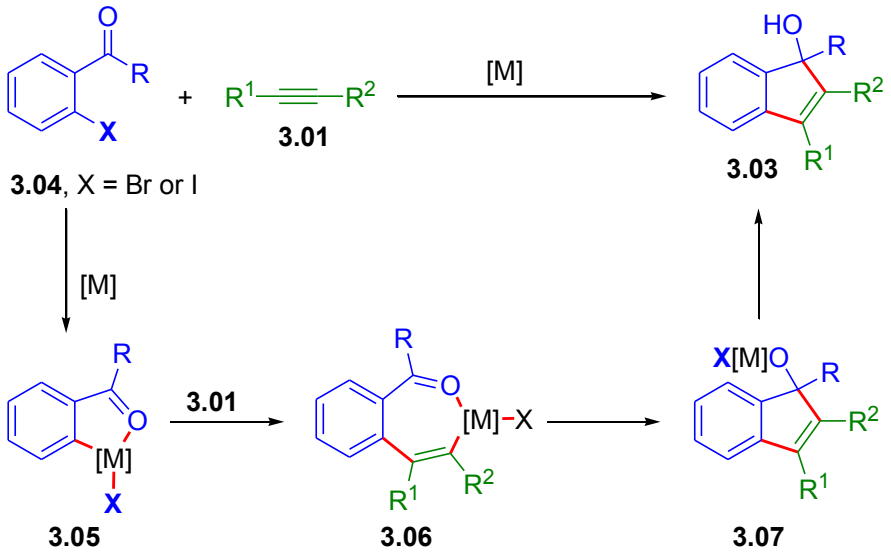

A: Yamamoto: **Pd**$(OAc)_2$ (5 mol%), KOAc (2 equiv), DMF, 100 ^oC, 51-86 %

B: Cheng: **Ni**(dppe)Br_2 (5 mol%), Zn (2.75 equiv), CH_3CN, 80 ^oC, 13h, 5-87 %

C: Cheng: **Co**(dppe)I_2 (5 mol%), Zn (2.75 equiv), CH_3CN, 80 ^oC, 3h, 35-99 %

Scheme 3.2. Transition metal-catalyzed carbocyclization with *o*-haloaromatic ketones and internal alkynes

Murakami and co-workers described a rhodium-catalyzed regioselective carbocyclization of *ortho*-formylphenylboronic acid (**3.06**) with alkynes to produce substituted indenol derivatives (Scheme 3.3).[13]

The proposed reaction mechanism was similar to the reaction using *ortho*-haloaromatic ketone/aldehydes (**3.04**) as substrates, except the first step was transmetalation instead of oxidative addition. All of these methods described above to synthesize indenols required prefunctionalized arene substrates, such as aryl halides and arylboronic acids, as starting materials, which needed extra synthetic steps to prepare and would generate stoichiometric amount of salt wastes.

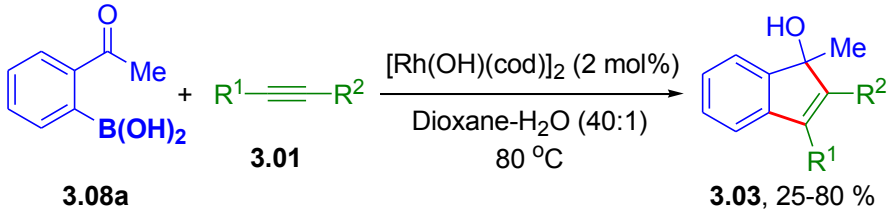

3.08a **3.01** **3.03**, 25-80 %

Scheme 3.3. Rhodium catalyzed carbocyclization with *o*-acetylphenylboronic acid and internal alkynes

Over the past two decades, the strategy based on transition metal-catalyzed C-H activation has evolved as an atom- and step-economic alternative to access indenols. In 1999, Woodgate reported the first example of indenol synthesis based on a carbonyl-directed C-H activation of aryl ketone with the assistance of a ruthenium complex (Scheme 3.4).[14] However, this rhodium catalysis led to a 1:1 mixture of alkenylated ketone (**3.10a**) and indenol (**3.03a**) with moderate yield in refluxing toluene.

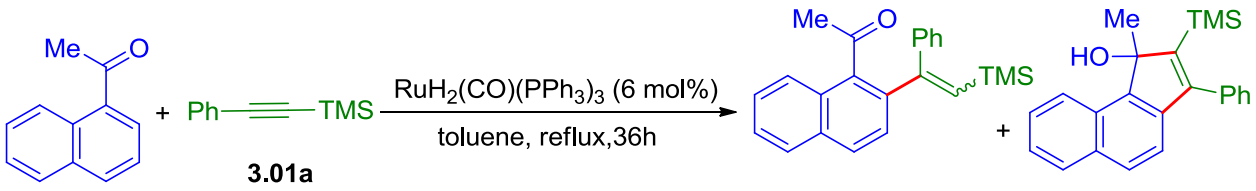

3.09a **3.01a** **3.10a**, 22.5% *E*/*Z* (7:1) **3.03a**, 22.5%

Scheme 3.4. Ruthenium catalyzed alkenylation and carbocyclization with 1-acetylnaphthalene and trimethyl(phenylethynyl)silane

Recently, based on their previous report on iridium catalyzed alkyne hydroarylation via directed *ortho*-C–H bond activation of aryl ketones,[15] Shibata and co-workers found an carbocyclization occurred when the counter anion of the iridium complex was changed, leading to indenol (**3.03b**) and benzofulvene (**3.13a**) instead of the *ortho*-alkenylated aryl ketone as shown in Scheme 3.5.[16] The iridium complex behaved as a catalyst in the *ortho*-C–H bond alkenylation of aryl ketones with alkynes giving intermediate **3.11** and as a Lewis acid catalyst in the cyclization of the alkenylated product, generating intermediate **3.12** and the subsequent dehydration product benzofulvene.

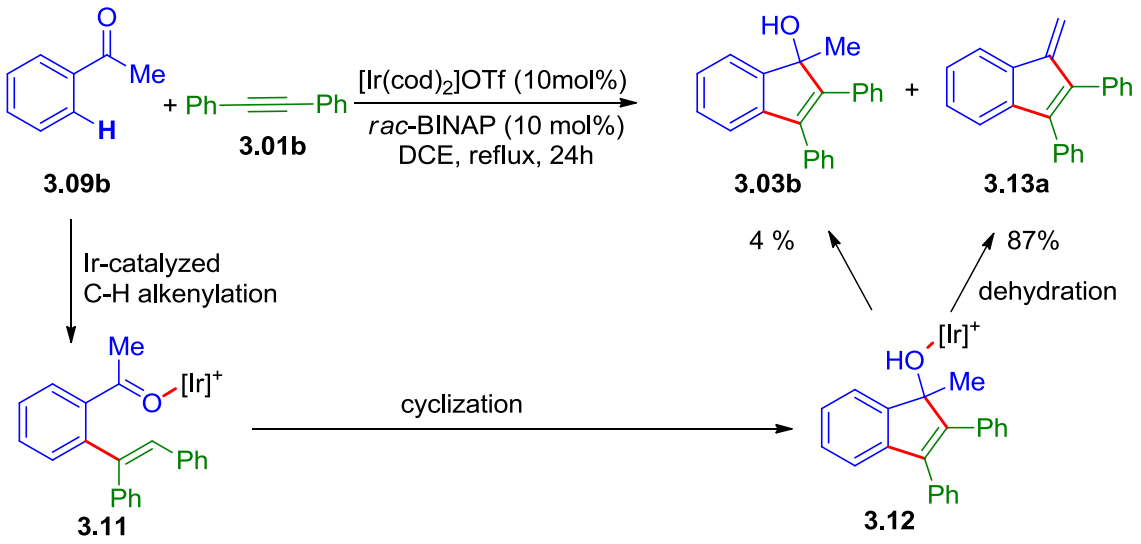

Scheme 3.5. Cationic iridium catalyzed carbocyclization with acetophenone and diphenylacetylene to form indenol and benzofulvene products

After Shibata's initial report, Glorius[18] and Cheng[17] independently developed a rhodium-catalyzed directed C–H activation of aromatic ketones and subsequent carbocyclization with alkynes to form indenols (Scheme 3.6). In their reaction systems, $AgSbF_6$ was required as co-catalyst and stoichiometric $Cu(OAc)_2$ was essential to facilitate the reaction by transmetalation with Rh–O species to release the rhodium catalyst from indenol product. Most recently, Jeganmohan developed a ruthenium catalytic system in which $Cu(OAc)_2$ was used in catalytic amount.[24] In the presence of higher loading of $AgSbF_6$ additive, benzofulvenes were produced through dehydration (Scheme 3.7).

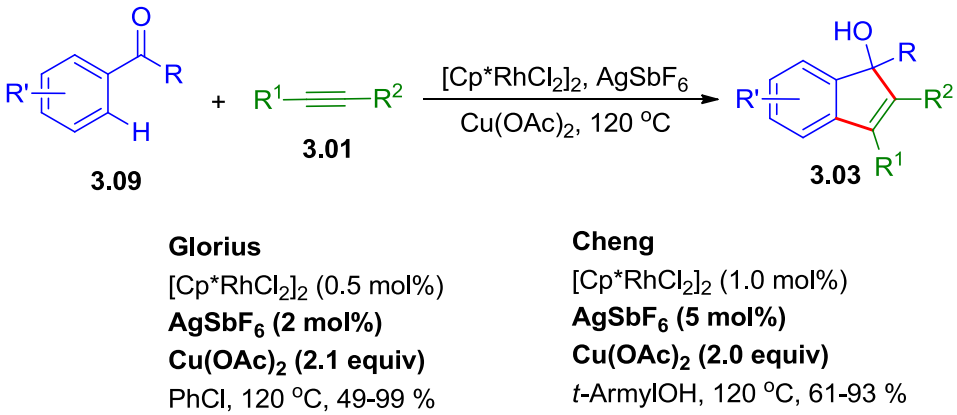

Scheme 3.6. Rhodium(III) catalyzed carbocyclization with aromatic ketones and internal alkynes initiated by C-H bond activation with the assistance of silver and copper salts

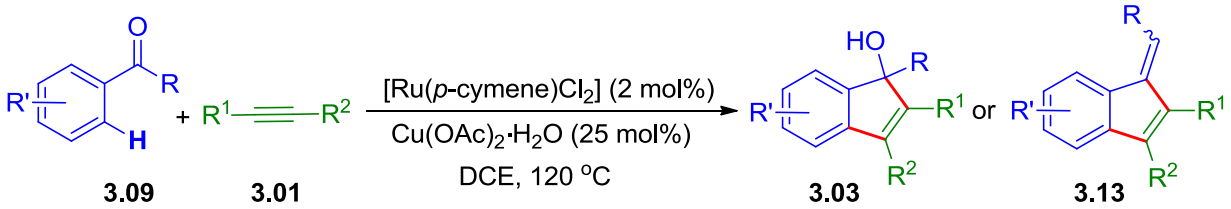

A: **$AgSbF_6$ (8 mol%)**, indinols, 69-88% %

B: **$AgSbF_6$ (10 mol%)**, benzofulvenes, 75-93 %

Scheme 3.7. Ruthenium(II) catalyzed carbocyclization with aromatic ketones and internal alkynes initiated by C-H bond activation with the assistance of silver and copper salts

These catalytic systems to access indenols were based on transition metal-catalyzed carbonyl directed C-H bond activation of aryl ketones and carbocyclization with alkynes, which eliminated the prefunctionalization of aryl ketones. However, all of them suffered from either low activity of the catalysts or harsh reaction conditions including high temperature and the requirement of heavy metal salt additives.

Our continuous interest in the development of ruthenium-catalyzed C-H activation and carbocylization reactions under mild conditions prompted us to explore the reaction of aryl ketones with alkynes to access indenols.[25] A ruthenium(II)-NHC catalyzed [3+2] carbocyclization with aryl ketones and internal alkynes under much milder conditions will be described in this chapter.

3.2. Initial Results

Based on our experience of Ru-NHC catalyzed carbocyclization of N-H ketimines and internal alkynes,[25] we began our study with stoichiometric cyclometalation with Ru(cod)(methylallyl)$_2$ and benzophenone (Scheme 3.8). A bis-cyclometalated Ru-complex with η^2-benzophenone ligand was produced and isolated. A structure that was similar to the imine analogue was confirmed by single crystal X-ray diffraction (Figure 3.1). However, the cyclometalation with benzophenone via ketone directed C-H bond activation was less efficient compared to N-H imines, and relatively higher reaction temperature (80 ^{o}C) was required to get satisfactory conversion.

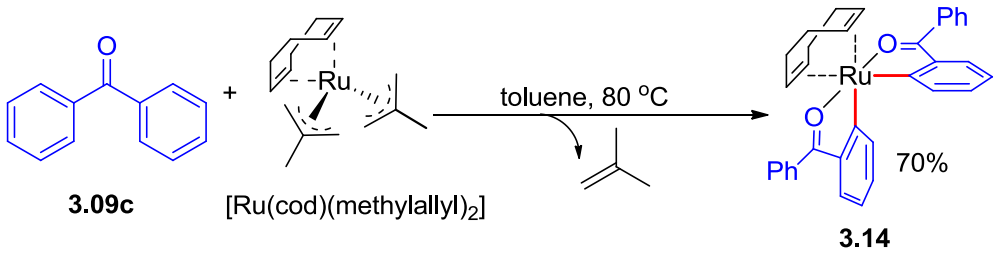

Scheme 3.8. Stoichiometric cyclometalation with [Ru(cod)(η^3-methylallyl)$_2$] and benzophenone to form bis-cyclometalated ruthenium(II) complex with η^2-[C,O] ketone ligand

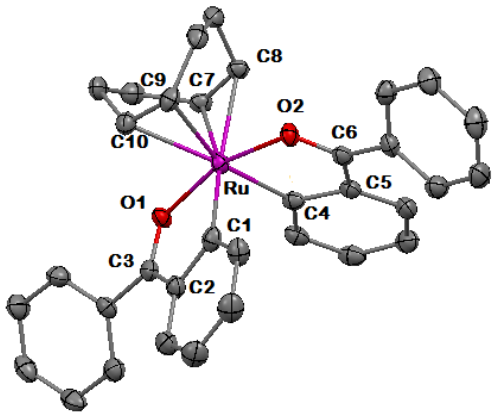

Figure 3.1. ORTEP diagram of {[Ru(cod)[η^2-OC(C_6H_5)C_6H_4]$_2$} (**3.14**) at 50% thermal ellipsoid.

The isolated ruthenacycle was tested as catalytic precursor for the coupling between benzophenone (**3.09c**) and diphenylacetylene (**3.01b**) (Scheme 3.9). The starting materials were recovered and no desired indenol product (**3.03c**) was detected even under elevated temperatures. N-heterocyclic carbene ligands (NHCs), including IPr, IMes, SIPr, and SIMes, could not facilitate the reaction. Therefore, it seemed that not only C-H bond activation but also alkyne insertion was difficult with {[Ru(cod)[η^2-OC(C_6H_5)C_6H_4]$_2$} (**3.14**).

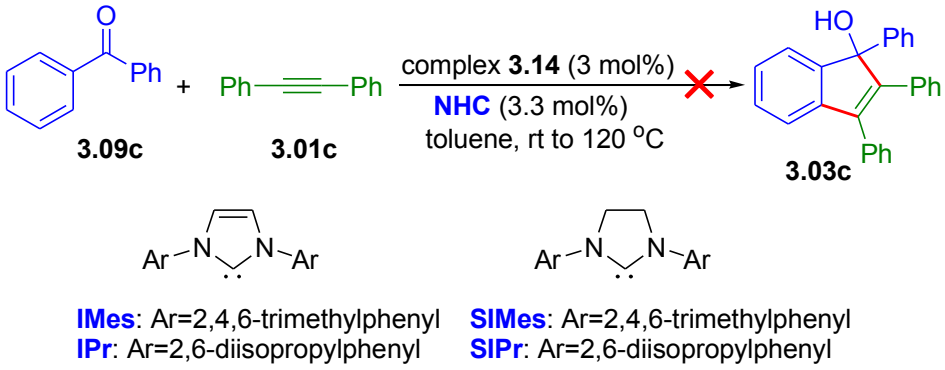

Scheme 3.9. Attempted catalytic reaction with benzophenone and diphenylacetylene using {[Ru(cod)[η^2-OC(C_6H_5)C_6H_4]$_2$} (**3.14**)/NHC-ligands

Compared with N-H imine, ketone is a less effective coordinating directing group based on lower Lewis basicity of oxygen *vs* nitrogen,[26] which likely induced the less efficient cyclometalation with benzophenone. With the weakly coordinating ketone as directing groups, the resulted metallacycle probably is not stable enough in the reaction system to enable the alkyne insertion. Therefore, using a cationic ruthenium complex was expected to enhance the interaction between the weakly coordinating carbonyl oxygen and the ruthenium metal. As a result of the stronger coordination with a more Lewis acidic ruthenium center, the cyclization step would be facilitated by a more electrophilic carbonyl group. In fact, during our study on this project, there were several transition metal-catalyzed carbocyclization with aryl ketone and alkynes reported, where cationic transition metal complexes were employed or generated *in situ* as catalyst precursors.[17,18,24]

It has been reported that Ru(π-arene)(carboxylate)$_2$ complexes tended to release a carboxylate ligand from the metal center and form a cationic Ru(II) mono-carboxylate complex with a ligated solvent molecule. Ru(π-arene)(carboxylate)$_2$ have been explored extensively in aromatic C-H bond functionalization and could be generated *in situ* from the readily available [Ru(*p*-cymene)Cl$_2$]$_2$ precursor and carboxylate salts (Scheme 3.10). Therefore, [Ru(*p*-cymene)Cl$_2$]$_2$ and NaOAc was selected in our first test for the coupling between benzophenone and diphenylacetylene in the presence of NHC ligand in toluene. We were delighted to find that the carbocyclization product, an indenol derivative (**3.03c**), was obtained in 42 % yield at 60 ^{o}C after 24h (Scheme 3.11).

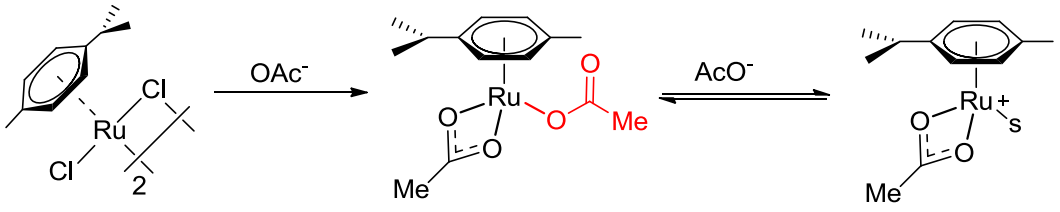

Scheme 3.10. *In situ* generation of cationic ruthenium-arene complex with the assistance of acetate anion and solvent molecule

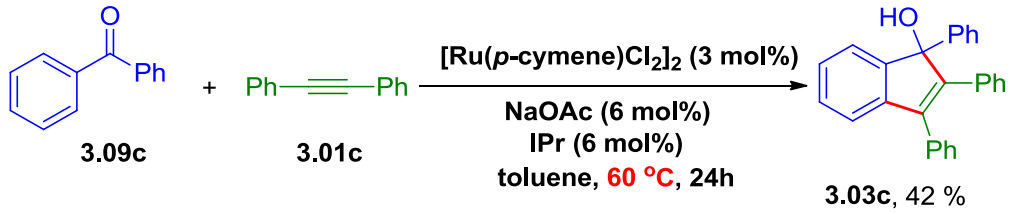

Scheme 3.11. [Ru(*p*-cymene)Cl$_2$]$_2$/NHC catalyzed carbocyclization with benzophenone and diphenylacetylene to form indenol derivative

3.3. Optimization of Reaction Conditions

Encouraged by the preliminary results, we next started the optimization of reaction conditions by evaluation of solvent effects (Table 3.1). Protic solvents such as MeOH, which has been used for ruthenium carboxylate catalyzed heterocyclization of arenes with alkynes, totally shut off the reaction (entry 11).[33-36] 1,2-Dichloroethane (DCE), which was used by Jeganmohan for the same transformation with a Ru-Ag-Cu catalytic system,[18] turned out to be unsuitable for our catalytic system (entries 6 and 7). N,N-Dimethylformamide (DMF), N,N-dimethylacetamide (DMA) and N-Methyl-2-pyrrolidone (NMP) also hindered the reaction significantly (entries 8-10). On the other hand, ethereal solvents were found to be superior to other solvents with tetrahedrofuran (THF) as the optimal solvent for this reaction (entries 2-5).

Table 3.1. Solvent effect in ruthenium(II)/NHC catalyzed carbocyclization with benzophenone and diphenylacetylene[a]

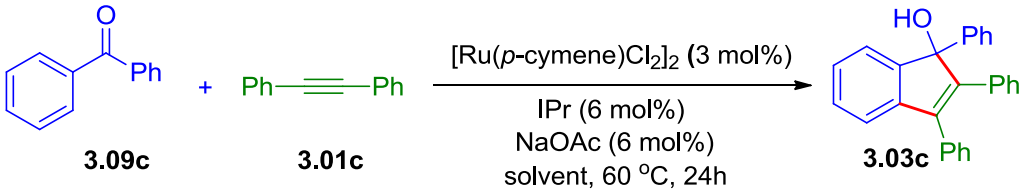

3.09c **3.01c** **3.03c**

entry	slovent	yield (%)[a]	entry	slovent	yield (%)[b]
1	toluene	49	7	DCE	8
2	THF	67	8	NMP	<2
3	dioxane	45	9	DMF	<2
4	Et_2O	39	10	DMA	<2
5	DME	47	11	MeOH	0
6	DCM	<2			

[a] Reaction condition: benzophenone imine (0.2 mmol, 1.0 equiv), diphenylacetylene (0.2 mmol), Ru(*p*-cymene)$Cl_2]_2$ (3 mmol%), IPr (6 mol%), $Na(OAc)_2$ (6 mol%), solvent (0.7 mL), 60 °C, 24h. [b] GC yields.

Next, we probed the effect of various carboxylate additives in THF (Table 3.2) and found that sodium acetate (NaOAc) gave rise to the most satisfactory results (entries 1−9). Either increase or decrease in the loading of NaOAc induced decrease in the yield of the product (entries 9-12), and no product was detected without NaOAc (entry 13). Attempts to use other ruthenium complexes as catalyst precursors were not successful (Table 3.3, entries 1-6). A control reaction showed that omission of the $[Ru(p\text{-cymene})Cl_2]_2$ resulted in complete inactivity of this catalytic system (entry 7). It was noteworthy that the addition of IPr was also critical for this reaction (entry 8), while other N-heterocyclic carbene ligands with similar backbone could not promote the reaction (entries 9-11). Increasing the catalyst loading to 5 mol% and using a slightly excess amount of aryl ketone led to quantitative yield of the indenol product with alkyne as the limiting reagent (entries 12-14).

Table 3.2. Effects of inorganic salt and ligand in ruthenium(II)/NHC catalyzed carbocyclization with benzophenone and diphenylacetylene[a]

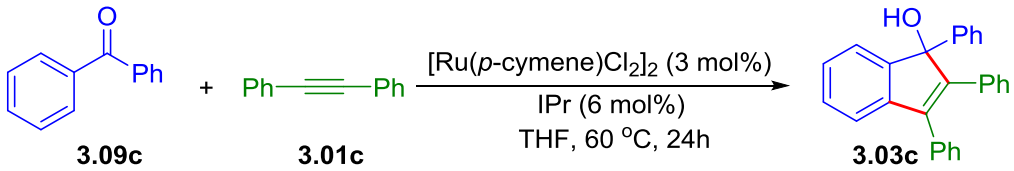

3.09c **3.01c** **3.03c**

entry	additive (mol%)	yield (%)[a]	entry	additive (mol%)	yield (%)[b]
1	LiOAc (6)	<2	8	NaOBz (6)	32
2	KOAc (6)	47	9	NaOAc (6)	67
3	CsOAc (6)	53	10	NaOAc (15)	52
4	NH_4OAc (6)	<2	11	NaOAc (30)	47
5	AgOAc (6)	3	12	NaOAc (3)	10
6	Cs_2CO3 (6)	0	13	NaOAc (0)	0
7	NaOPiv(6)	5			

[a] Reaction condition: benzophenone (0.2 mmol, 1.0 equiv), diphenylacetylene (0.2 mmol), $[Ru(p\text{-cymene})Cl_2]_2$ (3 mmol%), IPr (6 mol%), THF (0.7 mL), 60 °C 24h. [b] GC yield.

Table 3.3. Effects of catalyst precursor, ligand and catalyst loading in ruthenium(II)/NHC catalyzed carbocyclization with benzophenone and diphenylacetylene[a]

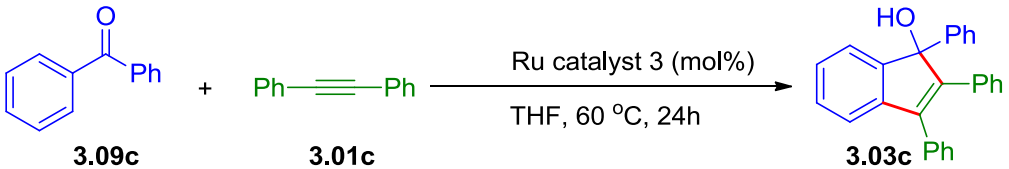

3.09c **3.01c** **3.03c**

entry	Ru-complex	yield (%)[b]	entry	Ru-complex	yield (%)[b]
1	$[Ru(benzene)Cl_2]_2$	67	8	$[Ru(p\text{-cymene})Cl_2]_2$	0
2	$[Ru(benzene)Cl_2]_2$	27	9	$[Ru(p\text{-cymene})Cl_2]_2$	<2[c]
3	$[Ru(cod)Cl_2]_n$	22	10	$[Ru(p\text{-cymene})Cl_2]_2$	0[d]
4	$[Ru(cod)(methylallyl)_2]$	2	11	$[Ru(p\text{-cymene})Cl_2]_2$	0[e]
5	$[RuCp^*Cl_2]_n$	0	12	$[Ru(p\text{-cymene})Cl_2]_2$	87[f]
6	$[RuCp^*(PPh_3)_2Cl]$	0	13	$[Ru(p\text{-cymene})Cl_2]_2$	95[f,g]
7	none	0	14	$[Ru(p\text{-cymene})Cl_2]_2$	100[f,h]

[a] Reaction condition: benzophenone (0.2 mmol, 1.0 equiv), diphenylacetylene (0.2 mmol), Ru-complex (3 mol%), THF (0.7 mL), 60 °C 24h. [b] GC yield. [c] With IMes (6 mol%). [d] With SIPr (6 mol%). [e] With SIMes (6 mol%). [f] Ru-complex (5 mol%), NaOAc (10 mol%), IPr (10 mol%). [g] Diphenylacetylene (0.24 mmol, 1.2 equiv), THF (1.0 mL). [h] Benzophenone (0.24 mmol, 1.2 equiv), THF (1.0 mL).

3.4. Substrate Scope

With the optimized reaction conditions in hand, we explored the aryl ketone substrate scope of Ru-catalyzed carbocyclization of aryl ketones and alkynes to form indenols. As shown in Figure 3.2, a variety of aryl ketones (**3.09**) were converted into the desired indenol products via reaction with diphenylacetylene (**3.01c**) as the alkyne substrate. Compared to diaryl ketones, aryl alkyl ketones gave relatively lower yields, which decreased with increasing steric bulkiness of the alkyl group (**3.03b**-**3.03f**). Acetophenones with both electron donating and electron withdrawing aromatic substituents (methyl, methoxy and halides) were suitable substrates in this catalytic system. Electron-deficient acetophenones gave higher yields (**3.03i**-**3.03l**) than their electron-rich analogues (**3.03g**, **3.03h**). When 2,2,2-

trifluoroacetopenone (**3.09m**) was subjected to the standard reaction conditions, quantitative yield of the corresponding indenol product (**3.03m**) was obtained.

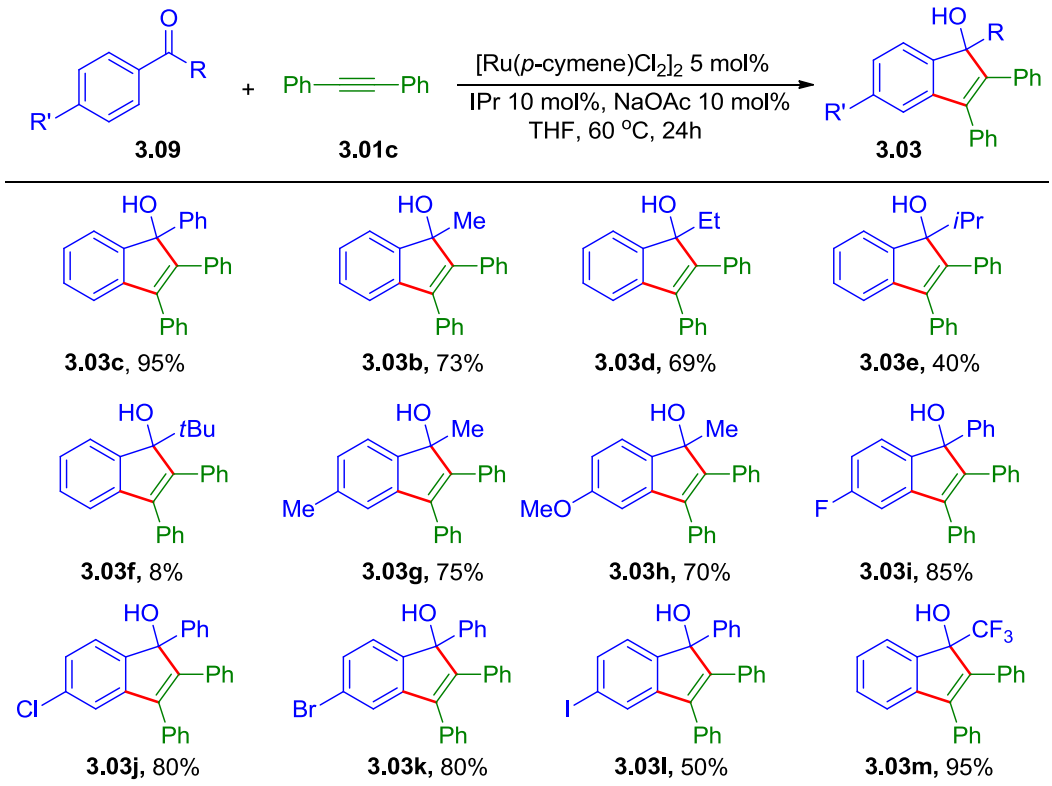

[a] Reaction conditions: aromatic ketone (0.6 mm, 1.2 eq.), diphenylacetylene (0.5 mm, 1.0 eq.), [Ru(*p*-cymene)Cl_2]$_2$ (5 mol%), IPr (10 mol%), NaOAc (10 mol%), THF (1.0 mL), 60 °C, 24h. [b] Isolated yields based on two runs.

Figure 3.2. Aromatic ketone substrate scope in ruthenium(II)/NHC catalyzed carbocyclization with aromatic ketones and internal alkynes[a,b]

Next, the alkyne substrate scope was examined with unsymmetrical arylalkyl acetylenes and symmetrical dialkyl acetylenes. However, these alkynes were inactive under the standard reaction conditions. Higher catalyst loading and higher reaction temperature was applied to the reaction between 1-phenyl-1-propyne (**3.01b**) and benzophenone (**3.09c**) (Scheme 3.12). Only 17% of the indenol product (**3.03n**) was isolated under elevated temperature of 140 °C and in the presence of 10 mol% Ru catalyst, which suggested a Ru-mediated stoichiometric transformation rather than catalytic reaction.

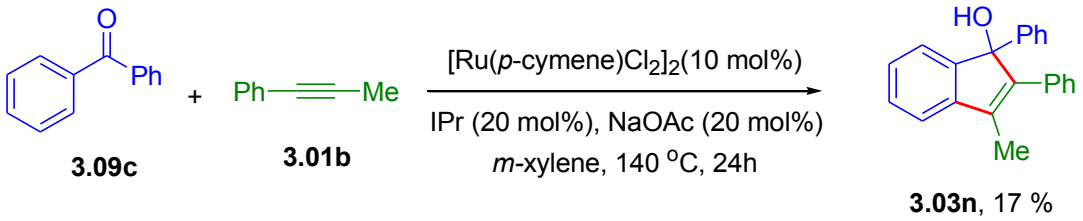

Scheme 3.12. Ruthenium(II)/NHC catalyzed carbocyclization with benzophenone and 1-phenyl-1-propyne

In Glorius and Cheng's Rh(III) catalyst systems, stoichiometric $Cu(OAc)_2$ was necessary to generate satisfactory yields.[17,18] In contrast, Jeganmohan's Ru(II) catalyst system required $Cu(OAc)_2$ as a co-catalyst.[24] Both $Cu(OAc)_2$ and $AgSbF_6$ additives were proposed to undergo transmetalation with Rh(II)-O or Ru(II)-O species to regenerate the catalyst. We hypothesized that the low reactivity with alkyl substituted alkyne substrates may be caused by slow transmetalation. However, when we introduced stoichiometric or catalytic amount of Cu and/or Ag salts in our catalytic system, no carbocyclization product was detected. It was also possible that Ag(I) and Cu(II) species competed against the Ru(II) catalyst precursor to coordinate with IPr ligand and deactivated the catalytic system. To test this hypothesis, a NHC-ligated Ru(II) complex, Ru(p-cymene)(IPr)Cl_2 was prepared[27] and evaluated as the catalyst precursor. However, the reactivity towards carbocyclization with alkyl substituted alkynes was not improved.

Based on these results, we proposed that the catalytic cycle for Ru-catalyzed carbocyclization with N-H ketimines and internal alkynes could also be applied to this Ru-catalyzed carbocyclization of aryl ketones and diphenylacetylene (Scheme 3.13). The cationic Ru catalyst would effectively coordinate to the carbonyl group and activate the *ortho*-C-H bond to generate a ruthenalcycle intermediate. This carbonyl-directed C-H activation likely proceeded by the concerted metalation-deprotonation (CMD) pathway in the presence of acetate additives. Next, alkyne insertion into the Ru-aryl bond gave a Ru alkenyl intermediate. Subsequent ketone insertion into the Ru-alkenyl linkage resulted in a Ru alkoxide intermediate, which released the indenol products upon protonation. The cationic nature of Ru complexes would facilitate both the C-H bond activation and cyclization steps. The nature of the rate-determining

step and other mechanistic details of this proposed catalytic cycle remain unclear and require a more systematic investigation in the future.

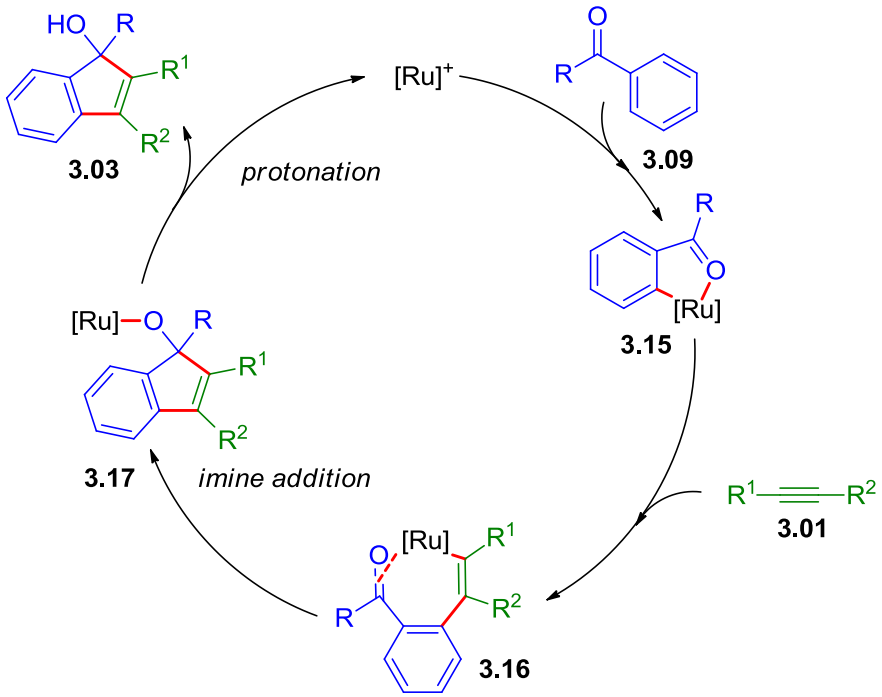

Scheme 3.13 Proposed reaction mechanism for ruthenium(II)/NHC catalyzed carbocyclization with aromatic ketones and internal alkynes

3.5. Conclusion

In summary, we have developed a Ru(II)-catalyzed [3+2] carbocyclization between aryl ketones and alkynes to form indenol derivatives under mild reaction conditions. Ketone-directed C-H bond activation and carbocyclization with alkynes was achieved without strong oxidant or heavy metal additives. The alkyne substrate scope was currently limited to diaryl-substituted alkynes, and further efforts are required to better understand the reaction mechanism and to improve the catalyst system for extended alkyne substrate scope.

3.6. Experimental Procedures

3.6.1. General Information

Unless otherwise noted, all manipulations were carried out under a nitrogen atmosphere using standard Schlenk-line or glovebox techniques. All glassware was oven-dried for at least 1 h prior to use. THF, toluene, ether, and hexane were degassed by purging with nitrogen for 45 min and dried with a solvent purification system (MBraun MB-SPS). DMF, dioxane, dimethoxyethane, dichloroethane, methanol, and ethanol were dried over activated 3 Å molecular sieves and degassed by purging with nitrogen. Other reagents and substrates were commercially available and used as received. TLC plates were visualized by exposure to ultraviolet light. Organic solutions were concentrated by rotary evaporation at ~10 torr. Flash column chromatography was performed with 32–63 microns silica gel. GC analyses were performed on a Shimadzu GC-2010 with *n*-dodecane as the internal standard. ^{1}H NMR spectra were obtained on a 400 MHz spectrometer, and chemical shifts were recorded relative to residual protiated solvent. ^{13}C NMR spectra were obtained at 100 MHz, and chemical shifts were recorded relative to the solvent resonance. Both ^{1}H and ^{13}C NMR chemical shifts were reported in parts per million downfield from tetramethylsilane (δ = 0 ppm). High-resolution mass spectra were obtained at a BrukerDaltronicsBioTOF HRMS spectrometer.

3.6.2. Preparation and X-Ray Diffraction Analysis of [Ru(cod)[η^2-OC(C_6H_5)C_6H_4]$_2$} (**3.14**)

Into a 20 mL scintillation vial equipped with a magnetic stir bar was added Ru(cod)(methylallyl)$_2$ (320 mg, 1.0 mmol), benzophenone (364 mg, 2.0 mmol) and 10 mL toluene. The mixture was stirred under 80 °C for 5 hours. All volatiles were removed under reduced pressure, and the residue was washed with hexane (3X), dried under vacuum, and afforded the desired complex as a brown powder (400 mg, 70 %). Recrystalization was carried out using a solvent system of toluene/pentane to afford single crystals that were suitable for X-ray diffraction analysis.

Single crystal X-ray diffraction data of Ru(cod)[η^2-OC(C_6H_5)C_6H_4]$_2$ (**3.14**) was collected on a Bruker Apex Duo diffractometer with a Apex 2 CCD area detector at T = 100K and using Cu radiation. Structures were processed with Apex 2 v2013.4-1 software package with the latest versions of SAINT

and SHELX software. Multi-scan absorption correction (SADABS 2012/1) was applied, and direct method was used to solve the structures. Details of data collection and refinement are given in Table 3.5 and 3.6.

Table 3.4. Summary of cell parameters, data collection and structural refinements for {Ru(cod)[η^2-OC(C_6H_5)C_6H_4]$_2$} (**3.14**)

Empirical formula	$C_{34}H_{30}O_2Ru$
Formula weight	573.67
Temperature, K	100
Wavelength, (Å)	1.54178
space group	$P2_1/c$
a/Å	16.9103(3)
b/Å	16.2919(3)
c/Å	18.8998(4)
α, deg	90
β,deg	103.222(1)
γ, deg	90
V, Å	5068.88(17)
Z	8
d_{calcd}, g/cm^3	1.503
μ, mm^{-1}	5.238
F(000)	2368.0
Theta range, deg	3.82 ÷ 66.61
h, k, l ranges	-20 ÷ 20, -19 ÷ 19, -21 ÷ 22
Reflections collected/unique	30544
Unique Reflections/gt	8821/7035
COOF on F^2	1.008
R_1, wR_2 ($I>2\sigma(I)$)[a]	3.17%, 7.34%
R_1, wR_2 (all data)	4.76%, 7.97%
Largest diff. peak and hole (e. Å $^{-3)}$	0.072

[a] R1 = $\Sigma||F_o| - |F_c|| / \Sigma|F_o|$, wR2 = $[\Sigma w[(F_o)^2 - (F_c)^2]^2 / \Sigma w(F_o^2)^2]^{1/2}$ for $F_o^2 > 2\sigma(F_o^2)$, w = $[\sigma^2(F_o)^2 + (AP)^2 + BP]^{-1}$ where P = $[[(F_o)^2 + 2(F_c)^2] / 3$ and A (B) = 0.0405 (2.2364);

Table 3.5. Selected average bond lengths [Å] and bond angles [degree] for {Ru(cod)[η^2-OC(C_6H_5)C_6H_4]$_2$} (**3.14**)

bond length [Å]		bond angles [degree]	
Ru(1)-O(1)	2.077(2)	O(1)-Ru-O(2)	162.52(8)
Ru-O(2)	2.077(2)	C(4)-Ru-C(10)	91.9(1)
Ru-C(1)	2.019(4)	C(4)-Ru-C(9)	92.2(1)
Ru-C(4)	2.018(3)	C(4)-Ru-C(8)	155.7(1)
Ru-C(7)	2.307(3)	C(4)-Ru-C(7)	167.9(1)
Ru-C(8)	2.275(3)	C(1)-Ru-C(4)	89.4(1)
Ru-C(9)	2.298(4)	C(1)-Ru-C(10)	155.7(1)
Ru-C(10)	2.260(3)	C(1)-Ru-C(9)	169.3(1)
C(1)-C(2)	1.427(4)	C(1)-Ru-C(8)	96.1(1)
C(2)-C(3)	1.441(4)	C(1)-Ru-C(7)	95.1(1)
C(3)-O(1)	1.261(4)	O(1)-Ru-C(7)	79.1(1)
C(4)-C(5)	1.431(4)	O(1)-Ru-C(8)	113.4(1)
C(5)-C(6)	1.451(4)	O(1)-Ru-C(9)	112.6(1)
C(6)-O(2)	1.266(4)	O(1)-Ru-C(10)	77.8(1)
C(7)-C(8)	1.373(4)	O(2)-Ru-C(7)	112.8(1)
C(9)-C(10)	1.363(4)	O(2)-Ru-C(8)	78.0(1)
		O(2)-Ru-C(9)	82.0(1)
		O(2)-Ru-C(10)	116.0(1)
		O(2)-Ru-C(4)	78.5(1)
		O(1)-Ru-C(1)	77.9(1)
		Ru-C(1)-C(2)	114.9(2)
		C(1)-C(2)-C(3)	112.8(3)
		C(2)-C(3)-O(1)	117.1(3)
		C(3)-O(1)-Ru	117.2(2)
		C(4)-C(5)-C(6)	112.6(3)
		C(5)-C(6)-O(2)	117.1(3)
		Ru-C(4)-C(5)	114.6(2)
		C(7)-Ru-C(8)	34.9(1)
		C(6)-O(2)-Ru	116.5(2)
		C(9)-Ru-C(10)	34.8(1)
		C(8)-Ru-C(9)	78.4(1)
		C(7)-Ru-C(10)	79.4(1)

3.6.3. General Procedure for Ruthenium(II)/NHC-Catalyzed [3+2] Annulation

Into a 4.0 mL scintillation vial equipped with a magnetic stir bar was placed the alkyne substrate **3.01** (0.1 mmol, 1.0 equiv.), the ketone substrate **3.09** (1.1 equiv.) and a stock solution of Ru(II) catalyst and carbene ligand in hexane solvent (0.5 mL). The stock solution contains [Ru(cod)(methylallyl)$_2$] (0.03 equiv.) and IPr-NHC ligand (0.033 equiv.). The vial was sealed with a silicone-lined screw-cap and stirred at room temperature in glovebox for 24 h. In case heating is needed for complete conversion, the vial was transferred out of the glovebox and stirred in a 60 °C or 80 °C oil bath for 24 h. The reaction mixture was then cooled to room temperature, and all volatile materials were removed under reduced pressure. Further purification was achieved by flash column chromatography. Yields of the isolated products are based on the average of two runs under identical conditions.

3.6.4 Spectral Data for [3+2] Annulation Products

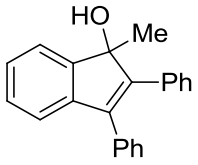

3.03b

1-Methyl-2,3-diphenyl-1H-inden-1-ol (**3.03b**): Chromatography (1:6 ethyl acetate/hexane, R_f = 0.35) gave **3.03b** as a yellow solid (109.0 mg, 73 %). ^{1}H NMR (400 MHz, $CDCl_3$): δ = 7.53 – 7.51 (m, 1H), 7.44–7.42 (m, 2H), 7.36–7.20 (m, 11H), 2.03 (s, 1H, -OH), 1.58 ppm (s, 3H); ^{13}C NMR (100 MHz, $CDCl_3$): δ = 149.7, 147.2, 142.4, 138.9, 135.0, 134.9, 129.6, 129.5, 128.72, 128.66, 128.2, 127.8, 127.5, 126.8, 122.1, 121.0, 83.5, 24.2 ppm; HRMS: m/z calcd for $C_{22}H_{18}ONa^+$: 321.1250; found: 321.1251.

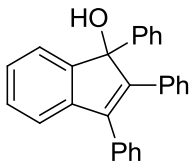

3.03c

1-Phenyl-2,3-diphenyl-1H-inden-1-ol (**3.03c**): Chromatography (1:6 ethyl acetate/hexane, R_f = 0.40) gave **3.03c** as a brown solid (180.2 mg, >98 %). ^{1}H NMR (400 MHz, $CDCl_3$): δ = 7.59–7.56 (m, 2H),

7.48–7.38 (m, 5H), 7.33–7.18 (m, 7H), 7.13–7.05 (m, 5H), 2.51 ppm (s, 1H, -OH); ^{13}C NMR (100 MHz, $CDCl_3$): δ = 151.0, 147.6, 142.9, 140.9, 135.0, 134.0, 129.7, 129.5, 129.0, 128.70, 128.66, 128.1, 127.5, 127.31, 127.29, 125.3, 123.3, 121.3, 87.2 ppm; HRMS: m/z calcd for $C_{24}H_{22}ONa^+$: 383.1406; found:383.1416.

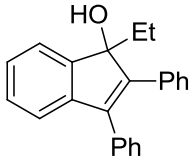

3.03d

1-Ethyl-2,3-diphenyl-1H-inden-1-ol (**3.03d**): Chromatography (1:6 ethyl acetate/hexane, R_f =0.40) gave **3.03d** as a brown solid (107.8 mg, 69 %). ^{1}H NMR (400 MHz, $CDCl_3$): δ = 7.47–7.42 (m, 3H), 7.35–7.29 (m, 5H), 7.26 – 7.23 (m, 2H), 7.22–7.19 (m, 4H), 2.11 (dq, *J* = 7.4, 14.9 Hz, 1H), 2.11 (m, 1H, OH), 1.93 (dq, *J* = 7.4, 14.9 Hz, 1H), 0.56 ppm (t, *J* = 7.4 Hz, 3H); ^{13}C NMR (100 MHz, $CDCl_3$): δ = 148.0, 145.4, 143.5, 140.6, 135.1, 135.0, 129.6, 129.5, 128.7, 128.6, 128.2, 127.8, 127.5, 126.7, 122.2, 120.8, 87.2, 30.1, 8.14 ppm; HRMS: m/z calcd for $C_{23}H_{20}ONa^+$: 335.1406; found:335.1406.

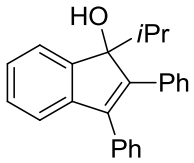

3.03e

1-Isoprppyl-2,3-diphenyl-1H-inden-1-ol (**3.03e**): Chromatography (1:6 ethyl acetate/hexane, R_f = 0.50) gave **3.03e** as a brown solid (65.3 mg, 40 %). ^{1}H NMR (400 MHz, $CDCl_3$): δ = 7.51 (dq, *J* = 6.2, 1.4 Hz, 1H), 7.45-7.42 (m, 2H), 7.34–7.19 (m, 11H), 2.86 ppm (s, 1H, -OH); ^{13}C NMR (100 MHz, $CDCl_3$): δ= 146.8, 146.5, 144.0, 140.5, 135.6, 134.9, 129.8, 129.5, 128.7, 128.5, 128.2, 127.7, 127.4, 126.2, 123.7, 120.8, 89.3, 34.2, 17.04, 16.98 ppm; HRMS: m/z calcd for $C_{24}H_{22}ONa^+$: 349.3163; found:349.3165.

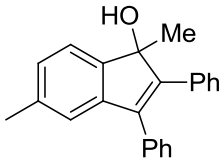

3.03g

1,5-Dimethyl-2,3-diphenyl-1H-inden-1-ol (**3.03g**): Chromatography (1:6 ethyl acetate/hexane, R_f = 0.40) gave **3.03g** as a yellow solid (117.2 mg, 75 %). ^{1}H NMR (400 MHz, $CDCl_3$): δ = 7.46–7.44 (m, 2H), 7.42 (d, *J* = 7.48 Hz, 1H), 7.38–7.32 (m, 5H), 7.25–7.22 (m, 3H), 7.10 (d, *J* = 7.47 Hz, 1H), 7.06 (s, 1H), 2.36 (s, 3H), 2.11 (s, 1H, -OH), 1.59 ppm (s, 3H); ^{13}C NMR (100 MHz, $CDCl_3$): δ = 147.5, 147.0, 142.6, 138.9, 138.5, 135.03, 135.02, 129.6, 129.5, 128.7,128.1, 127.7, 127.4, 127.3, 121.82, 121.77, 83.33, 24.3, 21.8 ppm; HRMS: m/z calcd for $C_{23}H_{20}ONa^+$: 335.1408; found: 335.1406.

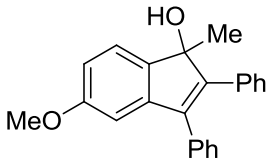

3.03h

5-Methoxy-1-methyl-2,3-diphenyl-1H-inden-1-ol (**3.03h**): Chromatography (1:6 ethyl acetate/hexane, R_f = 0.25) gave **3.03h** as a yellow solid (116.5 mg, 70 %). ^{1}H NMR (400 MHz, $CDCl_3$): δ = 7.44–7.40 (m, 3H), 7.35–7.29 (m, 5H), 7.23–7.21 (m, 3H), 6.79–6.75 (m, 2H), 3.76 (s, 3H), 2.18 (bs, 1H, -OH), 1.56 ppm (s, 3H); ^{13}C NMR (100 MHz, $CDCl_3$): δ = 160.6, 148.5, 144.1, 142.0, 138.5, 135.0, 134.9, 129.7, 129.5, 128.8, 128.2, 127.8, 127.5, 122.7, 111.3, 107.7, 83.0, 55.8, 24.4 ppm; HRMS: m/z calcd for $C_{23}H_{20}O_2Na^+$: 351.1356; found: 351.1353.

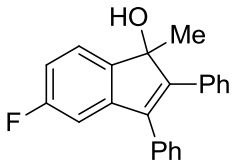

3.03i

5-Fluoro-1-methyl-2,3-diphenyl-1H-inden-1-ol (**3.03i**): Chromatography (1:6 ethyl acetate/hexane, R_f = 0.35) gave **3.03i** as a yellow solid (134.5 mg, 85 %). ^{1}H NMR (400 MHz, $CDCl_3$): δ= 7.45–7.41 (m, 3H), 7.36–7.27 (m, 5H), 7.24–7.21 (m, 3H), 6.95–6.89 (m, 2H), 2.21 (bs, 1H, -OH), 1.56 ppm (s, 3H); ^{13}C NMR (100 MHz, $CDCl_3$): δ = 163.7 (d, *J* = 244.8 Hz), 148.9, 145.1 (d, *J* = 2.7 Hz), 144.6 (d, *J* = 8.7 Hz), 138.0 (d, *J* = 2.8 Hz), 134.6, 134.3, 129.5, 129.3, 128.8, 128.2, 128.0, 127.8, 123.1 (d, *J* = 9.0 Hz), 112.9 (d, *J* = 22.9 Hz), 108.6 (d, *J* = 24.2 Hz), 82.9, 24.3 ppm; HRMS: m/z calcd for $C_{22}H_{17}OFNa^+$: 339.1156; found: 339.1152.

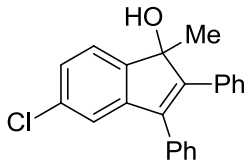

3.03j

5-Chloro-1-methyl-2,3-diphenyl-1H-inden-1-ol (**3.03j**): Chromatography (1:6 ethyl acetate/hexane, R_f = 0.50) gave **3.03j** as a yellow solid (133.2 mg, 80 %). ^{1}H NMR (400 MHz, $CDCl_3$): δ = 7.44–7.39 (m, 3H), 7.37–7.31 (m, 3H), 7.29–7.27 (m, 2H), 7.24–7.22 (m, 4H), 7.20 (d, *J* = 1.8 Hz, 1H), 2.25 (s, 1 H, -OH), 1.56 ppm (s, 3H); ^{13}C NMR (100 MHz, $CDCl_3$): δ = 148.6, 148.0, 144.7, 138.1, 134.6, 134.5, 134.2, 129.53, 129.45, 129.3, 128.9, 128.2, 128.0, 127.8, 124.1, 123.5, 122.6, 83.1, 24.1 ppm; HRMS: m/z calcd for $C_{22}H_{17}OClNa^+$: 355.0860; found: 355.0853.

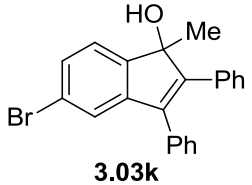

3.03k

5-Bromo-1-methyl-2,3-diphenyl-1H-inden-1-ol (**3.03k**): Chromatography gave **3.03k** as a yellow solid (133.2 mg, 80 %). ^{1}H NMR(400 MHz, $CDCl_3$): δ = 7.42–7.39 (m, 2H), 7.38 (d, *J* = 1.84 Hz, 1H), 7.35–7.31 (m, 5H), 7.28–7.26 (m, 2H), 7.23–7.21 (m, 3H), 2.18 (s, 1H, -OH), 1.55 ppm (s, 3H); ^{13}C NMR (100 MHz, $CDCl_3$): δ = 148.4, 144.5, 138.0, 134.4, 134.2, 134.3, 129.6, 129.4, 128.9, 128.3, 128.1, 127.9, 126.6, 123.1, 121.3, 83.1, 24.2 ppm; HRMS: m/z calcd for $C_{22}H_{17}OBrNa^+$: 399.0355; found: 399.0352.

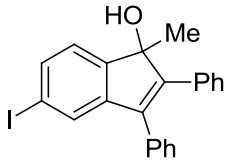

3.03l

5-Iodo-1-methyl-2,3-diphenyl-1H-inden-1-ol (**3.03l**): Chromatography (1:6 ethyl acetate/hexane, R_f = 0.40) gave **3.03l** as a brown solid (106.1 mg, 50 %). ^{1}H NMR(400 MHz, $CDCl_3$): δ = 7.60 (dd, *J* = 7.7, 1.5 Hz, 1H), 7.51 (d, *J* = 1.5 Hz, 1H), 7.41–7.38 (m, 2H), 7.36–7.30 (m, 3H), 7.27–7.25 (m, 3H), 7.22–7.20 (m, 3H), 2.01 (s, 1H, -OH), 1.55 ppm (s, 3H); ^{13}C NMR (100 MHz, $CDCl_3$): δ= 149.2, 148.2, 144.6,

138.0, 135.6, 134.4, 134.2, 130.0, 139.6, 129.3, 128.9, 128.3, 128.1, 127.8, 123.9, 94.3, 83.3, 24.1ppm; HRMS: m/z calcd for $C_{22}H_{17}OINa^+$: 447.0216; found: 447.0208.

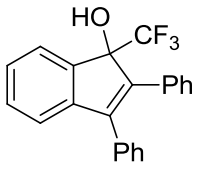

3.03m

1-Trifluoromethyl-2,3-diphenyl-1H-inden-1-ol (**3.03m**): Chromatography (1:6 ethyl acetate/hexane, R_f = 0.40) gave **3.03m** as a brown solid (176.1 mg, >98 %). ^{1}H NMR (400 MHz, $CDCl_3$): δ = 7.66 (d, *J* = 7.6 Hz, 1H), 7.39-7.423 (m, 13H), 2.18 (dt, *J* = 13.7, 6.8 Hz, 1H), 2.13 (bs, 1H, -OH), 1.23 (d, *J* = 6.8 Hz, 3H), 0.58 ppm (d, *J* = 6.8 Hz, 3H) ; ^{13}C NMR (100 MHz, $CDCl_3$): δ = 145.3, 144.2, 141.0, 140.2, 133.8, 133.4, 130.6, 129.8, 129.3, 128.7, 128.1, 127.5, 126.4, 124.4, 123.6, 121.7 ppm; HRMS: m/z calcd for $C_{24}H_{22}ONa^+$: 375.0967; found:375.0968.

3.7. References

1. Liebeskind, L. S.; Gasdaska, J. R.; McCallum, J. S.; Tremont, S. J. Ortho-Functionalization of Aromatic Ketones via Manganation. A Synthesis of Indenols. *J. Org. Chem.* **1989**, *54*, 669-677.

2. Cambie, R. C.; Metzler, M. R.; Rutledge, P. S.; Woodgate, P. D. Cyclomanganation of Diterpenoids; Functionalization of C14. *J. Organomet. Chem.* **1990**, *381*, C26-C30.

3. Cambie, R. C.; Metzler, M. R.; Rutledge, P. S.; Woodgate, P. D. Synthesis and Reactions of η^2-(2-Formylphenyl)tetracarbonylmanganese(I) Complexes; Cyclopentaanulation of a Diterpenoid. *J. Organomet. Chem.* **1990**, *398*, C22-C24.

4. Robinson, N. P.; Main, L.; Nicholson, B. K. Reactions of *ortho*-Manganated Aryl-Ketones, Aldehydes and Amides with Alkynes; A New Synthesis of Inden-1-ols and Indenones. *J. Organomet. Chem.* **1989**, *364*, C37-C39.

5. Vicente, J.; Abad, J.-A.; Gil-Rubio, J. Palladium-Assisted Formation of Carbon−Carbon Bonds. 6.1 Study of the Reactivity of (*o*-Formylaryl)- or (*o*-Acetylaryl)palladium Complexes with Alkynes. Synthesis of Indenones and Indenols. *Organometallics* **1996**, *15*, 3509-3519.

6. Vicente, J.; Abad, J.-A.; López-Peláez, B.; Martínez-Viviente, E. Synthesis and Reactivity toward Alkynes of 2-Formyl- and 2-Acetylarylpalladium(II) (Aryl = Phenyl and 5-Nitrophenyl) Complexes. Formation of Indenols and Indenones. *Organometallics* **2001**, *21*, 58-67.

7. Quan, L. G.; Gevorgyan, V.; Yamamoto, Y. Intramolecular Nucleophilic Addition of Vinylpalladiums to Aryl Ketones. *J. Am. Chem. Soc.* **1999**, *121*, 3545-3546.

8. Quan, L. G.; Gevorgyan, V.; Yamamoto, Y. Intramolecular Nucleophilic Addition of Vinylpalladiums to Aryl Ketones. *J. Am. Chem. Soc.* **1999**, *121*, 9485-9485.

9. Rayabarapu, D. K.; Cheng, C.-H. Nickel-Catalyzed Regioselective Carbocyclization of *ortho*-Halophenyl Ketones with Propiolates: An Efficient Route to Disubstituted Indenols. *Chem. Commun.* **2002**, 942-943.

10. Chang, K.-J.; Rayabarapu, D. K.; Cheng, C.-H. Cobalt-Catalyzed Carbocyclization of *o*-Iodobenzaldehydes and *o*-Iodophenylketones with Alkynes. *Org. Lett.* **2003**, *5*, 3963-3966.

11. Rayabarapu, D. K.; Yang, C.-H.; Cheng, C.-H. Regioselective Synthesis of Indenols via Nickel-Catalyzed Carbocyclization Reaction. *J. Org. Chem.* **2003**, *68*, 6726-6731.

12. Chang, K.-J.; Rayabarapu, D. K.; Cheng, C.-H. Cobalt-Catalyzed Regioselective Carbocyclization Reaction of *o*-Iodophenyl Ketones and Aldehydes with Alkynes, Acrylates, and Acrylonitrile: A Facile Route to Indenols and Indenes. *J. Org. Chem.* **2004**, *69*, 4781-4787.

13. Matsuda, T.; Makino, M.; Murakami, M. Synthesis of 1*H*-Inden-1-ol Derivatives via Rhodium-catalyzed Annulation of *o*-Acylphenylboronic Acids with Alkynes. *Chem. Lett.* **2005**, *34*, 1416-1417.

14. Harris, P. W. R.; Rickard, C. E. F.; Woodgate, P. D. Ruthenium-Catalysed *ortho* Vinylation of Aromatic Ketones with Alkynes; Unexpected Cyclopentaannulation. *J. Organomet. Chem.* **1999**, *589*, 168-179.

15. Tsuchikama, K.; Kasagawa, M.; Hashimoto, Y.-K.; Endo, K.; Shibata, T. Cationic Iridium–BINAP Complex-Catalyzed Addition of Aryl ketones to Alkynes and Alkenes via Directed C–H Bond Cleavage. *J. Organomet. Chem.* **2008**, *693*, 3939-3942.

16. Tsuchikama, K.; Kasagawa, M.; Endo, K.; Shibata, T. Sequential Catalytic Reactions for the Synthesis of Benzofulvenes Using an Iridium Complex with Dual Function. *Synlett* **2010**, *2010*, 97-100.

17. Muralirajan, K.; Parthasarathy, K.; Cheng, C. H. Regioselective Synthesis of Indenols by Rhodium-Catalyzed C-H Activation and Carbocyclization of Aryl Ketones and Alkynes. *Angew. Chem. Int. Ed.* **2011**, *50*, 4169-4172.

18. Patureau, F. W.; Besset, T.; Kuhl, N.; Glorius, F. Diverse Strategies toward Indenol and Fulvene Derivatives: Rh-Catalyzed C-H Activation of Aryl Ketones Followed by Coupling with Internal Alkynes. *J. Am. Chem. Soc.* **2011**, *133*, 2154-2156.

19. Lautens, M.; Klute, W.; Tam, W. Transition Metal-Mediated Cycloaddition Reactions. *Chem. Rev.* **1996**, *96*, 49-92.

20. Ojima, I.; Tzamarioudaki, M.; Li, Z.; Donovan, R. J. Transition Metal-Catalyzed Carbocyclizations in Organic Synthesis. *Chem. Rev.* **1996**, *96*, 635-662.

21. Frühauf, H.-W. Metal-Assisted Cycloaddition Reactions in Organotransition Metal Chemistry. *Chem. Rev.* **1997**, *97*, 523-596.

22. Zhang, X.-S.; Chen, K.; Shi, Z.-J. Transition Metal-Catalyzed Direct Nucleophilic Addition of C-H Bonds to Carbon-Heteroatom Double Bonds. *Chem. Sci.* **2014**, *5*, 2146-2159.

23. Zheng, Q.-Z.; Jiao, N. Transition-Metal-Catalyzed Ketone-Directed *ortho*-C–H Functionalization Reactions. *Tetrahedron Lett.* **2014**, *55*, 1121-1126.

24. Chinnagolla, R. K.; Jeganmohan, M. Ruthenium-Catalyzed Regioselective Cyclization of Aromatic Ketones with Alkynes: an Efficient Route to Indenols and Benzofulvenes. *Eur. J. Org. Chem.* **2012**, *2012*, 417-423.

25. Zhang, J.; Ugrinov, A.; Zhao, P. Ruthenium(II)/N-Heterocyclic Carbene Catalyzed [3+2] Carbocyclization with Aromatic N-H Ketimines and Internal Alkynes. *Angew. Chem. Int. Ed.* **2013**, *52*, 6681-6684.

26. Engle, K. M.; Mei, T.-S.; Wasa, M.; Yu, J.-Q. Weak Coordination as a Powerful Means for Developing Broadly Useful C–H Functionalization Reactions. *Acc. Chem. Res.* **2011**, *45*, 788-802.

27. Jafarpour, L.; Huang, J.; Stevens, E. D.; Nolan, S. P. (p-Cymene)RuLCl$_2$ (L = 1,3-Bis(2,4,6-trimethylphenyl)imidazol-2-ylidene and 1,3-Bis(2,6-diisopropylphenyl)imidazol-2-ylidene) and Related Complexes as Ring Closing Metathesis Catalysts. *Organometallics* **1999**, *18*, 3760-3763.

CHAPTER 4. EXPLORING BIS(CYCLOMETALATED) RUTHENIUM(II) COMPLEXES AS ACTIVE CATALYST PERCURSORS: ROOM-TEMPERATURE ALKENE-ALKYNE COUPLING FOR 1,3-DIENE SYNTHESIS

4.1. Background and Significance

The addition of aromatic C-H bonds across C-C triple bonds via transition metal-catalyzed functional group-directed C–H bond activation, pioneered by Murai (Scheme 1.7), provides a site-selective and atom-economical method to access alkenylated compounds.[1] A variety of transition metal catalysts have been developed for this transformation.[2-6] In contrast, the related addition of alkenyl C–H bonds across alkynes remains relatively underdeveloped.

Cross-coupling of alkynes with acrylate/acylamides was first reported by Mitsudo and Watanabe in 1991 to produce conjugated dienes in a highly regio- and stereoselective manner (Scheme 4.1).[7] In the presence of 2 mol% of Ru(cod)(cot), diphenylacetylene (**4.01**) reacted with acrylates (**4.02**) in pyridine at 80 ^{o}C to give α,β,γ,δ-unsaturated dienoates (**4.03**) in high yields. In comparison, N,N-dimethylacrylamide would react only in the absence of pyridine solvent with electron-rich internal alkynes, providing the desired products in moderate to good yields. This reaction was proposed to proceed via oxidative cyclization to form a ruthenacyclopentene complex (**4.04**) following coordination of an acetylene and an alkene to Ru(0) complex. Subsequent β-hydrogen elimination formed Ru-H complex (**4.05**) and successive C-H reductive elimination afforded the 1,3-diene product and regenerated the Ru(0) catalyst.

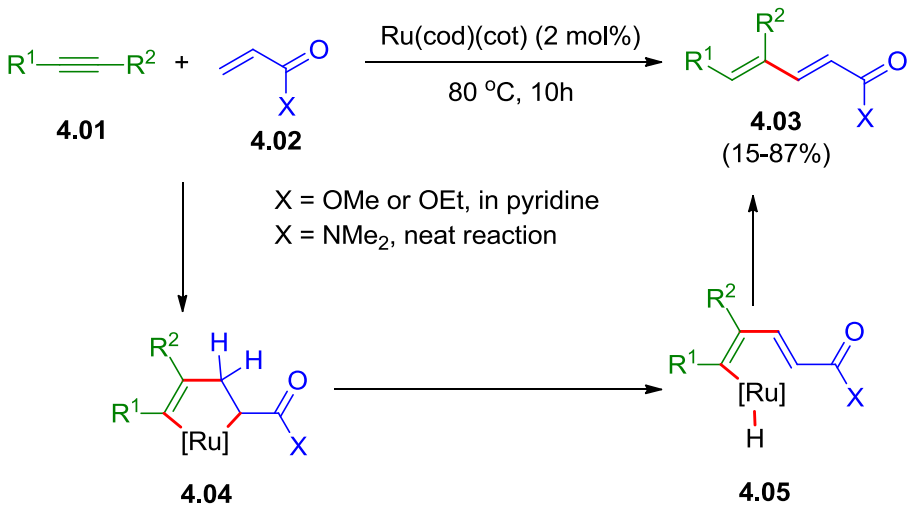

Scheme 4.1. Ruthenium catalyzed alkene-alkyne coupling to form 1,3-dienes via oxidative cyclization

In 1999, Yi described a cross-coupling of alkynes with ethylene to access conjugated dienes via a different reaction mechanism (Scheme 4.2).[8] A cationic ruthenium complex **4.06** was used as the catalyst precursor, which was proposed to generate a Ru-H species **4.07** *in situ* as the initial active intermediate in the catalytic cycle. Alkyne insertion into the Ru-H bond gave a vinyl-Ru intermediate **4.08**, followed by ethylene insertion in vinyl-Ru linkage to produce an alkyl-Ru intermediate **4.09**. Subsequent β-hydrogen elimination completed the catalytic cycle and gave the 1,3-diene product (**4.10**). Further vinylation of the product would generate a 1:2 coupling product **4.11**. For symmetric diaryl and dialkyl alkynes, high yields and stereoselectivity were achieved with trace amount of **4.11**. In comparison, terminal alkynes were more likely to give 1:2 coupling product **4.11**.

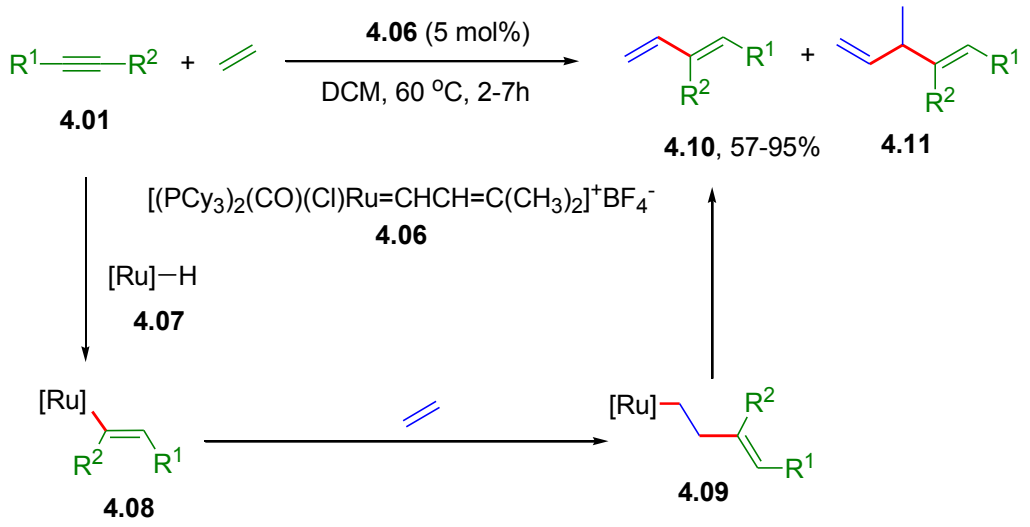

Scheme 4.2. Ruthenium catalyzed ethylene-alkyne coupling to form 1,3-dienes via alkyne insertion into Ru-H bond

In 2002, Murai extended the application of $[RuH_2(CO)(PPh_3)_3]$ catalyzed directed C-H bond activation to alkenylation of cyclic conjugate enones (**4.12**) with internal alkynes (**4.01**) (Scheme 4.3).[9] Cyclic conjugated dienones (**4.13**) was obtained in high yields in toluene under 135 °C, but the *E/Z* selectivity was highly dependent on the structure of the starting materials. The reaction proceeds via carbonyl directed C-H bond cleavage generating the ruthenacycle intermediate **4.14**, followed by alkyne coordination and migratory insertion gave the alkenyl ruthenium intermediate **4.15**. Subsequent C-C reductive elimination afforded conjugate dienone product (**4.13**).

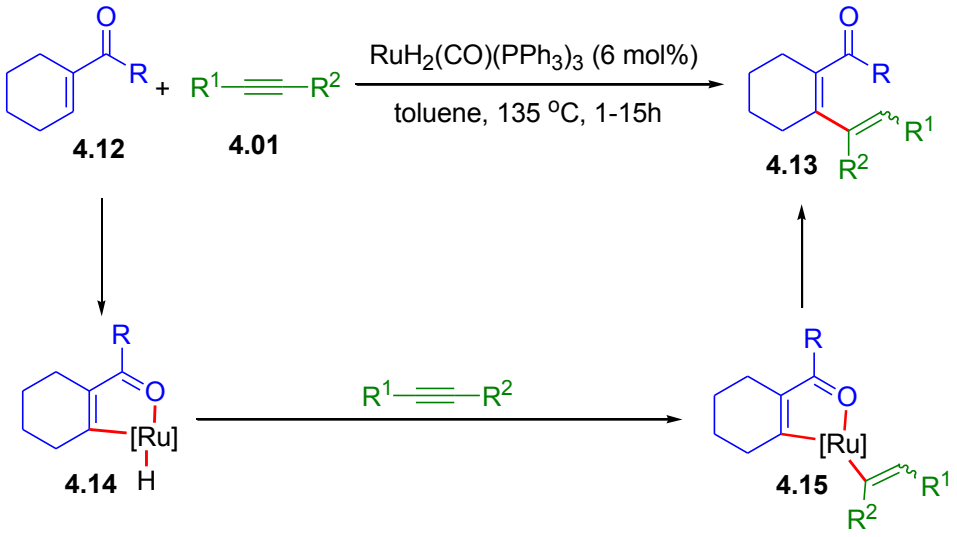

Scheme 4.3. Ruthenium catalyzed alkene-alkyne coupling to form 1,3-dienes via directed C-H bond activation

In these pioneering works, ruthenium complexes are used as catalyst precursors to promote alkene-alkyne cross-coupling to form 1,3-dienes via three different reaction pathways, which indicates ruthenium as a powerful metal with high potential to catalyze this transformation. Recently, several reports have been disclosed on further development of ruthenium catalysts.[10-13] For example, in 2007, Uemura reported cross-coupling of terminal phenylacetylenes (**4.01**) with acrylates (**4.02**) catalyzed by $Ru_3(CO)_{12}$.[10] The reaction was proposed to proceed via an alkyne insertion in Ru-H bond which was generated *in situ* from the catalyst precursor [$Ru_3(CO)_{12}$] (2 mol%) and LiI (10 mol%) (Scheme 4.4). However, conjugated dienoates (**4.03**) were only obtained in moderate yields with low stereoselectivity.

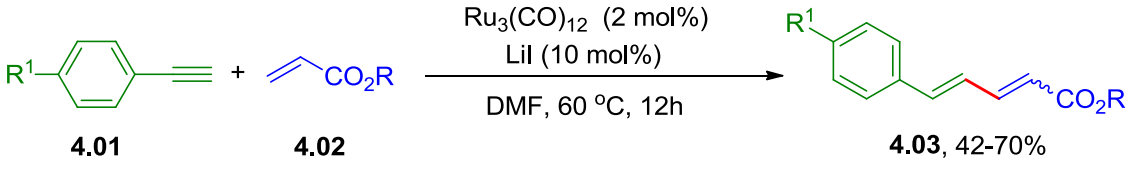

Scheme 4.4. Ruthenium catalyzed terminal alkyne-acrylate coupling via alkyne insertion into Ru-H bond

In 2009, Plietker reported a ruthenium catalyzed enyne coupling via directed C-H bond activation with broader alkene scope.[11] Highly substituted 1,3-dienes are accessible in good to excellent yields from the addition of vinyl C-H bond to internal alkynes using a readily accessible ruthenium hydride complex, [RuHCl(CO)(PPh_3)$_3$] (Scheme 4.5). However, the regio- and stereoselectivity were low for unsymmetrical internal alkynes and olefins with bulky substituents. In a follow-up study, the authors revealed that with the assistance of microwave radiance, intermolecular of terminal alkynes with methyl acrylates (**4.02a**) was much faster and gave conjugated olefins in good yield (Scheme 4.6).[12] However, in order to avoid the homocoupling of terminal alkynes, very high loading of methyl acrylate was required.

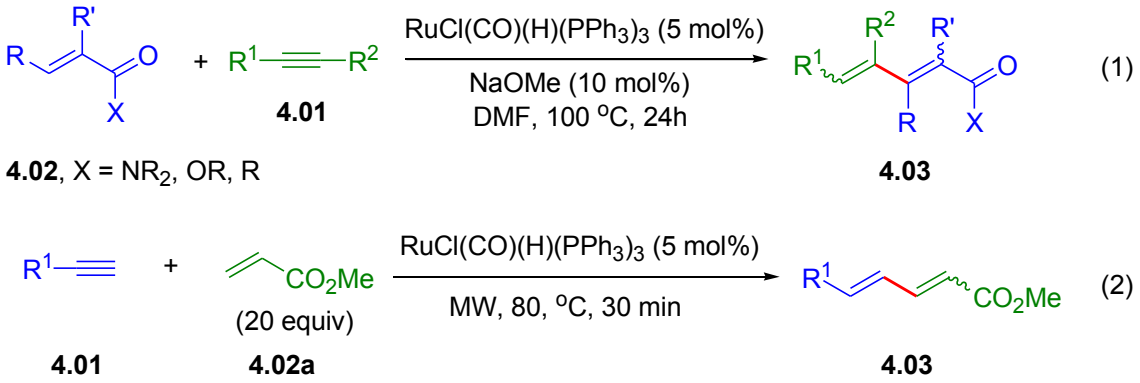

Scheme 4.5. Ruthenium catalyzed enyne coupling to form 1,3-dienes via directed C-H bond activation

More recently, Saito disclosed a ruthenium catalyzed cross-coupling of ynamides (**4.16**) with ethylene proceeded via oxidative cyclization under room temperature (Scheme 4.6).[13] In the presence of catalytic amount of [Cp*RuCl(cod)], 2-aminobuta-1,3-diene derivatives (**4.17**) were obtained in a highly regioselective manner. Terminal alkynes were not suitable substrates in this reaction. Besides, the olefin substrate was limited to ethylene.

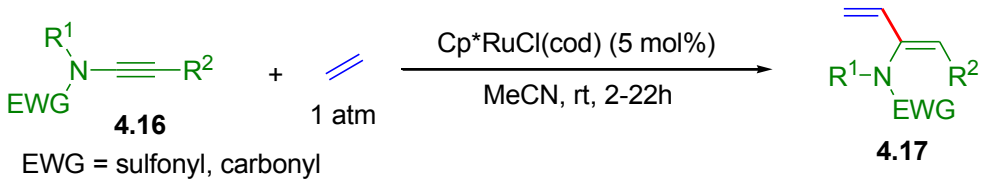

Scheme 4.6. Ruthenium catalyzed ynamide-ethylene coupling to form 2-aminobuta-1,3-diene via oxidative cyclization

Besides ruthenium, other transition metals have also been applied in alkenylation of vinyl C-H bonds with alkynes, including rhodium, palladium, cobalt and nickel.[14-20] Rhodium catalysts enable imine (**4.18**) directed C-H bond alkenylation of α,β-unsaturated imines with alkynes.[14-17] For example, Ellman, Bergman and Colby reported Rh-catalyzed cross-coupling of N-benzyl imines of tiglic aldehyde and *t*-butyl acetylene to access the conjugated aldehyde upon hydrolysis with good yield and selectivity (Scheme 4.7).[14] Later, Ellman and Cheng independently applied this transformation to prepare highly substituted pyridines.[15,16]

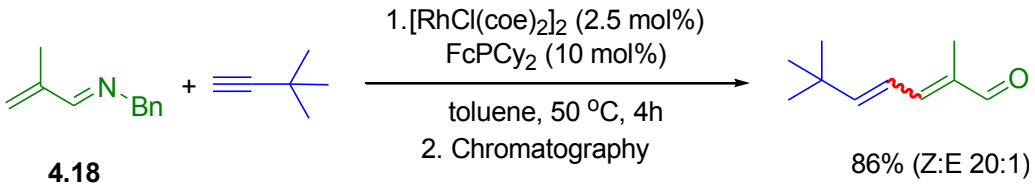

Scheme 4.7. Rhodium catalyzed enyne coupling to form conjugated aldehyde via imine directed C-H bond activation and hydroxylation

Skrydstrup developed a palladium-phosphine catalyzed enyne coupling via a proposed pathway of alkyne insertion into Pd-H bond.[18] With a catalyst system of $Pd(dba)_2$ and $P(tBu)_3$, disubstituted acetylenes reacted with olefins without α-hydrogen (acrylates, acrylamides and styrenes) in DMF under 50 °C to give 1,3-dienes (Scheme 4.8). This catalytic system exhibited not only high reactivity, but also good regioselectivity and functional group compatibility. Significant influence of the substituents in both alkyne and olefin had been observed on the *E/Z* ratios of the products.

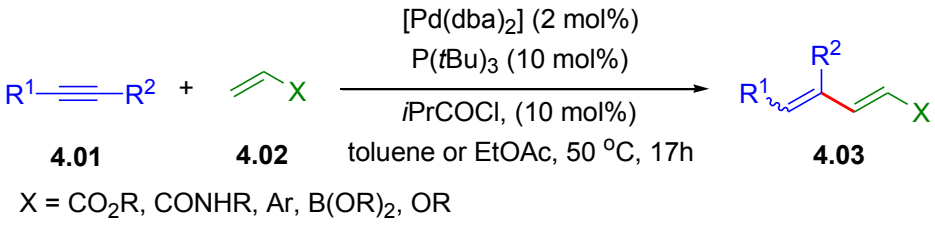

Scheme 4.8. Palladium catalyzed enyne coupling to form 1,3-dienes via alkyne insertion into Pd-H bond

Cheng revealed cobalt catalyzed cross-coupling of internal alkynes with styrenes under room temperature to form 1,3-dienes (Scheme 4.9).[20] Zn and ZnI_2 additives were crucial to generate the catalytically active Co(I) species, which could selectively coordinate with an alkyne and a styrene to form the key cobaltacyclopentene intermediate in the oxidative cyclization pathway. This coupling reaction proceeded with high regio- and stereoselectivity and was also compatible with both electron-rich and electron-deficient substituents attached to alkynes. However, the coupling reaction was not suitable for terminal alkynes, since it promoted a facile homocyclotrimerization of the alkynes.

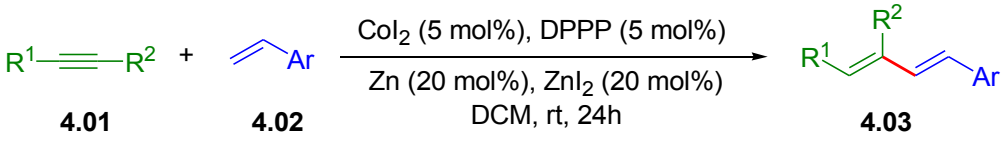

Scheme 4.9. Cobalt catalyzed alkyne-styrene coupling to form 1,3-dienes via oxidative cyclization

A new nickel-catalyzed codimerization of an acrylate and an alkyne was developed to provide 1,3-diene by Kurahashi (Scheme 4.10).[19] N-Aryl-2-aminopyridine played an essential role in prompting the formation of the 1:1 coupling product. In the proposed reaction mechanism, N-aryl-2-aminopyridine coordinated to nickel and chemoselectively formed hydrogen-bond with an acrylate. The resulting intermediate **4.19** led to 1,3-diene product via oxidative cyclization pathway. Moreover, N-phenyl-acrylamide was able to form a pseudodiene complex (**4.20**) with nickel(0); such a complex allowed exclusive intermolecular codimerization of N-phenyl-acrylamide and diphenylacetylene with good yields. In the case of N,N-disubstituted acrylamide, the 1:1 coupling product was not observed. These results

indicated the importance of intramolecular interaction of hydrogen-bonding to promote the desired reaction in a chemo-, regio- and stereoselective manner.

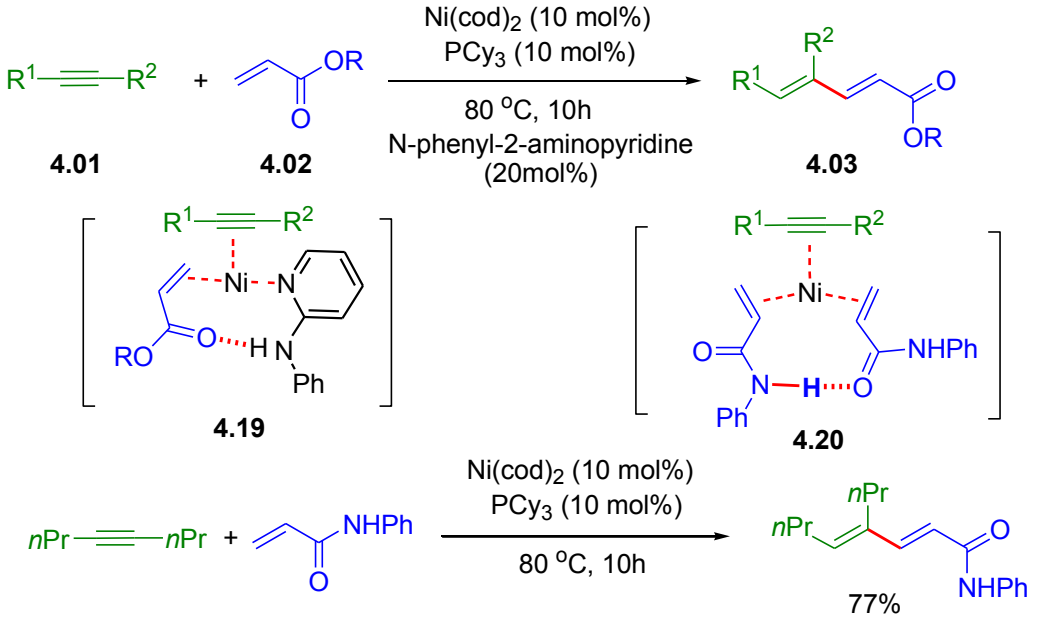

Scheme 4.10. Nickel catalyzed enyne coupling to form 1,3-dienes via oxidative addition with the assistance of intramolecular hydrogen-bonding

During our study of the ruthenium catalyzed [3+2] carbocyclization, we have synthesized several bis(cyclometalated) octahedral ruthenium(II) complexes (**4.21A**-**C**), {Ru(η^4-cod)[η^2-X=C(R)C_6H_4]$_2$} (X = O or NH; R = Ph or *n*Bu) (Scheme 4.11).[21,22] **4.21B** could be used as catalyst precursor to catalyze [3+2] cyclization between N-H ketimines and alkynes using the N-heterocyclic carbene ligand, IPr.[22] The proposed mechanism involves carbon-carbon bond formation by alkyne insertion into the Ru-C bond of a ruthenacycle intermediate, presumably facilitated by the IPr ligand that has replaced cod ligand on Ru center. Thus, the substrate-derived η^2-[C,N] imine ligands appear to play the dual role of actor ligand and spectator ligand, eventually incorporated into the cyclization product and replaced by incoming ketimine substrates via cyclometalation. It is noteworthy that **4.21B** did not react with alkyne substrates without added IPr ligand, suggesting significant ligand effect on its stability and reactivity.

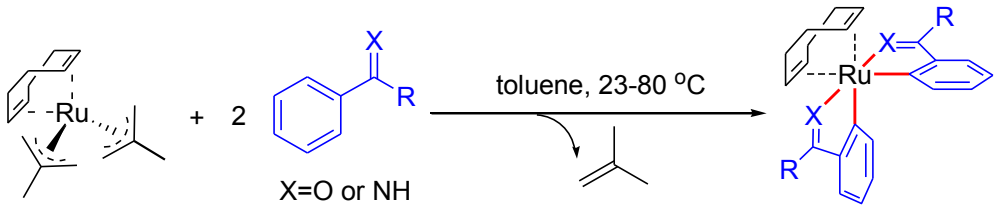

4.21A, X=O, R=*n*Bu, 85%
4.21B, X=NH, R=Ph, 95%
4.21C, X=O, R=Ph, 70%

Scheme 4.11. Preparation of bis-cyclometalated ruthenium(II) complexes with η^2-[C,X] ligands

We envision that these complexes can be explored as ruthenium(II) catalyst precursors (**4.21**) with η^2-[C,X] ligands solely as spectator ligands which occupy four of the six coordination sites and affect reactions occurring at the other two *cis* coordination sites. In particular, ancillary ligands (L) can be replaced by alkene/alkyne substrates through π-complexation, thus setting the stage for C-C bond formation by oxidative cyclization (Scheme 4.12). The latter transformation is a key step in a number of ruthenium-catalyzed C-C coupling reactions such as alkene–alkyne (enyne) couplings for diene synthesis,[23] [2+2] or [2+2+2] cycloadditions,[24] and [2+2+1] cycloadditions such as the Pauson–Khand reaction.[25,26] With easily accessible η^2-[C,X] ligands through C-H activation, bis(cyclometalated) ruthenium(II) complexes may serve as an attractive alternative to existing catalysts, allowing modular catalyst design and tunable ligands for catalyst efficiency and selectivity.

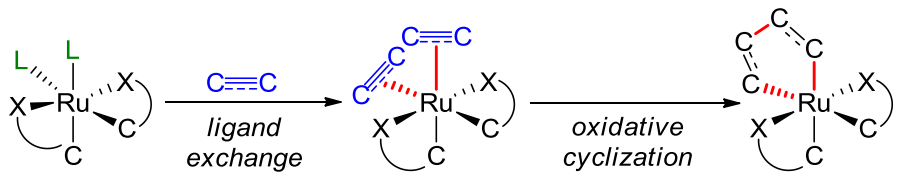

4.21 **4.22** **4.23**

Scheme 4.12. Envisioned C-C bond formation via oxidative cyclization with bis-cyclometalated ruthenium(II) complexes with η^2-[C,X] ligands

This chapter will describe the catalytic applications of several bis(cyclometalated) ruthenium(II) complexes with η^2-[C,N] and η^2-[C,O] ligands besides formal [3+2] carbocyclization. The potential of these ruthenacycles as catalyst precursors is demonstrated by a catalytic room-temperature alkene–alkyne coupling to synthesize α,β,γ,δ-unsaturated esters and amides.

4.2. Initial Results

Our study began with testing the hypothesis that the ancillary ligands (such as cod) can be replaced by other molecules through π-complexation in the complex **4.21B** and **4.21C** with the η^2-[C,X] ligands remained on Ru center as spectator ligands. The chelating cod ligand in both **4.21B** and **4.21C** could be replaced by two pyridine molecules to form the bis(pyridine)-ligated **4.22B** and **4.22C**, respectively (Scheme 4.13). The solid-state structures of **4.22B** and **4.22C** were determined by single crystal X-ray diffraction (Figure 4.1). In both of these bis(cyclometalated) ruthenium(II) complexes, the two *cis* η^2-[C,X] ligands remained intact and two pyridine replaced the chelating cod ligand, which was consistent with our hypothesis.

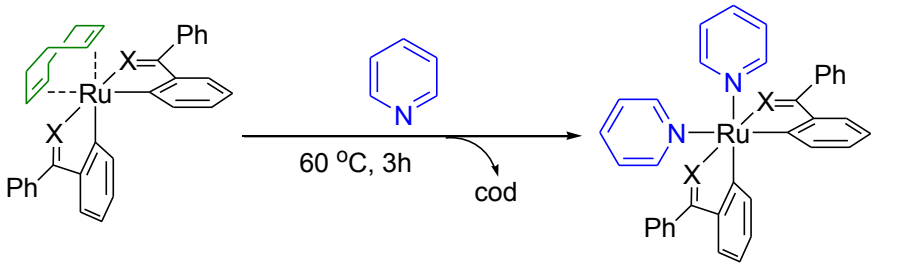

4.21B, X = NH
4.21C, X = O

4.22B, X = NH: (85%)
4.22C, X = O: (80%)

Scheme 4.13. Test of the hypothesis on ligand exchange with chelating 1,5-cyclooctadiene(cod) of {Ru(cod) [η^2-$HNC(C_6H_5)C_6H_4]_2$} (**4.21B**) and {Ru(cod)[η^2-$OC(C_6H_5)C_6H_4]_2$} (**4.21C**)

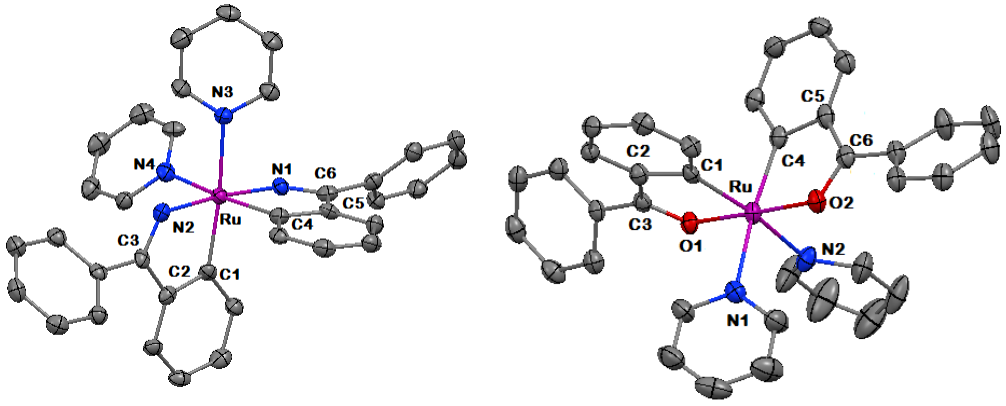

Figure 4.1 ORTEP diagram of {Ru(pyridine)$_2$[η^2-HNC(C_6H_5)C_6H_4]$_2$} (**4.22B**) and {Ru(pyridine)$_2$[η^2-OC(C_6H_5)C_6H_4]$_2$} (**4.22C**) at 50% thermal ellipsoid

With this stoichiometric observation, we first tested the catalytic reactivity of **4.21B** in the coupling between diphenylacetylene and methyl acrylate. In the presence of 5 mol% of **4.21B**, *(2E,4Z)*-1,3-dienoate product (**4.03A**) was obtained in 98% yield from the starting materials in toluene under 80 ^{o}C after 24h. In addition to enyne coupling, the dimerization of methyl acrylate was also observed. The major product is 1,3-dienoate (**4.03A**), indicating that enyne coupling is favored over acrylate dimerization. These results indicated the bis-cyclometalated ruthenium complexes were highly promising catalysts in the intermolecular alkene-alkyne cross-coupling reaction.

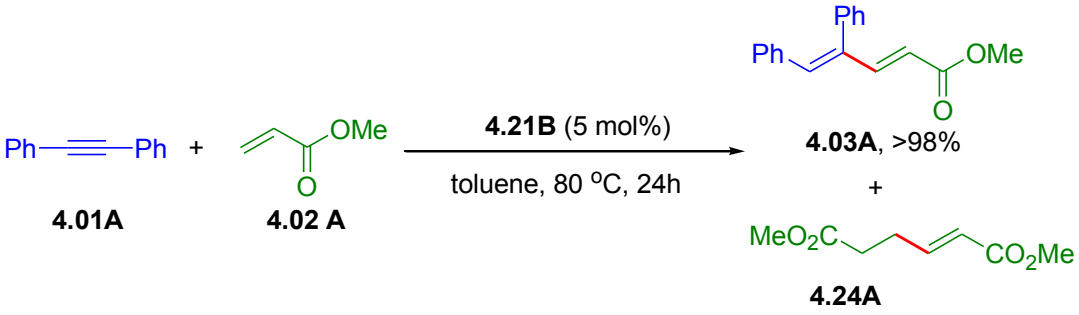

Scheme 4.14. Test of the catalytic reactivity of {Ru(cod)[η^2-NHC(C_6H_5)C_6H_4]$_2$} (**4.21B**) in alkene-alkyne coupling

4.3. Optimization of Reaction Conditions

The promising initial results encouraged us to further evaluate the catalytic activity of bis-cyclometalated Ru(II) complexes in intermolecular alkene-alkyne coupling between diphenylacetylene and methyl acrylate to form (*2E,4Z*)-1,3-diene products (**4.03**) (Table 4.1). Using 5 mol% [(cod)Ru(η^3-methallyl)$_2$] as catalyst precursor and no added ligands led to only 12% conversion after heating at 80 ^{o}C for 24 hours in toluene (entry 1). By contrast, *in situ* generated ruthenacycle **4.21B** via pre-activation of [(cod)Ru(η^3-methallyl)$_2$] with 2 equivalents of benzophenone imine ligand effectively promoted formation of conjugated diene in quantitative yield by GC analysis (entry 2). The structure of the ligands was found to be crucial to the effectiveness of the reaction. Compared to benzophenone imine ligand, much lower reactivity was observed when catalyst pre-activation was carried out using a number of aromatic compounds that are capable of generating bis-cyclometalated Ru(II) complexes (entries 3-14).[27,28] For example, using protected imines and benzophenone ligands gave less than 10% yields. Besides, 1-phenylethanamine provided moderated yield, which might due to its potential to form ketimine via *in situ* dehydrogenation. Without the pre-activation, benzophenone imine was ineffective in promoting this transformation (entry 15), indicating the active catalyst precursor was bis-cyclometalated ruthenium(II) complex **4.21B**.

Table 4.1. Ligand effect in ruthenium(II) catalyzed alkene-alkyne coupling[a]

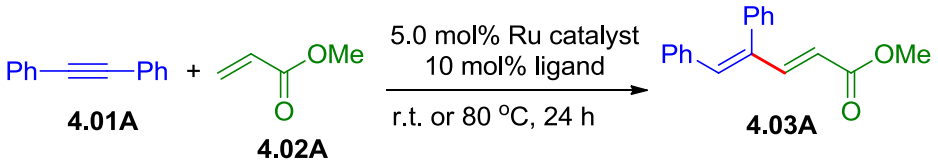

4.01A **4.02A** **4.03A**

Entry	Ru Catalyst	Ligand	Temp.	Yield (%)[b]
1	$[Ru(cod)(C_4H_7)_2]$	none	80 °C	12
2	$[Ru(cod)(C_4H_7)_2]$	$Ph_2C{=}NH$	80 °C	**>98**
3	$[Ru(cod)(C_4H_7)_2]$	2-phenylpyridine	80 °C	8
4	$[Ru(cod)(C_4H_7)_2]$	PhCN	80 °C	37
5	$[Ru(cod)(C_4H_7)_2]$	PhCONHPh	80 °C	14
6	$[Ru(cod)(C_4H_7)_2]$	Ph_2CHNH_2	80 °C	24
7	$[Ru(cod)(C_4H_7)_2]$	$PhCH(CH_3)NH_2$	80 °C	54
8	$[Ru(cod)(C_4H_7)_2]$	$Ph_2C{=}O$	80 °C	<5
9	$[Ru(cod)(C_4H_7)_2]$	Ph_2CNTs	80 °C	13
10	$[Ru(cod)(C_4H_7)_2]$	*o*-phenylenediamine	80 °C	15
11	$[Ru(cod)(C_4H_7)_2]$	benzophenone oxime	80 °C	34
12	$[Ru(cod)(C_4H_7)_2]$	N-benzylideneaniline	80 °C	11
14	$[Ru(cod)(C_4H_7)_2]$	2-phenyl-2-oxazoline	80 °C	25
15	$[Ru(cod)(C_4H_7)_2]$	$Ph_2C{=}NH$	r.t.	15
16	**4.21B**	none	r.t.	**>98**

[a] Reaction conditions: diphenylacetylene (0.20 mmol, 1 equiv), methyl acetate (2.0 equiv), Ru catalyst (0.05 equiv), ligand (0.10 equiv), solvent (0.5 mL), room temperature (20-22 °C) or 80 °C, 24 h. [b] GC yields.

Next, the solvent effect on the outcome of the reaction was studied (Table 4.2). THF and DMF were proved to be suitable solvent for this reaction, which provided extra choices for substrates with lower solubility in toluene (entry 1-5). Under optimized conditions, room-temperature coupling between diphenylacetylene (1.0 equiv.) and methyl acrylate (2.0 equiv.) proceeded smoothly in toluene solvent with 5.0 mol% **4.21B**, giving 1,3-diene product in quantitative yield by GC analysis (entry 1). The pyridine-ligated bis(imine) complex **4.22B** was less stable than **4.21B** in solution phase but displayed comparable

catalytic activity (entry 2). By contrast, the bis(ketone) analogues **4.21C** and **4.22C** were virtually unreactive as catalyst precursors (entries 6, 7 and 9). Such reactivity distinction is consistent with the mechanistic hypothesis that cod or pyridine ligands can be replaced by alkene/alkyne substrates (Scheme 4.12), thus having little effect on catalytic activity beyond the initial stage of catalyst preactivation. In contrast, the η^2-[C,X] imine or ketone ligands are expected to stay on the ruthenium center throughout catalytic cycles and play a dominant role on catalyst activity.

Table 4.2. Effects of catalyst precursor and solvent in ruthenium(II) catalyzed alkene-alkyne coupling[a]

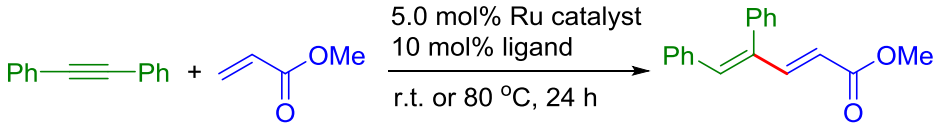

4.01A **4.02A** **4.03A**

Entry	Ru Catalyst	Solvent	Temp.	Yield (%)[b]
1	**4.21B**	toluene	r.t.	**>98**
2	**4.21B**	THF	r.t.	**96**
3	**4.21B**	DME	r.t.	66
4	**4.21B**	DMF	r.t.	**93**
5	**4.21B**	hexane	r.t.	82
6	**4.21C**	toluene	r.t.	<2
7	**4.21C**	toluene	80 °C	<2
8	**4.22B**	toluene	r.t.	**>98**
9	**4.22C**	toluene	r.t.	<2

[a] Reaction conditions: diphenylacetylene (0.20 mmol, 1 equiv), methyl acetate (2.0 equiv), Ru catalyst (0.05 equiv), ligand (0.10 equiv), solvent (0.5 mL), room temperature (20-22 °C) or 80 °C, 24 h. [b] GC yields.

4.4. Substrate Scope

With the standard reaction conditions established, various internal alkynes and acrylic esters or amides were studied for Ru-catalyzed room-temperature alkene-alkyne coupling (Figure 4.2). Coupling between diphenylacetylene and unsubstituted alkyl acrylates proceeded smoothly to form 1,3-diene products in over 90% yields and with exclusive stereoselectivity for the (*2E*,*4Z*)-isomers. For phenyl acrylate coupling product, the yield was improved from 58% to 87% by replacing **4.21B** with bis(pyridine) ruthenacycle **4.22B** as the catalyst precursor. Such reactivity enhancement is likely due to facile catalyst activation by substrate replacement of more labile pyridine ligands compared to the chelating diene ligand (Scheme 4.12). When coupling between diphenylacetylene and methyl acrylate was scaled up from 0.2 mmol to 20 mmol, the loading of **4.21B** could be reduced to 1.0 mol% to acquire the product in 90% isolated yield (4.8 gram purified product) over 48 hours. Coupling between diphenylacetylene and N,N-dimethyl acrylamide gave the product in 72% yield, and higher reaction temperature was needed to improve the yield of N,N-diethyl product from 50% at room temperature to 85% at 60 ºC. Compared to less reactive N,N-dialkylacrylamides, N-isopropyl- and N-*t*-butylacrylamide reacted with diphenylacetylene in good reactivity, although the latter required using **4.22B** as catalyst precursor for satisfactory yield.

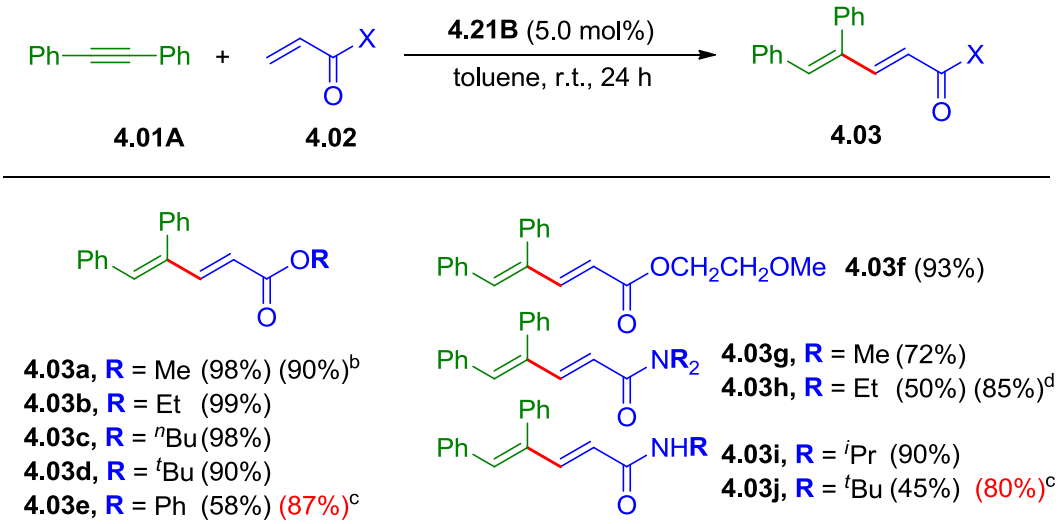

[a] Reaction conditions: diphenylacetylene (0.20 mmol, 1.0 equiv), methyl acrylate (2.0 equiv), **4.21B** (0.050 equiv), toluene (0.5 mL), room temperature (20-22 °C), 24h; averaged isolated yields of two runs. [b] 20 mmol scale reaction, **4.21B** (1 mol%), rt, in toluene 48h. [c] Using **4.22B** instead of **4.21B**. [d] At 60 °C.

Figure 4.2. Alkene substrate scope in bis-cyclometalated ruthenium(II) catalyzed alkene-alkyne coupling[a]

The scope of alkyne substrates was studied by coupling reactions with methyl acrylate (Figure 4.3). High reactivity and regioselectivity was observed for phenylacetylene derivatives with alkyl substituents, favoring the formation of 4-alkyl-5-aryl regioisomer in >10:1 selectivity. The mild reaction conditions allow very good compatibility with functional groups such as acyl, formyl, and Br substituents, providing synthetic handles for further functional group transformations. Aliphatic internal alkynes such as 3-hexyne and 4-octyne displayed lower reactivity than aromatic alkynes, and a 2:1 alkyne/acrylate stoichiometry was used to get coupling products in moderate yields. Coupling between methyl acrylate and terminal alkynes generally suffered from lower reactivity and gave a complex mixture of products, which meant the presence of competing reaction pathways.[29] Nevertheless, coupling between methyl acrylate and phenylacetylene was effectively catalyzed by **4.22B** to form product **4.03v** with (*E,E*)-stereoselectivity in 65% isolated yield. Substrate substitution was supposed to be easier for monodentate ligands than for chelating ligands, thus the accelerated coordination of substrate to **18** would account for the increased yield.

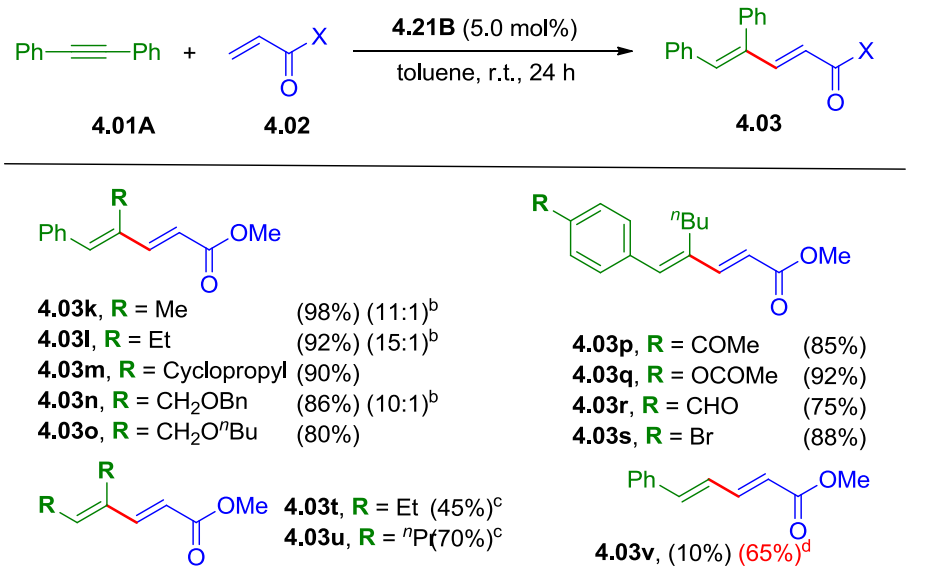

[a] Reaction conditions: diphenylacetylene(0.20 mmol, 1.0 equiv), methyl acrylate (2.0 equiv), **4.21B** (0.050 equiv), toluene (0.5 mL), room temperature (20-22 °C), 24h; averaged isolated yields of two runs. [b] Combined yield of two regioisomers; the ratio is determined by NMR analysis; structure of major isomer is shown. [c] Using 0.20 mmol methyl acrylate as limiting reagent and 2.0 equiv of alkyne. [d] Using **4.22B** istead of **4.21B**; isolated yield for the major stereoisomer in 5:1 selectivity; minor isomer was not purified

Figure 4.3. Alkyne substrate scope in bis-cyclometalated ruthenium(II) catalyzed alkene-alkyne coupling[a]

We should also mention that the current enyne coupling catalyst system did not work with more hindered acrylates (with α- or β-substituents) or less electron-deficient alkenes such as vinylarenes.

4.5. Reaction Mechanism Studies and Discussion

Three types of reaction mechanism have been proposed for Ru-catalyzed alkene-alkyne couplings to form 1,3-dienes (Scheme 4.15):[7-9] (1) C–C bond formation by alkene-alkyne oxidative cyclization, followed by β-H elimination and C–H reductive elimination (Path 1); (2) alkyne insertion into a Ru-hydride bond, followed by alkene insertion into the resulting Ru-alkenyl linkage and subsequent β-H elimination (Path 2); (3) sp^2 C–H bond activation of alkene, followed by alkyne insertion into Ru alkenyl, and C–H bond formation by either reductive elimination or protonation of Ru–C bond (Path 3).

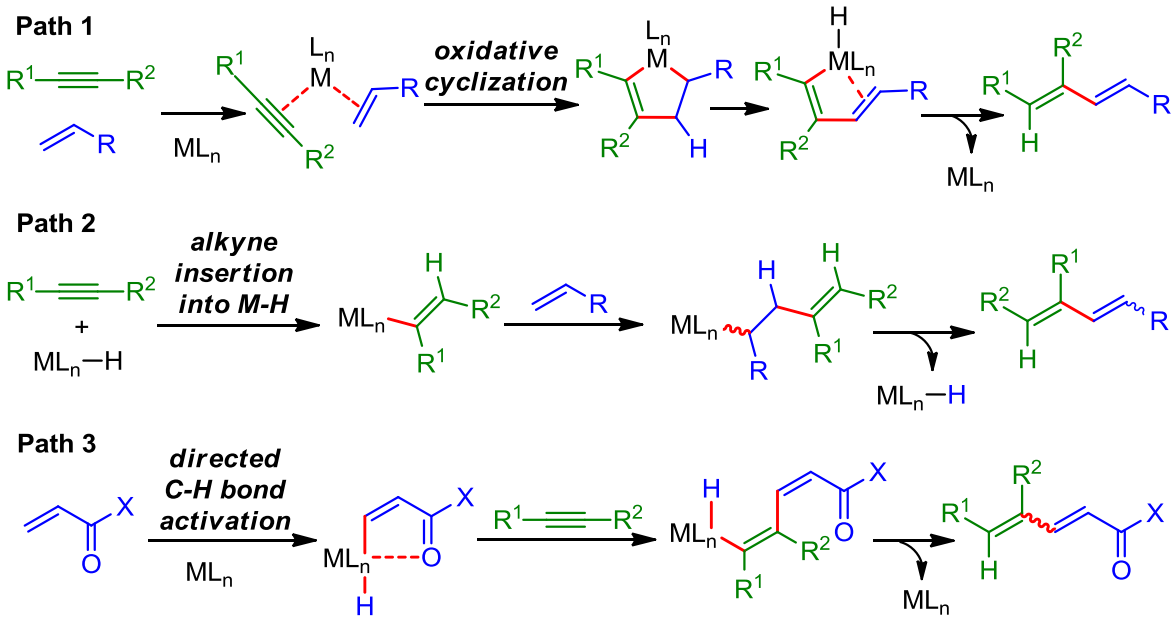

Scheme 4.15. Possible reaction mechanisms for transition metal-catalyzed alkene-alkyne cross-coupling

Although the latter two pathways cannot be completely ruled out, the oxidative cyclization mechanism[9] (Path 1) is most consistent with the observed regio- and stereochemistry in coupling products. In particular, high regioselectivity with non-symmetrical alkyne substrates supports C-C bond formation by oxidative cyclization (Path 1) or alkyne insertion into Ru-alkenyl linkage (Path 3), not by alkyne insertion into Ru-H linkage (Path 2).[18] The complete lack of (2*Z*)-stereoisomers in coupling products also argues against the proposed alkene C-H activation stereochemistry in Path 3, which should favor (2*Z*)-isomers by ester- or amide-directed C-H activation/cyclometalation.[8]

The proposed oxidative cyclization pathway has prompted us to extend our study to other mechanistically related C-C couplings using the current catalyst system. As mentioned in the initial result, the tail-to-tail methyl acrylate dimerization product was also detected in the reaction phenylacetylene and methyl acrylate. This inspired us to test whether the bis-cyclometalated ruthenium complexes (**4.21B, 4.21C**) could effectively catalyzed the dimerization of alkenes. In the presence of 5 mol% **4.21B**, methyl acrylate underwent dimerization giving (*E*)-dimethyl hex-2-enedioate (**4.24A**) in 70% yield under room temperature in toluene (Scheme 4.16).

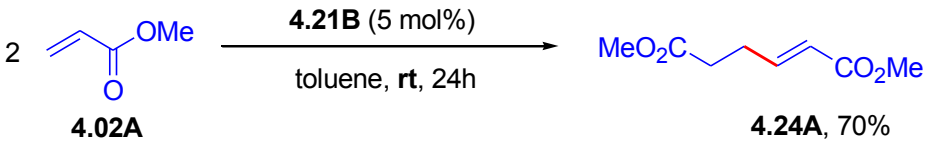

Scheme 4.16. Methyl acrylate dimerization catalyzed by {Ru(cod)[η^2-NHC(C_6H_5)C_6H_4]$_2$} (**4.21B**)

Compared with Kurahashi's nickel catalyst,[19] the bis-cyclometalated ruthenium complexes (**4.21B,C** and **4.22B, C**) possess two η^2-[C, X] ligands, which have the potential to form hydrogen-bonds with two molecules of acrylates. We hypothesized that the formation of hydrogen-bond between ligands and substrates would promote substrates coordination, increase the interaction between substrates and ruthenium center and facilitate oxidative cyclization, leading to higher efficiency of the catalysis. It is likely that the formation of hydrogen-bond could explain the high efficiency and regio- and stereoselectivity of our catalyst compared with previously reported works in acrylate dimerization.[29,30] Preliminary results from DFT calculations also suggested involvement of hydrogen-bonding interactions between cyclometalated imine NH moieties and carbonyl groups from the acrylate substrates (Figure 4.4).

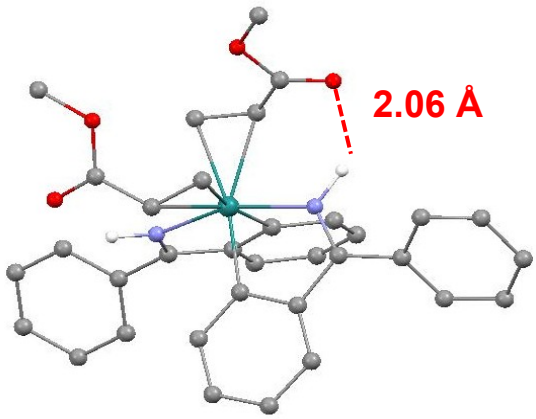

Figure 4.4. DFT-calculated structure of the formation of hydrogen-bond between cyclometalated imine NH moieties and carbonyl groups from the acrylate substrates

In addition, when norbornene was used as the alkene substrate, a cyclobutene derivative was formed via [2+2] cyclization under elevated temperature as shown in Scheme 4.17, which further supports the proposed Ru(II)/Ru(IV) catalytic cycle involving alkene/alkyne oxidative cyclization.[31,32]

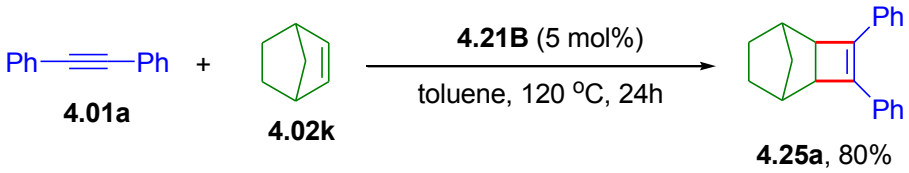

Scheme 4.17. [2+2] cycloaddition of diphenylacetylene and norbornene catalyzed by {Ru(cod)[η^2-NHC(C_6H_5)C_6H_4]$_2$} (**4.21B**)

4.6. Conclusion

In summary, we have developed a new class of bis(cyclometalated)ruthenium(II) catalyst precursors with readily available η^2-[C,X] ligands derived from aromatic NH ketimines and ketones. The catalytic activity of the bis(imine) Ru complex was evaluated in several catalytic C-C coupling reactions which are proposed to proceed by Ru(II)/Ru(IV) catalytic cycles involving oxidative cyclization. A room temperature alkene–alkyne coupling was promoted to form α,β,γ,δ-unsaturated esters and amides with high regio- and stereoselectivity, good functional-group tolerance, and very high catalyst efficiency in a representative gram-scale synthesis. The major limitation of the current catalyst system is the limited scope of alkene substrates and we aim to improve this scope through a more systematic study on structure–reactivity correlations of bis(cyclometalated) ruthenium(II) complexes with various η^2-[C,X] ligands.

4.7. Experimental Procedures

4.7.1. General Information

Unless otherwise noted, all manipulations were carried out under a nitrogen atmosphere using standard Schlenk-line or glove box techniques. All glassware was oven-dried for at least 1 h prior to use. THF, toluene, and hexane were degassed by purging with nitrogen for 45 min and dried with a solvent

purification system (MBraun MB-SPS). DMF, dioxane and dimethoxyethane were dried over activated 3 Å molecular sieves and degassed by purging with nitrogen. Other reagents and substrates were purchased from TCI-America, VWR, Strem, Aldrich or Alfa-Aesar and were used as received. TLC plates were visualized by exposure to ultraviolet light. Organic solutions were concentrated by rotary evaporation at ~10 torr. Flash column chromatography was performed with 32–63 microns silica gel.

GC analyses were performed on a Shimadzu GC-2010. ^{1}H NMR spectra were obtained on a 400 MHz spectrometer, and chemical shifts were recorded relative to residual protiated solvent. ^{13}C NMR spectra were obtained at 100 MHz, and chemical shifts were recorded to the solvent resonance. Both ^{1}H and ^{13}C NMR chemical shifts were reported in parts per million downfield from tetramethylsilane (δ = 0 ppm). High-resolution mass spectra were obtained at a Bruker Daltronics BioTOF HRMS spectrometer.

4.7.2. Preparation of Alkyne Substrates

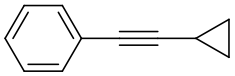

4.01m

(Cyclopropylethynyl)benzene were synthesized according to Procedure A:[33] To a solution of the iodo- or bromoarene (5.0 mmol) and terminal alkyne (6.0 mmol) in Et_3N (20 mL) was added $PdCl_2(PPh_3)_2$ (140 mg, 4 mol %). The mixture was then stirred for 5 min, and CuI (20 mg, 2 mol%) was added. The resulting mixture was stirred under a nitrogen atmosphere. The reaction was monitored by TLC to establish completion. The reaction mixture was then poured into water, and the aqueous layer was extracted three times with dichloromethane. After drying the combined organic layers over magnesium sulfate, the solvent was removed in vacuum. The residue was purified by flash column chromatography on silica gel using hexane/ethyl acetate to afford the pure alkynes.

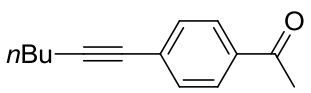

4.01p

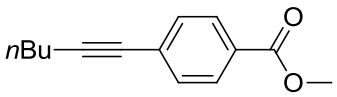

4,01q

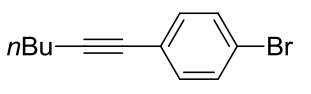

4.01s

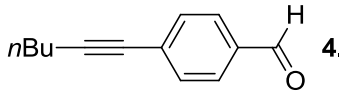

4.01r

1-(4-(Hex-1-yn-1-yl)phenyl)ethanone , methyl 4-(hex-1-yn-1-yl)benzoate , 4-(hex-1-yn-1-yl)benzaldehyde and 1-bromo-4-(hex-1-yn-1-yl)benzene were synthesized according to Procedure B:[34] A mixture of the iodo- or bromoarenes (5.0 mmol), terminal alkyne (6 mmol), $Pd(PPh_3)_2Cl_2$ (175mg, 5 mol %), PPh_3 (33 mg, 2.5 %), and Et_3N (0.76g, 1.5 eq.) in 20 mL of THF was stirred for 20 min at room temperature, and CuI (12 mg, 1.25 mol %) was then added. The reaction was monitored by TLC to establish completion. The workup procedure is same as Method A.

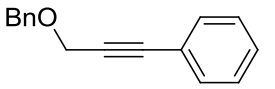

4.01n

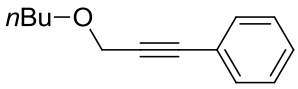

4.01m

(3-Butoxyprop-1-yn-1-yl)benzene and (3-(benzyloxy)prop-1-yn-1-yl)benzene was synthesized according to a known procedure (Procedure C):[35] To a solution of 3-phenyl-2-propyn-1-ol (0.66g, 5 mmol) in THF (20 mL) was added portionwise NaH (0.15g, 12mmol) at 0°C over 2h and the mixture was kept under stirring for 2h at 0°C. Upon the end of the H_2 formation, Benzyl or butyl bromide (5.5 mmol) and TBAI (0.1g, 0.25 mmol) was added. The mixture was then stirred at room temperature overnight. The reaction mixture was quenched with a saturated solution of NH_4Cl, extracted with ethyl acetate (3x); dried over $MgSO_4$ and concentrated under reduced pressure. Purification by flash column chromatography afforded the pure alkynes.

4.7.3. Preparation and X-Ray Diffraction Analysis of Ruthenium(II) Catalyst Precursors

{Ru(cod)[η^2-HNC(C_6H_5)C_6H_4]$_2$} (**4.21B**): Into a 20 mL scintillation vial equipped with a magnetic stir bar was added Ru(cod)(methylallyl)$_2$ (320 mg, 1.0 mmol), benzophenone imine (362 mg, 2.0mmol) and 10 mL toluene. The mixture was stirred overnight at room temperature. Then, the solvent was removed under reduced pressure. The residue was washed with hexane (3X), dried under vacuum, and afforded an orange powder (513 mg, 90 %).

{Ru(cod)[η^2-OC(C_6H_5)C_6H_4]$_2$} (**4.21C**): Into a 20 mL scintillation vial equipped with a magnetic stir bar was added Ru(cod)(methylallyl)$_2$ (320 mg, 1.0 mmol), benzophenone (364 mg, 2.0 mmol) and 10 mL toluene. The mixture was stirred under 80 °C for 5 hours. Then the solvent was removed under reduced

pressure, and the residue was washed with hexane (3X), dried under vacuum, and afforded a brown powder (400 mg, 70 %).

{Ru(pyridine)$_2$[η^2-HNC(C_6H_5)C_6H_4]$_2$} (**4.22B**): Into a 4 mL scintillation vial equipped with a magnetic stir bar was added Ru(cod)(N,C-benzophenone imine)$_2$ (**4.21B**) (50.0 mg, 0.088 mmol) and 1.5 mL of pyridine. The mixture was stirred under 60 °C for 3 hours. After cooling to room temperature, 2mL of hexane was added and precipitate was generated. The mixture was stored under -30 °C overnight. Then mother liquor was removed, and the residue was washed by cool hexane (3X), dried under vacuum, and afforded a purple powder (46.4 mg, 85%).

{Ru(pyridine)$_2$[η^2-OC(C_6H_5)C_6H_4]$_2$} (**4.22C**) was prepared from **4.21C** by the same procedure as **4.22B** and gave a dark green powder (43.8 mg, 80%).

Single crystal X-ray diffraction data of {Ru(pyridine)$_2$[η^2-HNC(C_6H_5)C_6H_4]$_2$} (**4.22B**) and {Ru(pyridine)$_2$[η^2-OC(C_6H_5)C_6H_4]$_2$} (**4.22C**) were collected on a Bruker Apex Duo diffractometer with a Apex 2 CCD area detector at T = 100K. Cu radiation was used for all 3 samples. Structures were process with Apex 2 v2013.4-1 software package with the most recent SAINT and SHELX software. Multi-scan absorption correction (SADABS 2012/1) was applied to all 3 data sets. Direct method was used to solve the structures of **4.21C,** while Intrinsic phasing was used for **4.22C**. Details of data collection and refinement are given in Table 4.3.

Table 4.3. Summary of cell parameters, data collection and structural refinements for {Ru(pyridine)$_2$[η^2-HNC(C_6H_5)C_6H_4]$_2$} (**4.22B**) and {Ru(pyridine)$_2$[η^2-OC(C_6H_5)C_6H_4]$_2$} (**4.22C**).

	4.22B	**4.22C**
Empirical formula	$C_{36}H_{30}N_4Ru \cdot C_3H_7$	$C_{36}H_{28}N_2O_2Ru \cdot 1/2C_6H_6 \cdot C_7H_8$
Formula weight	662.79	752.86
Temperature, K	100	100
Wavelength, (Å)	1.54178	1.54178
space group	C2/c	P-1
a/Å	14.2160(9)	10.5700(3)
b/Å	21.6320(14)	17.0020(14)
c/Å	21.1498(11)	20.4407(11)
α, deg	90	90.826(2)
β,deg	106.714(4)	95.963(2)
γ, deg	90	91.517(2)
V, Å	6229.2(7)	3651.7(2)
Z	8	4
d_{calcd}, g/cm^3	1.413	1.369
μ, mm^{-1}	4.331	3.792
F(000)	2744.0	1556
Theta range, deg	3.836 ÷ 66.671	4.207 ÷ 66.593
h, k, l ranges	-16 ÷ 16, -25 ÷ 24, -21 ÷ 25	-8 ÷ 12, -20 ÷ 20, -24 ÷ 22
Reflections collected/unique	28536	44552
Unique Reflections/gt	5155/3708	12508/9746
COOF on F^2	1.077	1.028
R_1, wR_2 ($I>2\sigma(I)$)[a]	6.63%, 16.22%	4.87%, 11.72%
R_1, wR_2 (all data)	10.08%, 17.46%	6.88%, 12.77%
Largest diff. peak and hole (e. Å $^{-3)}$	0.072	0.072

[a] R1 = $\Sigma||F_o| - |F_c|| / \Sigma|F_o|$, wR2 = $[\Sigma w[(F_o)^2 - (F_c)^2]^2 / \Sigma w(F_o^2)^2]^{1/2}$ for $F_o^2 > 2\sigma(F_o^2)$, w = $[\sigma^2(F_o)^2 + (AP)^2 + BP]^{-1}$ where P = $[[(F_o)^2 + 2(F_c)^2] / 3$ and A (B) = **4.22B** 0.0995 (11.4750); **4.22C** 0.0626(6.5504).

Table 4.4. Selected average bond lengths [Å] and bond angles [degree] for {Ru(pyridine)$_2$[η^2-HNC(C_6H_5)C_6H_4]$_2$} (**4.22B**)

bond length [Å]		bond angles [degree]	
Ru-N(1)	2.028(4)	N(1)-Ru-C(1)	97.8(2)
Ru-N(2)	2.018(4)	N(1)-Ru-C(4)	77.6(2)
Ru-N(3)	2.173(6)	N(1)-Ru-N(3)	92.3(2)
Ru-N(4)	2.174(6)	N(1)-Ru-N(4)	92.6(2)
Ru-C(1)	2.020(6)	N(2)-Ru-C(4)	97.8(2)
Ru-C(4)	2.020(6)	N(2)-Ru-C(1)	78.0(2)
N(1)-C(6)	1.296(9)	N(2)-Ru-N(3)	91.8(2)
N(2)-C(3)	1.301(9)	N(2)-Ru-N(4)	91.8(2)
C(1)-C(2)	1.430(9)	N(3)-Ru-C(1)	169.8(2)
C(2)-C(3)	1.466(8)	N(4)-Ru-C(4)	170.0(2)
C(4)-C(5)	1.416(9)	N(1)-Ru-N(2)	174.0(2)
C(5)-C(6)	1.475(8)	Ru-C(1)-C(2)	115.0(4)
		C(1)-C(2)-C(3)	113.3(5)
		C(2)-C(3)-N(2)	113.0(6)
		Ru-N(2)-C(3)	120.6(5)
		Ru-C(4)-C(5)	115.7(4)
		C(4)-C(5)-C(6)	113.2(5)
		C(5)-C(6)-N(1)	112.8(5)
		Ru-N(1)-C(6)	120.7(4)

Table 4.5. Selected average bond lengths [Å] and bond angles [degree] for {Ru(pyridine)$_2$[η^2-OC(C_6H_5)C_6H_4]$_2$} (**4.22C**)

bond length [Å]		bond angles [degree]	
Ru-O(1)	2.017(3)	O(1)-Ru-C(1)	79.4(1)
Ru-O(2)	2.022(3)	O(1)-Ru-C(4)	99.7(1)
Ru-N(1)	2.189(4)	O(2)-Ru-C(4)	79.5(1)
Ru-N(2)	2.188(4)	O(2)-Ru-C(1)	99.8(1)
Ru-C(1)	1.998(4)	N(1)-Ru-C(1)	93.5(1)
Ru-C(4)	1.999(4)	N(2)-Ru-C(4)	94.6(2)
O(1)-C(3)	1.278(6)	N(1)-Ru-C(4)	168.8(1)
O(2)-C(6)	1.278(6)	N(2)-Ru-C(1)	168.9(1)
C(2)-C(3)	1.447(6)	C(1)-Ru-C(4)	86.7(2)
C(5)-C(6)	1.442(6)	O(1)-Ru-O(2)	178.3(1)
C(1)-C(3)	1.434(6)	N(1)-Ru-N(2)	87.5(2)
C(4)-C(6)	1.434(6)	O(1)-Ru-N(1)	91.9(1)
		O(1)-Ru-N(2)	89.5(1)
		O(2)-Ru-N(1)	89.6(6)
		O(2)-Ru-N(2)	90.9(1)

4.7.4. General Procedures for Ruthenium(II) Catalyzed Alkene-Alkyne Coupling

Into a 4.0 mL scintillation vial equipped with a magnetic stir bar was placed the alkyne substrate (0.2 mmol, 1.0 eq.), the alkene substrate (0.4 mmol, 2.0 eq.) and 0.5 mL of a stock solution containing Ru(II) catalyst (0.05 eq.). The vial was sealed with a silicone-lined screw-cap, stirred at room temperature in glove box for 24 h (room temperature reactions), or transferred out of the glove box and stirred in a heated oil bath for 24 h (heated reactions). After the reaction mixture was cooled to room temperature, all volatile materials were removed under reduced pressure. Further purification was achieved by flash column chromatography. Yields of the isolated products are based on the average of two runs under identical conditions.

For reactions using *in situ* generated catalysts, a 4 mL scintillation vial equipped with a magnetic stir bar was charged with Ru(cod)(methylallyl)$_2$ (1.0 eq.), ligand (2.0 eq.) and toluene. The vial was sealed with a silicone-lined screw-cap, transferred out of the glove box, and heated up to 80 ^{o}C for 30 min. Then the vial was transferred into glove box and the resulted mixture was used as a stock solution of ruthenium catalyst precursor.

4.7.5. Ruthenium(II) Catalyzed [2+2] Cycloaddition of Diphenylacetylene and Norbornene

Into a 4.0 mL scintillation vial equipped with a magnetic stir bar was added {Ru(cod)[η^2-HNC(C_6H_5)C_6H_4]$_2$} (**4.21B**) (0.1 mmol, 0.05 eq.), diphenylacetylene (0.2 mmol, 1.0 eq.), norbornene (0.4 mmol, 2.0 eq.) and 0.5 mL of toluene. The vial was sealed with a silicone-lined screw-cap, transferred out of the glove box, and heated up and stirred for 24 h. After the reaction mixture was cooled to room temperature, all volatile materials were removed under reduced pressure. Further purification by flash column chromatography gave 3,4-diphenyltricyclo[4.2.1.02,5]non-3-ene **4.25A** (white powder, 43.6 mg, 80 %).

4.7.6. Ruthenium(II) Catalyzed Dimerization of Methyl Acrylate

Into a 4.0 mL scintillation vial equipped with a magnetic stir bar was added {Ru(cod)[η^2-HNC(C_6H_5)C_6H_4]$_2$} (**4.21B**) (0.1 mmol, 0.025 eq.), methyl acrylate (0.4 mm) and 0.5 mL of toluene. The vial was sealed with a silicone-lined screw-cap, and stirred under room temperature for 24 h. Then all volatile materials were removed under reduced pressure. Further purification by flash column chromatography gave compound (*E*)-dimethyl hex-2-enedioate (yellow oil, 24.1 mg, 70 %).

4.7.7. Spectral Data for Isolated Products

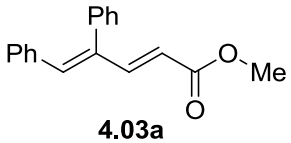

4.03a

(*2E*,*4Z*)-Methyl 4,5-diphenylpenta-2,4-dienoate: Chromatography (1:6 ethyl acetate/hexane, R_f = 0.45) gave **4.03a** as a white solid (52.2 mg, >98 %). ^{1}H NMR (400 MHz, $CDCl_3$): δ = 7.68 (dd, *J* = 15.5, 0.7 Hz, 1H), 7.42-7.34 (m, 3H), 7.15-7.08 (m, 5H), 6.95-6.93 (m, 2H), 6.91 (s, 1H), 5.50 (dd, *J* = 15.5, 0.5 Hz, 1H), 3.71 ppm (s, 3H); ^{13}C NMR (100 MHz, $CDCl_3$): δ = 167.9, 150.0, 139.8, 138.9, 137.1, 135.9, 130.2, 129.41, 129.38, 128.5, 128.4, 128.1, 120.1, 51.7 ppm; HRMS: m/z calcd for $C_{18}H_{16}O_2Na^+$: 287.1043; found: 287.1035.

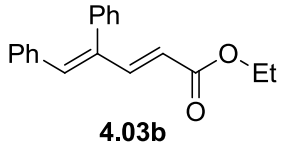

4.03b

(*2E*,*4Z*)-Ethyl 4,5-diphenylpenta-2,4-dienoate: Chromatography (1:6 ethyl acetate/hexane, R_f = 0.50) gave **4.03b** as a white solid (55.0 mg, >98 %). ^{1}H NMR (400 MHz, $CDCl_3$): δ = 7.67 (dd, J_1 = 15.5, 0.7 Hz, 1H), 7.40-7.34 (m, 3H), 7.11-7.08 (m, 5H), 6.95-6.91 (m, 2H), 6.90 (s, 1H), 5.48 (d, *J* = 15.5 Hz, 1H), 4.17 (q, *J* = 7.1 Hz, 2H), 1.25 ppm (t, *J* = 7.1 Hz, 3H); ^{13}C NMR (100 MHz, $CDCl_3$): δ = 167.5, 149.8, 139.9, 138.8, 137.2, 135.9, 130.3, 129.46, 129.41, 128.44, 128.40, 128.1, 120.6, 60.5, 14.5 ppm; HRMS: m/z calcd for $C_{19}H_{18}O_2Na^+$: 301.1199; found: 301.1196.

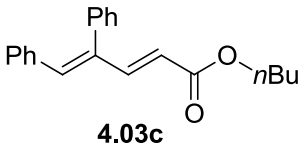

4.03c

(*2E*,*4Z*)-Butyl 4,5-diphenylpenta-2,4-dienoate: Chromatography (1:6 ethyl acetate/hexane, R_f = 0.50) gave **4.03c** as a white solid (60.6 mg, >98 %). ^{1}H NMR (400 MHz, $CDCl_3$): δ = 7.65 (dd, *J* = 15.5, 0.7 Hz, 1H), 7.40-7.34 (m, 3H), 7.15-7.07 (m, 5H), 6.93-6.91 (m, 2H), 6.90 (s, 1H), 5.47 (d, *J* = 15.4 Hz, 1H), 4.17 (t, *J* = 6.7Hz, 2H), 1.61 (m, 2H), 1.36 (m, 2H), 0.91 ppm (t, *J* = 7.4 Hz, 3H); ^{13}C NMR (100 MHz, $CDCl_3$): δ = 167.6, 149.7, 139.9, 138.8, 137.2, 136.0, 130.3, 129.47, 129.41, 128.43, 128.40, 128.1, 120.6, 64.5, 31.0, 19.4, 14.0 ppm; HRMS: m/z calcd for $C_{21}H_{22}O_2Na^+$: 329.1512; found: 329.1520.

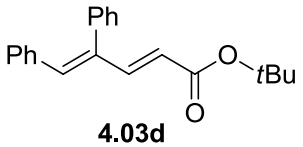

4.03d

(*2E*,*4Z*)-Tert-butyl 4,5-diphenylpenta-2,4-dienoate: Chromatography (1:6 ethyl acetate/hexane, R_f = 0.57) gave **4.03d** as a white solid (55.0 mg, 90 %). ^{1}H NMR (400 MHz, $CDCl_3$): δ = 7.58 (dd, J_1 = 15.5, J_2 = 0.8 Hz, 1H), 7.42-7.36 (m, 3H), 7.15-7.08 (m, 5H), 6.93-6.91 (m, 2H), 6.88 (s, 1H), 5.41 (dd, *J* = 15.4, 0.5 Hz, 1H), 1.46 ppm (s, 9H); ^{13}C NMR (100 MHz, $CDCl_3$): δ = 166.8, 148.8, 139.9, 138.7, 136.0, 130.2, 129.5, 129.3, 128.33, 128.25, 128.0, 122.5, 80.4, 28.4 ppm; HRMS: m/z calcd for $C_{21}H_{22}O_2Na^+$: 329.1512; found: 329.1513.

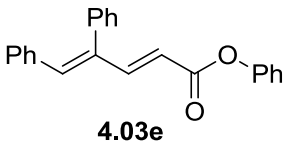

4.03e

(*2E*,*4Z*)-Phenyl 4,5-diphenylpenta-2,4-dienoate: Chromatography (1:6 ethyl acetate/hexane, R_f = 0.57) gave **4.03e** as a white solid (55.0 mg, 90 %). ^{1}H NMR (400 MHz, $CDCl_3$): δ = 7.58 (dd, *J* = 15.5, 0.8 Hz, 1H), 7.42-7.36 (m, 3H), 7.15-7.08 (m, 5H), 6.93-6.91 (m, 2H), 6.88 (s, 1H), 5.41 (dd, *J* = 15.4, 0.5 Hz, 1H), 1.46 ppm (s, 9H); ^{13}C NMR (100 MHz, $CDCl_3$): δ = 166.8, 148.8, 139.9, 138.7, 136.0, 130.2, 129.5, 129.3, 128.33, 128.25, 128.0, 122.5, 80.4, 28.4 ppm; HRMS: m/z calcd for $C_{21}H_{22}O_2Na^+$: 329.1512; found: 329.1513.

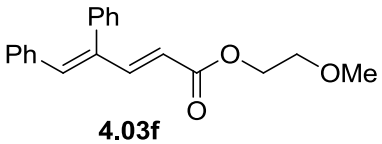

4.03f

(*2E*,*4Z*)-2-Methoxyethyl 4,5-diphenylpenta-2,4-dienoate: Chromatography (1:6 ethyl acetate/hexane, R_f = 0.20) gave **4.03f** as a white solid (57.4 mg, 93 %). ^{1}H NMR (400 MHz, $CDCl_3$): δ = 7.70(dd, *J* = 15.5, 0.7 Hz, 1H), 7.41-7.35 (m, 3H), 7.14-7.08 (m, 5H), 6.94-6.91 (m, 3H), 5.55 (d, *J* = 15.4 Hz, 1H), 4.29-4.26 (m, 12H), 3.59-3.57 (m, 2H), 3.36 ppm (s, 3H); ^{13}C NMR (100 MHz, $CDCl_3$): δ =

167.4, 150.3, 139.8, 139.0, 137.1, 135.8, 130.2, 129.38, 129.36, 128.4, 128.3, 128.1, 120.1, 70.7, 63.5, 59.2 ppm; HRMS: m/z calcd for $C_{20}H_{20}O_3Na^+$: 331.1305; found: 331.1296.

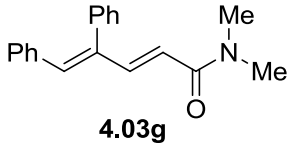

4.03g

(*2E*,*4Z*)-N,N-Dimethyl-4,5-diphenylpenta-2,4-dienamide: Chromatography (1:6 ethyl acetate/hexane, R_f = 0.48) gave **4.03g** as a white solid (62.0 mg, 95 %). ^{1}H NMR (400 MHz, $CDCl_3$): δ = 7.85(dd, *J* = 15.4, 0.7 Hz, 1H), 7.47-7.34 (m, 5H), 7.20-7.08 (m, 8H), 6.98-6.895 (m, 3H), 5.67 ppm (d, *J* = 15.4 Hz, 2H); ^{13}C NMR (100 MHz, $CDCl_3$): δ = 165.9, 151.7, 151.1, 139.9, 139.8, 137.0, 135.8, 130.4, 129.5, 128.7, 128.5, 128.3, 125.9, 121.9, 119.5 ppm; HRMS: m/z calcd for $C_{23}H_{18}O_2Na^+$: 349.1199; found: 349.1204.

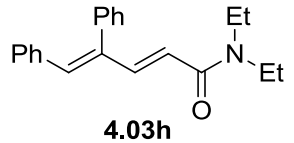

4.03h

(*2E*,*4Z*)-N,N-Diethyl-4,5-diphenylpenta-2,4-dienamide: Chromatography (ethyl acetate/hexane, R_f = 0.48) gave **4.03h** as a white solid (rt, 36.7 mg, 60%; 60 °C, 52.0 mg, 85 %). ^{1}H NMR (400 MHz, $CDCl_3$): δ = 7.65 (d, *J* = 14.9 Hz, 1H), 7.43-7.34 (m, 3H), 7.16-7.14 (m, 2H), 7.09-7.06 (m, 3H), 6.92-6.90 (m, 2H), 6.86 (s, 1H), 5.83 (d, *J* = 14.9 Hz, 1H), 3.40 (q, *J* = 7.0 Hz, 2H), 3.11 (q, *J* = 7.0 Hz, 2H), 1.10 (t, *J* = 7.0 Hz, 3H), 0.98 ppm (t, *J* = 7.0 Hz, 3H); ^{13}C NMR (100 MHz, $CDCl_3$): δ = 166.2, 147.3, 140.3, 138.0, 137.1, 136.3, 130.0, 129.5, 129.2, 128.3, 128.0, 127.9, 120.6, 42.4, 41.2, 14.9, 13.4 ppm; HRMS: m/z calcd for $C_{21}H_{23}NONa^+$: 328.1672; found: 328.1672.

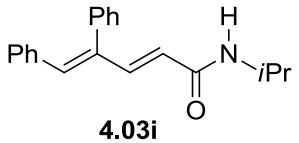

4.03i

(*2E*,*4Z*)-N-Isopropyl-4,5-diphenylpenta-2,4-dienamide: Chromatography (1:4 ethyl acetate/hexane, R_f = 0.23) gave **4.03i** as a white solid (52.5 mg, 90 %). ^{1}H NMR (400 MHz, $CDCl_3$): δ = 7.59(dd, *J* = 15.0, 0.6 Hz, 1H), 7.40-7.33 (m, 3H), 7.15-7.05 (m, 5H), 6.91-6.87 (m, 2H), 6.85 (s, 1H), 5.36 (m, 2H), 4.10 (m, 1H), 1.10 ppm (d, *J* = 6.6 Hz, 6H); ^{13}C NMR (100 MHz, $CDCl_3$): δ = 165.4, 146.0, 139.7, 137.8, 137.4, 136.1, 130.0, 129.5, 129.3, 128.3, 128.0, 127.8, 123.4, 41.5, 22.9 ppm; HRMS: m/z calcd for $C_{20}H_{21}NONa^+$: 314.1515; found: 314.1515.

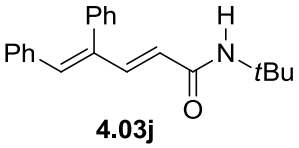

4.03j

(*2E*,*4Z*)-N-tert-Butyl-4,5-diphenylpenta-2,4-dienamide: Chromatography (1:1 ethyl acetate/hexane, R_f = 0.50) gave **4.03*J*** as a white solid (27.5 mg, 45 %). ^{1}H NMR (400 MHz, $CDCl_3$): δ = 7.56 (d, *J* = 15.0 Hz, 1H), 7.41-7.36 (m, 3H), 7.15-7.13 (m, 2H), 7.09-7.06 (m, 3H), 6.91-6.88 (m, 2H), 6.84 (s, 1H), 5.833 (d, *J* = 15.0 Hz, 1H), 5.25 (bs, 1H), 1.33 ppm (s, 9H); ^{13}C NMR (100 MHz, $CDCl_3$): δ = 165.6, 145.6, 139.7, 138.0, 137.3, 136.2, 130.0, 129.6, 129.3, 128.3, 128.0, 127.8, 124.3, 51.5, 29.0 ppm; HRMS: m/z calcd for $C_{21}H_{23}NONa^+$: 328.1672; found: 328.1666.

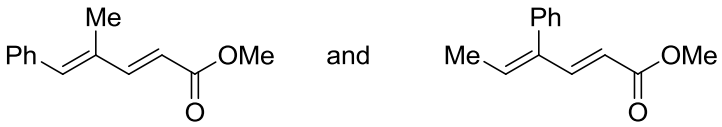

4.03k and **4.03k'**

(*2E*,*4E*)-Methyl 4-methyl-5-phenylpenta-2,4-dienoate: Chromatography (1:6 ethyl acetate/hexane, R_f = 0.50) gave **4.03k** and **4.03k'** as a colorless oil (**4.03k: 4.03k'** = 11:1, 40.0 mg, > 98 %). ^{1}H NMR (400 MHz, $CDCl_3$): δ = 7.49 (dd, *J* = 15.4, 0.7 Hz, 1H), 7.38-7.23 (m, 5H), 6.82 (s, 1H), 5.96 (d, *J* = 15.6 Hz, 1H), 3.76 (s, 3H), 2.02 ppm (d, *J* = 1.2 Hz, 2H); ^{13}C NMR (100 MHz, $CDCl_3$): δ = 167.9, 150.2, 139.2,

136.9, 134.3, 129.7, 128.5, 127.9, 117.3, 51.7, 13.9 ppm; HRMS: m/z calcd for $C_{13}H_{14}O_2Na^+$: 225.0886; found: 225.0896.

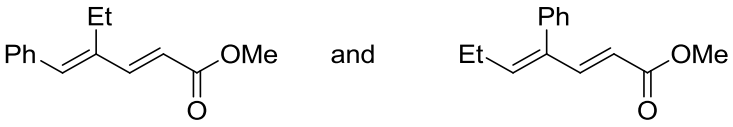

4.03l **4.03l'**

(*2E*,*4E*)-Methyl 4-ethyl-5-phenylpenta-2,4-dienoate: Chromatography (1:6 ethyl acetate/hexane, R_f = 0.52) gave **4.03l** and **4.03l'** as a colorless oil (**4.03l**:**4.03l' = 15**:**1,** 39.8 mg, 92 %). ^{1}H NMR (400 MHz, $CDCl_3$): δ = 7.39 (d, *J* = 15.9 Hz, 1H), 7.37-7.23 (m, 5H), 6.67 (s, 1H), 5.99 (d, *J* = 15.8 Hz, 1H), 3.76 (s, 3H), 2.49 (q, *J* = 7.6 Hz, 2H), 1.17 ppm (t, *J* = 7.6 Hz, 3H); ^{13}C NMR (100 MHz, $CDCl_3$): δ = 168.0, 149.2, 140.4, 138.7, 136.7, 129.2, 128.7, 128.0, 116.9, 51.7, 20.5, 13.7 ppm; HRMS: m/z calcd for $C_{14}H_{16}O_2Na^+$: 239.1043; found: 239.1046.

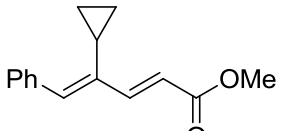

4.03m

(*2E*,*4E*)-Methyl 4-ethyl-5-phenylpenta-2,4-dienoate: Chromatography (1:6 ethyl acetate/hexane, R_f = 0.43) gave **4.03m** as a white solid (41.1 mg, 90 %). ^{1}H NMR (400 MHz, $CDCl_3$): δ = 7.50 (d, *J* = 7.4 Hz, 2H), 7.38 (d, 15.6 Hz, 1H), 7.32 (t, *J* = 7.4 Hz, 2H), 7.27-7.24 (m, 1H), 6.81 (s, 1H), 6.33 (d, *J* = 15.6 Hz, 1H), 3.76 (s, 3H), 1.61-1.55 (m, 1H), 0.89-0.84 (m, 2H), 0.24-0.20 ppm (m, 2H); ^{13}C NMR (100 MHz, $CDCl_3$): δ = 168.1, 149.8, 140.4, 138.7, 136.3, 130.3, 128.2, 128.1, 118.1, 51.7, 9.9, 9.1 ppm; HRMS: m/z calcd for $C_{15}H_{16}O_2Na^+$: 251.1043; found: 251.1050.

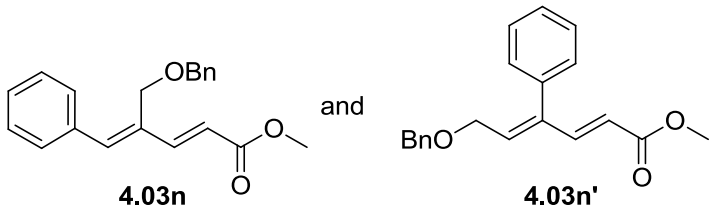

4.03n **4.03n'**

(*2E*,*4Z*)-Methyl 4-(benzyloxymethyl)-5-phenylpenta-2,4-dienoate: Chromatography (1:4 ethyl acetate/hexane, R_f = 0.43) gave **4.03n** and **4.03n'** as a white solid (**4.03n**: **4.03n'** = 10:1, 53.0 mg, 86 %). ^{1}H NMR (400 MHz, $CDCl_3$): δ = 7.54 (d, *J* = 15.6 Hz), 7.48 (d, *J* = 15.8 Hz), 7.35-7.29 (m, 10H), 7.09 (d, *J* = 8.2 Hz), 7.04 (s, 1H), 4.57 (s, 2H), 4.41 (s), 4.26 (s, 1H), 3.99 (d, *J* = 6.5 Hz), 3.77 (s, 3H), 3.70 ppm (s); ^{13}C NMR (100 MHz, $CDCl_3$): δ = 167.9, 147.7, 142.6, 137.8, 135.8, 134.5, 129.6, 128.72, 128.70, 128.6, 128.5, 128.2, 118.5, 73.1, 65.0, 51.8 ppm; HRMS: m/z calcd for $C_{20}H_{20}O_3Na^+$: 331.1305.37; found: 331.1312. The minor diastereomer was assigned based on the different coupling constants and the spectrum of the known isomer.

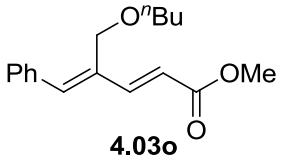

4.03o

(*2E*,*4Z*)-Methyl 4-butoxy-5-phenylpenta-2,4-dienoate : Chromatography (1:4 ethyl acetate/hexane, R_f = 0.40) gave **4.03o** as a white solid (42.0 mg, 80 %).^{1}H NMR (CDCl3, 300 MHz): δ = 7.45 (d, *J* = 15.8 Hz, 1H), 7.38-7.29 (m, 5H), 7.02 (s, 1H), 6.15 (d, *J* = 15.8 Hz, 1H), 4.19 (s, 2H), 3.76 (s, 3H), 3.48 (t, *J* = 6.5 Hz, 2H), 1.63-1.56 (m, 2H), 1.45-1.36 (m, 2H), 0.92 ppm (t, *J* = 7.4 Hz, 3H); ^{13}C NMR (CDCl3, 75 MHz): δ = 167.9, 147.8, 142.3, 136.0, 134.8, 129.6, 128.7, 128.6, 118.4, 70.83, 65.8, 51.8, 32.0, 19.7, 14.1 ppm; HRMS: calculated for $C_{16}H_{20}Na^+$: m/z = 297.1461; found: m/z = 297.1454.

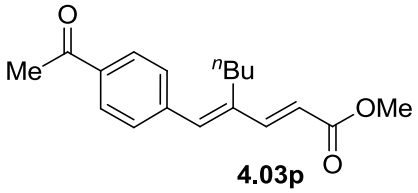

4.03p

(*2E*,*4E*)-Methyl 4-(4-acetylbenzylidene)oct-2-enoate: Chromatography (1:4 ethyl acetate/hexane, R_f = 0.32) gave **4.03p** as a white solid (48.7 mg, 85 %). ^{1}H NMR (400 MHz, $CDCl_3$): δ = 7.93-7.90 (m, 2H), 7.38-7.33 (m, 3H), 6.75 (s, 1H), 5.99 (d, *J* = 15.8 Hz, 1H), 3.74 (s, 3H), 2.56 (s, 3H), 2.44-2.40 (m, 2H), 1.53-1.45 (m, 2H), 1.40-1.31 (m, 2H), 0.88 ppm (t, *J* = 7.3 Hz, 3H); ^{13}C NMR (100 MHz, $CDCl_3$): δ = 197.6, 167.7, 148.9, 141.5, 141.2, 137.3, 136.1, 129.3, 128.7, 118.1, 51.8, 31.2, 27.4, 26.8, 23.2 ppm; HRMS: m/z calcd for $C_{18}H_{22}O_3Na^+$: 309.1416; found: 309.1455.

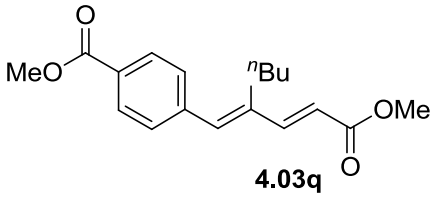

4.03q

Methyl 4-((E)-2-((E)-3-methoxy-3-oxoprop-1-enyl)hex-1-enyl): Chromatography (1:6 ethyl acetate/hexane, R_f = 0.32) gave **4.03q** as a white solid (39.8 mg, 92 %). ^{1}H NMR (400 MHz, $CDCl_3$): d = 7.85(dd, *J* = 15.4, 0.7 Hz, 1H), 7.47-7.34 (m, 5H), 7.20-7.08 (m, 8H), 6.98-6.895 (m, 3H), 5.67 ppm (d, *J* = 15.4 Hz, 2H); ^{13}C NMR (100 MHz, $CDCl_3$): δ = 165.9, 151.7, 151.1, 139.9, 139.8, 137.0, 135.8, 130.4, 129.5, 128.7, 128.5, 128.3, 125.9, 121.9, 119.5 ppm; HRMS: m/z calcd for $C_{18}H_{22}O_4Na^+$: 325.1410; found: 325.1401.

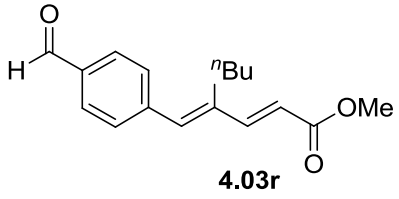

4.03r

(*2E*,*4E*)-Methyl 4-(4-formylbenzylidene)oct-2-enoate: Chromatography (1:4 ethyl acetate/hexane, R_f = 0.36) gave **4.03r** as a white solid (40.9 mg, 75 %). ^{1}H NMR (400 MHz, $CDCl_3$): δ = 9.96 (s, 1H), 7.83 (d, *J* = 8.3 Hz, 2H), 7.41 (d, *J* = 8.2 Hz, 2H), 7.35 (d, *J* = 15.8, 1H), 6.75 (s, 1H), 6.00 (d, *J* = 15.8 Hz, 1H), 3.74 (s, 3H), 2.44-2.40 (m, 2H), 1.52-1.44 (m, 2H), 1.39-1.30 (m, 2H), 0.87 ppm (t, *J* = 7.3 Hz, 3H); ^{13}C NMR (100 MHz, $CDCl_3$): δ = 191.7, 167.6, 148.7, 142.9, 141.7, 137.0, 135.4, 130.0, 129.7, 118.4, 51.8, 31.2, 27.4, 23.1, 14.0 ppm; HRMS: m/z calcd for $C_{17}H_{20}O_3Na^+$: 295.1305; found: 295.1313.

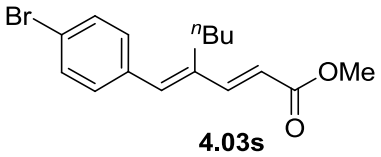

4.03s

(*2E*,*4E*)-Methyl 4-(4-cyanobenzylidene)oct-2-enoate: Chromatography (1:10 ethyl acetate/hexane, R_f = 0.37) gave **4.03s** as a white solid (40.9 mg, 75 %). ^{1}H NMR (400 MHz, $CDCl_3$): δ = 7.44 (d, *J* = 8.5 Hz, 2H), 7.34 (d, *J* = 15.8 Hz, 1H), 7.13 (d, *J* = 8.5 Hz, 2H), 6.65 (s, 1H), 5.96 (d, *J* = 15.8 Hz, 1H), 3.74 (s, 3H), 2.38 (t, *J* = 8.0 Hz, 2H), 1.50-1.43 (m, 2H), 1.34 (m, 2H), 0.89 ppm (t, *JJ* = 7.24 Hz, 3H); ^{13}C NMR (100 MHz, $CDCl_3$): δ = 167.9, 149.2, 140.0, 137.4, 135.7, 131.9, 130.8, 122.1, 117.5, 51.8, 31.1, 27.3, 23.2, 14.1 ppm; HRMS: m/z calcd for $C_{17}H_{19}NO_2Na^+$: 3470442; found: 347.0452.

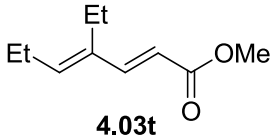

4.03t

(*2E*,*4E*)-Methyl 4-ethylhepta-2,4-dienoate: Chromatography (1:6 ethyl acetate/hexane, R_f = 0.50) gave **4.03t** as yellow oil (15.2 mg, 45 %). ^{1}H NMR (400 MHz, $CDCl_3$): δ = 7.20 (d, *J* = 15.9 Hz, 1H), 5.82-5.78 (m, 2H), 3.72 (s, 3H), 2.25-2.13 (m, 4H), 1.02-0.96 ppm (m, 6H); ^{13}C NMR (100 MHz, $CDCl_3$): δ = 168.3, 148.9, 143.7, 138.7, 114.8, 51.6, 22.0, 19.8, 13.9, 13.6 ppm; HRMS: m/z calcd for $C_{10}H_{16}O_2Na^+$: 191.1043; found: 191.1042.

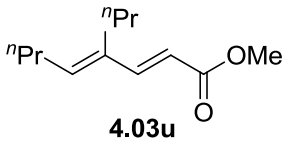

4.03u

(*2E*,*4E*)-Methyl 4-propylocta-2,4-dienoate: Chromatography (1:6 ethyl acetate/hexane, R_f = 0.52) gave **4.03u** as a yellow oil (27.5 mg, 70 %). ^{1}H NMR (400 MHz, $CDCl_3$): δ = 7.22 (d, *J* = 15.8 Hz, 1H), 5.85 (t, *J* = 7.5 Hz, 1H), 5.77 (d, *J* = 15.9 Hz, 1H), 3.71 (s, 3H), 2.16 (dt, J_1 = 14.7, J_2 = 7.6 Hz, 4H), 1.46-1.34 (m, 4H), 0.92-0.88 ppm (m, 6H); ^{13}C NMR (100 MHz, $CDCl_3$): δ = 168.3, 149.4, 142.9, 137.6, 114.8, 51.6, 31.0, 28.8, 22.6, 22.1, 14.4, 14.1 ppm; HRMS: m/z calcd for $C_{12}H_{20}O_2Na^+$: 219.1356; found: 219.1359.

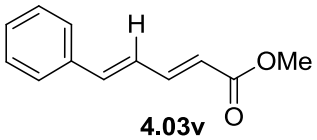

4.03v

(*2E*,*4E*)-Methyl 5-phenylpenta-2,4-dienoate: Chromatography (1:10 ethyl acetate/hexane, R_f = 0.33) gave **4.03v** as a white solid (26.7 mg, 71 %). ^{1}H NMR (400 MHz, $CDCl_3$): δ = 7.47-7.41 (m, 3H), 7.37-7.24 (m, 3H), 6.91-6.851 (m, 2H), 5.98 (m, 1H), 3.75 ppm (m, 3H); ^{13}C NMR (100 MHz, $CDCl_3$): δ = 167.8, 145.1, 140.8, 136.3, 129.4, 129.1, 127.5, 126.5, 121.1, 51.9 ppm; HRMS: m/z calcd for $C_{12}H_{12}O_2Na^+$: 211.0730; found: 211.0731.

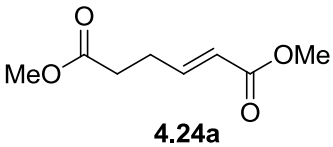

4.24a

(*E*)-Dimethyl hex-2-enedioate: Chromatography (hexane, R_f = 0.36) gave **4.24a** as yellow oil (24.1 mg, 70 %). ^{1}H NMR (400 MHz, $CDCl_3$): δ = 6.93 (dt, *J* = 15.7, 6.4 Hz, 1H), 5.84 (dt, *J* = 15.6, 1.5 Hz, 1H), 3.71 (s, 3H), 3.67 (s, 3H), 2.55-2.42 ppm (m, 4H); ^{13}C NMR (100 MHz, $CDCl_3$): δ = 172.8, 166.9, 147.0, 122.1, 52.0, 51.7, 32.4, 27.4 ppm. HRMS: calcd for $C_8H_{12}O_4Na^+$: m/z = 195.0628; found: m/z = 195.0622.

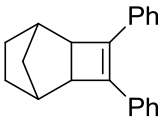

4.25a

3,4-Diphenyltricyclo[4.2.1.02,5]non-3-ene: Chromatography (hexane, R_f = 0.36) gave **4.25a** as a white solid (43.6 mg, 80 %). ^{1}H NMR (CDCl3, 400 MHz): δ = 7.59-7.53 (m, 4H), 7.33-7.29 (m, 4H), 7.26-7.22 (m, 2H), 2.81 (s, 2H), 2.26-2.25 (m, 2H), 1.68-1.60 (m, 3H), 1.245-1.20 (m, 2H), 1.057-1.04 (m, 1H); ^{13}C NMR ($CDCl_3$, 100 MHz): δ = 139.7, 135.8, 128.5, 127.7, 126.6, 47.4, 35.2, 31.0, 28.8. HRMS: calcd for C21H20: m/z = 272.1565; found: m/z = 272.1568.

4.8. References

1. Kakiuchi, F.; Yamamoto, Y.; Chatani, N.; Murai, S. Catalytic Addition of Aromatic C-H Bonds to Acetylenes. *Chem. Lett.* **1995**, *24*, 681-682.

2. Kakiuchi, F.; Murai, S. Catalytic C−H/Olefin Coupling. *Acc. Chem. Res.* **2002**, *35*, 826-834.

3. Ritleng, V.; Sirlin, C.; Pfeffer, M. Ru-, Rh-, and Pd-Catalyzed C−C Bond Formation Involving C−H Activation and Addition on Unsaturated Substrates: Reactions and Mechanistic Aspects. *Chem. Rev.* **2002**, *102*, 1731-1770.

4. Colby, D. A.; Bergman, R. G.; Ellman, J. A. Rhodium-Catalyzed C−C Bond Formation via Heteroatom-Directed C−H Bond Activation. *Chem. Rev.* **2010**, *110*, 624-655.

5. Kitamura, T. Transition-Metal-Catalyzed hHdroarylation Reactions of Alkynes through Direct Functionalization of C-H Bonds. A Convenient Tool for Organic Synthesis. *Eur. J. Org. Chem.* **2009**, 1111-1125.

6. Messaoudi, S.; Brion, J.-D.; Alami, M. Transition-Metal-Catalyzed Direct C–H Alkenylation, Alkynylation, Benzylation, and Alkylation of (Hetero)arenes. *Eur. J. Org. Chem.* **2010**, *2010*, 6495-6516.

7. Mitsudo, T.-a.; Zhang, S.-W.; And, M. N.; Watanabe, Y. Ruthenium Complex-Catalysed Highly Selective Codimerisation of Acetylenes and Alkenes. *J. Chem. Soc., Chem. Commun.* **1991**, 598-599.

8. Yi, C. S.; Lee, D. W.; Chen, Y. Hydrovinylation and [2+2] Cycloaddition Reactions of Alkynes and Alkenes Catalyzed by a Well-Defined Cationic Ruthenium−Alkylidene Complex. *Organometallics* **1999**, *18*, 2043-2045.

9. Kakiuchi, F.; Uetsuhara, T.; Tanaka, Y.; Chatani, N.; Murai, S. Ruthenium-Catalyzed Addition of Olefinic C–H Bonds in Conjugate Enones to Acetylenes to Give Conjugate Dienones. *J. Mol. Catal. A: Chem.* **2002**, *182-183*, 511-514.

10. Nishimura, T.; Washitake, Y.; Uemura, S. Ruthenium/Halide Catalytic System for C-C Bond Forming Reaction between Alkynes and Unsaturated Carbonyl Compounds. *Adv. Synth. Catal.* **2007**, *349*, 2563-2571.

11. Neisius, N. M.; Plietker, B. The Ruthenium-Catalyzed Hydrovinylation of Internal Alkynes by Acrylates: An Atom Economic Approach to Highly Substituted 1,3-Dienes. *Angew. Chem. Int. Ed.* **2009**, *48*, 5752-5755.

12. Schabel, T.; Plietker, B. Microwave-Accelerated Ru-Catalyzed Hydrovinylation of Alkynes and Enynes: A Straightforward Approach toward 1,3-Dienes and 1,3,5-Trienes. *Chem. - Eur. J.* **2013**, *19*, 6938-6941.

13. Saito, N.; Saito, K.; Shiro, M.; Sato, Y. Regio- and Stereoselective Synthesis of 2-Amino-1,3-Diene Derivatives by Ruthenium-Catalyzed Coupling of Ynamides and Ethylene. *Org. Lett.* **2011**, *13*, 2718-2721.

14. Colby, D. A.; Bergman, R. G.; Ellman, J. A. Stereoselective Alkylation of α,β-Unsaturated Imines via C−H Bond Activation. *J. Am. Chem. Soc.* **2006**, *128*, 5604-5605.

15. Colby, D. A.; Bergman, R. G.; Ellman, J. A. Synthesis of Dihydropyridines and Pyridines from Imines and Alkynes via C-H Activation. *J. Am. Chem. Soc.* **2008**, *130*, 3645-3651.

16. Parthasarathy, K.; Jeganmohan, M.; Cheng, C.-H. Rhodium-Catalyzed One-Pot Synthesis of Substituted Pyridine Derivatives from α,β-Unsaturated Ketoximes and Alkynes. *Org. Lett.* **2008**, *10*, 325-328.

17. Shibata, Y.; Hirano, M.; Tanaka, K. Rhodium-Catalyzed Regio- and Stereoselective Codimerization of Alkenes and Electron-Deficient Internal Alkynes Leading to 1,3-Dienes. *Org. Lett.* **2008**, *10*, 2829-2831.

18. Lindhardt , A. T.; Mantel, M. L. H.; Skrydstrup, T. Palladium-Catalyzed Intermolecular Ene–Yne Coupling: Development of an Atom-Efficient Mizoroki–Heck-Type Reaction. *Angew. Chem. Int. Ed.* **2008**, *47*, 2668-2672.

19. Horie, H.; Koyama, I.; Kurahashi, T.; Matsubara, S. Nickel-Catalyzed Intermolecular Codimerization of Acrylates and Alkynes. *Chem. Commun.* **2011**, *47*, 2658-2660.

20. Mannathan, S.; Cheng, C.-H. Cobalt-Catalyzed Regio- and Stereoselective Intermolecular Enyne Coupling: an Efficient Route to 1,3-Diene Derivatives. *Chem. Commun.* **2010**, *46*, 1923-1925.

21. Zhang, J.; Ugrinov, A.; Zhao, P. Ruthenium(II)/N-Heterocyclic Carbene Catalyzed [3+2] Carbocyclization with Aromatic N-H Ketimines and Internal Alkynes. *Angew. Chem. Int. Ed.* **2013**, *52*, 6681-6684.

22. Zhang, J.; Ugrinov, A.; Zhang, Y.; Zhao, P. Exploring Bis(cyclometalated) Ruthenium(II) Complexes as Active Catalyst Precursors: Room-Temperature Alkene–Alkyne Coupling for 1,3-Diene Synthesis. *Angew. Chem. Int. Ed.* **2014**, *53*, 8437-8440.

23. Trost, B. M.; Frederiksen, M. U.; Rudd, M. T. Ruthenium-Catalyzed Reactions—A Treasure Trove of Atom-Economic Transformations. *Angew. Chem. Int. Ed.* **2005**, *44*, 6630-6666.

24. Vovard-Le Bray, C.; Dérien, S.; Dixneuf, P. H. Cp*RuCl(COD) in Catalysis: a Unique Role in the Addition of Diazoalkane Carbene to Alkynes. *C. R. Chim.* **2010**, *13*, 292-303.

25. Morimoto, T.; Chatani, N.; Fukumoto, Y.; Murai, S. $Ru_3(CO)_{12}$-Catalyzed Cyclocarbonylation of 1,6-Enynes to Bicyclo[3.3.0]octenones. *J. Org. Chem.* **1997**, *62*, 3762-3765.

26. Kondo, T.; Suzuki, N.; Okada, T.; Mitsudo, T.-a. First Ruthenium-Catalyzed Intramolecular Pauson−Khand Reaction. *J. Am. Chem. Soc.* **1997**, *119*, 6187-6188.

27. Flower, K. R.; Howard, V. J.; Pritchard, R. G.; Warren, J. E. Synthesis and Characterization of Cycloruthenated 2-(Phenylimino)phenyls: A Useful Probe for the Elucidation of the Tautomeric Process in 2-Hydroxyphenyl-Schiff Bases. *Organometallics* **2002**, *21*, 1184-1189.

28. Scherl, P.; Wadepohl, H.; Gade, L. H. Hydrogenation and Silylation of a Double-Cyclometalated Ruthenium Complex: Structures and Dynamic Behavior of Hydrido and Hydridosilicate Ruthenium Complexes. *Organometallics* **2013**, *32*, 4409-4415.

29. Hirano, M.; Sakate, Y.; Komine, N.; Komiya, S.; Bennett, M. A. Isolation of *trans*-2,5-Bis(methoxycarbonyl)ruthenacyclopentane by Oxidative Coupling of Methyl Acrylate on Ruthenium(0) as an Active Intermediate for Tail-to-Tail Selective Catalytic Dimerization. *Organometallics* **2009**, *28*, 4902-4905.

30. Sustmann, R.; Hornung, H. J.; Schupp, T.; Patzke, B. Dimerization of Methyl Acrylate by Homogeneous Transition-Metal Catalysis. Part I. Activation of Hydrido (Carbonyl) Chloro-[Bis(Triisopropylphosphane)] Ruthenium by CF_3SO_3Ag. *J. Mol. Catal.* **1993**, *85*, 149-152.

31. Butenschön, H. Construction of Carbon Frameworks with the Help of Ruthenium Complexes: 1,5-Cyclooctadiene as a Reagent in Transition Metal Catalyzed Reactions. *Angew. Chem. Int. Ed.* **1994**, *33*, 636-638.

32. Mitsudo, T.-a.; Naruse, H.; Kondo, T.; Ozaki, Y.; Watanabe, Y. [2 + 2] Cycloaddition of Norbornenes with Alkynes Catalyzed by Ruthenium Complexes. *Angew. Chem. Int. Ed.* **1994**, *33*, 580-581.

33. Thorand, S.; Krause, N. Improved Procedures for the Palladium-Catalyzed Coupling of Terminal Alkynes with Aryl Bromides (Sonogashira Coupling). *J. Org. Chem.* **1998**, *63*, 8551-8553.

34. Singh, R.; Just, G. Rates and Regioselectivities of the Palladium-Catalyzed Ethynylation of Substituted Bromo- and Dibromobenzenes. *J. Org. Chem.* **1989**, *54*, 4453-4457.

35. Bolte, B.; Odabachian, Y.; Gagosz, F. Gold(I)-Catalyzed Rearrangement of Propargyl Benzyl Ethers: A Practical Method for the Generation and in Situ Transformation of Substituted Allenes. *J. Am. Chem. Soc.* **2010**, *132*, 7294-7296.

CHAPTER 5. A DECARBOXYLATIVE APPROACH FOR REGIOSELECTIVE HYDROARYLATION OF ALKYNES

5.1. Background and Significance

Aryl-substituted alkenes are prevalent structures in biologically active compounds and used extensively as synthetic intermediates for fine chemicals and materials. The addition of an aromatic C-H bond to a C-C triple bond allows convenient and modular synthesis of arylalkenes using readily available alkyne and arene building blocks.[1-7] These alkyne hydroarylation processes feature high atom efficiency and significantly reduced production of salt wastes in contrast to transition metal-catalyzed alkyne coupling with aryl halides and their analogs or main-group metal aryl nucleophiles (Scheme 5.1).[8-12]

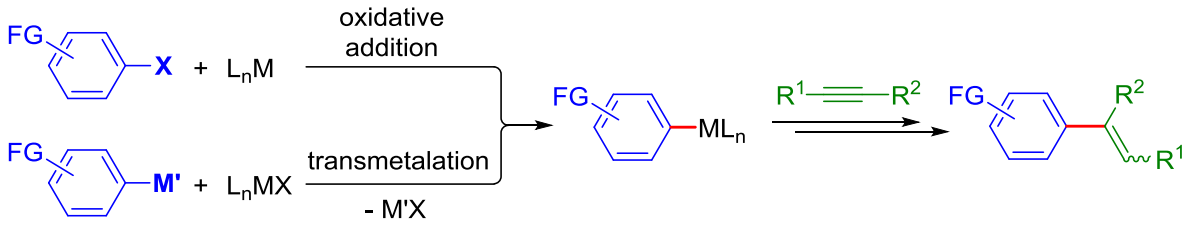

Scheme 5.1. Transition metal-catalyzed alkyne hydroarylation with aryl halides and arylmetallic reagents

A long-standing challenge for practical applications of alkyne hydroarylation is to achieve controlled and versatile regioselectivity with unsymmetrically substituted arenes. The classic method of alkyne hydroarylation by Lewis acid-catalyzed Friedel-Crafts reactions generally requires electron-donating aromatic substituents to achieve satisfactory reactivity. The resulting *ortho*- and *para*-directing effects often lead to a hard-to-separate mixture of *ortho*- and *para*-substituted alkenylarene isomers in low regioselectivity (Scheme 5.2, EDG = electron-donating group).[13-20] In addition, Friedel-Crafts alkyne hydroarylation often suffers from low stereoselectivity for *E/Z* isomeric alkene products and byproduct formation from over-alkenylation of the arene substrates.

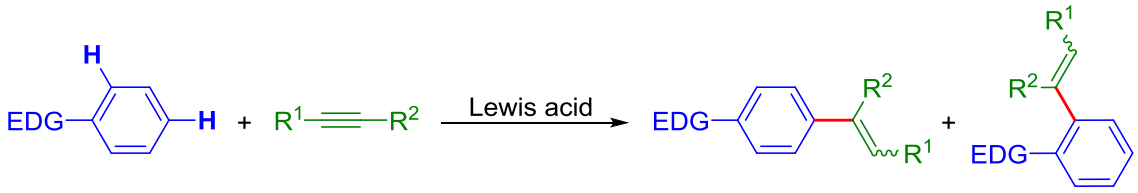

Scheme 5.2. Lewis acid-catalyzed alkyne hydroarylation with electron-rich arenes

In recent years, a variety of transition metal-based catalysts have been developed for alkyne hydroarylation via formal activation of arene C-H bonds to form nucleophilic metal aryl intermediates. A number of these reported catalysts involve an electrophilic aromatic substitution (EAS) pathway for C-H activation with Lewis acidic transition metal catalysts, which is mechanistically related to the Friedel-Crafts chemistry and leads to similar limitation in regioselectivity (Scheme 5.3).[21,22]

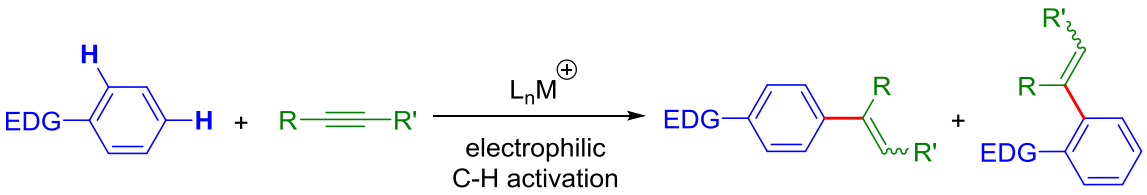

Scheme 5.3. Transition metal-catalyzed alkyne hydroarylation via electrophilic C-H bond activation

Another major strategy is to utilize σ-donating functionality as *ortho*-directing groups for aromatic C-H bond activation, which leads to exclusive *ortho*-selectivity for catalytic alkyne hydroarylation as described in Chapter 1 (Scheme 5.4, DG = directing group).[23-30] However, removal of these *ortho*-directing groups from the hydroarylation products usually requires additional chemical transformations and is not always achievable.[31] Thus, the limitation on regiochemistry of alkyne hydroarylation methods is highlighted by the difficulty to selectively form *meta*- or *para*-substituted alkenylarene products.

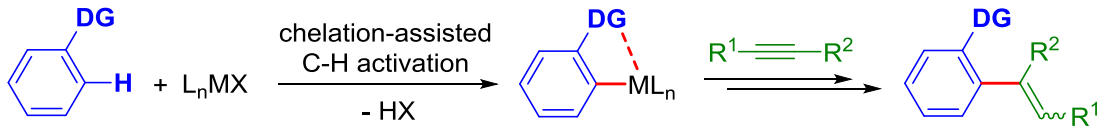

Scheme 5.4. Transition metal-catalyzed alkyne hydroarylation via directed C-H bond activation

Recently, a handful of strategies for *meta*-selective C-H activation based C-C bond forming reactions have been developed to access *meta*-substituted arenes.[32-39] Notably, Yu and coworkers elegantly devised a template approach to activate remote *meta*-C–H bonds, which could be used to prepare *meta*-alkenylarenes (**5.03**) via oxidative alkenylation (Scheme 5.5).[40] High regio- and stereoseletivity were achieved with various olefins (**5.02**) in the presence of catalytic amount of $Pd(OPiv)_2$ and stoichiometric amount of oxidant in DCE at 90 ^{o}C. It was also proved that the *meta*-directing group concept could also be applied to alkenylation of hydrocinnamic acids, phenols and anilines.[40-42] However, the development of the template would require extensive engineering and extra steps to install and remove the template before and after alkenyation. Beside, oxidative alkenylation requires stoichiometric amount of silver salt as oxidant. Thus it is highly desirable to develop an alkyne hydroarylation method that allows controllable and versatile regiochemistry of aromatic substitution.

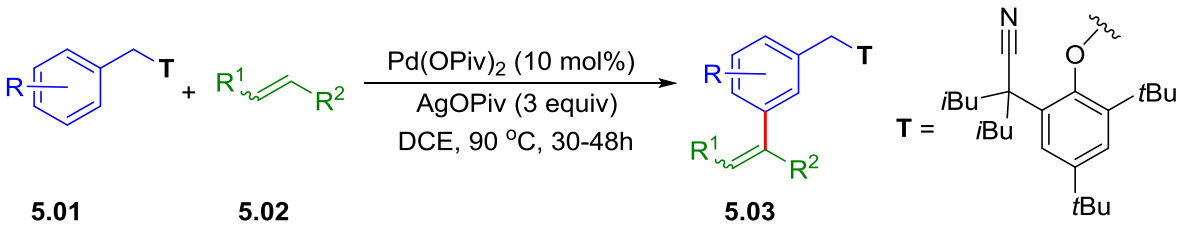

Scheme 5.5. Palladium catalyzed template directed *meta*-C-H bond alkenylation

The strategy of traceless directing group allows site-selective C-H bond activation at an *ortho*-position of the directing group and *meta*-/*para*-selective functionalization depending on the substitution

pattern of the substrate. Thus, it provides an attractive tactic to access *meta*-/*para*-functionalized arenes in a single step (Scheme 5.6).

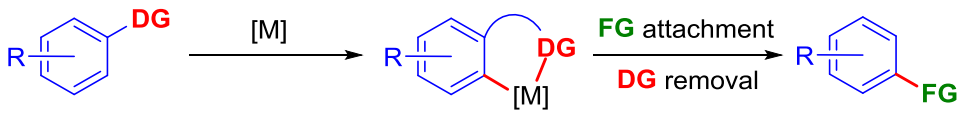

Scheme 5.6. Transition metal-catalyzed C-H bond functionalization using traceless directing group

Given the wide availability and low costs of arenecarboxylic acids, transition metal-catalyzed decarboxylative transformations of arenecarboxylic acids have attracted significant attention in the past decade.[43-46] A variety of transition metals have been successfully applied in these transformations via the formation of aryl-metal intermediate (Scheme 5.7). Usually an *ortho*-inductive electron-withdrawing aromatic substituent would be required to facilitate these transformations. For example, our group has developed a rhodium-catalyzed decarboxylative Heck-Mizoroki reaction of perfluorobenzoic acids (**5.04**) with electron-deficient olefins (**5.02**) to produce alkenylarenes (**5.03**) (Scheme 5.8).[33]

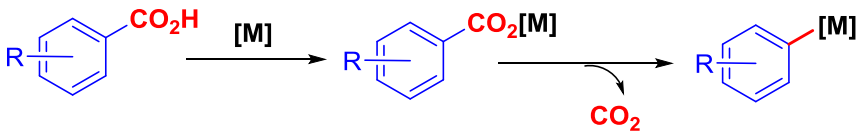

Scheme 5.7. Transition metal-mediated protodecarboxylation of arenecarboxylic acids

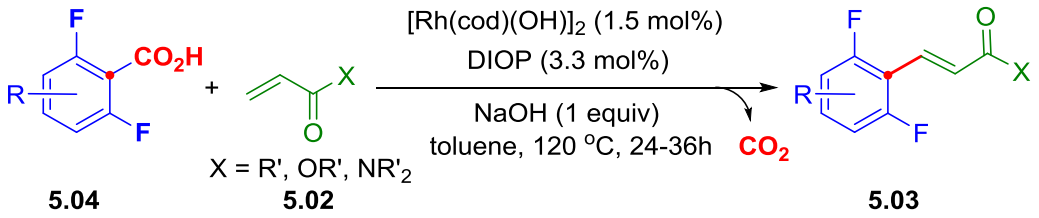

Scheme 5.8. Rhodium catalyzed decarboxylative Heck-Mizoroki reaction of perfluorobenzoic acids with electron-deficient olefins

On the other hand, carboxylic acid has been used as directing group in transition metal-catalyzed C-H bond activation to introduce a C-C bond in its *ortho*-position.[47-54] In alkyne hydroarylation with arenecarboxylic acids (**5.04**), isocoumarins (**5.06**) are usually formed via a tandem reaction of carboxylic acid directed C-H bond activation, alkyne insertion and oxidative heterocyclization.[55,56] For example, Miura and coworkers reported a rhodium-catalyzed heterocyclization of arenecarboxylic acids (**5.04**) and internal alkynes (**5.05**) in the presence of stoichiometric $Cu(OAc)_2$ as oxidant under N_2 or catalytic $Cu(OAc)_2$ under air (Scheme 5.9).[55] Besides isocoumarins, the minor products (**5.07**) from [2+2+2] decarboxylative cyclization were also detected for some substrates. The authors found iridium could selectively catalyze the decarboxylative cyclization with the assistance of stoichiometric amount of Ag_2CO_3 at higher temperature (Scheme 5.10).[55] The reaction was proposed to proceed via carboxylic acid directed C-H bond activation, followed by alkyne insertion and decarboxylation. Subsequent second alkyne insertion and reductive elimination gave the cyclization product. Successive oxidation of Ir(I) back to Ir(III) by Ag_2CO_3 completed the catalytic cycle.

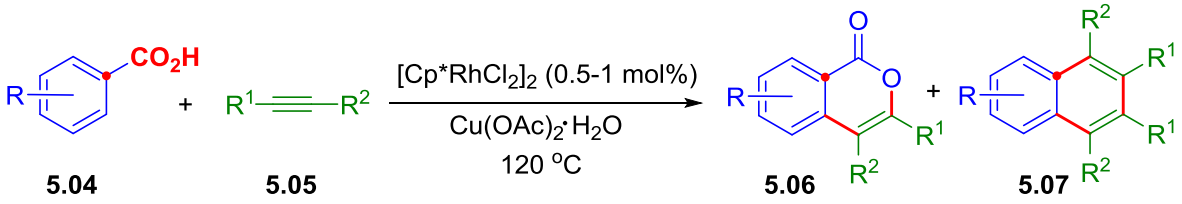

Scheme 5.9. Rhodium catalyzed oxidative heterocyclization with arenecarboxylic acid and internal alkynes initiated by carboxyl directed C-H bond activation

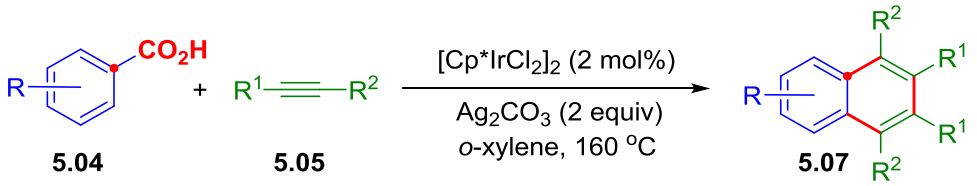

Scheme 5.10. Iridium catalyzed decarboxylative [2+2+2] cyclization with arenecarboxylic acids and internal alkynes initiated by carboxyl directed C-H bond activation

We hypothesized that a potential solution for the regiochemistry challenge in alkyne hydroarylation is to use arenecarboxylic acids (**5.04**) as arene equivalents, with the carboxylic acid functionality as an *ortho*-directing group that is removed by metal-mediated decarboxylation after C-H alkenylation (Scheme 5.11). This decarboxylative approach for alkyne hydroarylation is a redox-neutral reaction and has the advantage of using ubiquitous benzoic acids as easily accessible aromatic building blocks, with CO_2 as the only byproduct and no production of salt waste.

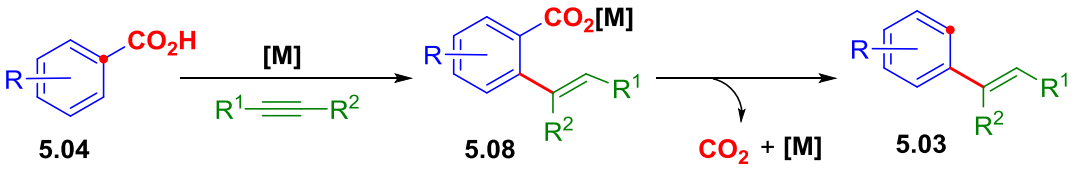

Scheme 5.11. Hypothesis on transition metal-catalyzed decarboxylative alkyne hydroarylation with carboxyl group as traceless directing group

However, achieving versatile regiochemistry and practical tolerance of functional groups has been very difficult for transition metal-catalyzed decarboxylative transformations. For example, Miura disclosed a rhodium catalyzed *meta*-selective decarboxylative alkenylation of arenecarboxylic acids (**5.04**) with styrenes (**5.02**).[57,58] The reaction was a two-step, one-pot reaction: first, rhodium catalyzed carboxylic acid directed *ortho* C-H bond alkenylation; second, silver mediated decarboxylation of the alkenylated arenecarboxylic acid (Scheme 5.12). Larrosa revealed a one-step palladium catalyzed *meta*-selective arylation of *ortho*-substituted arenecarboxylic acids (**5.04**) with aryl iodide (**5.09**). This reaction was carried out in acetic acid and with the assistance of stoichiometric Ag_2CO_3 at 130 °C (Scheme

5.13).[35] Notably, in all of these reported examples of using a removable carboxyl directing group, substrate activation with an *ortho*-aromatic substituent to carboxylic acid group is necessary to promote the reaction. This pre-requisite for substrate activation limited the scope and regiochemistry of C-H functionalization products regarding aromatic substituents. In addition, the requirement of stoichiometric sliver salt and high reaction temperature would limit the tolerance of synthetically useful functional groups such as the oxidation-sensitive phenol and unprotected aniline functionality. Thus, applying traceless directing group strategy to an alkyne hydroarylation with arenecarboxylic acids needs to overcome these limitations to achieve controllable and versatile regiochemistry of aromatic substitution.

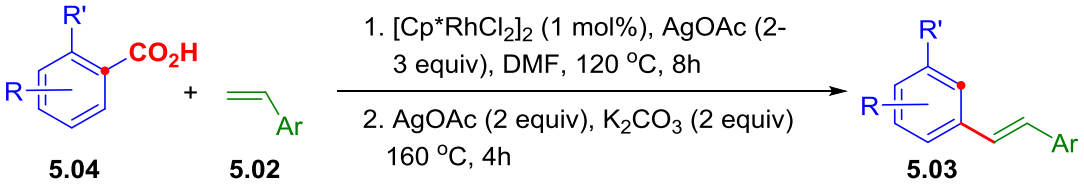

Scheme 5.12. Rhodium catalyzed decarboxylative alkenylation with arenecarboxylic acids and styrenes

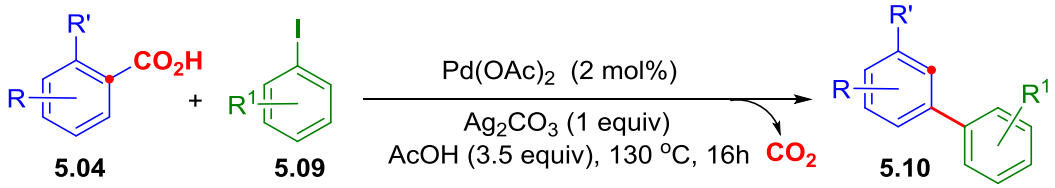

Scheme 5.13. Palladium catalyzed decarboxylative arylation with arenecarboxylic acids and aryl iodides

This chapter will describe our discovery of a catalyst system for decarboxylative alkyne hydroarylation with various benzoic acids that overcomes the limitation on decarboxylation substrate scope, providing alkenylarene products with a broad scope of aromatic substituents that feature versatile regiochemistry and synthetically useful functional group tolerance.

5.2. Initial Results

Formation of isocoumarins and naphthalenes, in rhodium and ruthenium catalyzed coupling between alkynes and benzoic acids was preferred, which required the presence of oxidants, such as copper(II) and silver(I) salts.[55,57,59,60] Thus, oxidants should be avoided in the design of alkyne hydroarylation with the same substrates.

As mentioned above, substrate activation with an *ortho* aromatic substituent to carboxylic acid group is required for decarboxylation after C-C coupling in palladium catalyzed decarboxylative arylation and rhodium catalyzed Heck-Mizoroki reaction. However, the formation of naphthalene derivatives via [2+2+2] decarboxylative cyclization does not require substrate preactivation. These results indicate that there might be an unusual intermediate involved in the process of the formation of naphthalenes. Such an intermediate consists of a special structural feature, which could interact with the metal catalyst and promote the decarboxylation. If the reaction could be stopped after alkenylation and decarboxylation, we would get the desired alkyne hydroarylation product.

With these consideration, we proposed a tandem sequence of “double chelation assistance” that is initiated by a carboxylic acid-directed C-H bond activation and alkyne coupling to form an *ortho*-alkenylbenzoic acid intermediate (**I**) as shown in Scheme 5.14. In the subsequent decarboxylation stage, the newly installed alkenyl moiety “returns the favor” of chelation assistance by coordinating to the metal center of a carboxylate intermediate and facilitates the C-C bond activation for CO_2 release (**II** in Scheme 5.14).

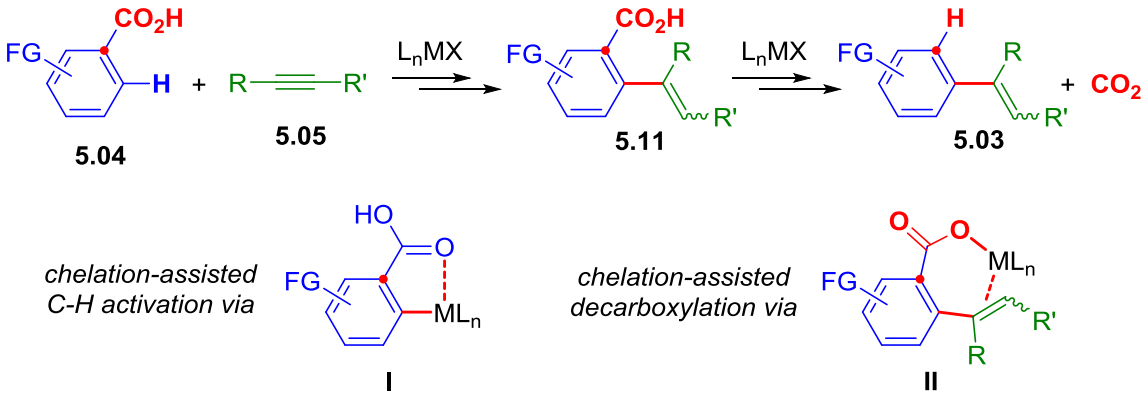

Scheme 5.14. Hypothesis on transition metal-catalyzed decarboxylative alkyne hydroarylation via a tandem sequence of "double chelation assistance"

With this envisioned low-activation energy decarboxylation process via alkene chelation, we began our investigation with a model reaction between benzoic acid (**5.04a** in Figure 5.1) and diphenylacetylene (**5.05a**), targeting 1,1,2-triphenylethylene (**5.03a**) as the desired product by decarboxylative hydroarylation. We have focused our attention on ruthenium(II)-based catalysts, which have played an important role both in chelation-assisted C-H activation and in decarboxylative allylation reactions.[61,62] A major challenge for our catalyst development is to achieve high chemoselectivity to promote formation of **5.03a** over multiple byproducts that can be formed by reported catalytic couplings between **5.04a** and **5.05a**, which include alkyne hydrocarboxylation (**5.12a**),[63] oxidative [4+2] heterocyclization (**5.06a**),[59,60] and oxidative [2+2+2] carbocyclization via decarboxylation (**5.07a**).[55,57,59] We found that in the presence of 5 mol% of [Ru(*p*-cymene)Cl_2]$_2$ and 20 mol% NaOAc, diphenylacetylene reacted with 1.5 equivalent of benzoic acid producing 40% of triphenylethene with 13% of all of the three byproducts as mentioned above at 100 °C (Figure 5.1). This result confirmed our hypothesis: alkyne hydroarylation was favored in the absence of oxidant and decarboxylation occurred under milder reaction conditions without silver additives.

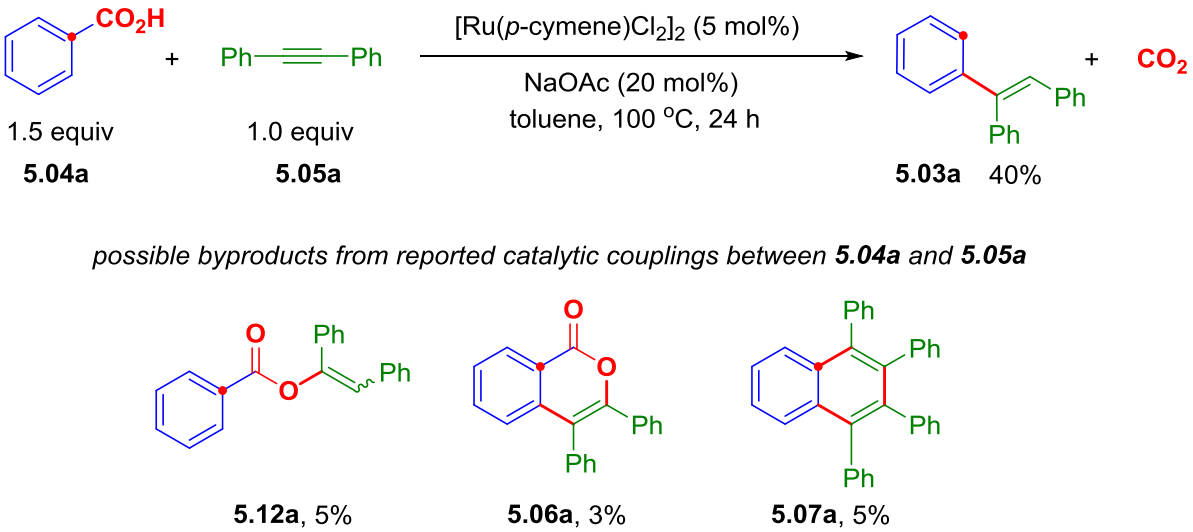

Figure 5.1. Initial result of ruthenium catalyzed decarboxylative hydroarylation with benzoic acid and diphenylacetylene

5.3. Optimization of Reaction Conditions

With this promising initial result, we started to evaluate the catalytic parameters including the ratio of **5.04a**:**5.05a**, additives, solvents and reaction temperature (Table 5.1). With 2 equivalent of benzoic acid, the yield of **5.03a** was increased to 55% while the yields of the byproducts were reduced (entry 2). Increasing the amount of diphenylacetylene would produce less **5.03a** and more [2+2+2] cyclization product (entries 3 and 4). Because benzoic acid and its substituted analogs are mostly available through commercial sources and inexpensive, we conducted the decarboxylative hydroarylation reaction with 2 equivalents of the benzoic acid substrate to maximize the conversion of the alkyne in all of the following reactions. Raising the loading of NaOAc did not affect the yield of **5.03a** (entries 5 and 6). Acetates with different cations, such as potassium and cesium had negligible influence on the yield of **5.03a** (entries 11 and 12). Acid additives, such as acetic acid, trifluoroacetic acid and pivalic acid, strongly retarded the reaction (entries 7-9). Lowering the reaction temperature to 80 ^{o}C dramatically decreased the yield of **5.03a** (entry 10). Polar solvents such as DCE, DME, 1,4-dioxane, and NMP, were not effective to promote the alkyne hydroarylation (entries 13-16).

Table 5.1. Initial test for effects of substrate ratios, additive, solvent, and temperature in ruthenium(II) catalyzed decarboxylative alkyne hydroarylation with arenecarboxylic acids[a]

Entry	ratio **5.04a:5.05a**	temperature (^{o}C)	salt additive (mol%)	solvent	Yield (%)[b] **5.03a**	**5.12a**	**5.06a**	**5.07a**
1	1.5:1	100	NaOAc (20)	toluene	40	5	3	5
2	2:1	100	NaOAc (20)	toluene	55	4	2	3
3	1:1	100	NaOAc (20)	toluene	37	4	2	5
4	1:2	100	NaOAc (20)	toluene	19	4	<2	8
5	2:1	100	NaOAc (50)	toluene	54	2	<2	3
6	2:1	100	NaOAc (100)	toluene	53	3	<2	2
7	2:1	100	PivOH (20)	toluene	8	3	<2	<2
8	2:1	100	AcOH (20)	toluene	<2	<2	<2	<2
9	2:1	100	TFA (20)	toluene	<2	<2	<2	<2
10	2:1	80	NaOAc (20)	toluene	7	<2	<2	<2
11	2:1	100	KOAc (20)	toluene	55	3	4	5
12	2:1	100	CsOAc (20)	toluene	56	3	3	7
13	2:1	100	NaOAc (20)	DCE	<2	4	<2	<2
14	2:1	100	NaOAc (20)	NMP	<2	3	<2	<2
15	2:1	100	NaOAc (20)	Dioxane	10	<2	<2	<2
16	2:1	100	NaOAc (20)	DME	15	<2	<2	<2

[a] Reaction conditions: benzoic acid (0.4 mmol, 2.0 equiv), diphenylacetylene (1.0 equiv), Ru precatalyst (10 mol%), salt additive (10-100 mol%), solvent (1.0 mL), 24h. [b] GCyields.

To improve the reaction, different types of ligands, such as N-heterocyclic carbenes (NHCs), mono- and bisphosphines, diamines and bipyridine, were tested at 100 ^{o}C (Table 5.2). However, all of these ligands would hinder the reaction (entries 1-11). The combination of [Ru(*p*-cycmene)Cl_2]$_2$ and NaOAc was supposed to generate ruthenium complexes with anionic acetate ligand. To increase the efficiency of the catalyst, [Ru(*p*-cymene)$(OAc)_2$] (**5.13**) was prepared and used as the catalyst precursor, generating 66% of **5.03a** with a trace amount of byproducts at 100 ^{o}C (entry 12). Even at a lower temperature 80 ^{o}C, there was still 25% of **5.03a** formed using **5.13** as catalyst precursor (entry 14). However, lowing the loading of **5.13** to 5 mol% would reduce the yield significantly (entry 13). Another ruthenium(II) carboxylate, [Ru(*p*-cymene)$(OBz)_2$], turned out to be as effective as **5.13** (entries 15, 16).

Ru(cod))(methylallyl)$_2$, which was used as the catalyst precursor for [3+2] carbocyclizations in Chapter 2 and 3, favored the alkyne hydrocarboxylation reaction (entry 14). All other Ru(0) and Ru(II) complexes were ineffective to promote the coupling between benzoic acid and diphenylacetylene (entries 17-22). [Ru(*p*-cymene)(OAc)$_2$] (**5.13**) was selected as the catalyst precursor to further improve the reaction at 80 ^{o}C.

Table 5.2. Effects of ligand and catalyst precursor in ruthenium catalyzed decarboxylative alkyne hydroarylation with arenecarboxylic acids[a]

Entry	Ru Precatalyst (mol%)	temperature (^{o}C)	Ligand (mol%)	Yield (%)[b] **5.03a**	**5.12a**	**5.06a**	**5.07a**
1	[Ru(*p*-cymene)Cl$_2$]$_2$ (5)	100	IPr (10)	14	<2	<2	<2
2	[Ru(*p*-cymene)Cl$_2$]$_2$ (5)	100	PPh$_3$ (10)	<2	5	<2	<2
3	[Ru(*p*-cymene)Cl$_2$]$_2$ (5)	100	PCy$_3$ (10)	<2	5	<2	<2
4	[Ru(*p*-cymene)Cl$_2$]$_2$ (5)	100	P(C$_6$F$_5$)$_3$ (10)	18	<2	<2	<2
5	[Ru(*p*-cymene)Cl$_2$]$_2$ (5)	100	P(*o*-tolyl)$_3$ (10)	10	<2	<2	<2
6	[Ru(*p*-cymene)Cl$_2$]$_2$ (5)	100	DPPP (10)	<2	<2	<2	<2
7	[Ru(*p*-cymene)Cl$_2$]$_2$ (5)	100	BINAP (10)	<2	<2	<2	<2
8	[Ru(*p*-cymene)Cl$_2$]$_2$ (5)	100	BPPBenzene	<2	<2	<2	<2
9	[Ru(*p*-cymene)Cl$_2$]$_2$ (5)	100	2,2'-Bipyridine (10)	<2	5	5	5
10	[Ru(*p*-cymene)Cl$_2$]$_2$ (5)	100	Phen (10)	<2	70	<2	<2
11	[Ru(*p*-cymene)Cl$_2$]$_2$ (5)	100	diamino-1,1'-biphenyl (10)	11	6	6	6
12	Ru(*p*-cymene)(OAc)$_2$] (10)[c]	100	none	66	<2	<2	<2
13	[Ru(*p*-cymene)(OAc)$_2$] (5)[c]	100	none	16	<2	<2	<2
14	[Ru(*p*-cymene)(OAc)$_2$] (10)[c]	80	none	25	<2	<2	<2
15	[Ru(*p*-cymene)(OBz)$_2$] (10)[c]	100	none	66	<2	<2	<2
16	[Ru(*p*-cymene)(OBz)$_2$] (10)[c]	80	none	30	<2	<2	<2
17	[Ru(cod)(methylallyl)$_2$] (10)[c]	80	none	no	no	no	no
18	[Ru(cod)Cl$_2$] (10)[c]	80	none	no	no	no	no
19	Ru$_3$CO$_{12}$ (3.4)[c]	80	none	no	no	no	no
20	[Ru(Cp)(PPh$_3$)$_2$Cl] (10)[c]	80	none	no	no	no	no
21	[RuCl$_3$*xH$_2$O] (10)[c]	80	none	no	no	no	no
22	RuH(CO)(PPh$_3$)$_3$ (10)[c]	80	none	no	no	no	no

[a] Reaction conditions: benzoic acid (0.4 mmol, 2.0 equiv), diphenylacetylene (1.0 equiv), Ru precatalyst (5-10 mol%), ligand (10 mol%), NaOAc (20 mol%), toluene (1.0 mL), 24h. [b] GC Yields; "no" indicates no detection of the product. [c] without NaOAc.

Arene solvents were found to be the best type of solvent for high chemoselectivity towards **5.03a** over other byproducts, although the yields were low in the presence of 10 mol% of **5.13** at 80 ^{o}C. Other solvents, such as ethereal solvents, DMF, DCM, acetone, and *t*-armyl alcohol were less effective in promoting this transformation (Table 5.3, entries 1-14). Through high throughput screening on solvent conditions, we found an effective solvent system containing 2:2:1 dioxane, mesitylene and heptane. In this mixed solvent system, the coupling between **5.04a** and **5.05a** could be promoted by 10 mol% Ru(p-cymene)$(OAc)_2$ (**5.13**) as catalyst at 80 ^{o}C to selectively form **5.03a** in 65% yield over 24 hours. Other analogous ruthenium complexes with different carboxylate anions, such as [Ru(*p*-cymene)$(OBz)_2$] and [Ru(*p*-cymene)$(OPiv)_2$], showed similar catalytic ability under the same reaction conditions. Notably, [Ru(*p*-cymene)$(O_2CCF_3)_2$] was a much less effective catalyst precursor (entries 17-19). Ruthenium complexes with different π-arene ligand, such as toluene and benzene, led to lower yields of **5.03a** (entries 20 and 21). The reaction time was found to have substantial impact on the outcome of the reaction. Under otherwise identical reaction conditions, 90% of **5.03a** was obtained when extending the reaction time to 48 hours, whereas less than 5% combined yield of byproducts **5.12a**, **5.06a**, and **5.07a** were detected by GC analysis.

Table 5.3. Effects of solvent and catalyst precursor in ruthenium catalyzed decarboxylative alkyne hydroarylation with arenecarboxylic acids[a]

Entry	Ru Precatalyst (mol%)	solvent	Yield (%)[b] **5.03a**	**5.12a**	**5.06a**	**5**
1	[Ru(*p*-cymene)$(OAc)_2$] (10)	toluene	25	<2	<2	
2	[Ru(*p*-cymene)$(OAc)_2$] (10)	mesitylene	27	<2	<2	
3	[Ru(*p*-cymene)$(OAc)_2$] (10)	benzene	22	<2	<2	
4	[Ru(*p*-cymene)$(OAc)_2$] (10)	*p*-cymene	20	14	<2	
5	[Ru(*p*-cymene)$(OAc)_2$] (10)	THF	12	<2	<2	
6	[Ru(*p*-cymene)$(OAc)_2$] (10)	1,4-dioxane	15	<2	<2	
7	[Ru(*p*-cymene)$(OAc)_2$] (10)	acetone	15	<2	<2	
8	[Ru(*p*-cymene)$(OAc)_2$] (10)	heptane	17	<2	<2	
9	[Ru(*p*-cymene)$(OAc)_2$] (10)	NMP	2	<2	<2	
10	[Ru(*p*-cymene)$(OAc)_2$] (10)	DME	16	<2	<2	
11	[Ru(*p*-cymene)$(OAc)_2$] (10)	DMF	<2	<2	<2	
12	[Ru(*p*-cymene)$(OAc)_2$] (10)	acetonitrile	20	5	<2	
13	[Ru(*p*-cymene)$(OAc)_2$] (10)	DCM	13	<2	<2	
14	[Ru(*p*-cymene)$(OAc)_2$] (10)	*t*-amyl-OH	4	<2	<2	
15	[Ru(*p*-cymene)$(OAc)_2$] (5)	mixed[c]	10	<2	<2	
16	[Ru(*p*-cymene)$(OAc)_2$] (10)	mixed[c]	65	<2	<2	
17	[Ru(*p*-cymene)$(OBz)_2$] (10)	mixed[c]	65	<2	<2	
18	[Ru(*p*-cymene)$(OPiv)_2$] (10)	mixed[c]	65	<2	<2	
19	[Ru(*p*-cymene)$(O_2CCF_3)_2$] (10)	mixed[c]	5	<2	<2	
20	[Ru(benzene)$(OAc)_2$] (10)	mixed[c]	20	<2	<2	
21	[Ru(toluene)$(OAc)_2$] (10)	mixed[c]	29	<2	<2	

[a] Reaction conditions: benzoic acid (0.4 mmol, 2.0 equiv), diphenylacetylene (1.0 eq
Ru precatalyst (5-10 mol%), ligand (10 mol%), solvent (1.0 mL), 80 ^oC, 24h. [b] GC Yi

5.4. Substrate Scope

With the optimized catalytic procedure in hand, we investigated decarboxylative alkyne hydroarylation with a variety of substituted benzoic acids (Figure 5.2). All reactions occurred with high stereoselectivity to form *syn*-hydroarylation products as the dominant stereoisomers. Results on

regiochemistry of the products were consistent with the envisioned tandem sequence of *ortho*-C-H alkenylation and subsequent decarboxylation (Scheme 5.14). Thus, *para*-substituted benzoic acids reacted with diphenylacetylene (**5.05a**) in exclusive regioselectivity to give *meta*-substituted alkenylarene products **5.03ba** and **5.03c**-**l** (Figure 5.2). High yields were achieved with electron-donating *para*-substituents including methyl, methoxy, and N-protected amino groups (products **5,03ba**, **5,03c**, **5,03d**, **5,03g**). The redox-neutral nature of current catalyst system also allowed tolerance of unprotected phenol and aniline functionality, leading to formation of *meta*-hydroxy- or amino-substituted products **5.03e** and **5.03f** in 85% and 63% yield respectively. On the other hand, significantly reduced reactivity was observed with electron-withdrawing *para*-substituents such as halogen atoms and the CF_3 group. As a result, products **5.03h-l** were formed in low yields even at a higher reaction temperature of 100 ^{o}C.

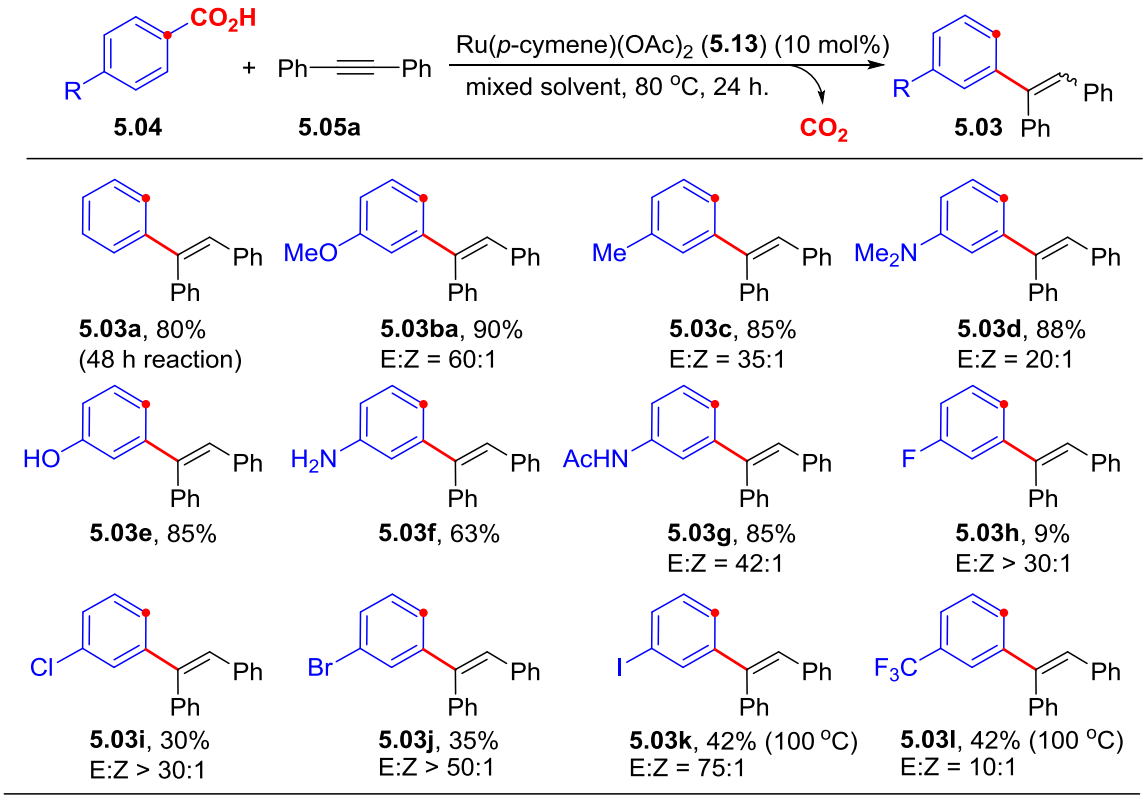

[a] Reaction conditions: arenecarboxylic acid (0.4 mmol, 2.0 equiv), diphenylacetylene (1.0 equiv), Ru-precatalyst (10 mol%), mixed solvent (dioxane: toluene: heptane=2:2:1) (1.0 mL), 80 °C, 24h. [b] average isolated yields based on at least two run, *E/Z* ratio was determined by ^{1}H-NMR.

Figure 5.2. Substrate scope of *para*-substituted benzoic acids in ruthenium catalyzed decarboxylative alkyne hydroarylation with diphenylacetylene[a,b]

With *ortho*-substituted benzoic acids, the same *meta*-substituted alkenylarene products should be formed as with the *para*-substituted analogs. This envisioned regiochemistry was confirmed with successful reactions between **5.05a** and several benzoic acids with *ortho*-substituents including methyl, methoxy, hydroxy, and phenyl groups (Figure 5.3). The *meta*-substituted benzoic acids were envisioned as a more challenging class of substrates due to competitive functionalization at two unsymmetrical aromatic C-H bonds that are both *ortho* to the carboxyl directing group. Indeed, 3-methoxybenzoic acid (3-anisic acid) reacted with **5.05a** to give an inse*para*ble mixture of 4 regio- and stereoisomers of corresponding hydroarylation products in 50% overall yields and low selectivities (products **5.03n**/**n'**). We hypothesized that both electronic and steric properties of *meta*-substituents should affect the regioselectivity, and more sterically demanding *meta*-substituents should inhibit formation of *ortho*-

alkenylation products and promote the corresponding *para*-alkenylation regioisomers. Gratifyingly, having sterically demanding dimethylamino, isopropyl and *tert*-butyl groups as *meta*-substituents did lead to exclusive formation of *para*-alkenylation products **5.03o-q** in 50-74% yields. The substituent-enabled high regioselectivity was also demonstrated with two protocatechuic acid (3,4-dihydroxybenzoic acid) derivatives having both *meta*- and *para*-substituents. The exclusive formation of *ortho*-alkenylation product **3r** suggested a dominant electronic effect and negligible steric effect with formaldehyde acetyl-protected 3,4-dihydroxy moiety. By contrast, the reaction with vanillic acid led to exclusive formation of product **3s** via regioselective C-H activation/alkenylation at the aromatic site that is *para* to methoxy and *meta* to hydroxy.

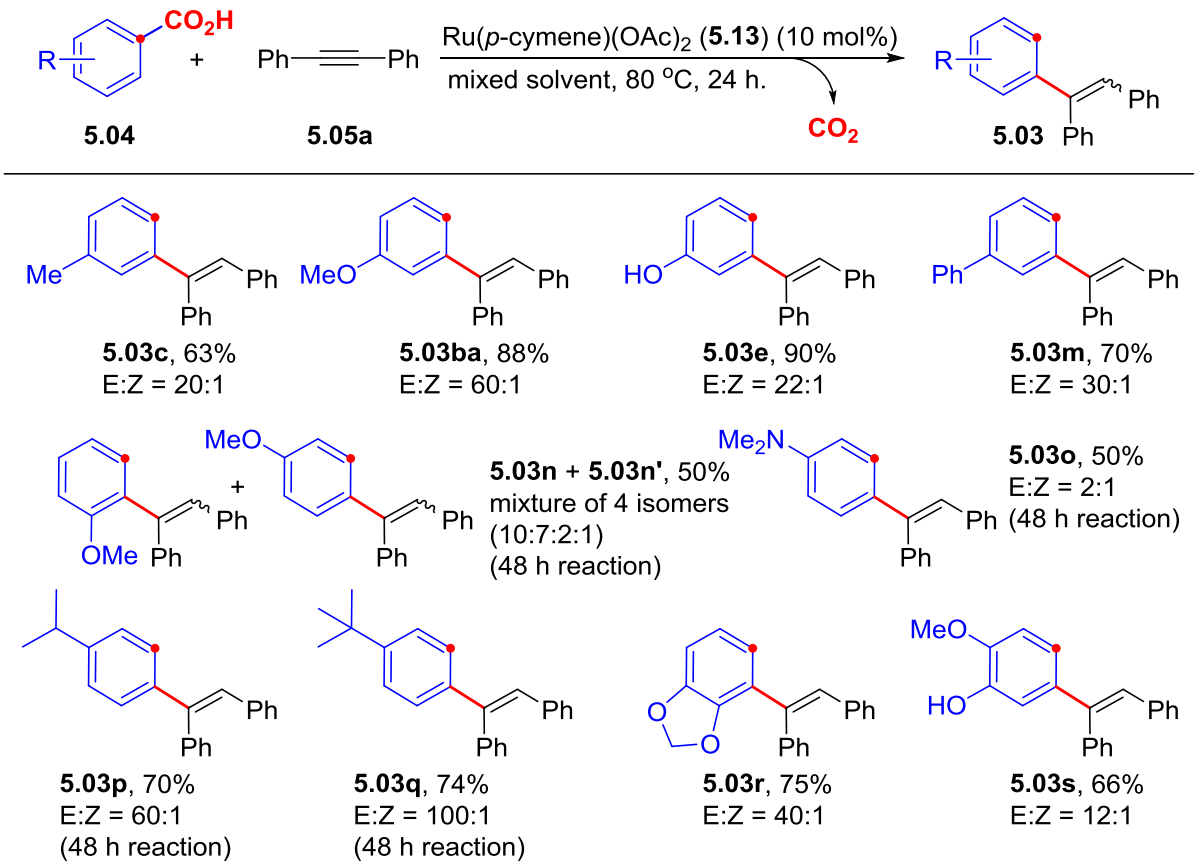

[a] Reaction conditions: arenecarboxylic acid (0.4 mmol, 2.0 equiv), diphenylacetylene (1.0 equiv), Ru-precatalyst (10 mol%), mixed solvent (dioxane: toluene: heptane=2:2:1) (1.0 mL), 80 °C, 24h. [b] Average isolated yields based on at least two run, *E/Z* ratio was determined by ^{1}H-NMR.

Figure 5.3. Substrate scope of *ortho*- and *meta*-substituted benzoic acids in ruthenium catalyzed decarboxylative alkyne hydroarylation with diphenylacetylene[a,b]

The scope of internal alkyne substrates were investigated with 4-methoxybenzoic acid as the reaction partner (Figure 5.4). Unsymmetrically substituted alkyl/aryl alkynes reacted with exclusive regioselectivity to form 1-alkyl-1-*m*-anisyl alkene products (**5.03bb**-**5.03bf**). However, methyl-, ethyl-, and n-butyl-substituted phenylacetylenes showed much lower reactivity than diphenylacetylene (**5.05a**) and required 20 mol% $Cu(OAc)_2$ additive to give products **5.03bb**-**5.03bd** in 60-77% yields. Compared to simple alkyl groups, higher reactivity was observed with methoxymethyl-substituted arylacetylenes, and no $Cu(OAc)_2$ additive was required to achieve good yields (products **5.03be**, **5.03bf**). This reactivity enhancement by methoxymethyl substituent was also demonstrated with symmetrical dialkylacetylenes (products **5.03bg**-**5.03bi**). Results from reactions with several symmetrical diarylacetylenes provided additional information on structural effects on alkyne reactivity (products **5.03bj**-**5.03bo**). In particular, relatively higher yields were observed with alkynes having *ortho*-substituted aryl groups (products **5.03bj**, **5.03bm**) than *meta*- and *para*-substituted analogs. On the other hand, the electronic properties of aromatic substituents appeared to have little effects on hydroarylation reactivity.

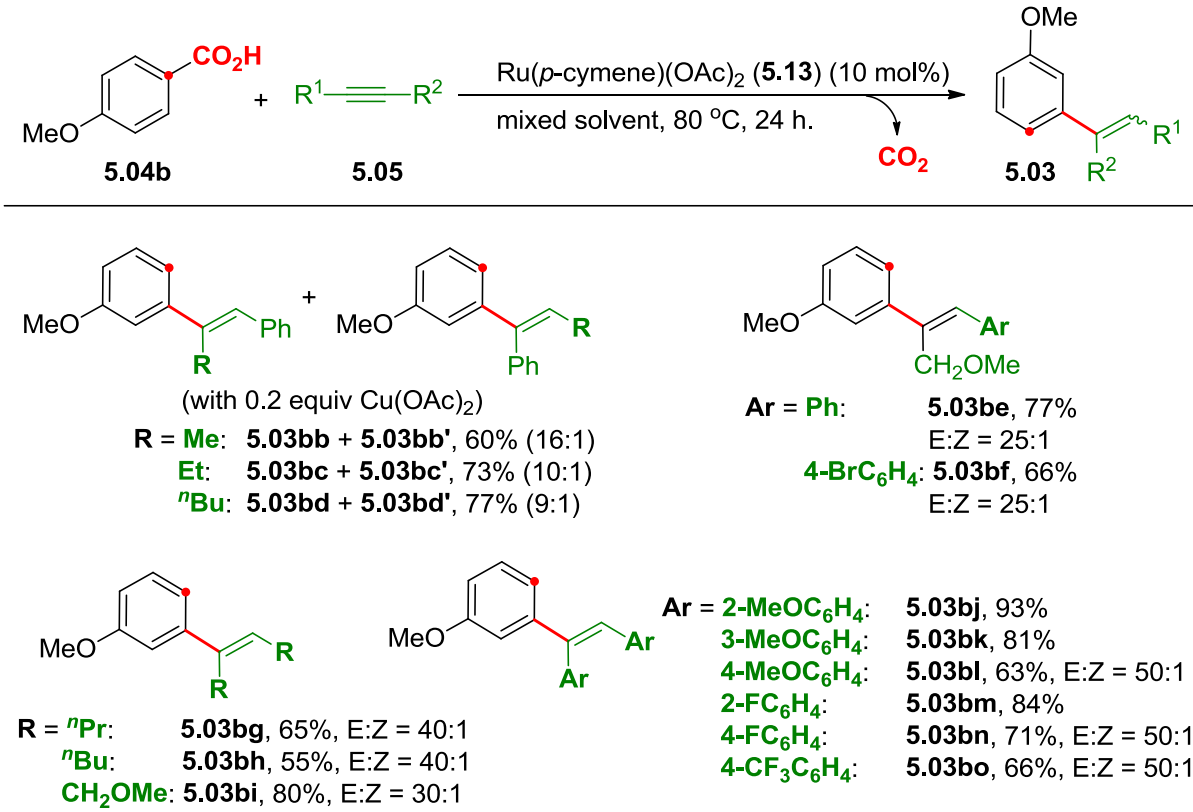

[a] Reaction conditions: *p*-anisic acid (0.4 mmol, 2.0 equiv), internal alkyne (1.0 equiv), Ru-Precatalyst (10 mol%, mixed solvent (dioxane: toluene: heptane=2:2:1) (1.0 mL), 80 °C, 24h. [b] Average isolated yields based on at leat two run, *E/Z* ratio was determined by ^{1}H-NMR.

Figure 5.4. Substrate scope of internal alkynes in ruthenium catalyzed decarboxylative alkyne hydroarylation with *p*-anisic acid[a,b]

Notably, most of benzoic acid substrates employed in the current procedure are commercially available and relatively inexpensive compared to other aromatic building blocks used in regioselective catalytic alkyne hydroarylation. In particular, the current catalyst system provides new opportunities for biomass-based phenolic acids as novel, sustainable aromatic building blocks in chemical synthesis (products **5.03ba**-**5.03bo**, **5.03e**, **5.03n**/**n'**, **5.03r**, **5.03s**) . As a leading example, 4-hydroxybenzoic acid can be separated from a number of biomass sources such as lignin, and is commercially available at ~60 US$/1kg (8.3 US$/mol) from Sigma-Aldrich. Decarboxylative hydroarylation with 4-hydroxybenzoic acid gave *meta*-alkenylphenol product **5.03e** in high yield and dominant stereoselectivity for the (*E*)-isomer. In

comparison, other reported alkyne hydroarylation procedures were either incompatible with unprotected phenol functionality, giving inseparable mixtures of *ortho*/*para*-alkenylation products with phenol ether substrates, or requiring the use of much more expensive halogenated phenol substrates (e.g. 3-iodophenol at ~780 US$/mol from Sigma-Aldrich) and generating stoichiometric halide salt waste.[64]

5.5. Reaction Mechanism Studies and Discussion

Based on the envisioned decarboxylative hydroarylation pathway via "double chelation assistance" (Scheme 5.14), we proposed that a cyclometalated alkenylruthenium(II) carboxylate complex (Figure 5.5, **IV**) was formed via carboxylate-directed C-H activation and subsequent alkyne insertion into the Ru-aryl linkage. Protonation of the Ru-alkenyl linkage in intermediate **IV** generated the alkenyl-chelated Ru(II) carboxylate intermediate **III** (Path A), which led to desired hydroarylation product **5.03** via chelation-assisted decarboxylation and subsequent protonation. Alternatively, C-O bond formation via direct reductive elimination with **IV** would generate an isocoumarin **5.06** as the byproduct of oxidative [4+2] annulation (Path B).[59,60] A third possible reactivity of **IV** was insertion into the Ru-alkenyl linkage by a second equivalent of alkyne substrate **5.05** (Path C), leading to formation of the oxidative [2+2+2] byproduct **5.07** via sequential decarboxylation and ring-closure by C-C reductive elimination.[65] The proposed chemoselectivity dependence on divergent reactivity of intermediate **IV** was supported by a number of experimental results and guided our efforts in further catalyst improvement. Firstly, the protonation steps in Path A may be facilitated by acid additives and promote formation of hydroarylation product **5.03** over other byproducts. This hypothesis was evaluated by a modified decarboxylative hydroarylation catalyst system with 50 mol% of added pivalic acid (Figure 5.6), which has been utilized as a common acid additive in a number of catalytic systems for C-H bond activation.[64] Indeed, hydroarylation reactivity of *para*-halogenated benzoic acids towards **5.05a** was promoted to give products **5.03h**-**j** in decent yields, with the most significant reactivity enhancement observed with 4-fluorobenzoic acid (from 7% to 42% yield). In addition, reactivity of 4-methoxybenzoic acid was also improved to give product **5.03be** in 91% yield as compared to 77% yield without acid additive.

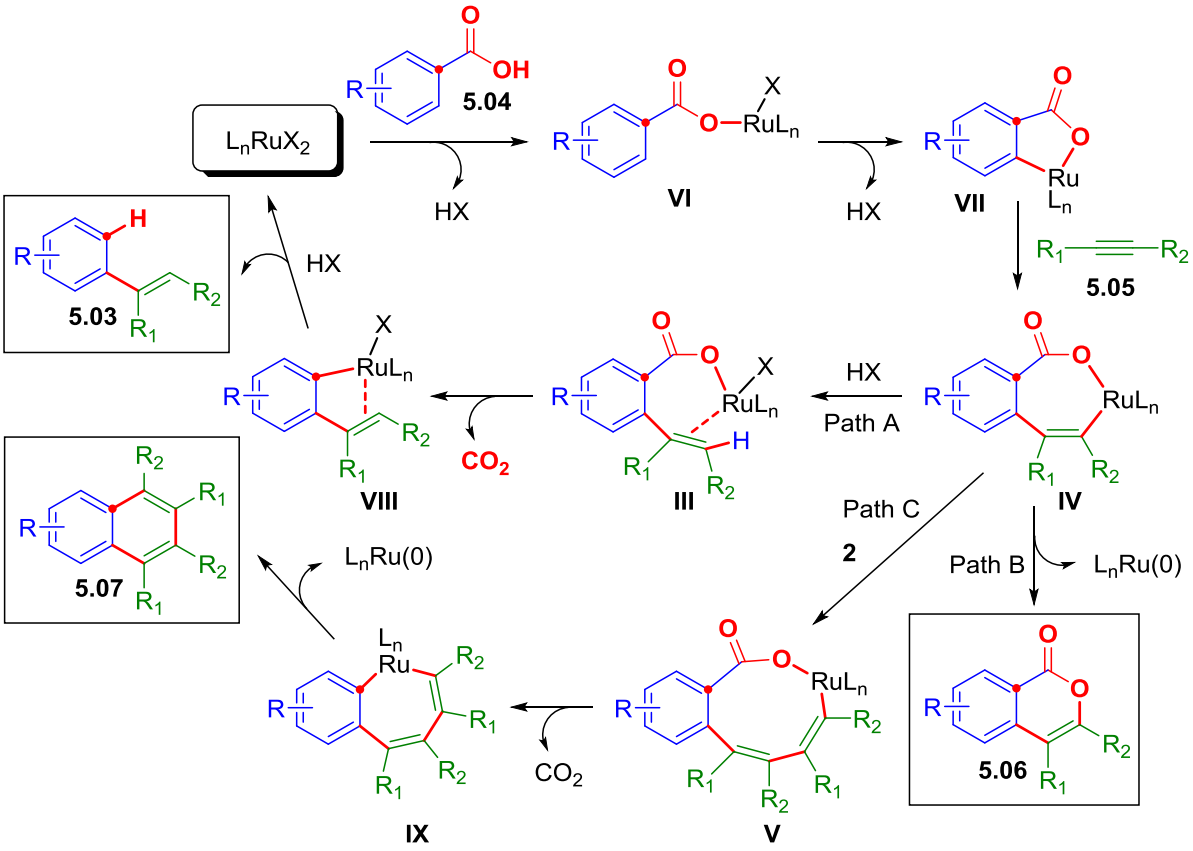

Figure 5.5. Proposed reaction mechanism for ruthenium catalyzed decarboxylative alkyne hydroarylation and byproduct formation

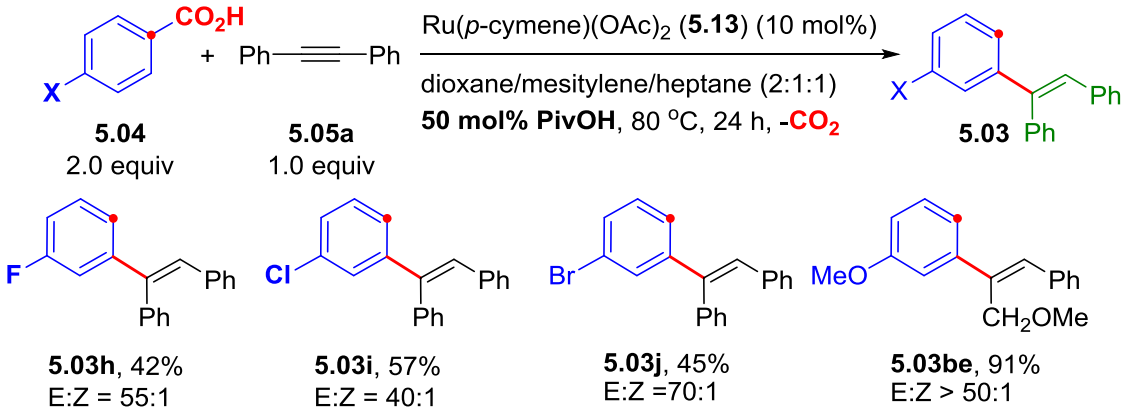

Figure 5.6. Effect of acid additive (PivOH) in ruthenium catalyzed decarboxylative alkyne hydroarylation

Secondly, a 2:1 reaction between diphenylacetylene (**5.05a**) and a Ru(II) benzoate complex, Ru(*p*-cymene)$(OBz)_2$ (**5.14**) at room temperature over 48 hours has led to quantitative formation of a Ru(0) complex **5.15** (Scheme 5.15). Solid-state structure of complex **5.15** was established by single crystal X-ray diffraction (Figure 5.7). Besides the η^6-p-cymene ligand, complex **5.15** was also stabilized by a η^4-1,2,3,4-tetraphenylnaphthalene ligand that was presumably generated by [2+2+2] annulation in Path C.[55,57,65] Notably, complex **5.14** has displayed comparable catalytic reactivity as Ru(*p*-cymene)$(OAc)_2$ (**5.13**) for decarboxylative alkyne hydroarylation with benzoic acid (**5.04a**). By contrast, complex **5.15** showed no catalytic reactivity under similar reaction conditions. The mild temperature for stoichiometric formation of complex **5.15** and its lack of catalytic activity suggested that Path C could be highly competitive against desired hydroarylation process. In addition, formation of stable Ru(0) complexes by Path C could serve as a catalyst sink and significantly lower the overall catalyst efficiency. In fact, 1,2,3,4-tetrasubstituted naphthalenes (**5.07**) were generally detected as the major byproducts for electron-poor benzoic acids that displayed low reactivity towards decarboxylative hydroarylation (products **5.03h**-**l** in Figure 5.2).

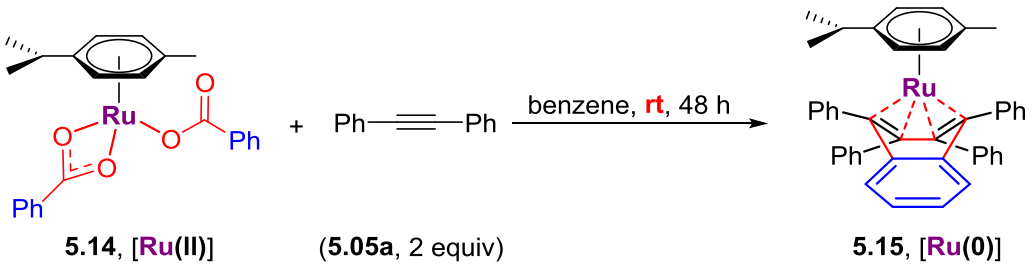

5.14, [**Ru(II)**] (**5.05a**, 2 equiv) **5.15**, [**Ru(0)**]

Scheme 5.15. Formation of ruthenium(0) complex via stoichiometric [2+2+2] cyclization

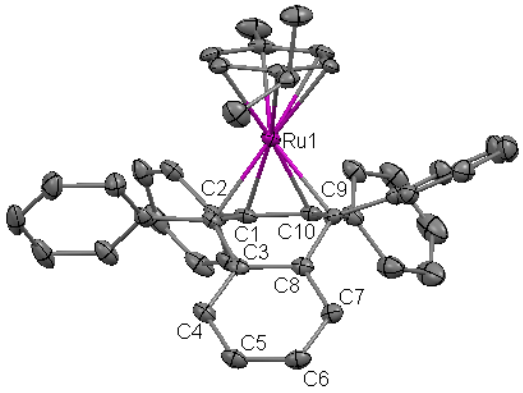

Figure 5.7. ORTEP diagram of complex [Ru(*p*-cymene)(η^4-1,2,3,4-tetraphenylnaphthalene)] (**5.15**) at 50% thermal ellipsoid

Based on the proposed mechanism (Scheme 5.16), formation of desired product **5.03** could be further promoted by slowing down the process of 2nd alkyne insertion in Path C and suppressing formation of byproduct **5.07**. This hypothesis was consistent with the observation of higher hydroarylation product yields with more sterically demanding diarylacetylenes (**5.03bi**, **5.03bm** in Figure 5.4). The yield improvement with 1,2-*ortho*-anisylacetylene (**5.05b**) was further demonstrated with electron-deficient benzoic acid substrates (Figure 5.8). 4-Fluorobenzoic acid and 4-trifluoromethylbenzoic acid both reacted with **5.05b** to give significantly higher yields (products **5.03t**, **5.03u**) compared to analogous reactions with diphenylacetylene (**5.05a**) (products **5.03h**, **5.03l** in Figure 5.2) and without the need of added pivalic acid or higher reaction temperature. 4-Cyanobenzoic acid also reacted with **5.05b** to achieve **5.03v** 73% yield, which was virtually unreactive towards **5.05a** at 80-100 ^{o}C.

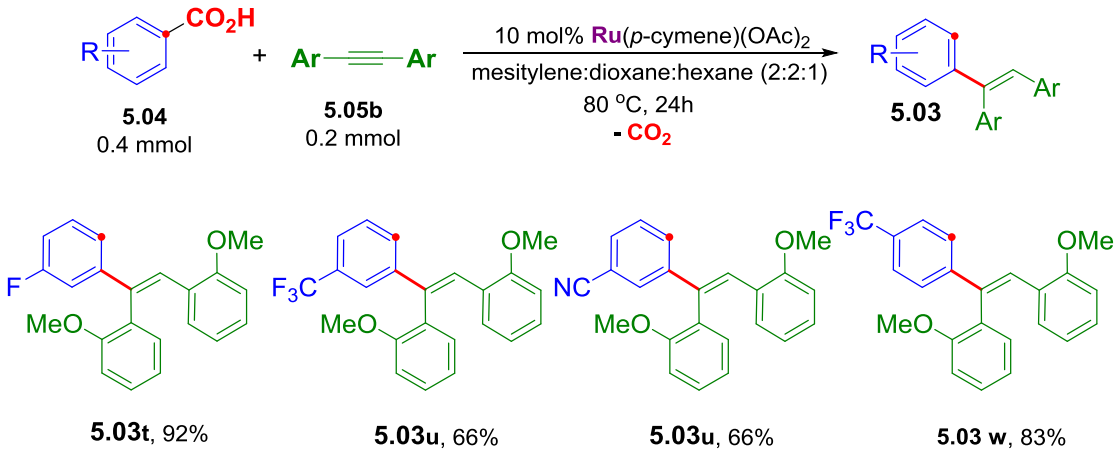

Figure 5.8. Improved ruthenium catalyzed decarboxylative alkyne hydroarylation with less reactive arenecarboxylic acids using steric demanding diaryl alkynes

In addition, chemoselectivity for hydroarylation could also be improved with higher ratios of benzoic acid vs. alkyne substrates. While keeping the alkyne as limiting reagent with 2 equivalents of benzoic acids, we were pleased to find that slow addition of alkyne substrates into the reaction system further improved the yields of hydroarylation products. Using Ru(*p*-cymene)$(OAc)_2$ (**5.13**) as the catalyst, this modified catalytic procedure was successfully scaled up to 4.0 mmol for reactions between **5.05a** and several substituted benzoic acids in higher percentage yields than the corresponding 0.1 mmol-scale reactions (Scheme 5.20) and allowed gram-scale synthesis of hydroarylation products.

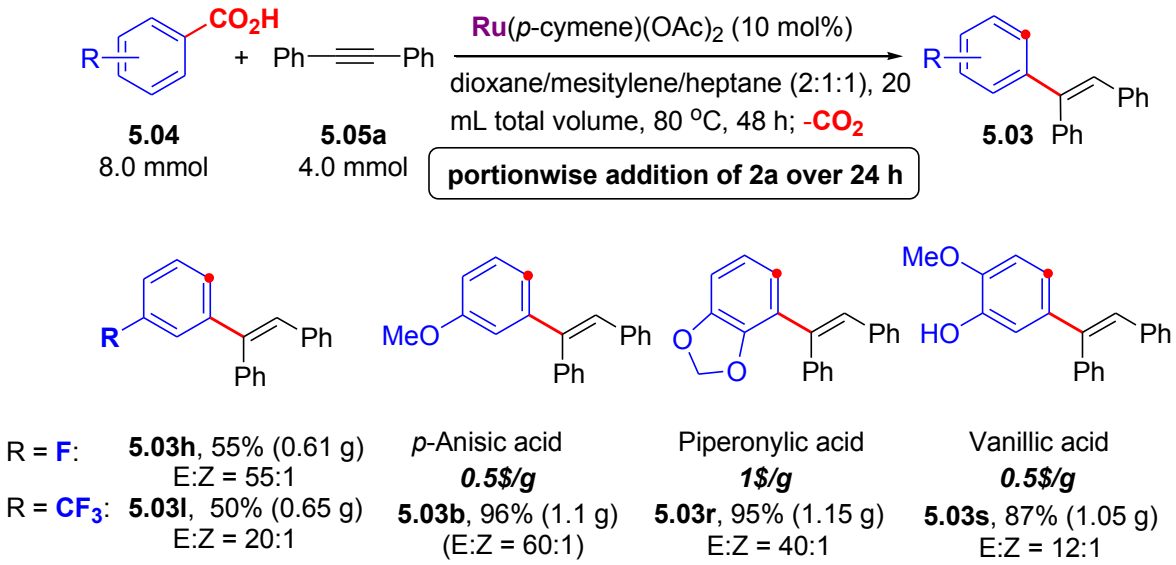

Figure 5.9. Reactions of ruthenium catalyzed decarboxylative alkyne hydroarylation via portionwise addition of the alkyne substrate

5.6. Conclusion

In summary, we have developed a decarboxylative approach for alkyne hydroarylation to synthesize arylalkenes with controlled and versatile regiochemistry of aromatic substituents. Following a tandem sequence of C-H bond activation and alkyne coupling, the subsequent decarboxylation is facilitated by the newly installed *ortho*-alkenyl moiety and is compatible with various aromatic substituents at *para*-, *meta*- and *ortho*-positions. This new decarboxylation strategy eliminates the prerequisite of substrate activation by *ortho*-substitution and allows a broad scope of substituted benzoic acids to serve as aromatic building blocks for alkyne hydroarylation. A number of *meta*- and *para*-substituted alkenylarenes, as well as alkenylarenes with unprotected phenol and aniline functionality can be conveniently prepared by this method, which are difficult to synthesize by conventional alkyne hydroarylation strategy. We expect that the chelation assistance demonstrated in current study can be further explored to facilitate other decarboxylative transformations, although details of this novel decarboxylation mechanism remain elusive at this stage.

5.7. Experimental Procedures

5.7.1. General Information

All decarboxylative hydroarylation reactions were assembled in an N_2-filled glovebox using oven-dried glassware and were stirred with Teflon-coated magnetic stirring bars. Benzene, pentane and toluene solvents were degassed by purging with nitrogen and then dried with a solvent purification system (MBraun MB-SPS). All other reagents and substrates were purchased from Sigma-Aldrich, VWR, Strem, Oakwood Chemical or Ark-Pharm and were used as received. Reaction temperatures above room temperature (~23 °C) refer to temperatures of an aluminum heating block or an oil bath, which were either controlled by an electronic temperature modulator or controlled manually and monitored using a standard alcohol thermometer. TLC plates were visualized by exposure to ultraviolet light using a dual-range UV lamp. Organic solutions were concentrated by rotary evaporation at ~10 torr. Flash column chromatography was performed with 32–63 microns silica gel. NMR spectra were acquired on a NMR spectrometer with 400 MHz for ^{1}H NMR and 100 MHz for ^{13}C NMR. Chemical shifts (δ) were reported in parts per million (ppm) relative to the residual solvent signal. Data for ^{1}H NMR spectra are reported as follows: chemical shift (multiplicity, coupling constants, and number of hydrogens). Abbreviations are as follows: s (singlet), d (doublet), t (triplet), q (quartet), m (multiplet), br (broad). ^{19}F NMR spectra were obtained at 282.4 MHz in $CDCl_3$, and all chemical shifts were reported in ppm upfield of CF_3COOH (δ = -78.5 ppm). GC analyses were performed on a Shimadzu GC-2010 system. GC-MS data were obtained on an Agilent 7890AGC system and an Agilent 5975C mass selective detector. High-resolution mass spectra were obtained at a Bruker Daltronics BioTOF HRMS spectrometer.

5.7.2. Preparation of Substrates and Ruthenium Complexes

Alkynes: (3-methoxyprop-1-yn-1-yl)benzene,[66] 1-bromo-4-(3-methoxyprop-1-yn-1-yl)benzene,[66] 1,2-bis(4-methoxyphenyl)ethyne,[67] 1,2-bis(4-methoxyphenyl)ethyne,[67] 1,2-bis(2-methoxyphenyl)ethyne,[66] 2-bis(2-fluorophenyl)ethyne,[67] 1,2-bis(4-fluorophenyl)ethyne,[67] and 1,2-bis(4-(trifluoromethyl)phenyl)ethyne[67] were prepared according to known procedures.

[Ru(benzene)Cl_2]$_2$,[68] [Ru(toluene)Cl_2]$_2$,[68] [Ru(benzen)$(OAc)_2$],[69] [Ru(toluene)$(OAc)_2$,[69] [Ru(*p*-ymene)$(OAc)_2$],[69] [Ru(*p*-cymene)$(OBz)_2$],[69] [Ru(*p*-cymene)$(O_2CCF_3)_2$][69] and [Ru(*p*-cymene)$(OPiv)_2$][70] were prepared according to reported methods.

5.7.3. Evaluation of Reaction Conditions for the Decarboxylative Hydroarylation of Alkynes

Reactions were conducted on a 0.2 mmol scale. In a nitrogen-filled glovebox, the metal complex as catalyst precursor, the additives, the solvent (1.0 mL), diphenylacetylene (**5.05a**, 0.2 mmol, 1.0 equiv.) and benzoic acid (**5.04a**) were combined in a 4-mL scintillation glass vial equipped with a magnetic stirrer. The vial was sealed with a Teflon-lined screwcap and electrical tape, transferred out of the glovebox and stirred at the indicated temperature for 24 h. The yields were determined by GC analysis with hexadecane as internal standard.

5.7.4. Preparation and X-Ray Diffraction Analysis of [Ru(*p*-cymene)(η^4-1,2,3,4-tetraphenylnaphthalene)] (**5.15**)

Into a 4 mL scintillation vial equipped with a magnetic stir bar was added [Ru(*p*-cymene)$(OBz)_2$] (47.8 mg, 0.1 mmol), diphenylacetylene (36.2 mg, 0.2mmol) and 2 mL benzene. The mixture was stirred for 48 hours at room temperature. Then, the solvent was removed under reduced pressure. The residue was washed with pentane (3X), dried under vacuum, and afforded an orange powder (65mg, 97%).

Single crystal X-ray diffraction data of **5.15** were collected on a Bruker Apex Duo diffractometer with a Apex 2 CCD area detector at T = 100K and using Cu radiation. Structures were processed with Apex 2 v2013.4-1 software package using the latest versions of SAINT and SHELX software. Multi-scan absorption correction (SADABS 2012/1) was applied, and direct method was used to solve the structures. Details of data collection and refinement are given in Table 5.4.

Table 5.4 Summary of cell parameters, data collection and structural refinements for [Ru(*p*-cymene)(η^4-1,2,3,4-tetraphenylnaphthalene)] (**5.15**)

Empirical formula	$C_{44}H_{38}Ru$
Formula weight	669.83
Temperature, K	100
Wavelength, (Å)	1.54178
space group	*P-1*
a/Å	10.0800
b/Å	10.3322(4)
c/Å	16.2742(6)
α, deg	89.290(2)
β,deg	83.725(1)
γ, deg	73.480(2)
V, Å	1614.92(11)
Z	2
d_{calcd}, g/cm^3	1.373
μ, mm^{-1}	4.147
F(000)	696.0
Theta range, deg	6.27 ÷ 66.64
h, k, l ranges	-11 ÷ 11, -12 ÷ 12, -16 ÷ 19
Reflections collected/unique	19644
Unique Reflections/gt	5536/5353
COOF on F^2	1.050
R_1, wR_2 $(I>2\sigma(I))^a$	2.79%, 7.04%
R_1, wR_2 *(all data)*	2.89%, 7.09%
Largest diff. peak and hole (e. Å $^{-3)}$	0.101

[a] $R1 = \Sigma||F_o| - |F_c|| / \Sigma|F_o|$, $wR2 = [\Sigma w[(F_o)^2 - (F_c)^2]^2 / \Sigma w(F_o^2)^2]^{1/2}$ for $F_o^2 > 2\sigma(F_o^2)$, $w = [\sigma^2(F_o)^2 + (AP)^2 + BP]^{-1}$ where $P = [[(F_o)^2 + 2(F_c)^2] / 3$ and A (B) = 0.0315 (1.9418);

Table 5.5 Selected bond lengths [Å] and bond angles [degree] of [Ru(*p*-cymene)(η^4-1,2,3,4-tetraphenylnaphthalene)] (**5.15**)

bond length [Å]		bond angles [degree]	
Ru(1)-C(1)	2.126(2)	C(1)-Ru(1)-C(2)	39.79(8)
Ru(1)-C(2)	2.193(2)	C(2)-Ru(1)-C(9)	74.08(8)
Ru(1)-C(9)	2.197(2)	C(1)-Ru(1)-C(10)	39.40(8)
Ru(1)-C(10)	2.126(2)	C(9)-Ru(1)-C(10)	39.75(8)
C(1)-C(2)	1.470(3)	C(1)-C(2)-C(3)	113.9(2)
C(2)-C(3)	1.494(3)	C(8)-C(9)-C(10)	112.8(2)
C(9)-C(10)	1.471(2)	C(3)-C(8)-C(9)	114.0(2)
C(8)-C(9)	1.501(3)	C(1)-C(10)-C(9)	114.4(2)
C(1)-C(10)	1.433(3)	C(2)-C(3)-C(8)	115.2(2)
C(3)-C(8)	1.397(3)	C(2)-C(1)-C(10)	114.0(2)
		Ru(1)-C(1)-C(2)	72.6(1)
		Ru(1)-C(2)-C(3)	110.5(1)
		Ru(1)-C(9)-C(8)	111.6(2)
		Ru(1)-C(9)-C(10)	67.5(1)
		Ru(1)-C(1)-C(10)	70.3(1)
		Ru(1)-C(10)-C(1)	70.3(1)

5.7.5. General Procedure for the Decarboxylative Hydroarylation of Alkynes

In a nitrogen-atmosphere glovebox, [Ru(*p*-cymene)$(OAc)_2$] (**5.13**, 71 mg, 0.2 mmol) and 10.0 mL of mixed solvent (4.0 mL dioxane, 4.0 mL mesitylene, and 2.0 mL heptane) were added into a 20-mL scintillation vial equipped with a magnetic stir bar. The mixture was stirred for 10 min to be used as a homogeneous stock solution of catalyst precursor. Into a 4-mL scintillation vial equipped with a magnetic stir bar was charged with the alkyne substrate (0.2 mmol, 1.0 equiv.), arenecarboxylic acid substrate (0.4 mmol), and 1.0 mL of stock solution for catalyst precursor (containing 0.02 mmol of complex **7**). The vial was then sealed with a Teflon-lined screwcap and secured with electrical tape, transferred out of the glovebox and stirred in a 80 °C oil bath for 24 h. After the reaction mixture was cooled to room

temperature, all volatile materials were removed under reduced pressure. Further purification was achieved by flash column chromatography using dichloromethane, ethyl acetate and hexanes as the eluent. The E/Z alkene stereoselectivity and regioselectivity for aromatic substitution was determined by ^{1}H NMR of the unpurified reaction mixture. Yields of the isolated products are based on the average of two runs under identical conditions.

5.7.6. Spectral Data of Isolated Products

Products **5.03a**,[71] **5.03b**,[72] **5.03c**,[71] **5.03l**,[72] (*E*)-*p*-**5.03n**,[71] *(Z)*-*p*-**5.03**n,[71] *(E)*-*p*-**5.03n'**,[71] (*Z*)-*p*-**5.03n'**,[71] **5.03p**,[12] **5.03**q,[12] and **5.03bb**[11] are known compounds and were identified by comparison of their NMR spectra with the respective reported data.

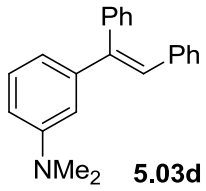

5.03d

(*E*)-3-(1,2-Diphenylvinyl)-N,N-dimethylaniline (**5.03d**): Colorless liquid, 46.0 mg, 85% (from 4-methylbenzoic acid); 34.1 mg, 63% (from 2-methylbenzoic acid). ^{1}H NMR (400 MHz, $CDCl_3$): δ = 7.41-7.37 (m, 3H), 7.30-7.27 (m, 4H), 7.21-7.15 (m, 5H), 7.11-7.09 (m, 2H), 7.03 (s, 1H), 2.40 ppm (s, 3H). ^{13}C NMR (100 MHz, $CDCl_3$): δ = 143.8, 143.1, 140.8, 138.0, 137.8, 130.7, 129.9, 128.9, 128.64, 128.58, 128.42, 128.38, 128.26, 127.7, 127.0, 125.2, 21.8 ppm. HRMS: m/z calcd for $C_{21}H_{19}^+$: 271.1487; found: 271.1485.

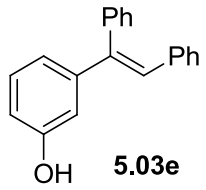

5.03e

(*E*)-3-(1,2-Diphenylvinyl)phenol (**5.03e**): Colorless liquid, 46.3 mg, 85% (from 4-Hydroxybenzoic acid); 49.0 mg, 90% (from 2-Hydroxybenzoic acid); ^{1}H NMR (400 MHz, $CDCl_3$): δ = 7.33-7.29 (m, 3H), 7.23-7.10 (m, 6H), 7.01-6.98 (m, 2H), 6.95-6.92 (m, 2H), 6.75-6.73 (m, 2H), 4.65 ppm (s, 1H). ^{13}C NMR

(100 MHz, $CDCl_3$): δ = 155.5, 145.4, 142.3, 140.4, 137.4, 130.6, 129.8, 129.6, 128.9, 128.6, 128.2, 127.7, 127.0, 120.4, 114.8, 114.7 ppm. HRMS: m/z calcd for $C_{20}H_{17}O^+$: 273.1279; found: 273.1289.

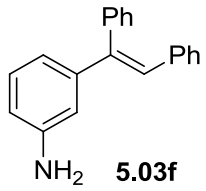

5.03f

(*E*)-3-(1,2-Diphenylvinyl)aniline (**5.03f**): Colorless liquid, 34.2 mg, 63%. ^1H NMR (400 MHz, $CDCl_3$): δ = 7.39-7.35 (m, 3H), 7.29-7.25 (m, 2H), 7.20-7.14 (m, 4H), 7.08-7.05 (m, 2H), 7.01 (s, 1H), 6.83-6.81 (m, 1H), 6.67-6.65 (m, 2H), 3.65 ppm (s, 2H). ^{13}C NMR (100 MHz, $CDCl_3$): δ = 146.3, 144.6, 142.7, 140.5, 137.5, 130.4, 129.6, 129.1, 128.6, 127.974, 127.967, 127.4, 126.7, 118.2, 114.51, 114.45 ppm. HRMS: m/z calcd for $C_{20}H_{17}NH^+$: 272.1434; found: 272.1434.

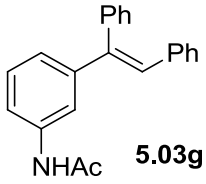

5.03g

(*E*)-N-(3-(1,2-diphenylvinyl)phenyl)acetamide (**5.03g**): White solid, 53.3 mg, 85%. ^1H NMR ($CDCl_3$, 300 MHz): δ = 7.64 (d, J = 8.0 Hz, 1H), 7.37-7.21 (m, 8H), 7.16-7.14 (m, 4H), 7.03 (dd, J = 7.5, 1.9 Hz, 2H), 6.99 (s, 1H), 2.16 ppm (s, 3H). ^{13}C NMR ($CDCl_3$, 75 MHz): δ = 168.4, 144.3, 142.0, 140.2, 137.9, 137.2, 130.4, 129.6, 128.9, 128.71, 128.67, 128.0, 127.5, 126.9, 123.6, 119.3, 119.0, 24.6 ppm. HRMS: calculated for $C_{21}H_{19}NONa^+$: m/z = 336.1359; found: m/z = 336.1359.

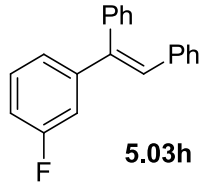

5.03h

(*E*)-(1-(3-Fluorophenyl)ethene-1,2-diyl)dibenzene (**5.03h**): White solid, 23.1 mg, 42%. ^1H NMR ($CDCl_3$, 300 MHz): δ = 7.36-7.33 (m, 3H), 7.27 (td, J = 8.0, 6.0 Hz, 1H), 7.22-7.20 (m, 2H), 7.15-7.11 (m,

4H), 7.05-7.02 (m, 3H), 7.00-6.95 ppm (m, 2H). ^{13}C NMR ($CDCl_3$, 75 MHz): δ = 163.1 (d, *J* = 145.2 Hz), 146.0 (d, *J* = 7.3 Hz), 141.7 (d, *J* = 2.3 Hz), 140.0, 137.2, 130.5, 129.9. 129.8 (d, *J* = 8.3 Hz), 129.3, 129.0, 128.3, 127.9, 127.3, 123.4 (d, *J* = 2.7 Hz), 114.6 (d, *J* = 22.2 Hz), 114.5 ppm (d, *J* = 21.4 Hz); ^{19}F NMR (282.4 MHz): δ = -113.42 ppm. HRMS: calculated for $C_{20}H_{16}F^+$: m/z = 275.1236; found: m/z = 275.1236.

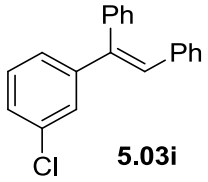

5.03i

(*E*)-(1-(3-Chlorophenyl)ethene-1,2-diyl)dibenzene (**5.03i**): White solid, 33.2 mg, 57%. ^{1}H NMR (400 MHz, $CDCl_3$): δ = 7.35-7.32 (m, 4H), 7.27-7.22 (m, 2H), 7.21-7.17 (m, 3H), 7.15-7.11 (m, 3H), 7.03-7.01 (m, 2H), 6.96 ppm (s, 1H). ^{13}C NMR (100 MHz, $CDCl_3$): δ = 145.7, 141.6, 140.0, 137.3, 134.6, 130.6, 129.9, 129.7, 129.6, 129.1, 128.4, 128.0, 127.9, 127.8, 127.4, 126.1 ppm. HRMS: m/z calcd for $C_{20}H_{16}Cl^+$: 291.0941; found: 291.0956.

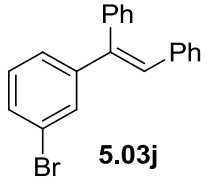

5.03j

(*E*)-(1-(3-Bromophenyl)ethene-1,2-diyl)dibenzene (**5.03j**): White solid, 30.2 mg, 45%. ^{1}H NMR ($CDCl_3$, 300 MHz): δ = 7.50 (t, *J* = 1.9 Hz, 1H), 7.42-7.39 (m, 1H), 7.36-7.31 (m, 3H), 7.24-7.11 (m, 7H), 7.04-7.01 (m, 2H), 6.95 ppm (s, 1H). ^{13}C NMR ($CDCl_3$, 75 MHz): δ = 146.0, 141.5, 140.0, 137.2, 130.8, 130.7, 130.6, 130.0, 129.9, 129.6, 129.1, 128.4, 128.0, 127.4, 126.6, 122.8 ppm. HRMS: m/z calcd for $C_{20}H_{16}Br^+$: m/z = 335.0435; found: m/z = 335.0436.

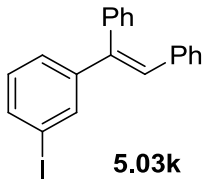

5.03k

(*E*)-(1-(3-Iodophenyl)ethene-1,2-diyl)dibenzene (**5.03k**): White solid, 32.1 mg, 42%. ^{1}H NMR (400 MHz, $CDCl_3$): δ = 7.71 (t, *J* = 1.8 Hz, 1H), 7.60 (ddd, *J* = 7.8, 1.6, 1.1 Hz, 1H), 7.35-7.31 (m, 3H), 7.25-7.22 (m, 1H), 7.19-7.11 (m, 5H), 7.04-7.00 (m, 3H), 6.92 ppm (s, 1H). ^{13}C NMR (100 MHz, $CDCl_3$): δ = 145.8, 141.2, 139.6, 136.9, 136.4, 130.3, 129.9, 129.7, 129.3, 128.8, 128.0, 127.7, 127.1, 127.0, 94.5 ppm. HRMS: m/z calcd for $C_{20}H_{15}INa^{+}$: 383.0297; found: 383.0297.

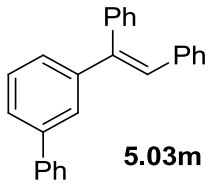

5.03m

(*E*)-3-(1,2-Diphenylvinyl)-1,1'-biphenyl (**5.03m**): Colorless liquid, 46.6mg, 70%. ^{1}H NMR ($CDCl_3$, 300 MHz): δ = 7.50 (t, *J* = 1.9 Hz, 1H), 7.42-7.39 (m, 1H), 7.36-7.31 (m, 3H), 7.24-7.11 (m, 7H), 7.04-7.01 (m, 2H), 6.95 ppm (s, 1H). ^{13}C NMR ($CDCl_3$, 75 MHz): δ = 144.3. 142.8. 141.5, 141.4, 140.5, 137.6, 130.7, 129.8, 129.0, 128.91, 128.85, 128.7, 128.2, 127.7, 127.6, 127.5, 127.1, 127.0, 126.69, 126.65 ppm. HRMS: calculated for $C_{26}H_{20}Na^{+}$: m/z = 333.1643; found: m/z = 333.1650.

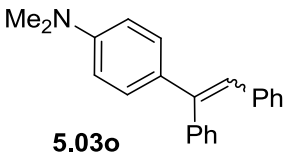

5.03o

4-(1,2-Diphenylvinyl)-N,N-dimethylaniline ((*E/Z*)- **5.03o**): Colorless oil, 30 mg, 50% (E:Z = 2:1). ^{1}H NMR (400 MHz, $CDCl_3$): δ = 7.37-6.98 (m, 12H), 6.88 (s, 0.67H), 6.83 (s, 0.33H), 6.69-6.66 (m, 2H), 2,98 (s, 2H), 2.96 ppm (s, 4H); ^{13}C NMR (100 MHz, $CDCl_3$): δ = 150.3, 150.0, 144.7, 143.1, 142.7, 141.1, 138.4, 138.2, 131.7, 131.6, 130.7, 129.7, 129.6, 128.7, 128.61, 128.56, 128.26, 128.18, 128.14, 128.08, 127.5, 127.4, 127.2, 126.5, 126.3, 125.0, 112.5, 112.2, 40.70, 44.66 ppm. HRMS: m/z calcd for $C_{22}H_{21}NNa^{+}$: 322.1566; found: 322.1558.

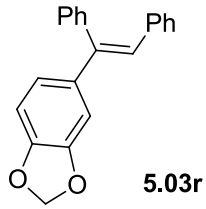

5.03r

(*E*)-5-(1,2-Diphenylvinyl)benzo[d][1,3]dioxolee (**5.03r**): Colorless liquid, 45.1 mg, 75 %. ^{1}H NMR (400 MHz, $CDCl_3$): δ = 7.85 (dd, *J* = 15.4, 0.7 Hz, 1H), 7.47-7.34 (m, 5H), 7.20-7.08 (m, 8H), 6.98-6.895 (m, 3H), 5.67 ppm (d, *J* = 15.4 Hz, 2H). ^{13}C NMR (100 MHz, $CDCl_3$): δ = 165.9, 151.7, 151.1, 139.9, 139.8, 137.0, 135.8, 130.4, 129.5, 128.7, 128.5, 128.3, 125.9, 121.9, 119.5 ppm. HRMS: m/z calcd for $C_{23}H_{18}O_2Na^+$: 349.1199; found: 349.1204.

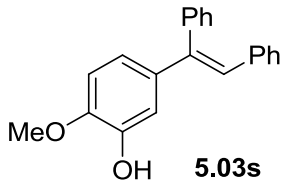

5.03s

(*E*)-5-(1,2-Diphenylvinyl)-2-methoxyphenol (**5.03s**): White solid, 39.9 mg, 66%. ^{1}H NMR ($CDCl_3$, 300 MHz): δ = 7.34-7.30 (m, 3H), 7.22-7.20 (m, 2H), 7.13-7.08 (m, 3H), 7.02-6.99 (m, 2), 6.98 (dd, *J* = 2.0, 0.4 Hz, 1H), 6.92 (s, 1H), 6.80 (d, *J* = 2.0 Hz, 1H), 6.79 (s, 1H) 5.58 (s, 1H), 3. 88 ppm (s, 3H). ^{13}C NMR ($CDCl_3$, 75 MHz): δ = 146.5, 145.5, 142.3, 140.6, 137.73, 137.30, 130.6, 129.7, 128.8, 128.2, 127.6, 127.1, 126.7, 119.9, 114.0, 110.5, 56.2 ppm. HRMS: calculated for $C_{21}H_{18}O_2Na^+$: m/z = 325.1199; found: m/z = 325.1207.

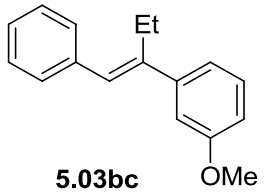

5.03bc

(*E*)-1-Methoxy-3-(1-phenylbut-1-en-2-yl)benzene (**5.03bc**): Colorless liquid, 34.8 mg, 73%. ^{1}H NMR (400 MHz, $CDCl_3$): δ = 7.38-7.23 (m, 6H), 7.07 (ddd, *J* = 7.6, 1.6, 0.9 Hz, 1H), 7.02-7.01 (m, 1H), 6.85 (ddd, *J* = 8.2, 2.6, 0.9 Hz, 1H), 6.70 (s, 1H), 3.84 (s, 3H), 2.73 (q, *J* = 7.5 Hz, 2H), 1.07 ppm (t, *J* =

7.5 Hz, 3H). ^{13}C NMR (100 MHz, $CDCl_3$): δ = 159.9, 144.59, 144.55, 138.5, 129.5, 128.9, 128.5, 127.9, 126.8, 119.4, 112.8, 112.6, 55.5, 23.6, 13.7 ppm. HRMS: m/z calcd for $C_{17}H_{19}O^+$: 239.1436; found: 239.1434.

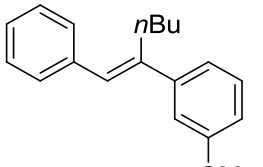

5.03bd

(*E*)-1-Methoxy-3-(1-phenylhex-1-en-2-yl)benzene (**5.03bd**): Colorless liquid, 41.0 mg, 77%. ^{1}H NMR (400 MHz, $CDCl_3$): δ = 7.43-7.29 (m, 6H), 7.11 (ddd, *J* = 7.7, 1.6, 1.0 Hz, 1H), 7.07-7.06 (m, 1H), 6.89 (ddd, *J* = 8.2, 2.6, 0.9 Hz, 1H), 6.76 (s, 1H), 3.87 (s, 3H), 2.76-2.72 (m, 2H), 1.52-1.33(m, 4H), 0.91 ppm (t, *J* = 7.2, 3H). ^{13}C NMR (100 MHz, $CDCl_3$): δ = 159.9, 145.1, 143.5, 138.5, 129.5, 129.0, 128.5, 128.4, 126.8, 119.4, 112.9, 112.6, 55.5, 31.2, 30.1, 23.1, 14.2 ppm. HRMS: m/z calcd for $C_{19}H_{22}ONa^+$: 267.1749; found: 267.1749.

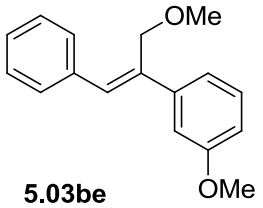

5.03be

(*Z*)-1-Methoxy-3-(3-methoxy-1-phenylprop-1-en-2-yl)benzene (**5.03be**): Colorless liquid, 39.2 mg, 77%. ^{1}H NMR (400 MHz, $CDCl_3$): δ = 7.44-7.36 (m, 4H), 7.32-7.28 (m, 2H), 7.18 (ddd, *J* = 7.7, 1.6, 1.0 Hz, 1H), 7.14-7.13 (m, 1H), 7.06 (s, 1H), 6.86 (ddd, *J* = 8.2, 2.5, 0.9 Hz, 1H), 4.36 (s, 2H), 3.84 (s, 3H), 3.38 ppm (s, 3H). ^{13}C NMR (100 MHz, $CDCl_3$): δ = 159.9, 143.3, 138.0, 137.3, 132.9, 129.6, 129.2, 128.5, 127.6, 119.1, 113.0, 112.5, 70.0, 58.4, 55.5 ppm. HRMS: m/z calcd for $C_{17}H_{19}O_2^+$: 277.1204; found: 277.1212.

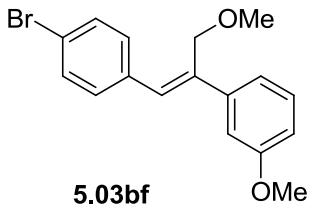

5.03bf

(*Z*)-1-(1-(4-Bromophenyl)-3-methoxyprop-1-en-2-yl)-3-methoxybenzene (**5.03bf**): White solid, 44.0 mg, 66%. ^{1}H NMR (400 MHz, $CDCl_3$): δ = 7.52-7.48 (m, 2H), 7.31-7.27 (m, 3H), 7.14 (ddd, *J* = 7.7, 1.7, 1.0 Hz, 1H), 7.11-7.10 (m, 1H), 6.96 (s, 1H), 6.85 (ddd, *J* = 8.2, 2.6, 0.9 Hz, 1H), 4.29 (s, 2H), 3.83 (s, 3H), 3.38 ppm (s, 3H). ^{13}C NMR (100 MHz, $CDCl_3$): δ = 159.9, 143.1, 138.7, 136.1, 131.70, 131.66, 130.9, 129.7, 121.7, 119.0, 113.1, 112.5, 70.4, 58.5, 55.5 ppm. HRMS: m/z calcd for $C_{16}H_{14}BrO^{+}$ (-OMe): 301.0220; found: 301.0228

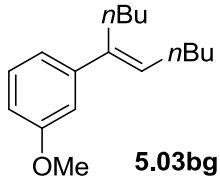

5.03bg

(*E*)-1-(Dec-5-en-5-yl)-3-methoxybenzene (**5.03bg**): Colorless liquid, 27.2 mg, 55%. ^{1}H NMR (400 MHz, $CDCl_3$): δ = 7.20 (t, *J* = 7.9 Hz, 1H), 6.93 (ddd, *J* = 7.7, 1.7, 1.0 Hz, 1H), 6.87 (dd, *J* = 2.5, 1.7 Hz, 1H), 6.76 (ddd, *J* = 8.2, 2.6, 0.9 Hz, 1H), 5.64 (t, *J* = 7.3 Hz, 1H), 3.80 (s, 3H), 2.48-2.44 (m, 2H), 2.18 (q, *J* = 7.24 Hz, 2H), 1.46-1.25 (m, 8H), 0.94-0.85 ppm (m, 6H). ^{13}C NMR (100 MHz, $CDCl_3$): δ = 159.7, 145.4, 140.2, 129.4, 129.2, 119.1, 112.6, 111.6, 55.4, 32.3, 31.2, 29.7, 28.4, 22.9, 22.7, 14.24, 14.18 ppm. HRMS: m/z calcd for $C_{17}H_{27}O^{+}$: 247.2062; found: 247.2062.

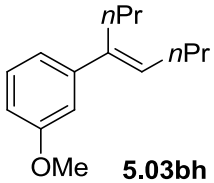

5.03bh

(*E*)-1-Methoxy-3-(oct-4-en-4-yl)benzene (**5.03bh**): Colorless liquid, 28.4 mg, 65%. ^{1}H NMR (400 MHz, $CDCl_3$): δ = 7.27 (t, *J* = 7.8 Hz, 1H), 7.00 (ddd, *J* = 7.7, 1.7, 0.9 Hz, 1H), 6.95 (dd, *J* = 2.6, 1.7 Hz,

1H), 6.82 (ddd, *J* = 8.2, 2.7, 1.0 Hz, 1H), 5.73 (t, *J* = 7.3 Hz, 1H), 3.86 (s, 3H), 2.53-2.50 (m, 2H), 2.26-2.20 (m, 2H), 1.52 (h, *J* = 7.4 Hz, 2H), 1.43 (h, *J* = 7.3 Hz, 2H), 1.02 (t, 7.4 Hz, 3H), 0.94 ppm (t, *J* = 7.4 Hz, 3H). ^{13}C NMR (100 MHz, $CDCl_3$): δ = 159.5, 145.2, 140.0, 129.3, 129.0, 119.0, 112.5, 111.5, 55.2, 31.8, 30.7, 23.1, 21.9, 14.02, 13.99 ppm. HRMS: m/z calcd for $C_{15}H_{23}O^+$: 219.1749; found: 219.1753.

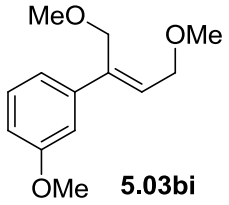

5.03bi

(*Z*)-1-(1,4-Dimethoxybut-2-en-2-yl)-3-methoxybenzene (**5.03bi**); Colorless liquid, 35.6 mg, 80%. ^{1}H NMR (400 MHz, $CDCl_3$): δ = 7.23 (t, *J* = 8.0 Hz, 1H), 7.23 (ddd, *J* = 7.7, 1.56, 0.9 Hz, 1H), 6.97-6.96 (m, 1H), 6.80 (ddd, *J* = 8.0, 2.4, 0.8 Hz, 1H), 6.07 (t, *J* = 6.4 Hz, 1H), 4.30 (s, 2H), 4.19 (d, *J* = 6.4 Hz, 2H), 3.79 (s, 3H), 3.38 (s, 3H), 3.32 ppm (s, 3H). ^{13}C NMR (100 MHz, $CDCl_3$): δ = 159.9, 142.6, 139.3, 130.0, 129.6, 119.2, 113.2, 112.5, 69.8, 69.3, 58.6, 58.3, 55.5 ppm. HRMS: m/z calcd for $C_{13}H_{18}O_3Na^+$: 245.1154; found: 245.1160.

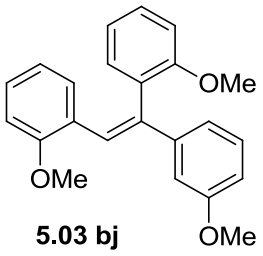

5.03 bj

(*Z*)-2,2'-(1-(3-Methoxyphenyl)ethene-1,2-diyl)bis(methoxybenzene) (**5.03bj**): Colorless liquid, 64.5 mg, 93%. ^{1}H NMR (400 MHz, $CDCl_3$): δ = 7.34 (s, 1H), 7.29 (td, *J* = 7.7, 1.5 Hz, 1H), 7.20 (t, *J* = 8.0 Hz, 1H), 7.11-7.07 (m, 3H), 6.97-6.95 (m, 2H), 6.91-6.87 (m, 2H), 6.83-6.79 (m, 3H), 6.59 (t, *J* = 7.5 Hz, 1H), 3.83 (s, 3H), 3.78 (s, 3H), 3.57 ppm (s, 3H). ^{13}C NMR (100 MHz, $CDCl_3$): δ = 159.7, 158.0, 157.9, 145.0, 139.0, 132.1, 129.8, 129.5, 129.2, 129.1, 128.3, 127.2, 124.4, 121.2, 120.1, 119.8, 112.8, 112.7, 111.8, 110.5, 55.84, 55.76, 55.5 ppm. HRMS: m/z calcd for $C_{23}H_{22}O_3Na^+$: 369.1461; found: 369.1468.

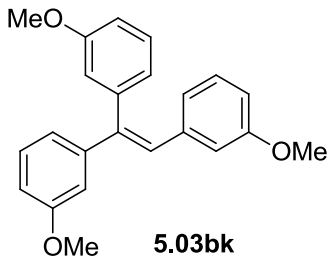

5.03bk

3,3',3''-(Ethene-1,1,2-triyl)tris(methoxybenzene) (**5.03bk**): Colorless liquid, 56.2 mg, 81%. ^{1}H NMR (400 MHz, $CDCl_3$): δ = 7.27 (t, *J* = 7.3 Hz, 1H), 7.23 (t, *J* = 7.3 Hz, 1H), 7.08 (t, *J* = 7.9 Hz, 1H), 6.97-6.83 (m, 6H), 6.78 (s, 1H), 6.71 (dd, *J* = 8.2, 1.1 Hz, 1H), 6.71 (dd, *J* = 8.7, 3.0 Hz, 1H), 6.58 (s, 1H), 3.78 (s, 3H), 3.72 (s, 3H), 3.54 ppm (s, 3H). ^{13}C NMR (100 MHz, $CDCl_3$): δ = 160.3, 159.8, 159.4, 144.8, 142.7, 142.0, 138.8, 130.1, 129.4, 129.2, 128.5, 123.0, 122.8, 120.4, 115.7, 114.1, 113.9, 113.70, 113.68, 113.15, 55.6, 55.1 ppm. HRMS: m/z calcd for $C_{23}H_{22}O_3Na^+$: 369.1461; found: 369.1459.

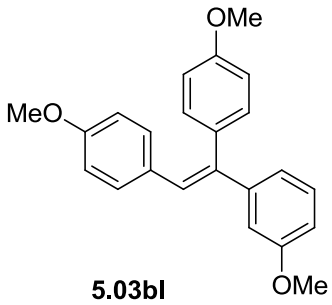

5.03bl

(*E*)-4,4'-(1-(3-Methoxyphenyl)ethene-1,2-diyl)bis(methoxybenzene) (**5.03bl**): White solid, 43.7 mg, 63 %. ^{1}H NMR (400 MHz, $CDCl_3$): δ = 7.21 (t, *J* = 7.9 Hz, 1H), 7.16-7.12 (m, 2H), 7.02-6.98 (m, 2H), 6.93-6.90 (m, 1H), 6.89-6.85 (m, 4H), 6.82 (ddd, *J* = 8.2, 2.6, 0.8 Hz, 1H), 6.71-6.68 (m, 2H), 3.83 (s, 3H), 3.78 (s, 3H), 3.75 ppm (s, 3H). ^{13}C NMR (100 MHz, $CDCl_3$): δ = 159.7, 159.1, 158.6, 145.8, 140.4, 132.9, 131.8, 131.0, 130.5, 129.3, 127.8, 120.4, 114.3, 113.7, 113.6, 112.8, 55.44, 55.42, 55.37 ppm; HRMS: m/z calcd for $C_{23}H_{22}O_3Na^+$: 369.1461; found: 369.1465.

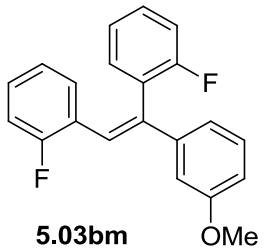

5.03bm

(*Z*)-2,2'-(1-(3-Methoxyphenyl)ethene-1,2-diyl)bis(fluorobenzene) (**5.03bm**): White solid, 54.2 mg, 84%. ^{1}H NMR (400 MHz, $CDCl_3$): δ = 7.35-7.31 (m, 1H), 7.29-7.24 (m, 2H), 7.18 (td, *J* = 7.4, 1.9 Hz, 1H), 7.15-6.96 (m, 5H), 6.94-6.93 (m, 1H), 6.89-6.86 (m, 1H), 6.84-6.78 (m, 2H), 3.79 ppm (s, 3H). ^{13}C NMR (100 MHz, $CDCl_3$): δ = 161.18 (d, *J* = 247.0 Hz), 160.65 (d, *J* = 246.4 Hz), 160.0, 143.6, 138.4, 132.5 (d, *J* = 3.5 Hz), 130.1 (d, *J* = 8.0 Hz), 129.8 (d, *J* = 2.8 Hz), 129.6, 129.1 (d, *J* = 8.3 Hz), 127.7 (d, *J* = 16.0 Hz), 125.4 (d, *J* = 12.8 Hz), 124.6 (d, *J* = 3.6 Hz), 123.8 (d, *J* = 3.6 Hz), 122.8 (d, *J* = 4.9 Hz), 119.9, 116.3 (d, *J* = 21.8 Hz), 115.5 (d, *J* = 22.2 Hz), 113.5, 113.2, 55.5 ppm. ^{19}F NMR (282.4 MHz): δ = -113.26, -115.43 ppm. HRMS: m/z calcd for $C_{21}H_{16}F_{23}Na^{+}$: 345.1061; found: 345.1064.

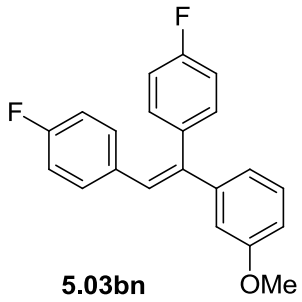

5.03bn

(*E*)-4,4'-(1-(3-Methoxyphenyl)ethene-1,2-diyl)bis(fluorobenzene) (**5.03bn**): Yellow solid, 45.8 mg, 71 %. ^{1}H NMR (400 MHz, $CDCl_3$): δ = 7.26-7.21 (m, 1H), 7.17-7.14 (m, 2H), 7.05-6.97 (m, 4H), 6.93 (s, 1H), 6.90-6.88 (m, 1H), 6.86-6.82 (m, 4H), 3.78 ppm (s, 3H). ^{13}C NMR (100 MHz, $CDCl_3$): δ = 162.5 (d, *J* = 246.9 Hz), 161.8 (d, *J* = 247.5 Hz), 159.8, 144.8, 141.5 (d, *J* = 2.0 Hz), 136.1 (d, *J* = 3.6 Hz), 133.5 (d, *J* = 3.4 Hz), 132.3 (d, *J* = 7.9 Hz), 131.3 (d, *J* = 7.8 Hz), 129.5, 127.6, 120.4, 116.0 (d, *J* = 21.3 Hz), 115.2 (d, *J* = 21.4 Hz), 113.7, 113.2, 55.4 ppm. ^{19}F NMR (282.4 MHz): δ = -114.27, -114, 45 ppm. HRMS: m/z calcd for $C_{21}H_{16}F_{2}ONa^{+}$: 345.1061; found: 345.1066.

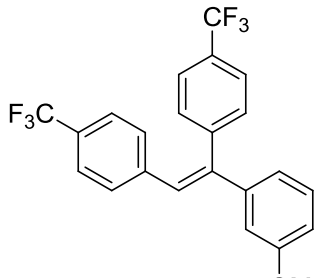

5.03bo

(*E*)-4,4'-(1-(3-Methoxyphenyl)ethene-1,2-diyl)bis((trifluoromethyl)benzene) (**5.03bo**): White solid, 55.8 mg, 66%. ^{1}H NMR (400 MHz, $CDCl_3$): δ = 7.59 (d, *J* = 8.0 Hz, 2H), 7.40 (d, *J* = 8.4 Hz, 2H), 7.30 (d, *J* = 8.0 Hz, 2H), 7.26 (t, *J* = 7.5 Hz, 1H), 7.09 (d, *J* = 8.1 Hz, 2H), 7.04 (s, 1H), 6.87 (tdd, *J* = 7.7, 2.1, 0.81 Hz, 2H), 6.82 (t, *J* = 2.1 Hz, 1H), 3.78 ppm (s, 3H). ^{13}C NMR (100 MHz, $CDCl_3$): δ = 159.7, 143.6, 143.46 (q, *J* = 1.3 Hz), 143.43, 140.3 (q, *J* = 1.6 Hz), 130.7, 130.0 (q, *J* = 32.3 Hz), 129.7, 129.5, 128.9 (q, *J* = 32.3 Hz), 127.9, 125.7 (q, *J* = 3.7 Hz), 125.1 (q, *J* = 3.8 Hz), 124.1 (q, *J* = 270.4 Hz), 124.0 (q, *J* = 270.3 Hz), 120.3, 113.8, 113.5, 55.3 ppm. ^{19}F NMR (282.4 MHz): δ = -62.60, -62.70 ppm. HRMS m/z calcd for C23H17F6O+: 423.1183; found: 423.1186.

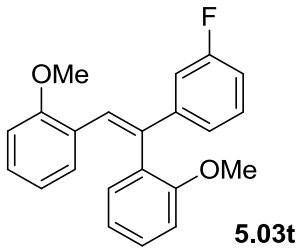

5.03t

(*Z*)-2,2'-(1-(3-Fluorophenyl)ethene-1,2-diyl)bis(methoxybenzene) (**5.03t**) :Yellow liquid, 62 mg, 92% (from *p*-fluorobenzoic acid); 48 mg, 72% (from *o*-fluorobenzoic acid). ^{1}H NMR (400 MHz, $CDCl_3$): δ = 7.32 (s, 1H), 7.28 (ddd, *J* = 8.3, 7.4, 1.8 Hz, 1H), 7.24-7.19 (m, 1H), 7.14-7.01 (m, 4H), 6.93-6.86 (m, 3H), 6.81 (dd, *J* = 8.3, 0.9 Hz, 1H), 6.76 (dd, *J* = 7.7, 1.7 Hz, 1H), 6.57 (t, *J* = 7.5 Hz, 1H), 3.82 (s, 3H), 3.96 ppm (s, 3H). ^{13}C NMR (100 MHz, $CDCl_3$): δ = 162.9 (d, *J* = 244.1 Hz), 157.67, 157.65, 145.6 (d, *J* = 7.5 Hz), 137.9 (d, *J* = 2.5 Hz), 131.8, 129.31 (d, *J* = 8.4 Hz), 129.30, 129.1, 129.0, 128.3, 126.6, 124.9, 122.4 (d, *J* = 2.6 Hz), 121.0, 119.9, 113.7 (d, *J* = 22 Hz), 113.5 (d, *J* = 22 Hz), 111.6, 110.3, 55.5 ppm. ^{19}F NMR (282.4 MHz): δ = -114.40 ppm. HRMS: m/z calcd for $C_{22}H_{20}FO_2^+$: 335.1447; found: 335.1451.

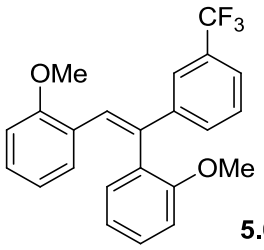

5.03u

(*Z*)-2,2'-(1-(3-(Trifluoromethyl)phenyl)ethene-1,2-diyl)bis(methoxybenzene) (**5.03u**): Yellow solid, 53.8 mg, 70%. ^{1}H NMR (400 MHz, $CDCl_3$): δ = 7.57 (d, *J* = 8.3 Hz, 2H), 7.48 (d, *J* = 7.15 Hz, 2H), 7.40 (s, 1H), 7.35 (ddd, *J* = 8.3, 7.4, 1.8 Hz, 1H), 7.18-7.14 (m, 1H), 7.10 (dd, *J* = 7.4, 1.7 Hz, 1H), 6.97-6.92 (m, 2H), 6.88 (dd, *J* = 8.3, 0.8 Hz, 1H), 6.83 (dd, *J* = 7.7, 1.6 Hz, 1H), 6.66-6.62 (m, 1H), 3.87 (s, 3H), 3.60 ppm (s, 3H). ^{13}C NMR (100 MHz, $CDCl_3$): δ = 157.7,157.6, 146.8 (q, *J* = 1.5 Hz), 137.8, 131.8, 129.3, 129.2, 128.76 (q, *J* = 32.2 Hz), 128.81, 128.5, 126.9, 126.4, 125.9, 125.0 (q, *J* = 3.8 Hz), 124.46 (q, *J* = 270 Hz), 121.0, 119.9, 111.5, 110.3, 55.49, 55.48 ppm. ^{19}F NMR (282.4 MHz): δ = -62.54 ppm. HRMS: m/z calcd for $C_{23}H_{20}F_3O_2^+$: 385.1415; found: 385.1414.

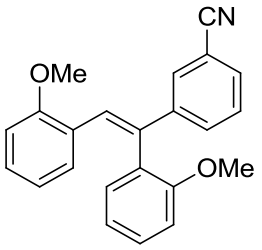

5.03v

(*Z*)-3-(1,2-Bis(2-methoxyphenyl)vinyl)benzonitrile (**5.03v**): Colorless liquid, 49.9 mg, 73%. ^{1}H NMR (400 MHz, $CDCl_3$): δ = 7.64-7.60 (m, 2H), 7.53 (dt, *J* = 7.7, 1.4 Hz, 1H), 7.40 (dt, *J* = 7.7, 0.8 Hz, 1H), 7.17-7.13 (m, 1H), 7.07 (dd, *J* = 7.4, 1.8 Hz, 1H), 6.96-6.91 (m, 2H), 6.87 (dd, *J* = 8.3, 0.9 Hz, 1H), 6.80 (dd, *J* = 7.7, 1.6 Hz, 1H), 6.63 (t, *J* = 7.6 Hz, 1H), 3.87 (s, 3H), 3.60 ppm (s, 3H). ^{13}C NMR (100 MHz, $CDCl_3$): δ = 157.7, 157.5, 144.5, 137.0, 131.7, 130.9, 130.3, 130.2, 129.5, 129.3, 128.8, 128.7, 128.2, 126.1, 126.0, 121.1, 119.9, 119.2, 112.2, 111.5, 110.3, 55.5, 55.4 ppm; HRMS: m/z calcd for $C_{23}H_{20}NO_2$: 342.1494; found: 342.1483.

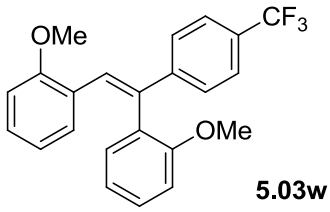

5.03w

(*Z*)-2,2'-(1-(4-(Trifluoromethyl)phenyl)ethene-1,2-diyl)bis(methoxybenzene) (**5.03w**) :Yellow solid, 63.8 mg, 83%. ^{1}H NMR (400 MHz, $CDCl_3$): δ = 7.62 (s, 1H), 7.48-7.46 (m, 2H), 7.38-7.36 (m, 1H), 7.31-7.27 (m, 2H), 7.12-7.08 (m, 1H), 7.05 (dd, *J* = 7.4, 1.8 Hz, 1H), 6.91-6.86 (m, 2H), 6.82 (dd, *J* = 8.3, 0.9 Hz, 1H), 6.77 (dd, *J* = 7.7, 1.7 Hz, 1H), 6.59 (td, *J* = 7.5, 0.7 Hz, 1H), 3.82 (s, 3H), 3.53 ppm (s, 3H). ^{13}C NMR (100 MHz, $CDCl_3$): δ = 157.81, 157.78, 144.2, 138.0, 132.0, 130.6 (q, *J* = 31.7 Hz), 130.21, 129.5, 129.4, 128.8, 128.62, 128.60, 126.6, 125. 7, 124.6 (q, *J* = 270.8 Hz), 123.7 (q, *J* = 3.9 Hz), 123.5 (q, *J* = 3.8 Hz), 121.2, 120.0, 111.7, 110.4, 55.67, 55.62 ppm. ^{19}F NMR (282.4 MHz): δ = -62.31 ppm. HRMS: m/z calcd for $C_{23}H_{20}F_3O_2^+$: 385.1415; found: 385.1425.

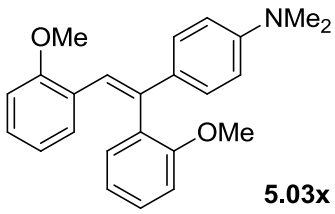

5.03x

(*Z*)-4-(1,2-Bis(2-methoxyphenyl)vinyl)-N,N-dimethylaniline (**5.03x**): White solid, 44.6 mg, 62%. ^{1}H NMR (400 MHz, $CDCl_3$): δ = 7.33-7.26 (m, 4H), 7.12-7.06 (m, 2H), 6.94-6.90 (m, 2H), 6.84 (dd, *J* = 8.3, 0.8 Hz, 1H), 6.79 (dd, *J* = 7.7, 1.5 Hz, 1H), 6.71-6.67 (m, 2H), 6.60 (t, *J* = 7.3 Hz, 1H), 3.86 (s, 3H), 3.61 (s, 3H), 2.98 ppm (s, 6H). ^{13}C NMR (100 MHz, $CDCl_3$): δ = 157.7, 157.4, 149.8, 138.6, 131.9, 131.4, 130.1, 129.0, 128.5, 127.58, 127.54, 127.3, 120.9, 120.4, 119.9, 112.2, 111.5, 110.2, 55.7, 55.6 ppm. HRMS: m/z calcd for $C_{24}H_{25}NO_2^+$: 360.1964; found: 360.1976.

5.8. References

1. Jia, C.; Piao, D.; Oyamada, J.; Lu, W.; Kitamura, T.; Fujiwara, Y. Efficient Activation of Aromatic C-H Bonds for Addition to C-C Multiple Bonds. *Science* **2000**, *287*, 1992-1995.

2. Jia, C.; Kitamura, T.; Fujiwara, Y. Catalytic Functionalization of Arenes and Alkanes via C−H Bond Activation. *Acc. Chem. Res.* **2001**, *34*, 633-639.

3. Nevado, C.; Echavarren, A. M. Transition Metal-Catalyzed Hydroarylation of Alkynes. *Synthesis* **2005**, 167-182.

4. Nakao, Y. Hydroarylation of alkynes catalyzed by nickel. *Chem. Rec.* **2011**, *11*, 242-251.

5. Bandini, M. Gold-Catalyzed Decorations of Arenes and Heteroarenes with C-C Multiple Bonds. *Chem. Soc. Rev.* **2011**, *40*, 1358-1367.

6. Mendoza, P. D.; Echavarren, A. M. Synthesis of Arenes and Heteroarenes by Hydroarylation Reactions Catalyzed by Electrophilic Metal Complexes. *Pure Appl. Chem.* **2010**, *82*, 801-820.

7. Kitamura, T. Transition-Metal-Catalyzed Hdroarylation Reactions of Alkynes through Direct Functionalization of C-H Bonds. A Convenient Tool for Organic Synthesis. *Eur. J. Org. Chem.* **2009**, 1111-1125.

8. Cacchi, S. The Palladium-Catalyzed Hydroarylation and Hydrovinylation of Carbon-Carbon Multiple Bonds: New Perspectives in Organic Synthesis. *Pure Appl. Chem.* **1990**, *62*, 713-722.

9. Cacchi, S.; Fabrizi, G.; Goggiamani, A.; Persiani, D. Palladium-Catalyzed Hydroarylation of Alkynes with Arenediazonium Salts. *Org. Lett.* **2008**, *10*, 1597-1600.

10. Artok, L.; Kuş, M.; Aksın-Artok, Ö.; Dege, F. N.; Özkılınç, F. Y. Rhodium Catalyzed Reaction of Internal Alkynes with Organoborons under CO Atmosphere: a Product Tunable Reaction. *Tetrahedron* **2009**, *65*, 9125-9133.

11. Xu, X.; Chen, J.; Gao, W.; Wu, H.; Ding, J.; Su, W. Palladium-Catalyzed Hydroarylation of Alkynes with Arylboronic Acids. *Tetrahedron* **2010**, *66*, 2433-2438.

12. Liu, S.; Bai, Y.; Cao, X.; Xiao, F.; Deng, G.-J. Palladium-Catalyzed Desulfitative Hydroarylation of Alkynes with Sodium Sulfinates. *Chem. Commun.* **2013**, *49*, 7501-7503.

13. Song, C. E.; Jun, D.-u.; Choung, S.-Y.; Roh, E. J.; Lee, S.-g. Dramatic Enhancement of Catalytic Activity in an Ionic Liquid: Highly Practical Friedel-Crafts Alkenylation of Arenes with Alkynes Catalyzed by Metal Triflates. *Angew. Chem. Int. Ed.* **2004**, *43*, 6183-6185.

14. Li, R.; Wang, S. R.; Lu, W. $FeCl_3$-Catalyzed Alkenylation of Simple Arenes with Aryl-Substituted Alkynes. *Org. Lett.* **2007**, *9*, 2219-2222.

15. Yoon, M. Y.; Kim, J. H.; Choi, D. S.; Shin, U. S.; Lee, J. Y.; Song, C. E. Metal Triflate-Catalyzed Regio- and Stereoselective Friedel–Crafts Alkenylation of Arenes with Alkynes in an Ionic Liquid: Scope and Mechanism. *Adv. Synth. Catal.* **2007**, *349*, 1725-1737.

16. Choi, D. S.; Kim, J. H.; Shin, U. S.; Deshmukh, R. R.; Song, C. E. Thermodynamically- and Kinetically-Controlled Friedel-Crafts Alkenylation of Arenes with Alkynes Using an Acidic Fluoroantimonate(v) Ionic Liquid as Catalyst. *Chem. Commun.* **2007**, 3482-3484.

17. Soriano, E.; Marco-Contelles, J. Mechanisms of the Transition Metal-Mediated Hydroarylation of Alkynes and Allenes. *Organometallics* **2006**, *25*, 4542-4553.

18. Tsuchimoto, T.; Maeda, T.; Shirakawa, E.; Kawakami, Y. Friedel-Crafts Alkenylation of Arenes Using Alkynes Catalysed by Metal Trifluoromethanesulfonates. *Chem. Commun.* **2000**, 1573-1574.

19. Bandini, M.; Emer, E.; Tommasi, S.; Umani-Ronchi, A. Innovative Catalytic Protocols for the Ring-Closing Friedel–Crafts-Type Alkylation and Alkenylation of Arenes. *Eur. J. Org. Chem.* **2006**, *2006*, 3527-3544.

20. Yamamoto, Y.; Gridnev, I. D.; Patil, N. T.; Jin, T. Alkyne Activation with Bronsted Acids, Iodine, or Gold Complexes, and Its Fate Leading to Synthetic Application. *Chem. Commun.* **2009**, 5075-5087.

21. Tsukada, N.; Mitsuboshi, T.; Setoguchi, H.; Inoue, Y. Stereoselective *cis*-Addition of Aromatic C−H Bonds to Alkynes Catalyzed by Dinuclear Palladium Complexes. *J. Am. Chem. Soc.* **2003**, *125*, 12102-12103.

22. Tsukada, N.; Murata, K.; Inoue, Y. Selective *cis*-Addition of C–H Bonds of Pyrroles and Thiophenes to Alkynes Catalyzed by a Dinuclear Palladium Complex. *Tetrahedron Lett.* **2005**, *46*, 7515-7517.

23. Kakiuchi, F.; Yamamoto, Y.; Chatani, N.; Murai, S. Catalytic Addition of Aromatic C-H Bonds to Acetylenes. *Chem. Lett.* **1995**, *24*, 681-682.

24. Satoh, T.; Nishinaka, Y.; Miura, M.; Nomura, M. Iridium-Catalyzed Regioselective Reaction of 1-Naphthols with Alkynes at the *peri*-Position. *Chem. Lett.* **1999**, *28*, 615-616.

25. Lim, Y.-G.; Lee, K.-H.; Koo, B. T.; Kang, J.-B. Rhodium(I)-Catalyzed *ortho*-Alkenylation of 2-Phenylpyridines with Alkynes. *Tetrahedron Lett.* **2001**, *42*, 7609-7612.

26. Cheng, K.; Yao, B.; Zhao, J.; Zhang, Y. $RuCl_3$-Catalyzed Alkenylation of Aromatic C−H Bonds with Terminal Alkynes. *Org. Lett.* **2008**, *10*, 5309-5312.

27. Tsuchikama, K.; Kasagawa, M.; Hashimoto, Y.-K.; Endo, K.; Shibata, T. Cationic Iridium–BINAP Complex-Catalyzed Addition of Aryl Ketones to Alkynes and Alkenes via Directed C–H Bond Cleavage. *J. Organomet. Chem.* **2008**, *693*, 3939-3942.

28. Schipper, D. J.; Hutchinson, M.; Fagnou, K. Rhodium(III)-Catalyzed Intermolecular Hydroarylation of Alkynes. *J. Am. Chem. Soc.* **2010**, *132*, 6910-6911.

29. Yamakawa, T.; Yoshikai, N. Cobalt-Catalyzed *ortho*-Alkenylation of Aromatic Aldimines via Chelation-Assisted C–H Bond Activation. *Tetrahedron* **2013**, *69*, 4459-4465.

30. Reddy, M. C.; Jeganmohan, M. Ruthenium-Catalyzed Highly Regio- and Stereoselective Hydroarylation of Aryl Carbamates with Alkynes via C-H Bond Activation. *Chem. Commun.* **2013**, *49*, 481-483.

31. Rousseau, G.; Breit, B. Removable Directing Groups in Organic Synthesis and Catalysis. *Angew. Chem. Int. Ed.* **2011**, *50*, 2450-2494.

32. Zhang, Y.-H.; Shi, B.-F.; Yu, J.-Q. Pd(II)-Catalyzed Olefination of Electron-Deficient Arenes Using 2,6-Dialkylpyridine Ligands. *J. Am. Chem. Soc.* **2009**, *131*, 5072-5074.

33. Yue, W.; Li, Y.; Jiang, W.; Zhen, Y.; Wang, Z. Direct Meta-Selective Alkylation of Perylene Bisimides via Palladium-Catalyzed C−H Functionalization. *Org. Lett.* **2009**, *11*, 5430-5433.

34. Ye, M.; Gao, G. L.; Yu, J. Q. Ligand-Promoted C-3 Selective C-H Olefination of Pyridines with Pd Catalysts. *J. Am. Chem. Soc.* **2011**, *133*, 6964-6967.

35. Cornella, J.; Righi, M.; Larrosa, I. Carboxylic Acids as Traceless Directing Groups for Formal meta-Selective Direct Arylation. *Angew. Chem. Int. Ed.* **2011**, *50*, 9429-9432.

36. Truong, T.; Daugulis, O. Directed Functionalization of C-H Bonds: Now also *meta* Selective. *Angew. Chem. Int. Ed.* **2012**, *51*, 11677-11679.

37. Juliá-Hernández, F.; Simonetti, M.; Larrosa, I. Metalation Dictates Remote Regioselectivity: Ruthenium-Catalyzed Functionalization of *meta* C_{Ar}-H Bonds. *Angew. Chem. Int. Ed.* **2013**, *52*, 11458-11460.

38. Wan, L.; Dastbaravardeh, N.; Li, G.; Yu, J.-Q. Cross-Coupling of Remote *meta*-C–H Bonds Directed by a U-Shaped Template. *J. Am. Chem. Soc.* **2013**, *135*, 18056-18059.

39. Hofmann, N.; Ackermann, L. *meta*-Selective C–H Bond Alkylation with Secondary Alkyl Halides. *J. Am. Chem. Soc.* **2013**, *135*, 5877-5884.

40. Leow, D.; Li, G.; Mei, T.-S.; Yu, J.-Q. Activation of Remote *meta*-C-H Bonds Assisted by an End-on Template. *Nature* **2012**, *486*, 518-522.

41. Dai, H.-X.; Li, G.; Zhang, X.-G.; Stepan, A. F.; Yu, J.-Q. Pd(II)-Catalyzed *ortho*- or *meta*-C–H Olefination of Phenol Derivatives. *J. Am. Chem. Soc.* **2013**, *135*, 7567-7571.

42. Tang, R.-Y.; Li, G.; Yu, J.-Q. Conformation-Induced Remote *meta*-C-H Activation of Amines. *Nature* **2014**, *507*, 215-220.

43. Gooßen, L. J.; Rodríguez, N.; Gooßen, K. Carboxylic Acids as Substrates in Homogeneous Catalysis. *Angew. Chem. Int. Ed.* **2008**, *47*, 3100-3120.

44. Rodriguez, N.; Goossen, L. J. Decarboxylative Coupling Reactions: a Modern Strategy for C–C-bond Formation. *Chem. Soc. Rev.* **2011**, *40*, 5030-5048.

45. Cornella, J.; Larrosa, I. Decarboxylative Carbon-Carbon Bond-Forming Transformations of (Hetero)aromatic Carboxylic Acids. *Synthesis* **2012**, *2012*, 653-676.

46. Dzik, W. I.; Lange, P. P.; Goo Carboxylates as Sources of Carbon Nucleophiles and Electrophiles: Comparison of Decarboxylative and Decarbonylative Pathways. *Chem. Sci.* **2012**, *3*, 2671-2678.

47. Giri, R.; Maugel, N.; Li, J. J.; Wang, D. H.; Breazzano, S. P.; Saunders, L. B.; Yu, J. Q. Palladium-Catalyzed Methylation and Arylation of sp^2 and sp^3 C-H Bonds in Simple Carboxylic Acids. *J. Am. Chem. Soc.* **2007**, *129*, 3510-3511.

48. Chiong, H. A.; Pham, Q.-N.; Daugulis, O. Two Methods for Direct ortho-Arylation of Benzoic Acids. *J. Am. Chem. Soc.* **2007**, *129*, 9879-9884.

49. Wang, D.-H.; Mei, T.-S.; Yu, J.-Q. Versatile Pd(II)-Catalyzed C−H Activation/Aryl−Aryl Coupling of Benzoic and Phenyl Acetic Acids. *J. Am. Chem. Soc.* **2008**, *130*, 17676-17677.

50. Shi, B.-F.; Zhang, Y.-H.; Lam, J. K.; Wang, D.-H.; Yu, J.-Q. Pd(II)-Catalyzed Enantioselective C−H Olefination of Diphenylacetic Acids. *J. Am. Chem. Soc.* **2009**, *132*, 460-461.

51. Wang, D. H.; Engle, K. M.; Shi, B. F.; Yu, J. Q. Ligand-Enabled Reactivity and Selectivity in a Synthetically Versatile Aryl C-H Olefination. *Science* **2010**, *327*, 315-319.

52. Ueyama, T.; Mochida, S.; Fukutani, T.; Hirano, K.; Satoh, T.; Miura, M. Ruthenium-Catalyzed Oxidative Vinylation of Heteroarene Carboxylic Acids with Alkenes via Regioselective C−H Bond Cleavage. *Org. Lett.* **2011**, *13*, 706-708.

53. Ackermann, L.; Pospech, J.; Potukuchi, H. K. Well-Defined Ruthenium(II) Carboxylate as Catalyst for Direct C–H/C–O Bond Arylations with Phenols in Water. *Org. Lett.* **2012**, *14*, 2146-2149.

54. Ackermann, L.; Pospech, J. Ruthenium-Catalyzed Oxidative C–H Bond Alkenylations in Water: Expedient Synthesis of Annulated Lactones. *Org. Lett.* **2011**, *13*, 4153-4155.

55. Ueura, K.; Satoh, T.; Miura, M. Rhodium- and Iridium-Catalyzed Oxidative Coupling of Benzoic Acids with Alkynes via Regioselective C−H Bond Cleavage. *J. Org. Chem.* **2007**, *72*, 5362-5367.

56. Mochida, S.; Hirano, K.; Satoh, T.; Miura, M. Synthesis of Functionalized α-Pyrone and Butenolide Derivatives by Rhodium-Catalyzed Oxidative Coupling of Substituted Acrylic Acids with Alkynes and Alkenes. *J. Org. Chem.* **2009**, *74*, 6295-6298.

57. Mochida, S.; Hirano, K.; Satoh, T.; Miura, M. Synthesis of Stilbene and Distyrylbenzene Derivatives through Rhodium-Catalyzed *ortho*-Olefination and Decarboxylation of Benzoic Acids. *Org. Lett.* **2010**, *12*, 5776-5779.

58. Mochida, S.; Hirano, K.; Satoh, T.; Miura, M. Rhodium-Catalyzed Regioselective Olefination Directed by a Carboxylic Group. *J. Org. Chem.* **2011**, *76*, 3024-3033.

59. Chinnagolla, R. K.; Jeganmohan, M. Regioselective Synthesis of Isocoumarins by Ruthenium-Catalyzed Aerobic Oxidative Cyclization of Aromatic Acids with Alkynes. *Chem. Commun.* **2012**, *48*, 2030-2032.

60. Ackermann, L.; Pospech, J.; Graczyk, K.; Rauch, K. Versatile Synthesis of Isocoumarins and α-Pyrones by Ruthenium-Catalyzed Oxidative C–H/O–H Bond Cleavages. *Org. Lett.* **2012**, *14*, 930-933.

61. Arockiam, P. B.; Bruneau, C.; Dixneuf, P. H. Ruthenium(II)-Catalyzed C–H Bond Activation and Functionalization. *Chem. Rev.* **2012**, *112*, 5879-5918.

62. Burger, E. C.; Tunge, J. A. Ruthenium-Catalyzed Stereospecific Decarboxylative Allylation of non-Stabilized Ketone Enolates. *Chem. Commun.* **2005**, 2835-2837.

63. Rotem, M.; Shvo, Y. Addition of Carboxylic Acids to Alkynes Catalyzed by Ruthenium Complexes. Vinyl Ester Formation. *Organometallics* **1983**, *2*, 1689-1691.

64. Cacchi, S.; Felici, M.; Pietroni, B. The Palladium-Catalyzed Reaction of Aryl Iodides with Mono and Disubstituted Acetylenes: a New Synthesis of Trisubstituted Alkenes. *Tetrahedron Lett.* **1984**, *25*, 3137-3140.

65. Wang, C.; Rakshit, S.; Glorius, F. Palladium-Catalyzed Intermolecular Decarboxylative Coupling of 2-Phenylbenzoic Acids with Alkynes via C-H and C-C Bond Activation. *J. Am. Chem. Soc.* **2010**, *132*, 14006-14008.

66. Xie, Y.; Yu, M.; Zhang, Y. Iron(II) Chloride Catalyzed Alkylation of Propargyl Ethers: Direct Functionalization of an sp^3 C-H Bond Adjacent to Oxygen. *Synthesis* **2011**, *2011*, 2803-2809.

67. Mio, M. J.; Kopel, L. C.; Braun, J. B.; Gadzikwa, T. L.; Hull, K. L.; Brisbois, R. G.; Markworth, C. J.; Grieco, P. A. One-Pot Synthesis of Symmetrical and Unsymmetrical Bisarylethynes by a Modification of the Sonogashira Coupling Reaction. *Org. Lett.* **2002**, *4*, 3199-3202.

68. Bennett, M. A.; Smith, A. K. Arene Ruthenium(II) Complexes Formed by Dehydrogenation of Cyclohexadienes with Ruthenium(III) Trichloride. *J. Chem. Soc., Dalton Trans.* **1974**, 233-241.

69. Tocher, D. A.; Gould, R. O.; Stephenson, T. A.; Bennett, M. A.; Ennett, J. P.; Matheson, T. W.; Sawyer, L.; Shah, V. K. Areneruthenium(II) Carboxylates: Reactions with Ligands and the X-ray Structure of the *p*-Cymene Pyrazine Complex $[Ru(\eta\text{-}p\text{-}MeC_6H_4CHMe_2)Cl(pyz)_2]PF_6$. *J. Chem. Soc., Dalton Trans.* **1983**, 1571-1581.

70. Arockiam, P. B.; Fischmeister, C.; Bruneau, C.; Dixneuf, P. H. C-H Bond Functionalization in Water Catalyzed by Carboxylato Ruthenium(II) Systems. *Angew. Chem. Int. Ed.* **2010**, *49*, 6629-6632.

71. He, Z.; Kirchberg, S.; Fröhlich, R.; Studer, A. Oxidative Heck Arylation for the Stereoselective Synthesis of Tetrasubstituted Olefins Using Nitroxides as Oxidants. *Angew. Chem. Int. Ed.* **2012**, *51*, 3699-3702.

72. Cacchi, S.; Fabrizi, G.; Goggiamani, A.; Persiani, D. Palladium-Catalyzed Hydroarylation of Alkynes with Arenediazonium Salts. *Org. Lett.* **2008**, *10*, 1597-1600.